

1-1-1988

## Mechanism and kinetics of the dicyandiamide cure of epoxy resins/

Michael D. Gilbert  
*University of Massachusetts Amherst*

Follow this and additional works at: [https://scholarworks.umass.edu/dissertations\\_1](https://scholarworks.umass.edu/dissertations_1)

---

### Recommended Citation

Gilbert, Michael D., "Mechanism and kinetics of the dicyandiamide cure of epoxy resins/" (1988). *Doctoral Dissertations 1896 - February 2014*. 737.  
<https://doi.org/10.7275/3w7s-4d76> [https://scholarworks.umass.edu/dissertations\\_1/737](https://scholarworks.umass.edu/dissertations_1/737)

This Open Access Dissertation is brought to you for free and open access by ScholarWorks@UMass Amherst. It has been accepted for inclusion in Doctoral Dissertations 1896 - February 2014 by an authorized administrator of ScholarWorks@UMass Amherst. For more information, please contact [scholarworks@library.umass.edu](mailto:scholarworks@library.umass.edu).

UMASS/AMHERST



312066007652621



Mechanism and Kinetics of the  
Dicyandiamide Cure of Epoxy Resins

A Dissertation Presented

by

Michael D. Gilbert

Submitted to the Graduate School  
of the University of Massachusetts in partial  
fulfillment of the requirements for the degree of

Doctor of Philosophy

MAY

1988

Polymer Science and Engineering Department

© Copyright by Michael David Gilbert

All Rights Reserved



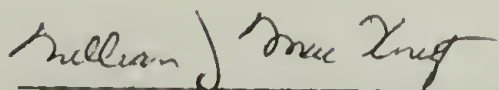
Mechanism and Kinetics of the  
Dicyandiamide Cure of Epoxy Resins

A Dissertation Presented

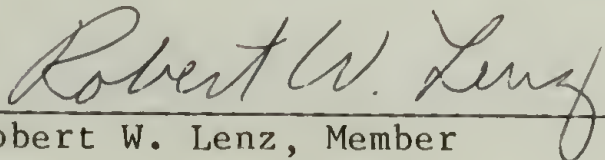
by

Michael D. Gilbert

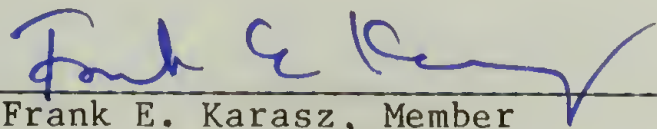
Approved as to style and content by:




William J. MacKnight, Chairman of Committee



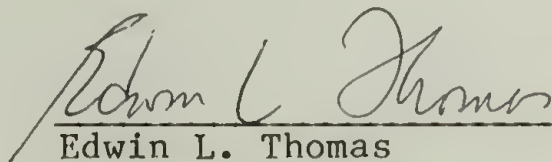
Robert W. Lenz, Member



Frank E. Karasz, Member



Nathan S. Schneider, Consultant



Edwin L. Thomas

Department Head

Department of Polymer Science and Engineering

This Work is Dedicated  
to the Memory of  
Frank Oliver Gilbert,  
Statesman, Orator, Philosopher,  
and my best friend.

## ACKNOWLEDGEMENTS

I would like to express my sincere appreciation to my advisor Professor William MacKnight for his support and guidance throughout the better part of the last decade. I would also like to thank Professors Lenz and Karasz for their time, patience, and the genuine interest they have shown in my work. My deepest gratitude goes to Dr. Nathan Schneider for providing opportunity, direction, motivation, money and a job. I am indebted to my friend and colleague Dr. Walter Zukas for his guidance in conducting this research, and for his help in preparing this manuscript. Further, I'd like to thank Drs. Catherine Byrne and Joseph Bornstein for insightful discussions.

I am especially thankful to my wife, Teri, without whose help this work never would have been completed. I am indebted to her for typing this document, preparing figures, and sacrificing "the best years of her life", during my graduate years.

Finally, thanks goes to David Dunn, for help with HPLC, Dr. James Sloan and Marianne Bachand, for FTIR, Dr. Paul Vouros and Jim Kyranos, for mass spectroscopy, Gretchen Richards and Dr. Lou Carreiro, for NMR, and Mike, Emily, Paul, Donna, Larry, Mark, Glenn, Rosie, Frank, Pete, Bernie, Jennie, Janice, Brian, Caryn, Alex, Jan, Lynn, Kelly, Reggie, Bob, Stan, Jane, Orna, Bob, Gary, Jason, Lisa, Bruce, Dom, Marie, Wenzel, Cheryl, Paul, Don, Bonnie, Linda, Tim, Debra, Donna, Steve, Michael, Amy, Joey, Sean, Christopher and others, too numerous to mention, for technical assistance.



## ABSTRACT

### Mechanism and Kinetics of the Dicyandiamide Cure of Epoxy Resins

May 1988

B.S., Rensselaer Polytechnic Institute

Ph.D. University of Massachusetts

Directed by: Professor William J. MacKnight

The uncatalyzed reaction of a monofunctional epoxide with dicyandiamide (dicy) was used to model the dicy cure of an epoxy resin. Due to the high temperatures required for the uncatalyzed reaction, a novel monoepoxide was synthesized for this purpose. Products formed in the model reaction were isolated by preparative liquid chromatography and were characterized by infrared and nuclear magnetic resonance spectroscopy, mass spectrometry and elemental analysis. Structures were identified and previously unknown reactions were discovered. A reaction mechanism was proposed, which clarified many of the ambiguities reported in the literature.

The rates and extents of formation of the various products were determined using calorimetry and liquid chromatography. The effect of temperature and compositional variation on final product distribution was determined. The isolated intermediates were further reacted with epoxide, allowing the chemical kinetics of the dicy/epoxide reactions to be probed, free of the complicating effects of dicy dissolution and diffusion. Calorimetric and dynamic mechanical techniques were used to

correlate aspects of the dicy/monoepoxide reaction mechanism with the development of network structure in the curing system. Network structure was found to be dependent upon the complex relationship between dicy dissolution, network vitrification and the dicy/epoxide reaction mechanism.

# TABLE OF CONTENTS

	<u>page</u>
ACKNOWLEDGEMENTS.....	v
ABSTRACT.....	vi
LIST OF TABLES.....	xi
LIST OF FIGURES.....	xii
Chapter	
1 INTRODUCTION.....	1
Dicyandiamide Cured Epoxies.....	1
The Structure and Physical Properties of Dicyandiamide.....	3
Epoxy Resins: Reactions and Structure.....	9
Previous Studies of the Dicy/Epoxy Cure Mechanism.....	16
Summary and Goals.....	25
2 THERMAL AND MECHANICAL ANALYSIS OF DICY CURED DGEBA.....	28
Introduction.....	28
Experimental.....	33
Materials.....	33
Dynamic Scanning Calorimetry.....	34
Torsional Braid Analysis.....	34
Results and Discussion.....	35
Dicy/DGEBA: Thermal Analysis.....	35
Isothermal Cures.....	39
Long Time Cures.....	42
Torsional Braid Analysis.....	43
Effect of Dicy Particle Size.....	46
Inhomogeneity and Vitrification.....	51
Summary.....	55
Cyanamide/DGEBA.....	57
3 KINETICS OF A DICY/MONOEPOXIDE REACTION.....	66
Introduction.....	66
Monoepoxide Studies.....	67
High Performance Liquid Chromatography.....	70
Experimental.....	71



Materials.....	71
Sample Preparation.....	72
Sample Analysis.....	73
Results and Discussion.....	74
Properties and Reactivity of MGEBA.....	74
Thermal Analysis of the Dicy/MGEBA Reaction.....	81
HPLC Analysis of the Dicy/MGEBA Reaction.....	84
Chromatographic Peak Identification.....	86
Detector Wavelength and Product Quantification.....	89
Effect of Solvent.....	92
Rates of Reactant Consumption and Product Formation....	95
Extended Reaction Times.....	103
Excess Epoxide.....	104
Base Catalyzed Reaction of Dicy with MGEBA.....	105
Summary.....	107
4 THE MECHANISM OF THE DICY/MGEBA REACTION.....	108
Introduction.....	108
Experimental.....	111
Materials.....	111
Preparatory Liquid Chromatography.....	111
Product Analysis.....	112
Results and Discussion.....	113
Dicy/MGEBA.....	113
Product Isolation.....	113
FTIR Analysis.....	115
Cyanamide/MGEBA.....	121
Product Isolation.....	122
FTIR Analysis.....	124
SEC Analysis.....	129
Further Reactions of Isolated Products.....	129
Less Polar Products.....	134
Model 2-Imino Oxazolidines.....	135
Purification and Identification of Isolated Products...	144
Mass Spectrometry.....	144
Carbon-13 NMR Analysis.....	149
Carbonyl Formation in the Dicy/MGEBA Reaction.....	155
Identification of the Less Polar Products.....	157
Review of Previous Results.....	165

	The Role of Water in the Dicy/Epoxide Reaction.....	167
	Uneluted Materials.....	170
	FTIR Studies of the Dicy/Epoxide Reaction.....	175
	Correlation of Results with Previous IR Studies.....	178
5	THE REACTION OF PRODUCT I WITH EPOXIES.....	183
	Introduction.....	183
	Experimental.....	186
	Results and Discussion.....	187
	Thermal Analysis.....	187
	HPLC Kinetic Analysis.....	192
	Concentrations of Eluting and Uneluting Species....	196
	Relative Rates of Product I and MGEBA Consumption..	200
	Uneluted Material in the Dicy/MGEBA Reaction.....	204
	Size Exclusion Chromatography.....	207
	Compositional Variation.....	209
	Variation of Reaction Temperature.....	210
	Analysis of the Product I/DGEBA Cure by TBA.....	212
	Summary.....	219
6	CONCLUSIONS.....	221
	The Dicy/Epoxide Reaction Mechanism.....	221
	The Mechanism.....	221
	Postulated Identity of the Uneluted Material.....	223
	Crosslinking and Long Term Stability.....	226
	Reaction Kinetics.....	228
	The Inhomogeneous Cure.....	230
	Future Work.....	231
	APPENDIX.....	233
	REFERENCES.....	241

## LIST OF TABLES

I.	Dicyandiamide Bond Lengths by X-ray Scattering.....	5
II.	Physical Properties of Dicyandiamide.....	6
III.	Heat of Reaction vs Dicy/DGEBA Composition.....	38
IV.	T <sub>g</sub> for Milled and Unmilled 1:4 Dicy/DGEBA Cured at 167°C..	53
V.	MS and Elemental Analysis of Isolated Products.....	147
VI.	Heats of Reaction of I/MGEBA and I/DGEBA.....	191
VII.	Tg Midpoint vs Composition for Product I/DGEBA Cure.....	217
VIII.	Times to TBA Gel Point for I/DGEBA Cure (min).....	218



## LIST OF FIGURES

Figure 2-1:	DSC temperature scan of 1:5 dicy/DGEBA at 5°C/min.....	36
Figure 2-2:	Plot of DSC conversion vs composition for uncatalyzed dicy/DGEBA cured at 177°C.....	40
Figure 2-3:	(a) TBA trace of 1:4 dicy/DGEBA isothermally cured at 177°C. (b) TBA temperature scan at 1.5°C/min.....	45
Figure 2-4:	DSC temperature scan of milled and unmilled 1:4 dicy/DGEBA at 5°C/min.....	48
Figure 2-5:	(a) TBA trace of milled 1:4 dicy/DGEBA isothermally cured at 167°C. (b) TBA temperature scan at 1.5°C/min...	49
Figure 2-6:	DSC temperature scan of 1:2 cyanamide/DGEBA at 5°C/min.....	59
Figure 2-7:	DSC temperature scan of neat cyanamide at 5°C/min.....	61
Figure 2-8:	DSC temperature scan of 1:4 2-imino-3-phenyl oxazolidine/DGEBA at 5°C/min.....	62
Figure 2-9:	Plot of DSC conversion vs composition for uncatalyzed cyanamide/DGEBA cured at 107°C.....	64
Figure 3-1:	FTIR spectrum of MGEBA.....	75
Figure 3-2:	DSC temperature scan of 1:4 dicy/MGEBA at 5°C/min.....	76
Figure 3-3:	DSC temperature scan of 2:3 cyanamide/MGEBA at 5°C/min..	79
Figure 3-4:	HPLC chromatogram of 1:6 dicy/MGEBA reacted at 197°C for 30 min; THF/H <sub>2</sub> O = 50-90%, over 40 min, at grad 6, analyzed at 280nm.....	85
Figure 3-5:	HPLC chromatogram of 1:6 dicy/MGEBA reacted at 197°C for 30 min; THF/H <sub>2</sub> O = 50-90%, over 40 min, at grad 6, analyzed at 229nm.....	91
Figure 3-6:	HPLC chromatogram of 1:4 dicy/MGEBA reacted at 197°C for 30 min, Acetonitrile/H <sub>2</sub> O = 50-100%, 10 min, grad 6, analyzed at 214nm.....	93
Figure 3-7:	HPLC chromatogram of 1:2 cyanamide/MGEBA reacted at 127°C for 60 min, Acetonitrile/H <sub>2</sub> O = 50-100%, 10 min, grad 6, analyzed at 214nm.....	94
Figure 3-8:	Products and reactants vs time for 1:4 dicy/MGEBA reacted at 197°C.....	97

Figure 3-9: Products and reactants vs time for 1:6 dicy/MGEBA reacted at 197°C.....	97
Figure 3-10: Products and reactants vs time for 1:4 dicy/MGEBA reacted at 187°C.....	98
Figure 3-11: Products and reactants vs time for 1:6 dicy/MGEBA reacted at 187°C.....	98
Figure 3-12: Products and reactants vs time for 1:4 dicy/MGEBA reacted at 177°C.....	99
Figure 3-13: Products and reactants vs time for 1:6 dicy/MGEBA reacted at 177°C.....	99
Figure 3-14: Products and reactants vs time for 1:4 dicy/MGEBA reacted at 167°C.....	100
Figure 3-15: Products and reactants vs time for 1:6 dicy/MGEBA reacted at 167°C.....	100
Figure 3-16: Dicy consumption vs MGEBA consumption 167°C-197°C.....	101
Figure 3-17: HPLC chromatogram BDMA catalyzed 1:8 dicy/MGEBA reacted at 147°C for 24 min; Acetonitrile/H <sub>2</sub> O= 50-100%, 10 min, grad 6, analyzed at 214nm.....	106
Figure 4-1: HPLC chromatogram of dicy/MGEBA reacted at 187°C for 60 min; THF/H <sub>2</sub> O = 50-90%, over 40 min, at grad 6, analyzed at 229nm.....	114
Figure 4-2: FTIR spectrum of isolated peak C.....	116
Figure 4-3: FTIR spectrum of isolated peak D.....	117
Figure 4-4: FTIR spectrum of isolated peak A.....	119
Figure 4-5: HPLC chromatogram of cyan/MGEBA product mixture; THF/H <sub>2</sub> O = 50-90%, over 40 min, at grad 6, analyzed at 280nm.....	123
Figure 4-6: FTIR spectrum of product I.....	125
Figure 4-7: FTIR spectrum of product II.....	126
Figure 4-8: FTIR spectrum of product III.....	127
Figure 4-9: FTIR spectrum of product IV.....	128
Figure 4-10: Comparison of SEC chromatograms of MGEBA and products I, II, III and IV.....	130

Figure 4-11: HPLC chromatogram of (1:4.5) I/MGEBA reacted at 167°C for 15 min; THF/H <sub>2</sub> O = 50-90%, over 40 min, at grad 6, analyzed at 229nm.....	132
Figure 4-12: HPLC chromatogram of (1:9) product II/MGEBA reacted at 167°C for 120 min; THF/H <sub>2</sub> O = 50-90%, over 40 min, at grad 6, analyzed at 229nm.....	133
Figure 4-13: FTIR spectrum of 2-imino-3-phenyl oxazolidine.....	136
Figure 4-14: HPLC chromatogram of 1:2 2-imino-3-phenyl oxazolidine/DGEBA reacted at 167°C for 120 min; THF/H <sub>2</sub> O = 50-90%, over 40 min, at grad 6, analyzed at 229nm.....	138
Figure 4-15: <sup>1</sup> H NMR spectrum of 2-imino-3-phenyl oxazolidine.....	139
Figure 4-16: <sup>1</sup> H NMR spectrum of product III.....	140
Figure 4-17: FTIR spectrum of synthesized product III.....	142
Figure 4-18: <sup>1</sup> H NMR spectrum of synthesized product III.....	143
Figure 4-19: FABMS spectra of products I, II and III.....	146
Figure 4-20: Mechanism of product III formation.....	148
Figure 4-21: <sup>13</sup> C NMR spectrum of MGEBA.....	150
Figure 4-22: <sup>13</sup> C NMR spectrum of product I.....	151
Figure 4-23: <sup>13</sup> C NMR spectrum of product II.....	153
Figure 4-24: <sup>13</sup> C NMR spectrum of product III.....	154
Figure 4-25: <sup>1</sup> H NMR spectra and structures of products I, II and III.....	156
Figure 4-26: Structure and mechanism of product IV formation.....	158
Figure 4-27: FTIR spectrum of product V.....	160
Figure 4-28: (a) HPLC chromatogram of isolated peaks F and H. (b) HPLC chromatogram of peaks F and H heated at 167°C for 120 min. (c) HPLC chromatogram of F+H/MGEBA reacted at 167°C for 120 min.....	163
Figure 4-29: Comparison of SEC chromatograms of G+H heated neat and reacted with MGEBA.....	164
Figure 4-30: FTIR spectrum of uneluted material.....	172
Figure 4-31: FTIR spectrum of product II heated to 167°C for 120 min.....	174



Figure 4-32:	FTIR of unresolved product mixture formed by reacting 1:6 dicy/MGEBA at 190°C for 1 hour.....	176
Figure 4-33:	FTIR of unresolved product mixture formed by reacting BDMA catalyzed 1:6 dicy/MGEBA at 100°C for 1 hour.....	177
Figure 5-1:	DSC temperature scan of 1:2 product I/MGEBA at 5°C/min.....	188
Figure 5-2:	DSC temperature scan of 1:4.5 product I/DGEBA at 5°C/min.....	190
Figure 5-3:	HPLC chromatogram of product 1:4.5 I/MGEBA reacted at 127°C for 121 min. THF/H <sub>2</sub> O = 50-90%, over 40 min, at grad 6, analyzed at 229nm.....	194
Figure 5-4:	Products and Reactants vs time 1:4.5 product I/MGEBA reacted at 167°C.....	195
Figure 5-5:	Products and Reactants vs time 1:4.5 product I/MGEBA reacted at 147°C.....	197
Figure 5-6:	Products and Reactants vs time 1:4.5 product I/MGEBA reacted at 127°C.....	198
Figure 5-7:	Formation of eluted and uneluted materials vs MGEBA consumption for (1:4.5) product I/MGEBA at 127°C-167°C..	201
Figure 5-8:	Consumption of product I vs consumption of MGEBA consumption for (1:4.5) product I/MGEBA at 127°C-167°C..	203
Figure 5-9:	Product and reactant concentration vs time for 1:6 dicy/MGEBA reacted at 197°C.....	205
Figure 5-10:	(a) Formation of uneluted materials vs MGEBA consumption for dicy/MGEBA. (b) Formation of eluted materials vs MGEBA consumption for dicy/MGEBA. Temp. = 167-197°C.....	206
Figure 5-11:	Comparison of SEC chromatograms of product I/MGEBA reacted at 167°C for (a) 5 min, (b) 10 min, (c) 20 min, (d) 30 min.....	208
Figure 5-12:	(a) SEC chromatogram of 1:1 product I/MGEBA reacted at 167°C for 60 min. (b) SEC chromatogram of 1:4.5 product I/MGEBA reacted at 167°C for 60min.....	211
Figure 5-13:	(a) TBA trace of 1:5 product I/DGEBA cured at 127°C. (b) TBA temperature scan at 1.5°C/min.....	213
Figure 5-14:	(a) TBA trace of 1:7 product I/DGEBA cured at 147°C. (b) TBA temperature scan at 1.5°C/min.....	215
Figure 6-1:	Dicy/MGEBA reaction scheme.....	222

# CHAPTER 1

## INTRODUCTION

### Dicyandiamide Cured Epoxies

Dicyandiamide (dicy) has long been used as a latent hardener in epoxy resin formulations, providing many unique and advantageous properties [1]. Dicy/epoxy resin mixtures have a shelf life of a year or more at room temperature and cure rapidly at elevated temperatures, producing relatively high glass transition temperature ( $T_g$ ) materials, which have good mechanical properties and excellent resistance to attack by acids, bases, and many of the usual epoxy solvents. The cured resin is reasonably resistant to water, and forms strong bonds to copper, a material to which other epoxies do not readily adhere. Further, dicy is soluble in water and can be used in water-borne epoxy formulations, which are finding increased use in an effort to reduce atmospheric emissions of organic solvents in manufacturing [2]. Finally, dicy is inexpensive. While other curing agents can be tailored to have properties as good as or superior to those of dicy, none can do so more cheaply. Due to their low cost and favorable properties, dicy/epoxy mixtures are widely used in the formulation of powder coatings, single component structural adhesives, and in the manufacture of printed circuit boards.

Although dicy is one of the most important latent curing agents in current use, it is the least understood [1] due to the complexity of the reaction mechanism and the inhomogeneous nature of the dicy/epoxy cure. Consequently, there has been some difficulty in realizing the full

potential of this unique thermosetting system. Further, while the latent nature of dicy can be related in part to its high melting point and low solubility in the epoxy resin [3], the resultant inhomogeneity of the curing system leads to severe difficulties in the attainment of uniform properties. Dicy particles can segregate in the epoxy mixture due to resin flow, resulting in local stoichiometric imbalances and producing materials with poor mechanical properties [4]. In addition, many of the larger sized dicy particles can remain unreacted in the fully cured material. These particles promote water sorption, resulting in hydrolytic degradation and a reduction in the electrical resistivity of the cured epoxy resin. In order to insure a uniform product, it is necessary to enhance the solubility and dispersion of dicy in the resin. This requires that the dicy particles be intensively milled, increasing the expense of the curing agent.

Additional problems exist, which greatly limit the use of dicy/epoxy formulations. Due to the nature of the cure mechanism, the highly exothermic dicy/epoxide reactions rapidly accelerate at cure temperature. In large samples or at high cure temperatures, the resulting heat build up leads to the explosive evolution of ammonia and other gases and charring of the resin. Thus, dicy/epoxy formulations can only be used in thin sections from which heat can be easily dissipated. Temperatures in excess of  $150^{\circ}\text{C}$  are required to fully cure the uncatalyzed mixtures. Since these temperatures are too high for many of the applications of dicy/epoxy formulations, it has been necessary to lower the cure temperature by the addition of an accelerator to the resin mixture. Tertiary amines have been used for this purpose, but only at the expense of room



temperature latency. Substituted phenyl ureas, such as Monuron, have also been used. It has been shown that these compounds react with epoxide to yield dimethyl amine, which then accelerates the dicy/epoxy reaction [5,6]. While these substituted ureas are themselves latent curing agents, their addition to the dicy/epoxy mixture decreases the latency period of this system to 3-6 weeks. Thus, it is not possible to accelerate the dicy/epoxy cure reaction without a significant reduction in the shelf life of this system. Further, these formulations can not be readily B-staged, since even a 1% reaction results in the loss of room temperature latency [4,3].

#### The Structure and Physical Properties of Dicyandiamide

In the industrial preparation of dicyandiamide, hot calcium carbide is reacted directly with nitrogen to form the calcium salt of cyanamide [7]. Carbon dioxide and water are then used to liberate the free cyanamide. The cyanamide is converted to dicy via a controlled polymerization under slightly basic conditions. This industrially important process was at one time competitive with the Haber process as a means of nitrogen fixation. The low cost of the starting materials, the ease of synthesis and handling, and the stability of dicy all contribute to the economics favoring the continued use of this curing agent.

The structure of dicy has been the object of some controversy. The two isomeric structures shown below have been widely used in the literature to explain the various reactions of dicy. Since the amine proton alpha to the cyano group would be acidic enough to protonate the basic



imide nitrogen [8], the existence of structure B is improbable.

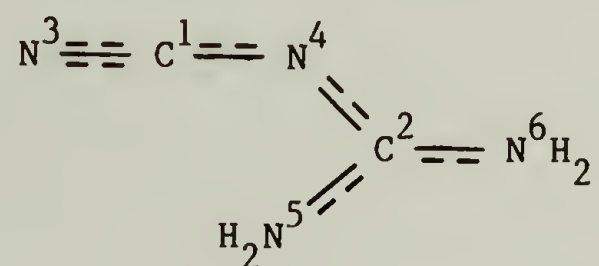
Further, structure A is favored by proton nuclear magnetic resonance



( $^1\text{H}$  NMR), which reveals a single amine proton peak at 6.078 ppm in the spectrum of dicy, supporting the equivalence of the amine protons [9]. In addition, bond lengths, measured by X-ray diffraction and listed in Table I [9], reveal that nitrogen  $\text{N}^4$  is attached to its neighboring carbon atoms by two pseudo double bonds, again favoring the unprotonated structure A. However, while the physical evidence supports structure A, the incorrect structure B has persisted in the literature and was used most notably in the mechanism proposed by Zahir and shown in a latter section of this chapter.

The dimerization reaction of cyanamide to form dicy liberates about 88 kJ of heat per mole of dicy, as determined by the heat of combustion of the two compounds [7]. It is believed that most of this energy difference is due to the added resonance stabilization of the dicy molecule. This conclusion is corroborated by the bond lengths shown in Table I, which also indicate a large extent resonance stabilization. The several resonance structures which can be drawn for the dicy molecule based on these bond lengths, reveal a high electron density at the cyano nitrogen, while the amine functionalities have a low electron density. This view is supported by the rather high dipole moment of  $8.16 \times 10^{-18}$  D, measured for this compound [10], and accounts for the

Table I  
Dicyandiamide Bond Lengths by X-ray Scattering [9]



Dicyandiamide		Model Compound	
$\text{C}^2 \text{N}^5$	1.35 A	C-N	1.47 A ( $\text{CH}_3\text{NH}_2$ )
$\text{C}^2 \text{N}^6$	1.35 A		
$\text{C}^2 \text{N}^4$	1.28 A	C=N	1.29 A ( $\text{CH}_3\text{C=NOH}$ ) <sub>2</sub>
$\text{C}^1 \text{N}^4$	1.28 A		
$\text{C}^1 \text{N}^3$	1.22 A	$\text{C}\equiv\text{N}$	1.16 A ( $\text{CH}_3\text{CN}$ )

Table II  
Physical Properties of Dicyandiamide [10]

---

---

Molecular Weight	84.08 g/mole
Melting Point	208-212°C
Specific Gravity (14°C)	1.404-1.405 g/cm <sup>3</sup>
Dipole Moment	8.16x10 <sup>-18</sup> D
Acid Dissociation Constant	6x10 <sup>-15</sup>
Basic Dissociation Constant	3x10 <sup>-15</sup>

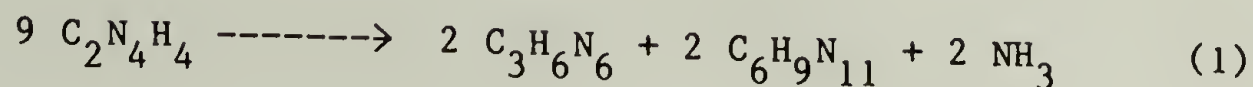
relatively high melting point of dicy. These values are listed in Table II along with other pertinent data. Dicy is an amphoteric compound having the weakly acidic and basic dissociation constants listed in Table II. It is capable of forming salts with both acids and bases only under anhydrous conditions, as water will decompose these salts. Due to its highly polar nature, dicy is soluble in water, liquid ammonia, dimethyl formamide, and alcohols. However, it is relatively insoluble in ether, benzene, and other less polar solvents, including liquid epoxy resins.

There are several factors contributing to dicy's behavior as a latent curing agent for epoxies. The most important appears to be dicy's high melting point and low solubility in the epoxy resin. This is supplemented by the neutral, non-nucleophilic nature of the dicy amine groups, which is imparted by the resonance stabilization of the molecule. However, under the right conditions, dicy can be an extremely reactive molecule and some of the relevant reactions of dicy are presented below.

While commercial dicy has been found to have a high moisture content [11], it is not hygroscopic, and is stable in air up to 170°C. However, upon melting dicy is converted into melamine along with ammonia and higher molecular weight triazines. Yields of 50% melamine are obtained in this reaction, shown in equation (1) [10]. Yields as high as 90% melamine have been obtained by heating dicy in methanol saturated with ammonia at 135-140°C for 4-6 hours. Heating dicy in certain organic amines also produces melamine, with the highest yields obtained by

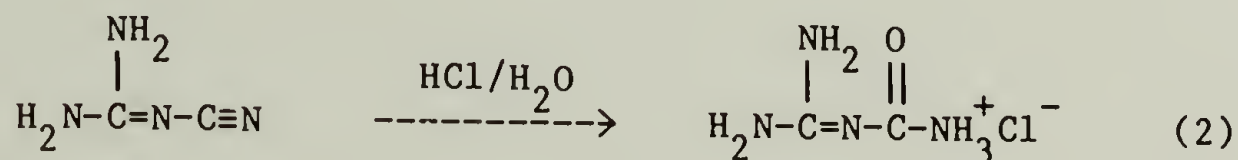


heating dicy in ethanol amine. This reaction may have some importance

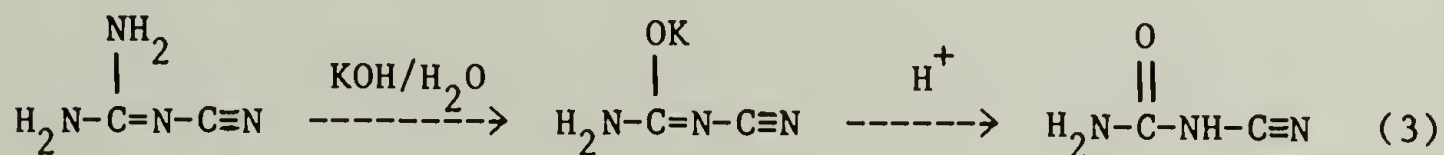


in the dicy/epoxy cure, since amine/epoxide products are essentially substituted ethanol amines.

Although neutral aqueous solutions of dicy are stable for many days at 80°C, the addition of acid or base will result in rapid hydrolysis of the molecule [7]. Acid hydrolysis quantitatively yields a guanyl urea salt as is shown in equation (2). Guanyl urea is a strong base, which



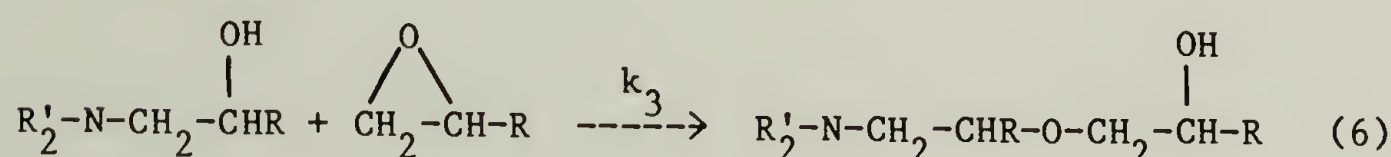
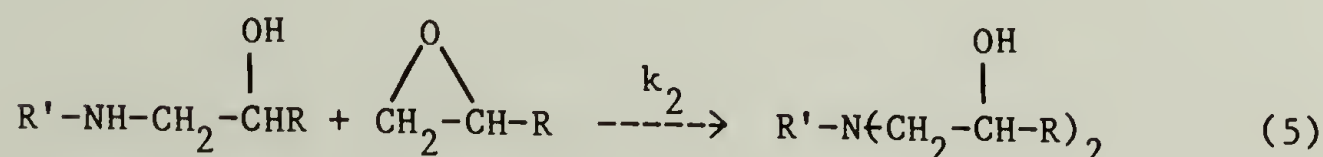
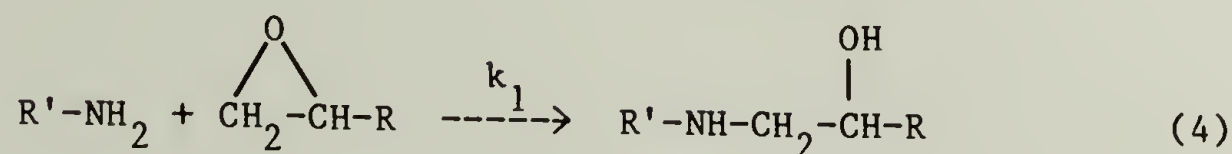
can be further hydrolyzed in the presence of acid to yield a guanidine salt. This is an industrially important method for the synthesis of guanidine derivatives. Hydrolysis of dicy in the presence of an inorganic base, shown in equation (3), results in the formation of a cyano



urea salt with a yield of about 50%. While the salt is stable, the free cyano urea is a highly reactive strong acid, which undergoes decomposition at 93°C. The reactions shown in equations (2) and (3), illustrate the prime mechanisms of hydroxyl attack on the dicy molecule. Each of



to the oxirane functionality. This last reaction, also known as etherification, is generally reported to be much slower than amine addition to



epoxide [12,13,14]. It has been found to occur to a significant extent in some amine cured mixtures containing excess epoxide. Further, it can be catalyzed by the addition of a tertiary amine, such as benzyl dimethyl amine (BDMA), to the reaction mixture, making it competitive in some cases with amine addition [15]. Although tertiary amines are generated by the reaction shown in equation (5), they are relatively ineffective as catalysts due to steric hindrance. A fourth reaction, the homopolymerization of the oxirane groups, has been reported to occur to some extent in the presence of a Lewis base such as BDMA [12]. While the reactions depicted in equations (4)-(6) also occur in the di-cure of epoxy resins, several additional reactions have been reported for this system, and these will be discussed later in this chapter.

It has been found that amine/epoxide addition will not occur without the presence of a proton donor, such as water, and that the rate of reaction is proportional to the concentration of the proton donating



species. It has been proposed that this proton donor is hydrogen bonded to both the amine and oxirane, thus aiding in proton exchange during the amine/epoxide reaction [16]. While some proton donating species are fortuitously present in commercial epoxy resins, the hydroxyl groups formed by the amine/epoxide reaction also act to catalyze the reaction. Thus, the rate of reaction increases with increasing extent of conversion, and this process is called autoacceleration.

The reaction of an epoxy resin such as DGEBA with a typical diamine leads to the formation of a three dimensional crosslinked network. This insoluble and intractable network is, in effect, a single molecule of virtually infinite molecular weight. The instant at which this intractable material or gel is first formed in the reaction mixture is called the gel point. Based on the functionality of the reactants and the amine to epoxy ratio ( $a/e$ ) of the mixture, the extent of reaction at gelation can be estimated using the Carothers [17] and Flory-Stockmayer [17] equations. Assuming that etherification and homopolymerization are negligible, DGEBA can be considered to be difunctional and the diamine, tetrafunctional. A stoichiometric mixture of these materials would thus contain two moles of DGEBA per mole of diamine. In this case, a general form of the Carother's equation, shown in (7), predicts an extent of reaction of 75% at the gel point, while the applicable form of the Flory-Stockmayer equation, shown in (8), predicts a 58% extent of reaction at gelation. In these equations,  $p_c$  is the extent of reaction of the amine protons,  $r$  is the ratio of the deficient reactant to that in excess, and  $f_A$  is the functionality of the amine. Since the Carothers equation predicts the extent of reaction at which the number average



degree of polymerization becomes infinite, the value predicted is usually too large, because many molecules reach the gel point before the

$$p_c = 1/2r + 1/f_A \quad (7)$$

$$p_c = 1/[r(f_E-1)(f_A-1)]^{1/2} \quad (8)$$

average does. The Flory-Stockmayer equation, on the other hand, predicts the extent of reaction at which the molecular weight of the largest molecule first becomes infinite and is therefore more correct. Due to cyclization and the unequal reactivities of the functional groups, experimental values usually fall somewhere between these two predictions. Should etherification and/or homopolymerization take place, then the effective functionality of the system would be higher and consequently gelation would occur at a much lower extent of amine conversion.

In the case of amine to epoxy addition, the rate of primary addition to epoxide is generally faster than that of secondary amine addition due to steric effects. Reactivity ratios ( $k_2/k_1$ ) have been determined for a number of model systems [18,19,20,21,22], and these appear to be dependent on the structure of the amine. As the value of  $k_2/k_1$  decreases, the net effect is to favor the formation of linear polymer in the early stages of the reaction with crosslinking occurring late in the reaction. As Bell [13] has pointed out, for stoichiometric mixtures the final structure of the crosslinked resin would not be changed, although the gel point would be shifted to higher extents of reaction. However, for

off-stoichiometric mixtures, a lower reactivity ratio would narrow the range of compositions within which gelation can occur. By determining this range for mixtures of these amines with DGEBA and comparing the results with those calculated from the Flory-Stockmayer equation, Lunak et al. [14] was able to calculate the reactivity ratios for several diamines. In this way,  $k_2/k_1$  values of 0.6-0.7 and 0.35-0.45 were calculated for alkyl and aryl amine addition to epoxide, respectively.

With continued reaction beyond the gel point, the gel content of the curing system is rapidly increased at the expense of the still soluble material or sol. The crosslink density of the material then continues to increase until the reaction is complete. If the temperature of the cure ( $T_{\text{cure}}$ ) is much lower than the ultimate  $T_g$  of the fully cured system, then the process of vitrification will stop the reaction and limit conversion. In order to complete the cure it is then necessary to increase the temperature to above the ultimate  $T_g$ . Both the modulus and the glass transition temperature ( $T_g$ ) of the material are proportionately increased by an increase in the crosslink density [23,13,24]. Thus, the physical properties of the material are dependent upon the final crosslinked density of the cured resin, which is again determined by the reactivity ratios of the component reactions, the stoichiometry of the mixture and the extent of reaction.

As previously discussed, etherification and homopolymerization will occur in mixtures containing excess epoxide or in mixtures catalyzed by the addition of a tertiary amine. Depending upon the relative extent to which these reactions contribute to epoxide consumption, both the stoi-

chiometry of the mixture and the effective functionality of the diepoxide will be altered. This would then change the onset of gelation, as well as the crosslink density and chemical structure of the crosslinks, affecting the final properties of the cured resin.

The temperature dependence of the rate constants for each of the reactions comprising an amine/epoxy cure can be fit to an Arrhenius expression, an example of which is shown in equation (9). In this expression,  $k$  is the reaction rate constant,  $T$  is the temperature, and

$$k = A \cdot \exp(-E_a/RT) \quad (9)$$

$E_a$  is the activation energy. For a cure composed of several competing reactions, an increase in the cure temperature will result in an increase in the relative contributions made by the reactions with higher activation energies. Since the structure of the crosslinked system is dependent upon the relative rates of the component reactions, a variation in the cure temperature could influence the final properties of the material. If an increase in temperature results in higher activation energy reactions becoming dominant in the cure, then the overall activation energy of the cure will increase. Further, should the difference be great, this increase in temperature will appear to change the mechanism of the cure.

Previous studies have indicated that the  $k_2/k_1$  reactivity ratio is independent of the temperature [19], indicating an equivalent energy of activation for primary and secondary amine addition to epoxide. How-



ever, the relative rates of etherification and homopolymerization appear to increase with decreasing temperature [25], apparently indicating a lower energy of activation for these two reactions compared to amine/epoxide addition. The dicy/epoxy cure consists of several component reactions in addition to those previously described as occurring in a typical amine/epoxy cure. As discussed below, these additional reactions appear to have different energies of activation. Thus, variations in the cure temperature may play an important role in determining the structure of the dicy cured resin.

Other factors which might influence the reactivity ratios of the component reactions in an amine/epoxy cure are autoacceleration and diffusion control of the reaction, caused by the onset of vitrification. Since autoacceleration activates the oxirane, it should have an equivalent effect on all addition reactions, and it has been shown that  $k_2/k_1$  values are apparently not affected by conversion [26,27,23]. Although diffusion control has been similarly found to have little effect on  $k_2/k_1$  values in a typical amine cured epoxy [22], its effect on the complex series of reactions in the dicy cure mechanism could be more pronounced. Finally, although the evidence is ambiguous [28], amine/epoxy cures have been reported to be inhomogeneous, resulting in the formation of regions of varying crosslink density in the cured material [29,30,31,32]. It has been postulated that these inhomogeneities are caused by thermodynamically controlled segregation. However, Bell [33] has shown that incomplete mixing of the reactants may be responsible for these observations. Due to the initial insolubility of dicy in the epoxy resin, it is likely that regions of varied structure are formed



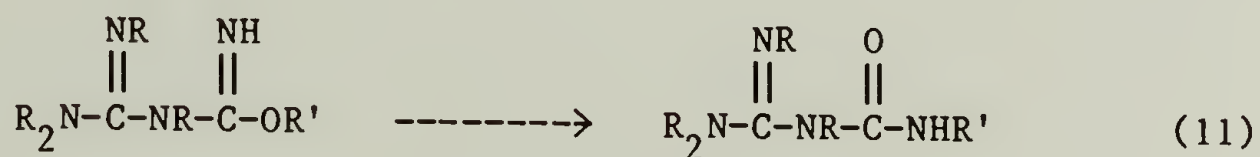
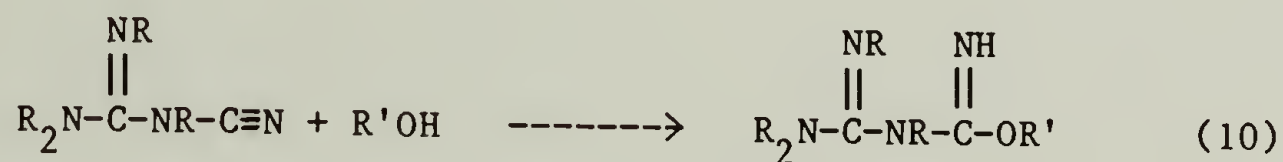
by this inherently inhomogeneous cure. These effects will be further discussed in the following section.

#### Previous Studies of the Dicy/Epoxy Cure Mechanism

Levine [34] was first to examine the dicy/epoxy cure mechanism in a commercial epoxy formulation. Using infrared (IR) spectroscopy, he was able to follow the disappearance of the oxirane absorbance band at  $915\text{ cm}^{-1}$ , and the increase in hydroxyl absorbance at  $3440\text{ cm}^{-1}$  anticipated for a normal amine/epoxide reaction. However, he also observed the appearance of several new absorbance bands at 1740, 1680, and  $1640\text{ cm}^{-1}$ , in the carbonyl and imide regions of the spectra. While he could tentatively assign structures to these absorbance bands, a mechanism for their formation could not be derived without encountering anomalies. Particularly troubling was the observed behavior of the doublet of cyano absorbance bands at 2144 and  $2188\text{ cm}^{-1}$ , in which the former appeared to disappear at a much faster rate than did the latter, while the absorbance band at  $1740\text{ cm}^{-1}$  continued to grow steadily until the end of the reaction.

In order to avoid the difficulties encountered in the structural analysis of a crosslinking system, Saunders et al. [35] investigated the BDMA catalyzed reaction of dicy with phenyl glycidyl ether (PGE) as a model for the dicy/epoxy cure. With this reaction, he was able to obtain a soluble product mixture, which could be readily characterized with  $^1\text{H}$  NMR and IR spectroscopy. By periodically analyzing aliquots from a curing mixture, Saunders was able to observe a two stage reac-

tion. The first stage, which took place at 90°C, appeared to result in the complete consumption of the epoxide via amine, imine and hydroxyl addition. The second stage of the reaction occurred at higher temperatures, after consumption of the epoxide was complete. IR analysis of the product mixture during this stage of the reaction revealed a decrease in the cyano absorbance band at 2180 cm<sup>-1</sup> and the growth of a carbonyl band at 1740 cm<sup>-1</sup>. Analysis of these same aliquots by <sup>1</sup>H NMR revealed a reduction in hydroxyl protons and a simultaneous increase in guanyl urea protons. To account for these observations, Saunders proposed a reaction scheme, in which hydroxyl groups, generated by the



amine/epoxide reaction, add to the cyano groups of the substituted dicy molecules to form guanyl esters, as shown in equation (10). These esters subsequently rearrange to form a guanyl ureas, as shown in equation (11). This proposed mechanism is akin to the acid catalyzed hydrolysis of dicy, previously shown in equation (2). Mechanical test data and solvent swelling studies indicated that the crosslink density of a dicy cured commercial epoxy was increased during this second stage. Saunders, therefore concluded that the reaction shown in equation (10), was an intermolecular addition, as opposed to an intramolecular cyclization. Further, hydroxyl addition appeared to be an important late-stage contributor to the crosslink structure of the cured resin.

Eyerer [4] used IR to follow the catalyzed cure of a commercial DGEBA type resin, and correlated the results with measurements of the microhardness, tensile strength and electrical conductivity of the curing sample. In this study, the cyano absorbance at  $2174\text{cm}^{-1}$  was observed to increase to a maximum and then decrease in intensity. Maximum absorbance was reached just prior to completion of the oxirane reactions. Again the appearance of a carbonyl band was observed, which increased steadily long after oxirane consumption was complete. Further, a large increase in tensile strength and a decrease in the electrical resistance of the cured material were observed to occur simultaneously and at a linear rate in this later stage of the cure. Eyerer believed these changes were due to the hydroxyl addition reactions proposed by Saunders. However, while Eyerer's results were in general agreement with the two-stage mechanism proposed by Saunders, additional complications were revealed.

Using a horizontally placed optical microscope to follow a BDMA catalyzed dicy cure of DGEBA, Eyerer observed the sedimentation of dicy crystals, forming a layer of dicy crystals at the bottom of the sample. This sedimentation was apparently caused by the higher specific gravity of the dicy crystals compared to the resin ( $1.404$  vs.  $1.15\text{ g/cm}^3$ ). Although the sedimentation occurred prior to substantial reaction of the epoxy, the top of the sample, opposite to the dicy layer was substantially crosslinked by the end of the reaction. Eyerer thus postulated that the dicy slowly diffused from the sedimentary layer into the resin during cure. In order to confirm this, microhardness tests were performed on a series of partially cured samples of varying thickness. It



was found that during the cure a gradient of crosslink densities existed across the sample, with the highest density near the dicy layer. With increasing cure time, the hardness gradually increased over the entire sample. Thus, dicy diffusion appeared to be the rate controlling step.

Sacher [36] used differential scanning calorimetry (DSC) to follow the uncatalyzed dicy cure of DGEBA at temperatures of  $170^{\circ}$  to  $220^{\circ}\text{C}$ . Although the dicy crystals initially appeared to dissolve in the resin, particles were subsequently observed to precipitate from the resin. Using IR to analyze the sedimentary layer, Sacher identified these particles as melamine and proposed that the dicy/epoxide products were in fact melamine derivatives. In addition, Sacher discovered that both the rate and energy of activation of the dicy/epoxy cure increased with decreasing particle size. In a similar study, Muroi et al. [37] found that the rate of the BDMA catalyzed dicy cure of DGEBA was also increased by decreasing the dicy particle size. Further, these authors proposed that the fast rate of reaction compared with diffusion resulted in the formation of shells of crosslinked resin around the dicy particles through which the dicy was forced to diffuse. Thus, the rate of the dicy/epoxy cure appeared to be controlled both by competing chemical reactions and by dicy diffusion.

As was discussed in the previous section of this chapter, an increase in temperature will increase the relative rates of those processes with higher energies of activation, thus resulting in a change in the overall activation energy and apparent mechanism of the cure. Such a change was observed by Eyerer between  $90^{\circ}$  and  $112^{\circ}\text{C}$ . However, it



was not readily apparent whether this change was due to a chemical reaction or dicy diffusion. A similar apparent change in mechanism with temperature was reported by Hagnauer et al. [38] for a dicy cured commercial epoxy accelerated with Monuron. Samples of this resin were partially cured, the sol was extracted with THF, and the percent gel content was measured. Analysis of the sol by high performance liquid chromatography (HPLC) revealed that, for identical amounts of gel, twice as many dicy molecules were consumed per epoxide molecule at 130°C than at 90°C. Further, while isothermal DSC revealed an overall activation energy of 55 kJoule/mole for the cure at 90° to 100°C, cures conducted at 120° to 130°C were found to have an overall activation energy of 147 kJ/mole. In addition, the HPLC and DSC results indicated that the extent of epoxide reaction at the onset of gelation increased with increasing temperatures. Again it was difficult to ascertain whether this mechanism change indicated a shift in the relative rates of the chemical reactions or was simply a manifestation of dicy dissolution and diffusion kinetics.

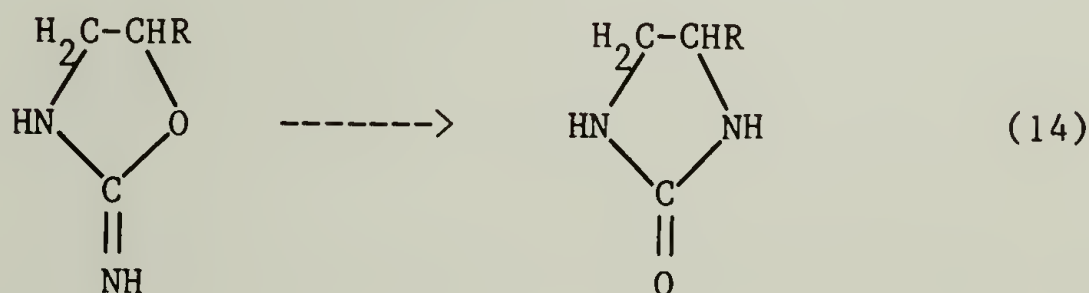
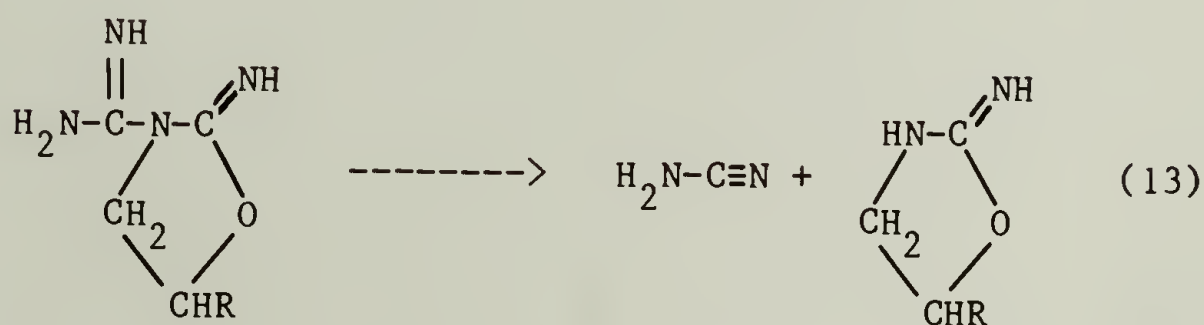
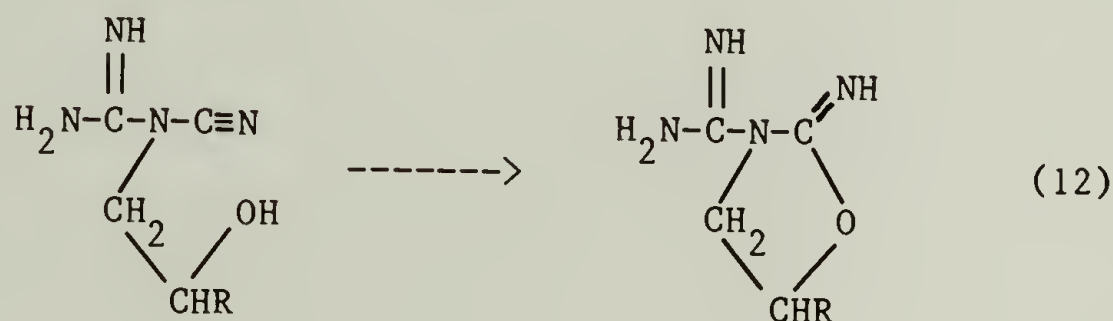
Schneider et al. [39] followed the cures of two commercial epoxy resins having different amine/epoxy (a/e) ratios, using DSC and torsional braid analysis (TBA). Arrhenius plots constructed from the isothermal DSC data indicated that the overall activation energies for the cures of both resins remained constant at 80-85 kJ/mole, over a broad temperature range. Thus, no apparent differences in the activation energies of the various component reactions could be discerned. However, the isothermal gel points determined by TBA were found to occur at extents of reaction far below those predicted by the Flory-Stockmayer

theory for a tetrafunctional amine. This may have been caused by the extra crosslink density contributed by Monuron and Diuron catalyzed homopolymerization. However, it was also possible that these low gel point extents of reaction were due to stoichiometric imbalances inherent in the dicy/epoxy cure. As proposed by Eyerer and Muroi, these imbalances could have led to the preferential crosslinking of the resin adjacent to the dicy crystals, in the early stages of the cure.

Recently, several investigators have conducted a more rigorous examination into the chemical mechanism of the dicy/epoxy cure. Among these, a model compound study by Zahir [40] was the first attempt to identify specific products of the dicy/epoxide reaction. Based on the results of this study, Zahir proposed a mechanism which is radically different from those assumed in the earlier studies and which indicates the true complexity of the dicy/epoxide reaction. Many of the subsequent studies by other investigators have been interpreted in terms of this mechanism, and the work presented in this manuscript was, in a large part, an effort to confirm and expound upon the Zahir mechanism, as described below.

Similar to the work of Saunders, Zahir obtained soluble product mixtures from the BDMA catalyzed reactions of PGE with both dicy and cyanamide, the monomeric form of dicy. Preparative size exclusion chromatography (PSEC) was used to separate the reaction mixtures into fractions of equivalent molecular size in order to facilitate product analysis. The resulting chromatographs revealed that cyanamide and dicy formed identical products in their reactions with epoxide. Using mass

spectroscopy (MS), Fourier Transform Infrared Spectroscopy (FTIR), and  $^{13}\text{C}$  NMR, Zahir identified these products as alkylated cyanamides and 2-imino oxazolidines. A mechanism was proposed in which the initial products of the dicy/epoxide reaction undergo intramolecular additions of hydroxyl to the dicy cyano group, as shown in equation (12). The cyclized substituted dicy then decomposes to form cyanamide and the 2-imino oxazolidine, as shown in equation (13). Zahir reported the formation of a titratable base during this stage of the reaction, thus supporting the formation of the highly basic 2-imino oxazolidine. This oxazolidine was thought to rearrange at a much slower rate, resulting in the formation of a cyclic urea, as shown in equation (14). The rate



controlling step in this mechanism appeared to be the initial dicy/epoxide reaction, while the cyclization reaction depicted in equation



(13) was thought to be relatively rapid. The cyclic products shown in this reaction scheme are capable of further addition of epoxide via the imino functionality and were thus believed to be trifunctional. Additional crosslinking was found to occur via the BDMA catalyzed etherification reactions.

More recently, Davidson [41] used the spectral subtractive capabilities of FTIR to study the uncatalyzed dicy cure of DGEBA. With this technique it was possible to quantify the amounts of dissolved and undissolved dicy in the reaction mixture at any time during cure. Although the dicy particle size was reduced by milling to diameters of less than 5 microns, spectra of the curing mixture at 140°C in some cases revealed that the dissolved dicy reacted faster than the remaining crystalline dicy could dissolve. The product absorbance bands which appeared in these spectra were generally similar to those reported for the catalyzed dicy/epoxide reactions [34,35,4,40] and could be interpreted in terms of the Zahir mechanism. Studies of mixtures with different compositions and at different cure temperatures indicated that, while the series of reactions remained the same, the extent to which each reaction occurred was significantly affected by the cure temperature.

Lin et al. [42] used FTIR to study the BDMA catalyzed dicy cure of DGEBA and confirmed a temperature dependence for the relative rates of the component reactions comprising the catalyzed cure mechanism. For cures conducted at 100°C, the spectra appeared to show a synchronous increase in the intensities of the imide and cyano absorbance bands during epoxide consumption. This synchronous increase was attributed to



the formation of alkylated dicy species. At cure temperatures of 140° to 160°C, the spectra revealed a more rapid growth in the intensity of the imide absorbance band compared to the growth of the cyano absorbance. This was interpreted as an indication of the formation of Zahir structures. Following consumption of the epoxy, the slow disappearance of cyano and imide groups was seen in the spectra of both the high and low temperature cures. Further, the steady growth of a carbonyl absorbance band at 1740 cm<sup>-1</sup> was seen at this time. Lin concluded that the cyano/hydroxyl addition reaction proposed by Zahir was favored at high temperatures, indicating a higher energy of activation for this reaction compared to amine/epoxy addition. The Lin study also indicated that etherification was favored at lower temperatures, and that the cyano/hydroxyl reaction appeared to be suppressed in mixtures with lower a/e ratios.

A study of the dicy cure by Galy et al. [43] revealed that the relationship between tertiary amine catalyzed etherification and the amine/epoxide reaction was complex. The rate of etherification was found to be proportional not only to the BDMA concentration, but also to the concentration of the hydroxyl groups generated by the amine/epoxide reaction. Therefore, the rate of etherification was believed to increase with the extent of amine conversion. Since etherification consumes the  $\beta$ -amino hydroxyl groups of the substituted dicy molecules, it is in direct competition with the cyclization reaction proposed by Zahir. Thus, an increase in the rate etherification, as caused by a decrease the cure temperature or an increase the concentration of tertiary amine, was reported to limit the extent of intramolecular hydroxyl

addition and subsequent dicy dissociation. Under these conditions, dicy would appear to act as a tetrafunctional amine.

In a further study by Galy et al. [44], preparative HPLC was used to isolate products from the BDMA catalyzed reaction of dicy with PGE. The products were analyzed by the techniques of FTIR, SEC, and  $^1\text{H}$  NMR and were identified as alkylated dicy molecules, contrary to the results of Zahir. Further, the primary products of the reaction appeared to be disubstituted dicy molecules from which oligomeric polyether chains extended. Thus, the rate of hydroxyl addition to the epoxide appeared to be much faster than secondary amine addition. Imide bonds appeared to be formed by the direct addition of the cyano group to an epoxide. However, products from this reaction appeared to be only minor components of the final mixture, resulting in only a partial disappearance of the cyano groups. HPLC chromatograms also revealed vast differences in the catalyzed and uncatalyzed product mixtures. A further discussion of the results of this study is presented in chapter 3.

### Summary and Goals

Based on the combined evidence presented in the literature, differences can be expected between the catalyzed and uncatalyzed dicy cures of epoxy resins. In the case of the catalyzed cure, etherification, as shown in equation (6), is competitive with the amine/epoxide additions reactions, shown in equations (4) and (5). Since these reactions have different energies of activation, their relative rates are controlled by the temperature of the cure, as well as the composition of the reaction

mixture. Further, a complex relationship exists between these reactions. Although etherification is competitive with amine/epoxide addition, its rate appears to be proportional to the concentration of amine/epoxide addition products. In addition, the relative contribution of each of these reactions to the cure is further controlled by the rate of dicy dissolution and diffusion, which in turn is dependent upon dicy particle size and the kinetics governing these two processes. Finally, since the products of the dicy/epoxy reaction might enhance the rate of dicy dissolution, this interrelationship is further complicated.

Two other types of reactions have been reported for the dicy/epoxy cure mechanism. These are the apparent reaction of the dicy cyano group with the generated hydroxyl functionalities, as shown in equations (10) and (12), and the structural rearrangement of the products formed by this reaction, as shown in equations (11) and (14). These reactions appear to have different energies of activation than those of the epoxy addition reactions and would, therefore, be favored by higher cure temperatures. Further, due to their dependence on hydroxyl group concentration, these reactions appear to be directly competitive with etherification and/or homopolymerization reactions. According to the Zahir mechanism, these reactions will result in a cleavage of the dicy molecule, dramatically changing the functionality and stoichiometry of the system and altering the chemical structure of the crosslink junctions. Thus, both an increase the cure temperature or a decrease in the amount of added tertiary amine would be expected to radically alter the apparent mechanism of the cure reaction.



The present study was premised on the assumption that the complex mechanism proposed by Zahir for the dicy/epoxy cure was correct. An attempt was made to measure rate of the intramolecular hydroxyl addition and dicy dissociation relative to amine/epoxide addition. In the initial study, presented in Chapter 2, the cure of a simplified cross-linking system was examined. Reactions were run without a catalyst, in order to limit the competitive process of etherification. By determining the effect of compositional variation on the thermal and mechanical properties of the curing system, it was hoped that the relative rates of component reactions could be ascertained. In the study presented in Chapter 3, this approach was refined by examining the relative rates of product formation in a model monofunctional epoxide system. Again, reactions were run without a catalyst, in order that correlations could be made with the results of the crosslinking study. The complications revealed by the model compound study necessitated a closer examination of the reaction mechanism. In the study presented in Chapter 4, products were isolated from the model reaction mixtures and were identified. Based on these identifications a novel reaction mechanism was proposed. In Chapter 5, the relative rates of the various reactions comprising this mechanism were assessed, and an attempt was made to correlate these reactions with the physical and mechanical changes observed during the cure of a dicy/epoxy system.



## CHAPTER 2

### THERMAL AND MECHANICAL ANALYSIS OF DICY CURED DGEBA

#### Introduction

The mechanism proposed by Zahir [40] for the dicy cure of epoxy resins was based on the study of a non-crosslinking model system. Therefore, it was considered necessary in the present investigation to test the validity of this mechanism for a crosslinking dicy/epoxy cure. For this purpose, a study was conducted in which the techniques of differential scanning calorimetry (DSC) and torsional braid analysis (TBA) were used to examine the uncatalyzed dicy cure of an epoxy resin, over a range of compositions. By determining the effect of compositional variation on the extent of reaction and development of physical properties in a curing system, it was hoped that the mechanism of the dicy/epoxy cure could be established. Although this study predates the work of Davidson [41], Lin et al. [42] and Galy et al. [43], advantage was taken of the observations made in those later studies in the interpretation of the results presented here.

In order to simplify the cure mechanism, a purified monomer of DGEBA was used as the epoxy resin and the cures were run without a catalyst, thus limiting interference from competitive etherification reactions. Since relatively high temperatures are required for the uncatalyzed dicy/epoxy cure reaction, it was believed that the solubility of the dicy in the epoxy resin would be enhanced [4,3] and the effects of dicy dissolution and diffusion on the rate of reaction would be diminished.

In accordance with the results of Zahir and those of later investigators [42,43], the reactions which were anticipated to occur under these conditions were amine addition to epoxide, followed by the intramolecular addition of hydroxyl to the cyano group and dissociation of the dicy to form 2-imino oxazolidine. Further reaction would then occur via imine addition to epoxide and the structural rearrangement of the oxazolidine to form a cyclic urea.

According to the Zahir mechanism, the dicy molecule is transformed from a tetra-functional diamine into two tri-functional cyclic amines, by its reaction with epoxy. Therefore, the overall functionality and stoichiometry of the curing system is different from that expected for a typical diamine cured epoxy. By determining the stoichiometric composition for the dicy/DGEBA cure, it was expected that the correct functionality of the dicy could be determined and the viability of the Zahir mechanism for a crosslinking system could be ascertained.

As was discussed in chapter 1, both the gel point conversion and the ultimate  $T_g$  of a crosslinking amine/epoxy system are dependent upon the degree to which the composition of the curing mixture matches the stoichiometry of the system. In the absence of etherification, the extent of reaction at gelation is lowest, and the ultimate  $T_g$  is highest, for a mixture at the stoichiometric composition. Compositional variation away from stoichiometry reduces the ultimate  $T_g$  of the cured resin and leads to an increase in the gel point extent of conversion of the deficient reactant. Therefore, by measuring the gel time and ultimate  $T_g$  for a

series of amine/epoxide cures, over a range of compositions, it should be possible to determine the stoichiometric mixture.

In the case of the dicy/DGEBA cure, this approach was expected to be limited due to the inherent inhomogeneity of the curing mixture. According to the results of Eyerer [4] and later Muroi et al. [37], the slow dissolution and diffusion of dicy into the epoxy resin leads to the formation of local gradients in dicy concentration, possibly resulting in premature gelation of the regions adjacent to the dicy particles. Since, even at high temperatures, large variations in the local composition of the curing system can be expected, no useful stoichiometric information was anticipated from measurements of gel point conversions for this system. In addition, all other kinetic events in the dicy/DGEBA cure were expected to be similarly affected by the system's inhomogeneity. Further, due to the formation of regions of varying crosslink density caused by the unequal distribution of dicy in the system, inaccurate  $T_g$  measurements were expected for the off-stoichiometric compositions.

However, it was believed that these difficulties could be avoided simply by measuring the effect of compositional variation on the extent of epoxide conversion in the curing mixtures. In the absence of etherification, the extent of epoxide conversion should be dependent upon the amount of available amine or imine functionalities. Ideally, in the case of deficient amine, epoxide conversion should vary linearly with amine concentration, and at stoichiometric or higher amine concentrations, 100% epoxide conversion should be achieved. Thus, a plot of the



epoxide conversion versus composition should show an abrupt change in slope at stoichiometry. Although the dicy/DGEBA mixture is inhomogeneous, it was believed that for a range of compositions, full conversion of the deficient reactant would eventually occur via diffusion, provided that the cure temperature exceeded the ultimate  $T_g$ . While some limitation on epoxide conversion was expected for dicy/epoxide system due to the constraints imposed by network formation [23], it was felt that the stoichiometric mixture could still be discerned by extrapolating from the highly off-stoichiometric portions of the conversion versus composition plots, where suppression of conversion would be less severe.

The extents of epoxide conversion were obtained for a range of uncatalyzed dicy/DGEBA compositions by isothermally curing samples in the DSC. This technique has been used in many previous studies of amine/epoxy systems, cured both isothermally and by scanning in temperature [23,26,27,45-48], and an extensive review of the literature on this subject has been published [49]. For a typical amine/epoxy cure, the heat of reaction measured by the DSC has been found to be proportional to the extent of epoxide consumption, and the rate of heat generation has been found to be directly proportional to the rate of cure. Thus, the overall kinetic parameters for a wide variety of amine/epoxy cures, including those of dicy containing systems [36,38,39,42,43,50-52], have been determined using this technique.

Amine/epoxide addition is also the largest source of heat generation in the dicy/epoxy cure. However, an additional heat of reaction, in a specific molar quantity, was expected for each of the several other



reactions described in the Zahir mechanism. Thus, the total heat of reaction was expected to be a sum of the contributions from each of the component reactions. These reactions were also expected to be limited or enhanced by variations in either the composition of the resin mixture or in the cure temperature. By quantifying the specific heat of each of these additional reactions and comparing with expected values, it was hoped that the identities of these additional reactions could be ascertained.

The effect of compositional variation on the development of mechanical properties was examined using TBA. This technique has been previously used to analyze a wide variety of amine/epoxy cures [53-55], including those of dicy containing, commercial formulations [39,56]. A glass braid, impregnated with resin is employed in this technique. By curing the resin on the braid and mechanically analyzing the composite specimen during cure, it is possible to follow relative changes in the storage and loss moduli of the resin from the liquid state to a point well beyond the onset of vitrification. The resulting TBA traces reveal transitions which have been associated with gelation and the onset of vitrification. Although, as previously discussed, no useful information about the stoichiometry of the dicy/DGEBA system was expected from the measurement of these transitions, it was believed that by correlating these transitions with the extent of reaction measured by the DSC, the inhomogeneity of the system could be evaluated. In an attempt to further probe the mechanism of the dicy/DGEBA cure, the techniques of DSC and TBA were also used to follow the uncatalyzed cyanamide cure of DGEBA. Due to the solubility of cyanamide in the epoxy resin, it was

hoped that mechanistic information could be obtained, free from the interfering effects of dicy insolubility.

## Experimental

### Materials

DGEBA was purified by recrystallization from a methyl ethyl ketone solution of a commercial resin, DER 332. The crystalline compound has a melting point of 40-45°C. Dicy, 97% pure, was obtained from Aldrich and was not further purified. No attempt was made to reduce the particle size. Cyanamide, stabilized with a small amount of boric or phosphoric acid, was also obtained from Aldrich with a purity of 99+%. Mixtures of dicy and DGEBA were prepared by dissolving the dicy in the DGEBA on a hot plate at 100°C. The mixture was quenched in liquid nitrogen and then intensively stirred. The process was repeated, and the mixture was allowed to slowly warm to room temperature, producing a uniform mixture. In several cases, Diuron was added to these mixtures for purposes of comparison. This was done by dissolving the Diuron in the preformed dicy/DGEBA mixture, heating to 50°C on a hot plate, quenching in liquid nitrogen and then allowing to warm to room temperature. The cyanamide/DGEBA mixtures were made by dissolving cyanamide in DGEBA at 50°C on a hot plate. These mixtures were then used immediately after preparation. For purposes of comparison several of the dicy/DGEBA and cyanamide/DGEBA compositions were catalyzed with benzyl dimethyl amine. This was done by adding the liquid amine to the preformed mixtures at room temperature. These samples were also used immediately after preparation. A model compound, 2-imino-3-phenyl oxazolidine, was synthesized by the

reaction of N-phenyl ethanol amine with cyanogen bromide. The details of this synthesis are presented in section 4 of the appendix. Mixtures of 2-imino-3-phenyl oxazolidine with DGEBA were made by dissolving the model compound in the DGEBA on a hot plate at 70°C.

#### Dynamic Scanning Calorimetry

Samples weighing 5 to 20mg were encapsulated in hermetically sealed aluminum pans (6.25 mm dia., 1.25 mm ht.) formed from 0.025 mm foil. Isothermal measurements were made using a Perkin Elmer DSC-2, under nitrogen and cooled with a circulating water bath for baseline stability. The instrument was calibrated for temperature and enthalpy with indium and lead. Strip-chart recorder traces were integrated using a Hewlett Packard 9830 programmable calculator equipped with a digitizer and plotter. Temperature scans were run on isothermally cured samples at 5°C/min to determine  $T_g$  and residual heat. Baselines for these scans were obtained by the subsequent rescanning of the fully cured samples. Temperature scans at 5°C/min were also run on several of the uncured compositions for purposes of comparison.

#### Torsional Braid Analysis

TBA specimens were prepared by impregnating glass braids, approximately 5.0 cm in length, with the neat resin mixtures. No solvents were used for this purpose. Isothermal TBA runs were made at approximately 1 Hz using an automated Plastics Analysis Instruments TBA system. The sample chamber was preheated to the cure temperature prior to sample introduction. Heating scans of the cured materials were run at 1.5°C/min. All runs were made under a helium atmosphere.



## Results and Discussion

### Dicy/DGEBA: Thermal Analysis

The cures of the uncatalyzed mixtures of dicy and DGEBA were initially analyzed by temperature scanning in the DSC. A typical scan at 5°C/min is shown in Figure 2-1 for a mixture containing a ratio of five epoxide equivalents per dicy molecule (dicy/epoxide = 1:5). The scan reveals a sharp exothermic peak I at 175° to 200°C, presumably due to amine/epoxide addition, followed by an endothermic spike at 208°C, associated with the melting of the residual dicy crystals. At temperatures above the dicy melt, there is a second broader exotherm II, showing one or two maxima. This DSC scan is similar to that reported by Schneider et al. [39] for dicy containing commercial formulations and later by Lin et al. [42] for the BDMA catalyzed dicy cure of DGEBA. In both of those studies the exothermic region above 250°C was attributed to degradation, as evidenced by weight loss and  $T_g$  reduction. Below 250°C the heat of reaction exhibited by exotherm II was assigned by Schneider et al. [39] to the consumption of residual epoxide groups via etherification reactions and the formation of melamine from the post melt reaction of residual dicy. Lin et al. [42], on the other hand, attributed the exotherm in this temperature range to the hydroxyl/cyano addition reaction described in the Zahir mechanism.

DSC scans were also run on mixtures catalyzed by BDMA, in order to test the effect of base catalysis on the dicy/epoxy cure. These scans revealed a shift in peak I to a lower temperature, comprising a broad exothermic region between 80° and 180°C. Exothermic region II, on the



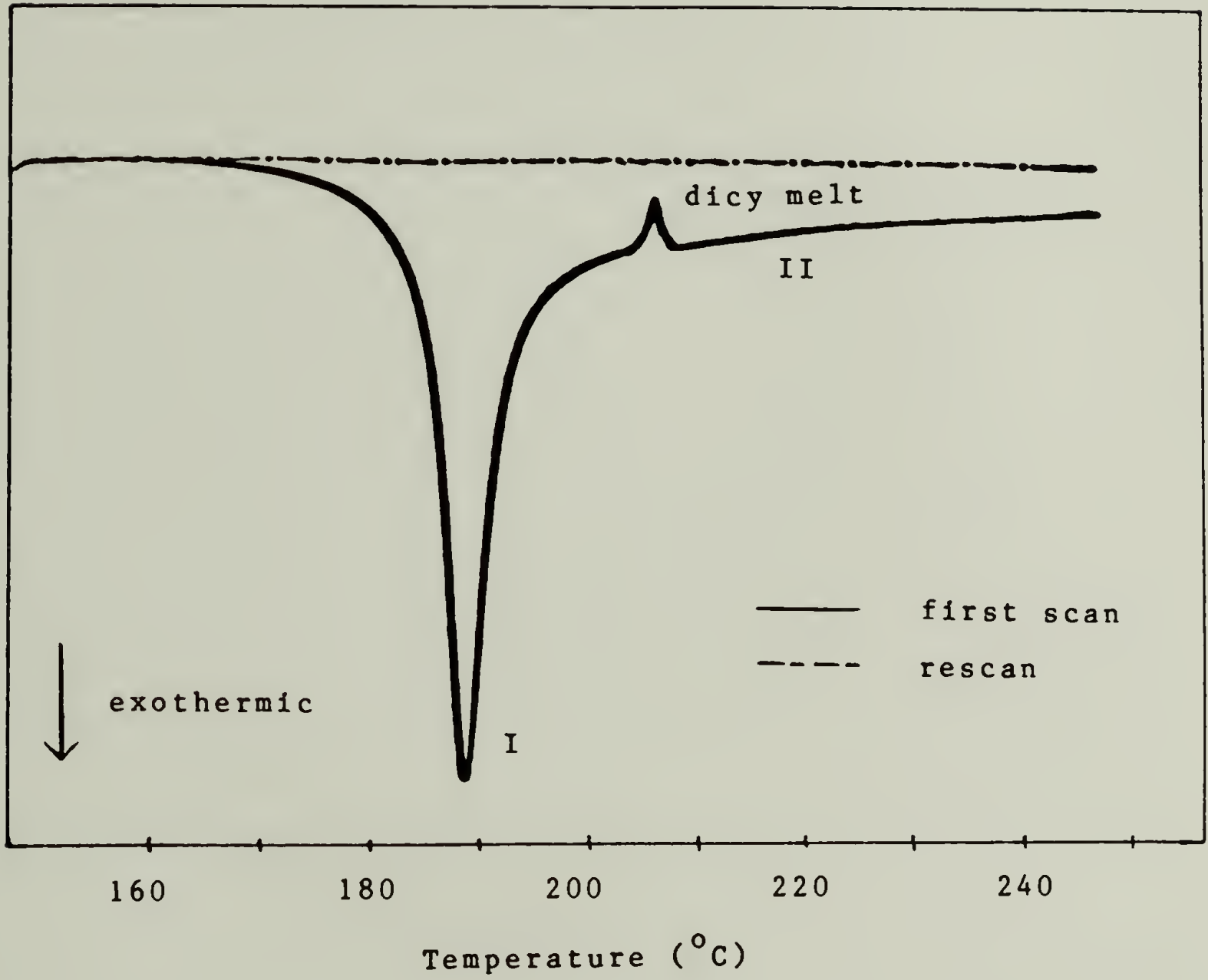


Figure 2-1: DSC temperature scan of 1:5 dicy/DGEBA at 5°C/min.

other hand, was not at all shifted by the addition of BDMA to the reaction mixture. Based on these observations, it appears that base catalysis lowers the activation energy of the reactions contained in peak I, while having no effect on the reactions encompassed by peak II.

The results of a cursory study showing the effect of compositional variation on the heats of reaction encompassed by peaks I and II, are listed in Table III. As can be seen, the heat of reaction approximated from the area of peak I was found to increase with increasing dicy concentration, reaching a maximum value of 85 kJ/mole equivalent (mol. eq.) of epoxide. Further study indicated that this limiting value for peak I was not significantly affected by the addition of catalytic amounts of the accelerator Diuron. The heat of reaction encompassed by exothermic region II increased to a maximum, then decreased as the amount of dicy in the mixture was increased, attaining a constant value of 60 kJ/mol. eq. epoxide at high dicy concentrations. At low dicy/epoxide ratios, the behavior of peak II was consistent with its assignment to high temperature etherification reactions, whereas at higher dicy loadings, the origin of this exotherm was not as readily apparent. As the amount of dicy was increased, the heat of combined exotherms I and II appeared to reach a constant total value of 140-150 kJ/mol. eq. epoxide. This value was not significantly increased by higher dicy loadings, thus indicating that any contributions attributable to melamine formation are not sizeable. At very high dicy loadings, complete consumption of epoxide should have occurred via the reactions of peak I. Therefore, the high heats of reaction measured in exothermic region II for these compositions was not understandable. One of the questions which arose out of this initial

Table III  
Heat of Reaction vs Dicy/DGEBA Composition

Composition	Peak I	Peak II	Total
epoxide/dicy	kJ/mol. eq.	kJ/mol. eq.	kJ/mol. eq.
14	35	75	110
7.5	44	99	138
3.7	61	74	135
2.5	81	54	135
1.9	79	65	144
1.2	89	63	152
1.0	81	62	143

study was whether this heat of reaction was due to the consumption of residual epoxy or to further reactions within the formed network.

### Isothermal Cures

In order to construct a conversion versus composition plot for the dicy/DGEBA system, isothermal cures of uncatalyzed dicy/DGEBA compositions, ranging from 1:64 to 1:2 dicy molecules per epoxide equivalent, were run in the DSC at a temperature of 177°C. This temperature was chosen, because it was well above the apparent ultimate  $T_g$  (150°C) of the cured materials, as is discussed below. It was felt that at this cure temperature the reactions of exotherm I could be driven to completion and thermally quantified without significant contributions from the slower reactions of exotherm II. It was expected that a plot of the isothermal heat of reaction obtained in this manner versus the dicy/epoxide ratio of the curing composition would reveal the true functionality and stoichiometry of the dicy/DGEBA system for the reactions of peak I. This, in turn, would indicate whether or not the cyclization reactions, as described by Zahir, were competitive with the amine/epoxide reactions in this temperature range.

A plot of the isothermal heat of reaction versus the composition of the uncatalyzed dicy/DGEBA mixtures is shown in Figure 2-2. Baselines for the isothermal cures were originally determined by allowing the strip chart recorder to run at the end of the reaction until no deflection was discernable over a reasonable length of time. Temperature scans of the isothermally cured materials revealed no evidence of an exothermic reaction until the temperature exceeded the dicy melting point at



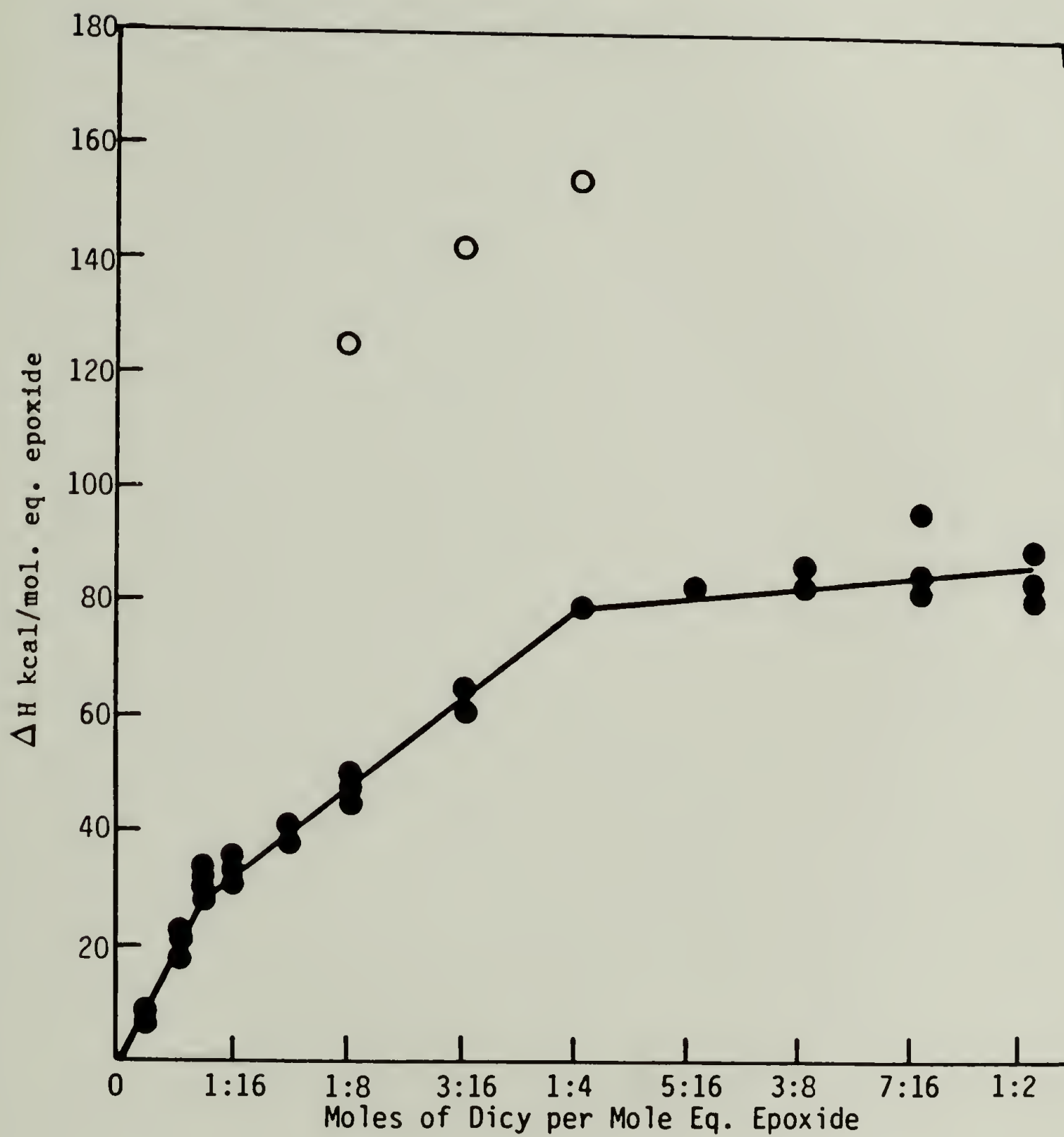


Figure 2-2: Plot of DSC conversion vs composition for uncatalyzed dicy/DGEBA cured at 177°C.

208°C. The dicy melt endotherm represented 5-10% of the original dicy in most cases. Rescans revealed that large increases in the  $T_g$ 's of the low dicy/epoxide ratio compositions had occurred by scanning through exotherm II. This behavior was an expected consequence of high temperature etherification. For these systems, maximum ultimate  $T_g$ 's of 150°C were measured. For compositions containing higher dicy loadings, the effect of post curing on  $T_g$  was more complex, resulting in both increases and decreases. Further discussion of this behavior is presented in a later section of this chapter.

An abrupt change in slope, at a composition of four epoxide groups per dicy molecule (1:4), is evident in the curve of the conversion versus composition plot. As was previously discussed, a change in slope is anticipated to occur at the stoichiometric composition. Thus, according to the initial interpretation of the isothermal data, dicy appeared to act as a tetrafunctional curing agent in its uncatalyzed reaction with DGEBA. A heat of reaction of approximately 85 kJ/mol. eq. epoxide was measured for this composition. Although this value is the same as the maximum heat of reaction reported by both Scheider et al. [39] and Lin et al. [42] for the isothermal cures of catalyzed mixtures with similar dicy/epoxide ratios, it is much less than the 104-108 kJ/mole eq. epoxide reported in the literature [23,27] for amine addition to epoxide. Some limitation on the total conversion was expected for a crosslinking system. A DSC study of the cures of DGEBA by various alkyl diamines, was conducted by Horie et al. [23]. Close to 100% conversion was found for the hexamethylene diamine cured system, while the ethylene diamine cure was limited to a conversion of 85%. Considering the size and func-

tionalities of both dicy and the 2-imino oxazolidine product of Zahir, it was expected that the extent of reaction for the dicy/DGEBA system at stoichiometry would be limited to a conversion similar to that of the ethylene diamine system. Therefore, the heat of reaction measured for the 1:4 dicy/epoxide mixture was in line with this expected limitation, assuming that amine/epoxide addition was the only reaction to occur during isothermal cure.

Although some limitation was anticipated for the extent of reaction of the stoichiometric mixture, at higher dicy loadings full conversion of the epoxide should have occurred. As can be seen in Figure 2-2, this was not the case. Compositions containing excess dicy were limited to a total isothermal heat of reaction of about 85 kJ/mol. eq. epoxide. The mechanism which limited conversion in the case of high dicy/epoxide eq. ratios was not readily apparent. Because the cure temperature ( $T_{\text{cure}}$ ) appeared to be above the ultimate  $T_g$  of the cured samples, vitrification did not initially appear to be a limiting factor. Since the total conversion was limited, no stoichiometric significance could be assigned to the changes in slope seen in Figure 2-2.

#### Long Time Cures

The cure times used in the above study were generally on the order of one to two hours. Completion of reaction was apparently confirmed by DSC temperature scans, which revealed no reaction exotherm below 200°C. However, further study of the uncatalyzed dicy/DGEBA cure by TBA revealed the presence of an extended reaction over a period of time exceeding twenty-four hours at 177°C. By adjusting the DSC to take

advantage of maximum sensitivity, it was possible to measure a very small heat output over a period of 24-48 hours for several of the dicy/DGEBA compositions. DSC temperature scans of the resins cured over these extended periods of time, exhibited neither a dicy melt endotherm at  $208^{\circ}\text{C}$ , nor any high temperature exotherm below  $250^{\circ}\text{C}$ . Thus, it appeared that complete reaction had taken place. Values for the long term heat of reaction are reproducible and equal the total combined heat of reaction from exothermic regions I and II, which are listed in Table III. The long-term total heat of reaction for several compositions are shown as open circles in Figure 2-2.

Clearly, the endpoints for the isothermal reactions used to construct the curve in Figure 2-2, were arbitrarily assigned based on the detector sensitivity. However, these reaction endpoints do approximate the point at which a rapid reduction in the rate of heat generation occurs. As such, this plot has some importance in understanding the reaction mechanism. The question which remained was whether this massive rate reduction was due to the occurrence of two or more consecutive chemical reactions, or was due to the imposition of some sort of physical control on the rate of dicy diffusion. Because the total heat of reaction measured by long-term isothermal DSC are equivalent to that measured by DSC temperature scans, it is assumed that the mechanisms of reaction for these two post cure methods are identical. Post cure behavior was further explored using TBA.

#### Torsional Braid Analysis

Isothermal cures of uncatalyzed dicy/DGEBA mixtures, ranging in



composition from 12:16 to 1:2 dicy molecules per epoxide equivalent, were run in the TBA for a variety of compositions at several cure temperatures. A typical trace is shown in Figure 2-3a, for a 1:4 dicy/epoxide mixture cured at 177°C. Large changes in the mechanical properties of the dicy/DGEBA system are evident, occurring over long periods of time. The trace of the log decrement, comparable to  $\tan \delta$ , contains three maxima, the first of which, a, has been associated with gelation [39,53,56]. The second damping peak, b, signifies the onset of vitrification and is accompanied by an increase to a maximum value in the rigidity, which is comparable to the storage modulus. This first rigidity maxima, 1, coincides with the massive rate reduction observed in the isothermal DSC cures and corresponds to a heat of reaction of 85 kJ/mol. eq. Further changes beyond this point in the TBA trace can be assigned to the long term reactions of exotherm II. As can be seen, these reactions result in a sizable decrease in damping, accompanied by a slight decrease in the stiffness. At still longer times, the stiffness increases to a second maxima, 2, and the development of a third larger damping peak c is seen. The rigidity maxima 2 corresponds to the completion of the long-term DSC reactions, and represents a total heat of reaction of 155 kJ/mol. eq. epoxide.

A TBA heating scan at a rate of about 1.5°C/min., is shown in Figure 2-3b for isothermally cured material. This scan reveals a  $T_g$  midpoint of 168°C, which is below the isothermal cure temperature. Further studies indicated that curing at or below the ultimate  $T_g$ , accentuates the changes observed in the long term cure. Compositions ranging from two to eight epoxy equivalents per dicy molecule (1:2-1:8) exhibited

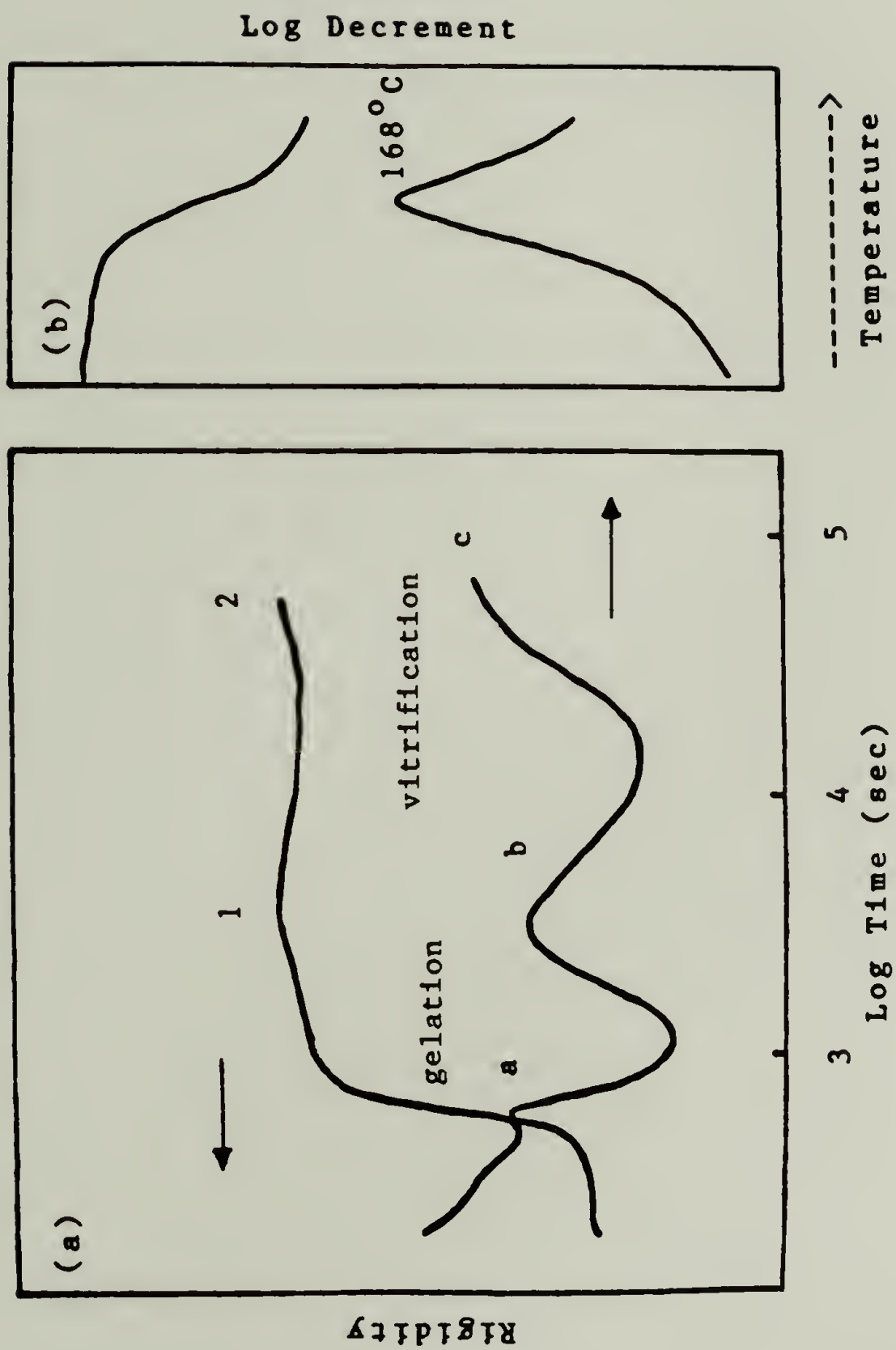


Figure 2-3: (a) TBA trace of 1:4 dicy/DGEBA isothermally cured at  $177^{\circ}\text{C}$ . (b) TBA temperature scan at  $1.5^{\circ}\text{C/min}$ .

similar long term curing behavior. Ultimate  $T_g$ 's of  $167^{\circ}$  to  $168^{\circ}\text{C}$  were observed for the 1:8 mixtures. Reduction of the dicy concentration below this amount resulted in the formation of materials with progressively lower ultimate  $T_g$ 's. However, increases in dicy concentration above this amount had little effect on the ultimate  $T_g$ , indicating that the excess dicy failed to take part in the reaction. Since etherification was thought to occur at extended reaction times [57], no stoichiometric significance were assigned to these  $T_g$  results.

The long time changes observed in the isothermal TBA traces of the dicy/DGEBA cures were caused by changes in the proximity of glass transition temperature to the temperature of cure. As such, these traces provide a measure of the slow variations in the  $T_g$  of the curing material, which occur over long periods of time. Three separate stages can be discerned in the isothermal cure mechanism. The first consists of the relatively rapid reactions of exotherm I, resulting in the formation of a crosslinked structure with a glass transition temperature approaching that of the cure. The completion of this stage appeared to be brought about either by the full consumption of reactants or some form of restriction on reactant mobility. Following its completion, a second stage is evident, which results in a slow decrease in the  $T_g$  of the material. This stage is followed by an even slower third stage, resulting in an increase in the  $T_g$  of the material presumably through further crosslinking reactions.

#### Effect of Dicy Particle Size

It was difficult to ascertain whether the long-term TBA behavior

represented a series of chemical reactions, or was instead a manifestation of the effects of dicy dissociation and diffusion on the crosslinking system. The dicy used in the above compositions consisted of a range of crystalline particle sizes. It is known from the work of Sacher [36] and later Muroi et al. [37] that the rate of dicy/epoxy reaction is directly proportional to the dicy particle size. Since 5-10% of the crystalline dicy, presumably the largest particles, remained at the end of the first stage of the cure, it was suspected that the differential in particle sizes might play a role in this long term cure behavior. Therefore, in order to test the effect of particle size, a sample with a composition similar to that used in the above TBA study, 1:4, was mechanically milled under liquid nitrogen, reducing the size of the dicy particles. Figure 2-4 shows the normalized DSC heating scan of the milled mixture at 5°C/min compared to that of an unmilled mixture of similar composition. In agreement with the results of Sacher [36] and Muroi et al. [37] the milled sample was found to react at a much faster rate than the unmilled sample. The total heat of reaction measured for this single, low temperature exotherm was only 108 kJ/mol. eq. epoxide. However, the milled mixture appeared to be completely cured by this low temperature reaction, since the scan of the mixture revealed neither a dicy melt endotherm nor a high temperature exotherm below 250°C.

A TBA trace of the isothermal cure of the milled 1:4 mixture at 167°C is shown in Figure 2-5a. Absent from this trace are any of the long term changes exhibited by the unmilled material when cured under identical conditions. A TBA heating scan of the isothermally cured material, shown in Figure 2-5b, reveals a  $T_g$  of 168°C. Since this was



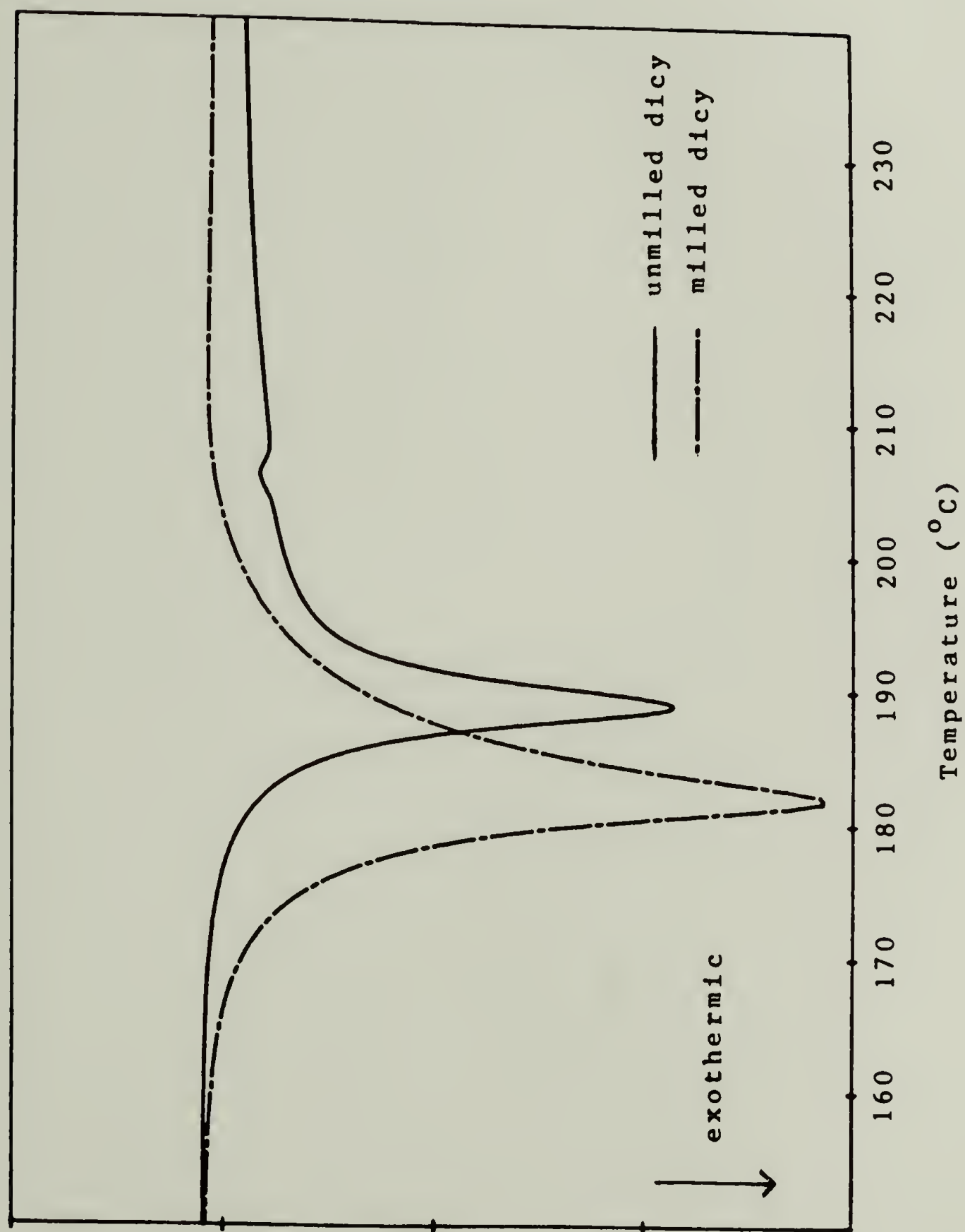


Figure 2-4: DSC temperature scan of milled and unmilled 1:4 dicy/DGEBA at 5°C/min.

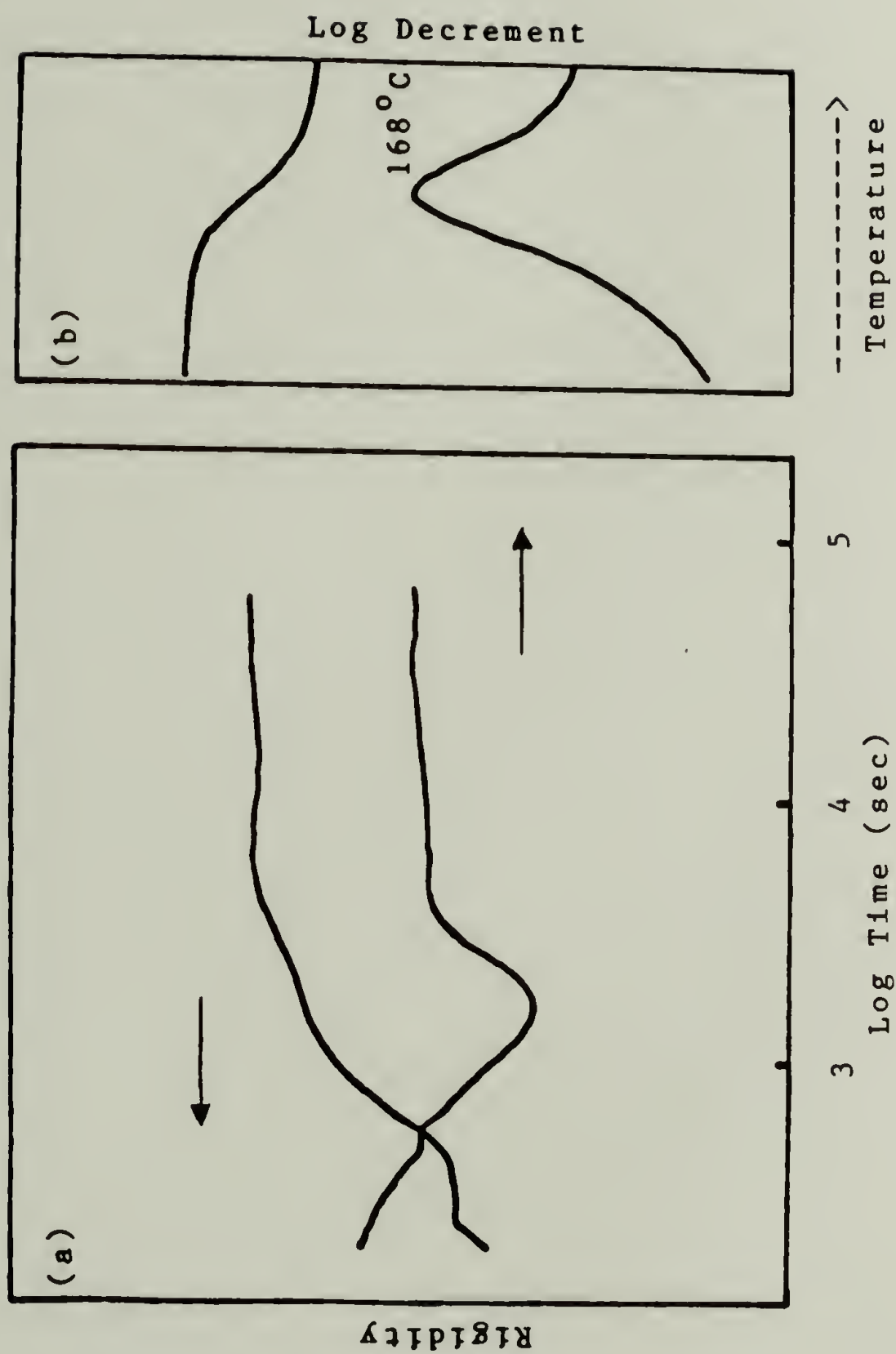


Figure 2-5: (a) TBA trace of milled 1:4 dicy/DGEBA isothermally cured at  $167^{\circ}\text{C}$ . (b) TBA temperature scan at  $1.5^{\circ}\text{C}/\text{min}$ .

identical to the ultimate  $T_g$  of the unmilled 1:4 mixture, the overall mechanism and crosslink densities for the milled and unmilled mixtures appeared to be similar. The milled composition was further analyzed by isothermally curing in the DSC at  $167^{\circ}\text{C}$  for an extended period of time. The end of the reaction appeared to be abrupt and coincided with the apparent completion of the isothermal TBA cure, yielding a total heat of reaction of  $121 \text{ kJ/mol. eq. epoxide}$ . This was less than the  $155 \text{ kJ/mol. eq. epoxide}$  measured for an unmilled sample of identical composition. However, the lack of any exotherm below  $250^{\circ}\text{C}$  in the DSC scan of the cured milled material again appeared to indicate that a complete reaction had occurred.

Based on these initial observations, it appeared that the presence of larger sized dicy particles was responsible for the appearance of three stages in the cure of the unmilled dicy/DGEBA mixtures. A possible explanation was that the initial stage of the cure consisted of the rapid reaction of the smaller dicy particles. As this stage approached completion, the less reactive, larger sized particles would act as a filler, stiffening the resin. At longer cure times, these particles would then dissolve, initially softening the resin, and then later stiffening the resin through further crosslinking reactions. However, the total heat of reaction for the milled and unmilled samples of similar composition should have been identical.

In order to find the missing heat of reaction, an isothermal cure of the milled 1:4 composition was run in the DSC at  $177^{\circ}\text{C}$ . An extended reaction was observed, lasting 19 hours, yielding a total heat of reac-

tion of 155 kJ/mol. eq. epoxide, identical to that measured for the unmilled composition. A TBA trace of the milled composition cured at the same temperature indicated no change in the stiffness trace at long times. However, the log decrement curve revealed extended behavior similar to that seen in the unmilled mixture, although the changes were less intense. A TBA heating scan of the cured resin indicated a  $T_g$  midpoint of only 158°C, explaining the low intensity of the changes seen in the isothermal trace. The higher cure temperature appeared to result in the partial degradation of the cured material. Thus, while particle size was found to influence the rate of the cure, it was not entirely responsible for the appearance of long time reactions in the cures of the unmilled materials. Therefore, the  $T_g$  reduction observed in the second stage of the TBA cures of the unmilled mixtures appears to be attributable to chemical degradation reactions.

#### Inhomogeneity and Vitrification

In the above investigation, incomplete reaction was observed for the milled material when isothermally cured at 167°C, as indicated by the comparatively low heat of reaction measured for this cure. The isothermal DSC trace indicated that the end of the reaction was abrupt. Continued heating at this temperature revealed no further heat generation and a correspondingly invariant TBA trace. This behavior appeared to be indicative of the massive rate reduction which occurs during the vitrification of a curing sample. A DSC temperature scan of the isothermally cured material revealed a  $T_g$  midpoint of 163°C and an onset of 161°C. Although this temperature was below the  $T_{cure}$ , it exceeds the highest  $T_g$  measured for the unmilled material (150°C), and is well above



the  $T_g$ 's of  $130^{\circ}$  to  $140^{\circ}\text{C}$ , reported in the literature for dicy/epoxy systems of similar composition [4,39,42,43,58,59]. The surprising discovery of such a high  $T_g$  for the milled sample reveals the true nature of the mechanism by which conversion is suppressed in the unmilled compositions.

As discussed in the introduction of this chapter, regions of varying crosslink density are expected to form in the cure of dicy/DGEBA mixtures due the presence of compositional gradients [4]. The highest  $T_g$  is expected for those regions in which the curing composition matches stoichiometry. The location and size of these regions is dependent upon the relative rate of dicy diffusion compared to epoxy reaction. Once formed, these regions separate areas deficient in epoxide from those deficient in dicy. Further reaction requires the diffusion of reactants through these high crosslink density regions, or the consumption of epoxide by alternative reactions. In the case of the unmilled dicy/DGEBA composition, the early vitrification of these intervening high crosslink density regions results in a large reduction in the rate of diffusion, and consequently, in the rate of reaction in the off-stoichiometric regions.

Evidence for the existence of regions of varying crosslink density in the cured unmilled sample can be found in the comparison of the  $T_g$ 's for milled and unmilled 1:4 dicy/DGEBA compositions isothermally cured at  $167^{\circ}\text{C}$ . Values are listed in Table IV. In general a much larger difference between the onset and midpoint values of the DSC  $T_g$  is observed for the unmilled as compared to the milled material. This

Table IV

$T_g$  for Milled and Unmilled 1:4 Dicy/DGEBA Cured at 167°C

	DSC $T_g$		DSC $T_g$ (post 250°C scan)		TBA $T_g$
	onset	midpoint	onset	midpoint	midpoint
Unmilled	128°C	142°C	128°C	130°C	167°C
Milled	161°C	163°C	149°C	151°C	168°C

behavior is indicative of a greater degree of inhomogeneity in the unmilled sample. Degradation by scanning to 250°C resulted in an equivalent decrease in the onset and midpoint  $T_g$  values of the milled sample. However, in the case of unmilled sample, degradation was found to reduce only the  $T_g$  midpoint value. The onset value was unaffected. Thus, it appears that the lower  $T_g$  regions of the unmilled sample have a greater degree of thermal stability than do the more highly crosslinked regions.

According to the TBA measurements, the milled and unmilled samples have identical  $T_g$  midpoints. This is at odds with the  $T_g$  midpoints measured by DSC. Of interest is not the discrepancy between the  $T_g$ 's measured by the two techniques. This is expected. Rather, it is the larger difference in values measured by these techniques for the unmilled as compared to the milled material. The glass transition temperature, measured by temperature scanning in the TBA, is indicative of the onset of long range molecular motions. As such, it is most sensitive to the higher  $T_g$  regions of an inhomogeneous system. The DSC, on the other hand, is a measure of the change in heat capacity which occurs at vitrification. Since the heat capacity change at  $T_g$  is greater for regions of lower crosslink density, than it is for those of high crosslink density [60], the apparent  $T_g$  measured by DSC will be weighted in favor of the low crosslink density regions in an inhomogeneous system. Thus, while the milled and unmilled samples were found to contain similar regions of high crosslink density, the unmilled sample also appears to contain a large fraction of low  $T_g$  material.

It has been reported that the conversion at maximum rate of reaction in an amine/epoxy cure is dependent on the balance between the accelerating effects of hydroxyl formation, and the decelerating effects of reactant consumption and is invariant with  $T_{\text{cure}}$  for a specific curing system [27]. In the dicy system, the maximum rate extent of conversion is dependent on the accelerating effects of the increasing solubility of dicy with increasing extents of conversion, balanced by the decelerating effects of reactant consumption. As such, maximum rate conversion is a measure of the availability of reactive dicy in a specific system. At the maximum rate of reaction, a partial heat of reaction of 35 kJ/mol. eq. epoxide was measured for the unmilled sample, while a heat of 60 kJ/mol. eq. epoxide was measured for the milled sample. Thus, the milled sample appeared to contain a higher overall concentration of available dicy, during this early stage of reaction. The lower apparent concentration of available dicy in the unmilled system was due to either the restriction of dicy dissolution by larger dicy particle size, or to limitations on dicy diffusion in the inhomogeneous unmilled sample. Studies in the following chapter of the reaction of unmilled dicy with a monoepoxide indicated that the latter scenario was correct.

### Summary

The long time physical behavior of the milled and unmilled cures can be explained in terms of the above mechanism. At the start of the initial stage of cure, an induction period exists, in which the dicy dissolves and diffuses into the epoxy resin. A pattern of compositional gradients is formed, which is dependent upon the size and distribution



of the dicy crystals. Reaction of the resin then occurs rapidly due to effects of autoacceleration. High crosslink density material is formed in regions in which composition is closest to stoichiometry and the process of vitrification results in an overall reduction in the rate of reaction. Simultaneously, a slow degradation reaction appears to occur in the regions of high crosslink density. In the case of the milled mixture the decreased particle size results in increased dicy dissolution in the initial stage of reaction. This leads to higher effective dicy concentrations, increased overall rate of cure, and increased homogeneity in the resin. Thus, a higher conversion of epoxide is achieved in the initial stage of reaction and the formation of high crosslink density material is more widespread. For a cure temperature of  $167^{\circ}\text{C}$ , vitrification leads to termination of the reaction. In the cure of the unmilled mixture, both the effective concentration of dicy and the overall homogeneity of the mixture are lower. This leads to a lower overall rate of conversion and the formation of a coarse pattern of high crosslink density material. The onset of vitrification in these regions results in the appearance of the first stiffness maxima in the TBA trace of the cure. Due to the lower rate of reaction and the high degree of inhomogeneity in the system, the degradation reaction prevents vitrification from entirely stopping the reaction. The later stages of cure involve the degradation of the high crosslink density material and the slow further reaction of the off-stoichiometric regions of the system.

Although the above study of the dicy/DGEBA cure provided little information about the chemical mechanism of the cure, it did indicate that large compositional variations can occur in the different regions

of the curing system. Due to the complexity of the chemical mechanism, discussed in chapter 4, these variations can be expected to alter the chemical structure of the networks formed in these regions. In the case of the milled material, it appears that a higher rate of reaction, combined with the effects of vitrification, can lead to the formation of a kinetically favored structure, radically different from the thermodynamically stable structure, formed at a slower rate.

#### Cyanamide/DGEBA

According to the results of the Zahir study, the cyanamide cure of DGEBA is expected to yield a network structure similar to that obtained from the dicy/DGEBA cure. Unlike dicy, cyanamide is completely soluble in DGEBA and forms a uniform mixture, alleviating the several problems associated with dicy insolubility. Therefore, a study was conducted in which the effects of compositional variation on the ultimate properties and heat of reaction were ascertained for the cyanamide/DGEBA cure. Since the curing mixtures were homogeneous, it was believed that the functionality and stoichiometry of the cyanamide/DGEBA system could be clearly discerned in this study, providing insight into the chemical mechanism of the dicy/DGEBA cure.

The reactions anticipated for this system were amine addition to epoxide, hydroxyl addition to cyano with formation of 2-imino oxazolidines, and imine addition to epoxide. An attempt was made to find evidence for these reactions and to examine their relative rates. Also anticipated for this system, was the dimerization of cyanamide to form

dicy and an effort was made to evaluate the extent to which this reaction occurred. Figure 2-6 shows a DSC heating scan at  $5^{\circ}\text{C}/\text{min}$  of a cyanamide/DGEBA mixture with a ratio of two equivalents of epoxide per cyanamide molecule (1:2). Two principle exothermic regions are observed consisting of a peak at  $125^{\circ}\text{C}$  I and a broad, higher temperature shoulder II. The relative areas of these exotherms were found to be dependent on compositional variation and it was believed that these exotherms encompassed the reactions outlined above. Two smaller exothermic regions, not readily evident in Figure 2-6, were also observed. The first peak III in the region of  $190^{\circ}$  to  $250^{\circ}\text{C}$ , appeared to be composed of the high temperature etherification reactions and the structural rearrangement reactions previously observed for the dicy/DGEBA cure in this temperature range. Exotherm IV, in the region above  $250^{\circ}\text{C}$ , is assigned to degradation, as indicated by a simultaneous weight loss and  $T_g$  reduction.

In an attempt to identify the component reactions of I and II, the effect of compositional variation on the relative areas of these exotherms was examined. It was found that as the concentration of cyanamide is increased, the areas of both low temperature exotherms increase to a certain point, after which the first increases at the expense of the second. Exotherm I and II both appear to contain epoxide addition reactions. Therefore, peak II was assigned to the reaction of epoxide with either a product formed by the initial cyanamide/DGEBA reaction or with dicy. As was previously discussed, cyanamide dimerization to dicy was expected as a potential side reaction. Due to its lower reactivity, it was expected that the exotherm of the dicy/DGEBA reaction would occur later in the DSC scan than that of the cyanamide/

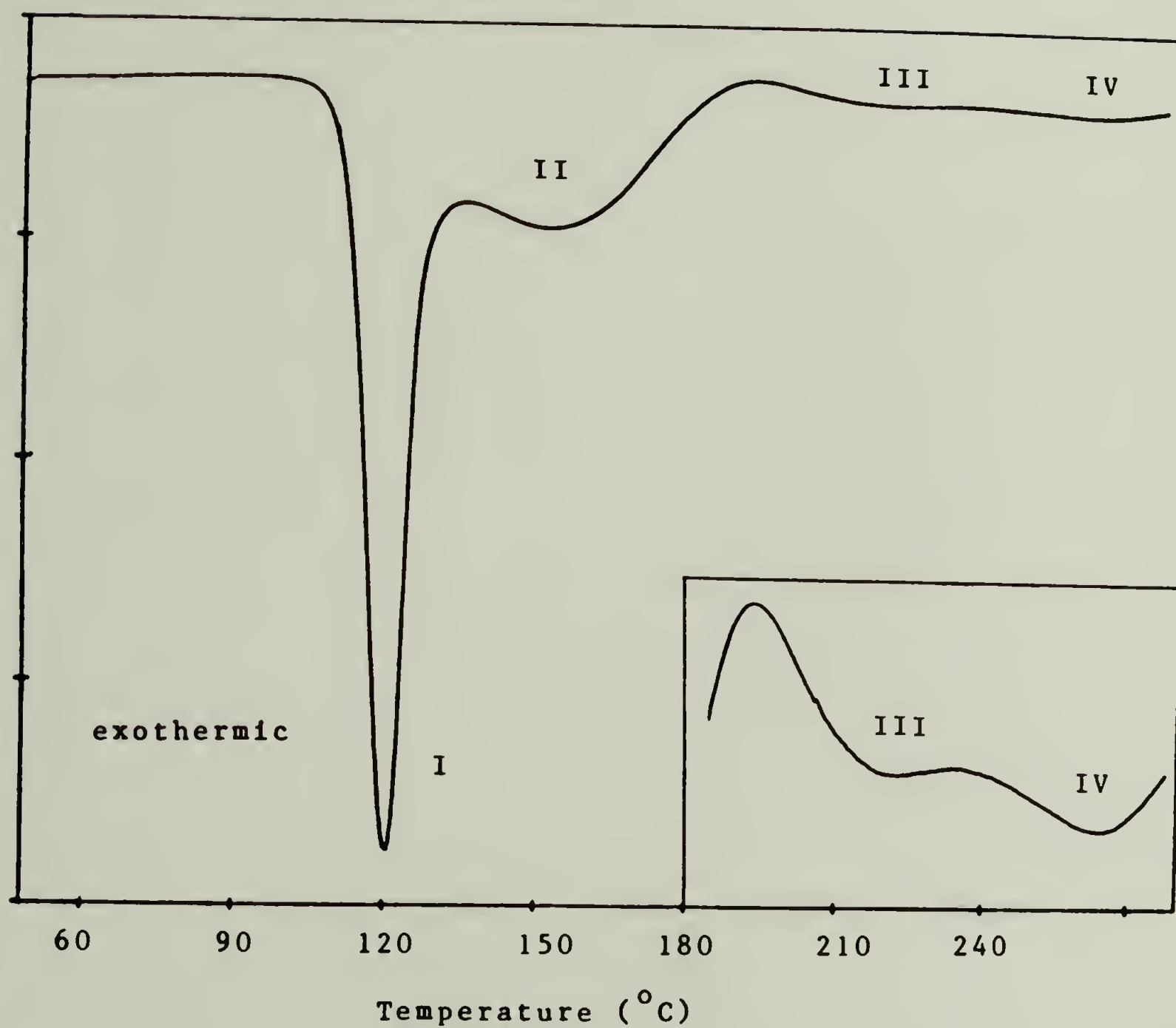


Figure 2-6: DSC temperature scan of 1:2 cyananide/DGEBA at 5°C/min.



DGEBA reaction. In order to examine the relative rate of dicy formation, a DSC temperature scan of the neat cyanamide was run at  $5^{\circ}\text{C}/\text{min}$ . The DSC trace, shown in Figure 2-7, reveals a dimerization exotherm with a maximum rate  $30^{\circ}\text{C}$  higher than that of peak I in Figure 2-6. Although the difference in the temperatures of onset for these two exotherms was only  $10^{\circ}\text{C}$ , it was believed that the dilution of the cyanamide by mixing with DGEBA would further lower the rate of dimerization. Therefore, cyanamide dimerization was only expected to occur to a significant extent in compositions with high cyanamide loadings.

Following the work of Catsiff et al. [61], the compound 2-imino-3-phenyl oxazolidine was synthesized as a model for the product which appears in Zahir's reaction scheme. A DSC scan,  $5^{\circ}\text{C}/\text{min}$ , of a mixture of this model compound with DGEBA at a ratio of four epoxide eq. per oxazolidine is shown in Figure 2-8. The first exothermic peak corresponds to peak II of the cyanamide/DGEBA DSC trace in both onset and maximum rate temperatures. This reaction was reported by Catsiff to be due to the addition of the imino functionality of the oxazolidine to an epoxide. Thus, it appeared that exotherm II in the cyanamide/DGEBA DSC temperature scan might also encompass the reaction of the generated 2-imino oxazolidine with DGEBA. Also evident in the DSC scan of the model compound/DGEBA mixture is a large, higher temperature exotherm. This was attributed to the consumption of excess epoxide by etherification and/or homopolymerization reactions catalyzed by the highly basic 2-imino oxazolidine. A further study of the reaction of this model compound with a monofunctional epoxide is presented in chapter 4.

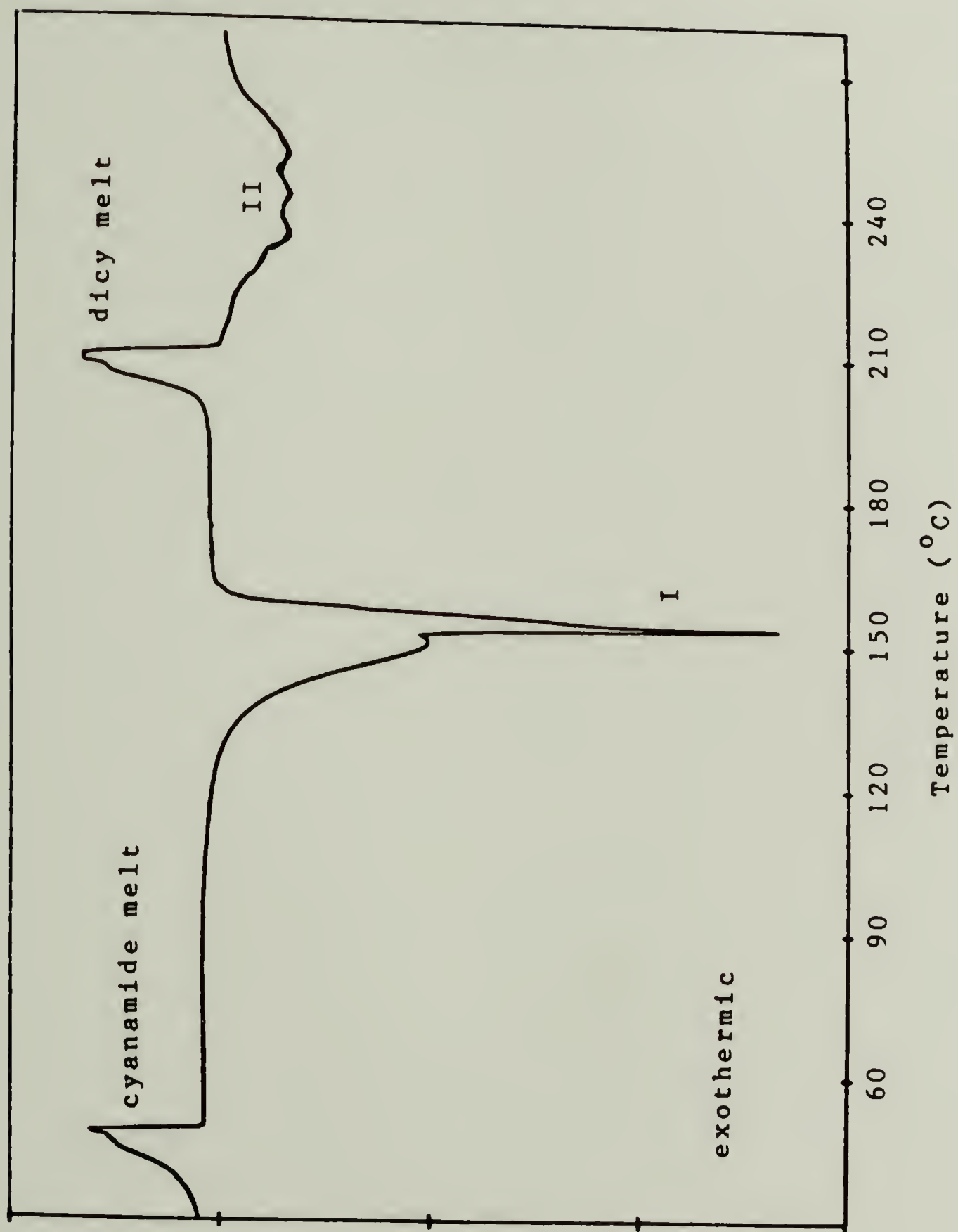


Figure 2-7: DSC temperature scan of neat cyanamide at 5°C/min.

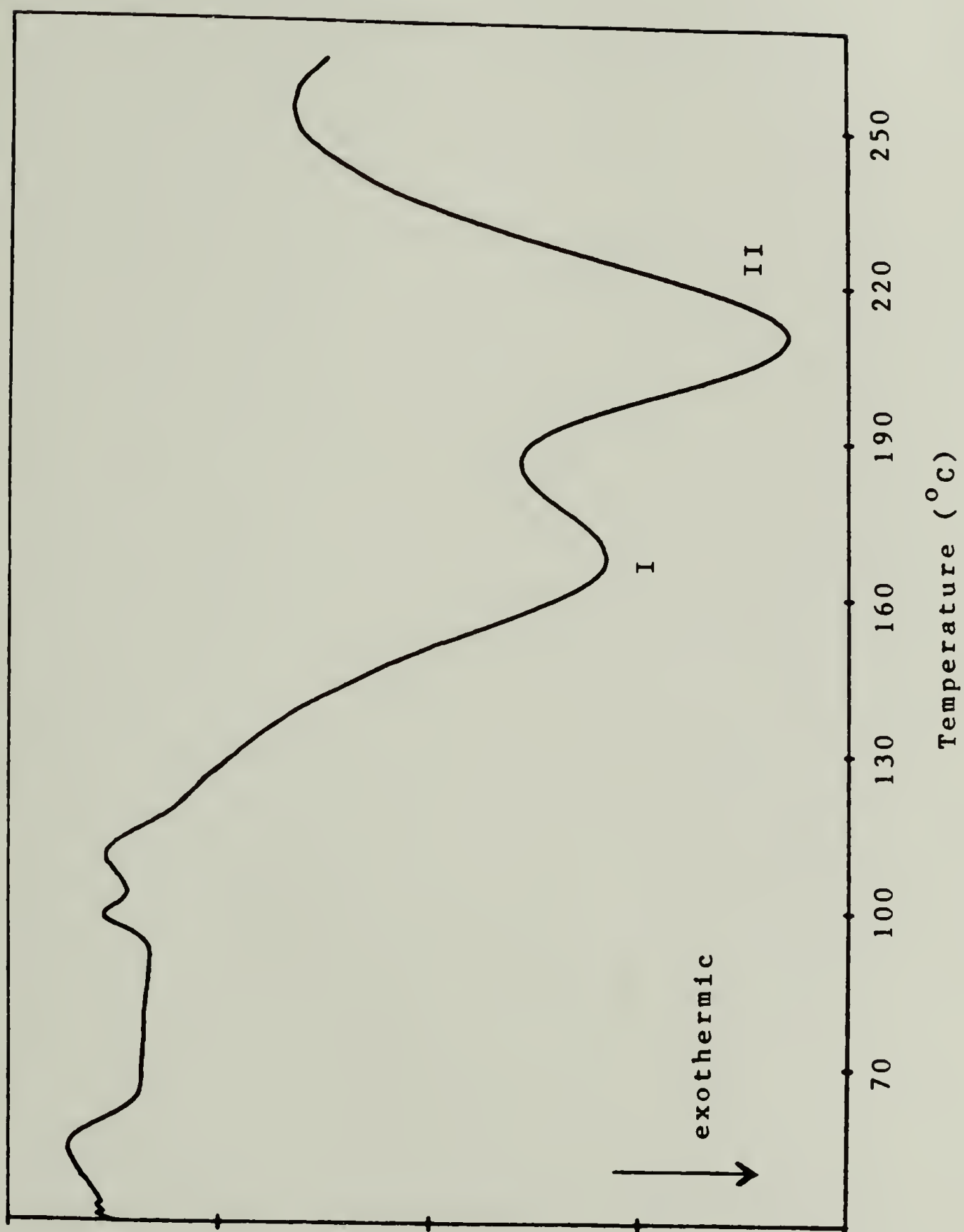


Figure 2-8: DSC temperature scan of 1:4 2-imino-3-phenyl oxazolidine/DGEBA at 5°C/min.

Based on the above results, peak I in the DSC heating scans of the cyanamide/DGEBA mixture was initially assigned to the reaction of the cyanamide amines with epoxide, dicy formation, and the formation of 2-imino oxazolidines by hydroxyl addition to cyano. Exotherm II was tentatively assigned to the reactions of the 2-imino oxazolidines and dicy with the remaining DGEBA. In an attempt to confirm those assignments, compositions were isothermal cured in the DSC at  $107^{\circ}\text{C}$ . It was believed that at this temperature the reactions of exotherm I would be much faster than those of exotherm II and could be independently quantified by thermal analysis. However, the endpoints for these reactions were somewhat arbitrary and it is likely that these cures did contain a significant contribution from the reactions of exotherm II. A plot of the isothermal heats of reaction versus composition for the cyanamide/DGEBA cure is shown in the upper curve of Figure 2-9. The lower trace is a plot of the heat generated in peak II, as determined by temperature scanning the isothermally cured resins in the DSC at  $5^{\circ}\text{C}/\text{min}$ . A break in the slope of the upper curve is seen at a composition of two epoxide groups per cyanamide molecule (1:2). This break appeared to confirm the assumption that cyanamide acted as a difunctional curing agent in exotherm I, reacting with epoxide via its amine functionality.

Based on bond energies a heat of reaction of 67 kJ/mole was calculated for hydroxyl addition to cyano. As previously discussed, a value of 104 to 108 kJ/mol. eq. epoxide is expected for amine/epoxy addition [23,27]. Together, these values yield an anticipated heat of reaction of 140 kJ/mol. eq. epoxide for the above composition. This value is in agreement with the 135 kJ/mol. eq. epoxide measured for 1:2 composition,



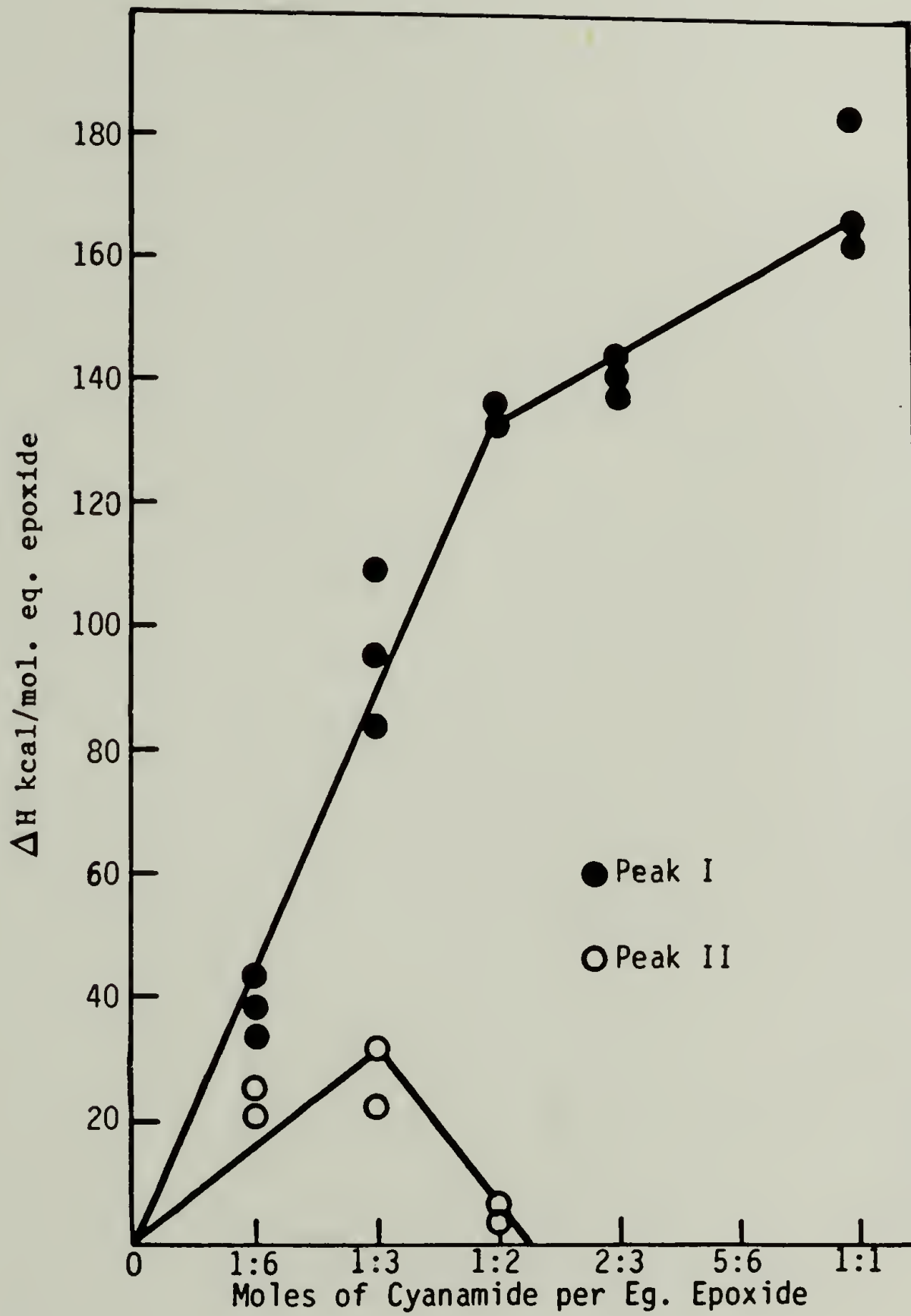


Figure 2-9: Plot of DSC conversion vs composition for uncatalyzed cyanamide/DGEBA cured at 107°C.

apparently indicating that oxazolidine formation also occurs in exotherm I. Finally, a break in the lower curve at a composition of 1:3 cyanamide/epoxide eq. appeared to support the designation of cyanamide as a trifunctional curing agent in exotherm II.

Thus, it originally appeared that the cyanamide/DGEBA cure consisted of amine/epoxide addition reactions and intramolecular hydroxyl addition to cyano to yield 2-imino oxazolidine at low temperatures. Imine addition appeared to occur only at higher temperatures. These observations were supported by TBA studies. Mixtures containing cyanamide/epoxide ratios of 1:2, were cured at 100°C for 19 hrs, and then were post cured at 177°C. Ultimate  $T_g$ 's of 100° to 110°C were measured for these samples. However, mixtures of identical composition, cured directly at 177°C, without a low temperature precure, attained ultimate  $T_g$ 's of 150° to 160°C. At low temperatures, it appeared that the cyanamide behaved as a difunctional crosslinker, consuming epoxide via amine/epoxide addition reactions and forming essentially linear polymer chains. Crosslinking, via imine/epoxide addition, appeared to become competitive with amine/epoxide addition only at higher temperatures, indicating a higher energy of activation for imine/epoxide addition. Based on this understanding of the mechanism, an attempt was made to determine the rates of these several reactions by examining the rate of formation of products in a cyanamide/monoepoxide reaction mixture. The results of this study are presented in the following chapter.

## CHAPTER 3

### KINETICS OF A DICY/MONOEPOXIDE REACTION

#### Introduction

Recently, several investigators have used the spectral subtraction capabilities of FTIR [62,63] and FT-NMR [64] to determine both structures and relative rates of the reactions comprising the cures of several amine/epoxy systems. However, the inhomogeneity of the dicy/DGEBA system, combined with the complexity of the spectra obtained from the curing system [41], precluded the use of these techniques for kinetic analysis of the dicy/DGEBA cure. Therefore, an attempt was made to model the reactions of the curing system using the reactions of dicy and cyanamide with a monoepoxide. Since these reactions produce soluble, relatively low molecular weight products, it was believed that HPLC could be used to separate and quantify the various product species formed by these model systems. Further, by isothermally reacting the model compound mixtures for various lengths of time and then analyzing the reaction mixtures with HPLC, the relative rates of both reactant consumption and product formation could be determined, allowing the relative rates of the component reactions of the dicy/DGEBA cure to be inferred.

The main impetus of this study was to test the validity of the Zahir [40] mechanism for the uncatalyzed dicy/DGEBA cure. An attempt was made to conduct the reactions of the model compound mixtures under conditions similar to those used in the cure studies presented in Chapter 2. To

that end, uncatalyzed mixtures were isothermally reacted in the DSC, in the temperature range previously used in the study of the dicy/DGEBA cure. In order to establish an additional correlation between the model reactions and the dicy/DGEBA cures, the isothermal heat of reaction for the model systems was determined by DSC. By relating product formation, as determined by HPLC, with specific heats of reaction, it was hoped that a further mechanistic interpretation could be applied to the thermal analysis measurements presented in the previous chapter.

### Monoepoxide Studies

Monoepoxide reactions have been widely used by previous investigators as models for epoxy thermoset cures. Based on studies of these model systems, early workers were able to deduce both product structures [18] and reaction mechanisms [12,19] for the curing systems. More recently, the techniques of SEC [20,65] and HPLC [15,21,25,66] have been used to separate and quantify the components of these model reaction mixtures allowing kinetic parameters to be assigned to reactions, such as primary and secondary amine addition to epoxide and etherification. The relative rates of reactions measured in these models systems have been directly applied to crosslinking systems and have shown a good correlation to those values, measured for the crosslinking systems by independent means [65].

Despite widespread use, some questions have remained as to the adequacy of the monoepoxide reactions in modeling the cures of the thermosetting systems due to constraints imposed on the reactivity of the curing system by the development of the network structure and the onset



of vitrification. Comparing the reactivities of a series of amine cured DGEBA resins with an amine/PGE model reaction mixture, Horie et al. [23] found that identical kinetic parameters governed the overall rates of reaction for both curing and model systems prior to a conversion of 55 to 75%. However, beyond this point, a drastic reduction in the overall rate of reaction was observed for the crosslinking systems, even at temperatures above ultimate  $T_g$ , due to the limitation on the mobility of reactive species by their incorporation in the network structure.

Similarly, the onset of vitrification in a curing system results in a lower overall rate of reaction by the imposition of diffusion control. As was discussed in chapter 1, Lunak et al. [22] found that for a typical amine/epoxy cure, diffusion control seems to have very little effect on the relative rates of component reactions since all functional groups appear to be equally affected. However, it is unlikely that the relative rates of the reactions comprising the complex mechanism of the dicy/DGEBA cure are similarly unaffected. In particular, the relative rates of the intramolecular hydroxy/cyano addition and dicy dissociation reactions, described by Zahir, were expected to be enhanced compared to amine/epoxide addition, under conditions of diffusion control.

As discussed in chapter 1, dicy/monoepoxide reactions have been previously used by Saunders et al. [35], Zahir [40], and more recently by Galy et al. [44] to model the cures of dicy/epoxy resin systems. The ability of these systems to model the reactions occurring in the dicy/DGEBA cure has been demonstrated by the reasonable correlation which exists between the IR spectra of these model compound mixtures and those

of the curing resins [4,41,42]. In each of these investigations the reactions were catalyzed by BDMA and the monoepoxide of choice was PGE. However, this compound could not be used in the present study, due to its high volatility at the temperatures required by the uncatalyzed dicy/epoxide reaction. Therefore, it was necessary to synthesize a higher molecular weight monoepoxide which could be used at these temperatures without appreciable weight loss. For this purpose, the methyl glycidyl ether of bisphenol A (MGEBA), a monoepoxide analog of DGEBA, was synthesized. The synthesis and structure of this compound are discussed in a later section of this chapter.

Due to the low solubility of dicy in MGEBA, this model system is, to a large degree, inhomogeneous. As in the case of the dicy/DGEBA cure, the slow dissolution and diffusion of dicy into the monoepoxide was expected to lead to the formation of compositional gradients in the reaction mixture. Both the local composition and overall rate of reaction for the model monoepoxide system are dependent on the rates of dicy dissolution and diffusion. The similarity of this situation to that found in the curing system might initially appear to be beneficial in allowing the monoepoxide reaction to more accurately model the conditions found in the early stages of reaction in the curing system. However, differences between these systems were expected due to the anticipated differences in the rates of dicy dissolution in DGEBA and the MGEBA. Further, it has been suggested that the rate of dicy dissolution is enhanced by the formation of dicy/epoxide products [3,37]. In the case of the curing systems, constraints on the mobility of dicy/epoxide

products in the regions adjacent to the dicy crystals, caused by the rapid formation of a network structure may in fact enhance dicy dissolution early in the reaction, while limiting dicy diffusion through vitrification at a later stage of the cure. In the model system diffusion of both dicy and the resulting low molecular weight products was expected to continue unabated throughout the course of the reaction, thus acting to homogenize the reaction mixture. These differences must be taken into account when attempting to draw mechanistic conclusions from the model compound study.

#### High Performance Liquid Chromatography

A wide variety of products were anticipated from the uncatalyzed dicy/MGEBA reaction. These were expected to include the mono through tetra substituted adducts of dicy, the mono through tri substituted adducts of both 2-imino oxazolidine and its cyclic urea rearrangement product, and the mono and di substituted adducts of cyanamide. Since many of these products are only marginally different in molecular size, they can not be readily separated by SEC, as used by Zahir. It was believed that better separation of these products could be obtained using reverse-phase HPLC. This technique separates compounds based on differences in polarity. As such, it is more sensitive to the changes brought about by the intramolecular reactions and rearrangements which were expected to occur in this system. An excellent review of reverse-phase HPLC as applied to the study of epoxy resin systems has been recently published [67], and a general introduction to this technique can be found in the book "Practical Liquid Chromatography" by Yost et al. [68].



Due to the large number of anticipated products, it was expected that the HPLC chromatograms of the dicy/MGEBA reaction mixture would be quite complex. Therefore, it was felt that there would be some difficulty in optimizing the separation of each of the individual products. Since the primary goal of this study was to determine the relative rate of cyclical product formation, effort was concentrated on identifying the peaks in the chromatogram associated with these products. It was believed that this could be readily accomplished, by comparing chromatograms of the dicy/MGEBA reaction mixture with those of the simpler cyanamide/MGEBA mixture. It was expected that this latter mixture would contain only the cyclic dissociation products described in the Zahir mechanism, without the corresponding linear substituted dicy adducts.

The results of previous HPLC studies of amine/monoepoxide reaction mixtures [15,25,66], including that of the dicy/PGE reaction [44], have revealed that higher molecular weight species generally elute at progressively longer times. Thus, it was believed that approximate molecular weights could be assigned to specific product peaks, based on HPLC retention times. Further identification of individual peaks was made by following the growth of product peaks as the reaction proceeded, and interpreting in terms of the Zahir mechanism.

## Experimental

### Materials

MGEBA was synthesized by a two step process. In the first step, bisphenol A (Aldrich, Gold Label, 99<sup>+</sup>% pure) was partially methylated



using dimethyl sulfate (Kodak). The monomethyl bisphenol A (mMBPA) was then separated from the resulting product mixture and purified by solvent extraction. In the second step, the mMBPA was reacted with excess epichlorohydrin (Aldrich, Gold Label, 99<sup>+</sup>% pure) in refluxing THF, producing MGEBA. The details of this synthesis are presented in sections 1 and 2 in the appendix. Following purification by solvent extraction, this compound was found to have a purity of 98<sup>+</sup>% by HPLC. The MGEBA was then characterized by FTIR, <sup>1</sup>H and <sup>13</sup>C NMR and MS. A description of these techniques can be found in the experimental section of chapter 4.

Dicy (Aldrich, 97% pure) and cyanamide (Aldrich, 99<sup>+</sup>% pure) were used without further purification. Reagent grade BDMA was used without further purification.

#### Sample Preparation

Weighed amounts of dicy and MGEBA were mixed in a vial on a hot plate at 160°C. The mixtures were then quenched in liquid nitrogen and allowed to warm to room temperature. The mixtures were then mixed by hand, reheated and requeched, producing a uniform composition. Catalyzed samples were made by adding BDMA to the mixtures just prior to use. Cyanamide/MGEBA mixtures were made by stirring the reactants together on a hot plate at 50°C.

DSC samples were prepared in a manner identical to that used in chapter 2 and a general description, both of this procedure and the operation of the DSC, can be found in the experimental section of that chapter. Samples were isothermally cured in the DSC for specific

lengths of time. The reactions were then quenched by quick-cooling in the DSC. The sample pans were reweighed, opened with a scalpel, and placed in a vial with 2mls of a mixture of 90% THF and 10% H<sub>2</sub>O. The vials were then allowed to stand for several hours after which they were shaken for five minutes with a mechanical vibrator allowing complete dissolution of the product mixture. The samples were filtered through a 0.2 micron disposable Acrodisc filter (Gehman) and the sample vials were washed with an additional 2mls of THF, then filtered and combined with the original solution, bringing the total solvent volume to 4mls.

#### Sample Analysis

Samples were analyzed using a Waters HPLC system equipped with a Model 660 Solvent Programmer, two M-6000A Pumps, a Model 441 UV Detector and a Model 730 Data Module. A reverse-phase, micron Bondapak C18 Column (30cmX3.9mm ID) packed with 10 micron packing material was used. Solvent mixtures of THF:H<sub>2</sub>O = 50:50 to 90:10 were run at a flow rate of 1.0ml/min, using a variety of programmed gradients and run times. Solvent mixtures of acetonitrile:H<sub>2</sub>O = 60:40 to 100:0 were also used. Detector wavelengths of 280nm and 229nm were independently used. Each injection contained 15 microliters of sample solution.

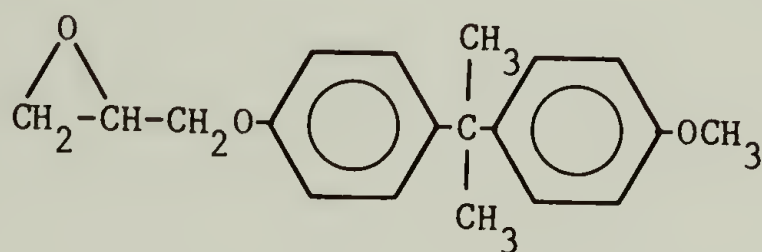
Samples were also analyzed with a Waters HPLC system equipped with two M-6000A pumps, a model 840 System Controller for Solvent Programming and Data Acquisition, and a WISP 710B Auto-Injector. A Waters, Reverse-phase, Resolve C-18 column (15cmx3.9mm I.D.) packed with 5 micron spherical packing material was used. The mobile phase consisted of an acetonitrile:H<sub>2</sub>O mixture of 50:50 to 100:0 on a 10 min linear gradient,

at a flow rate of 1.7mm/min. Injection volumes of 10 microliters and a detector wavelength of 214nm were used.

## Results and Discussion

### Properties and Reactivity of MGEBA

The structure of MGEBA, shown below, was confirmed by MS, which revealed the anticipated molecular weight of 198 AMU, and by  $^1\text{H}$  and  $^{13}\text{C}$  NMR. The results of these analyses are discussed in chapter 4. An FTIR



spectrum of this monoepoxide, shown in Figure 3-1, is nearly identical to that of DGEBA. The MGEBA resin is a colorless, low viscosity liquid at room temperature and is slightly volatile at the temperatures required for the uncatalyzed dicy/epoxide reaction. A weight loss of 15% was observed for a sample heated to 190°C for two hours in an open DSC pan. However, no weight loss was observed for a similarly heated sample, when encapsulated in an aluminum DSC pan. Thus, the thermal and HPLC kinetic analysis of the uncatalyzed dicy/MGEBA reaction could be conducted without interference from MGEBA vaporization when reaction mixtures were similarly encapsulated.

The uncatalyzed dicy/MGEBA reaction was initially examined using temperature scanning DSC. A typical DSC trace is shown in Figure 3-2

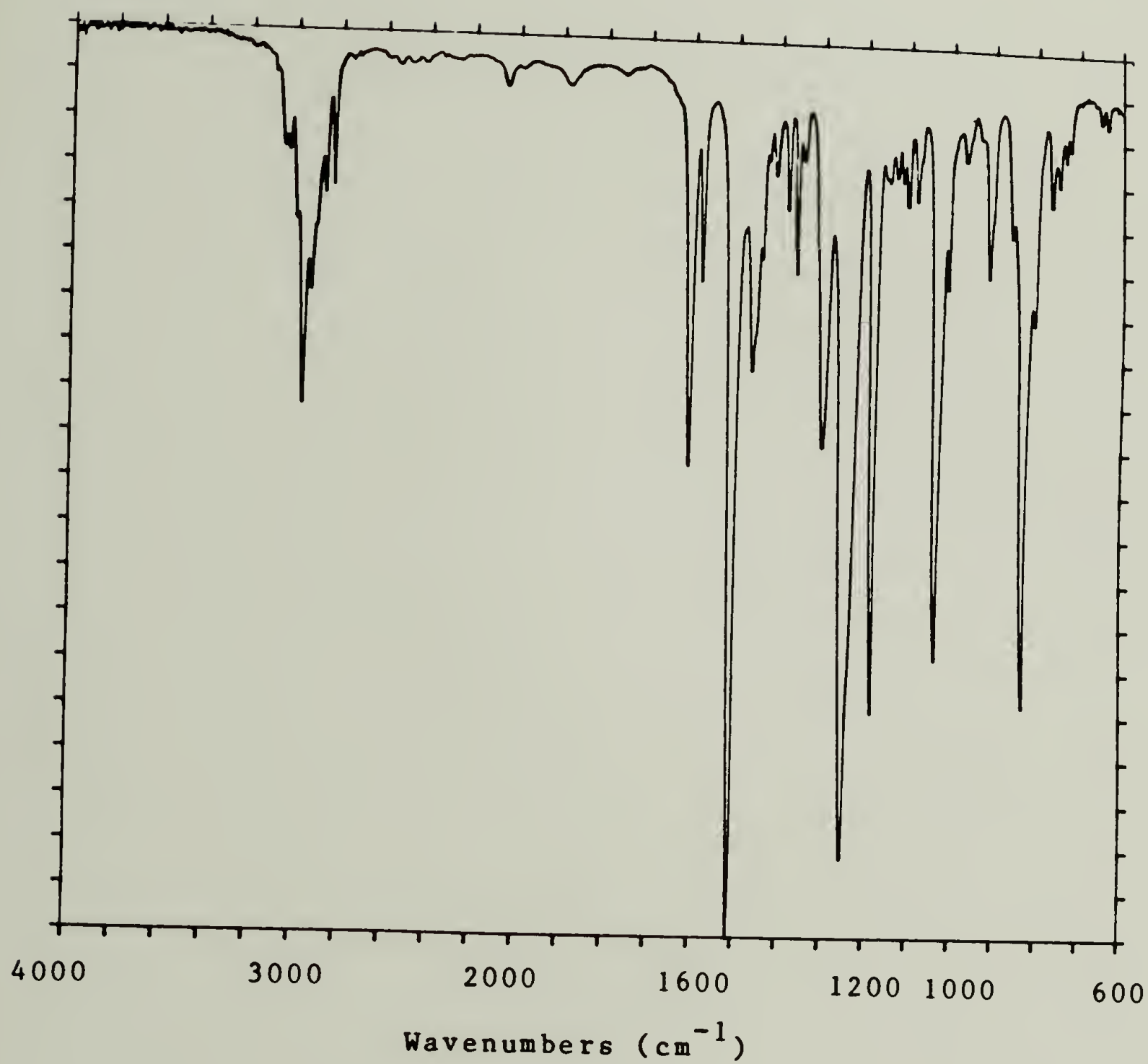


Figure 3-1: FTIR spectrum of MGEBA



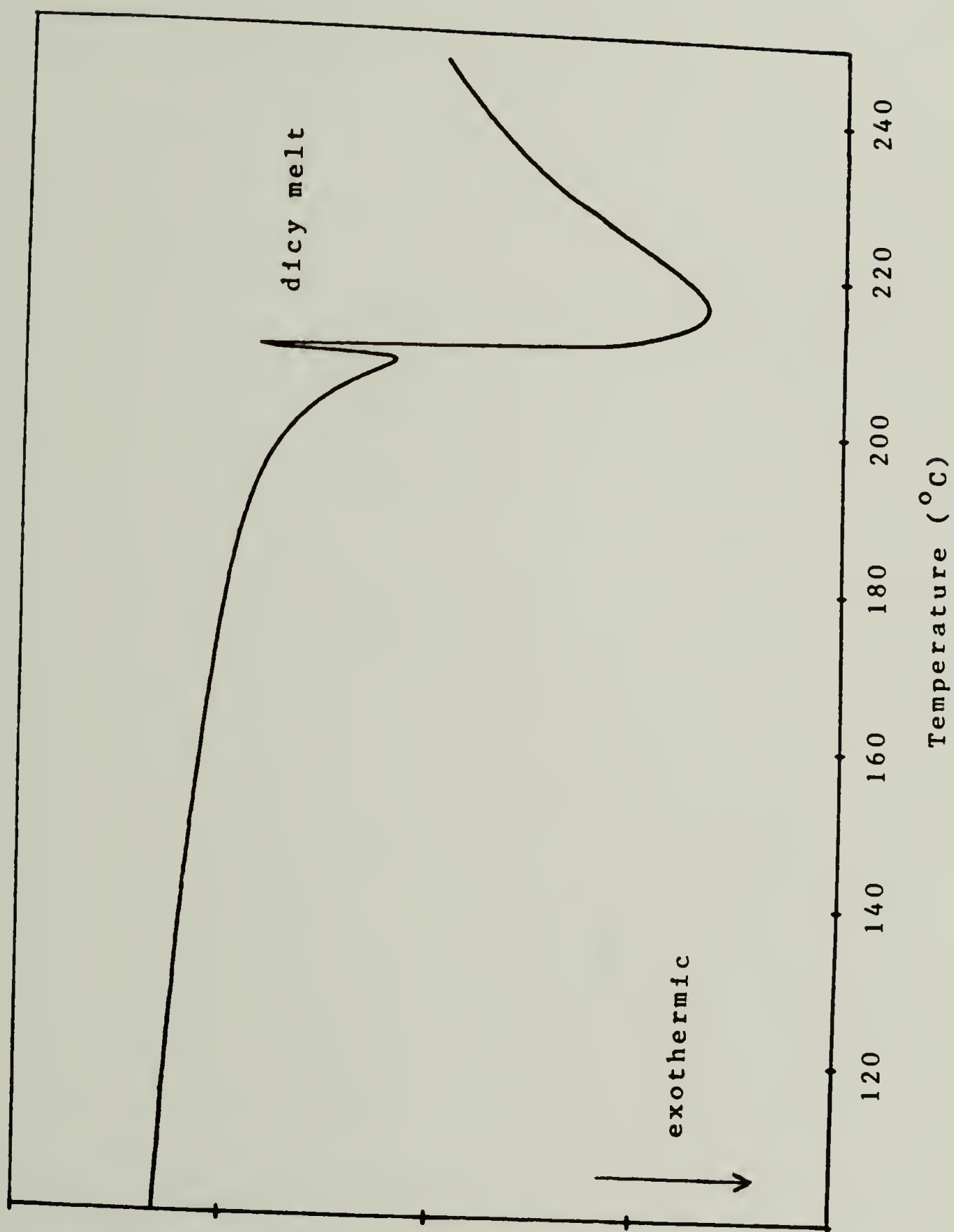


Figure 3-2: DSC temperature scan of 1:4 dicy/MGEBA at 5°C/min.

for a mixture containing four epoxide equivalents per dicy molecule (1:4), scanned at 5°C/min. A single exothermic peak is evident in this trace with an onset temperature of 190°C and a peak maximum at 215°C. Also evident is an endothermic spike associated with the dicy melt, superimposed over the exothermic region at a temperature of 209°C. A comparison with the DSC trace of the uncatalyzed dicy/DGEBA mixture shown in Figure 2-1 reveals that the exothermic region of the model compound system occurred in a temperature range which is 30°C higher than that observed for the principal exothermic region of the dicy/DGEBA cure, when scanned at an identical rate in the DSC.

The lower reactivity of the model system is an anticipated consequence of the relatively high weight to functionality ratio of the MGEBA molecule. This ratio, known as the epoxide equivalent weight (EEW), has a value of 298g/epoxide eq. for MGEBA compared with an EEW of 170g/epoxide eq. for purified DGEBA and 150g/epoxide eq. for PGE. In the dicy/MGEBA mixtures, the excess weight of the monoepoxide acts as a diluent, reducing the effective concentrations of both the oxirane functionalities and the relatively low molecular weight dicy molecules. This, in turn, results in a reduction in the overall rate of the dicy/DGEBA reaction. Intermolecular reactions, such as amine and imine addition to epoxide, should be equally affected by the dilution of reactive species in the monoepoxide system. Therefore, it was expected that the rates of these reactions, relative to one another, would be the same in this system as in the curing system. However, the dilution of reactive species was expected to have little, if any, effect upon intramolecular reactions. Thus, the rates of reactions,

such as cyclization, dicy dissociation and structural rearrangements, relative to those of the intermolecular additions, are expected to be higher in the monoepoxide system than in the uncatalyzed dicy/DGEBA cure. This relative enhancement must be taken into account when attempting to apply the results of the monoepoxide reaction study to the curing system.

Further complications were encountered, due to the lower solubility of dicy and cyanamide in MGEBA relative to DGEBA. Both MGEBA and DGEBA consist of polar oxirane functionalities attached to an essentially non-polar molecule. Because of the lower concentration of oxirane functionalities in the MGEBA resin, this material is less polar and is, consequently, a poorer solvent for the highly polar cyanamide and dicy molecules than DGEBA. In the case of dicy, this lower solubility further contributes to lower overall reactivity of the system. In the case of cyanamide, this lower solubility results in the formation of inhomogeneous cyanamide/MGEBA mixtures. The effects of this inhomogeneity on the reaction kinetics of this particular model system, are discussed below.

The uncatalyzed cyanamide/MGEBA reaction was also analyzed by temperature scanning mixtures in the DSC. A typical trace, shown in Figure 3-3 for a mixture scanned at a rate of  $5^{\circ}\text{C}/\text{min}$ , reveals two principal exothermic peaks, similar in appearance to those observed in the DSC scan of the cyanamide/DGEBA mixture shown in Figure 2-8. However, an exothermic spike associated with dicy crystallization is clearly evident in the scan of the cyanamide/monoepoxide mixture at a

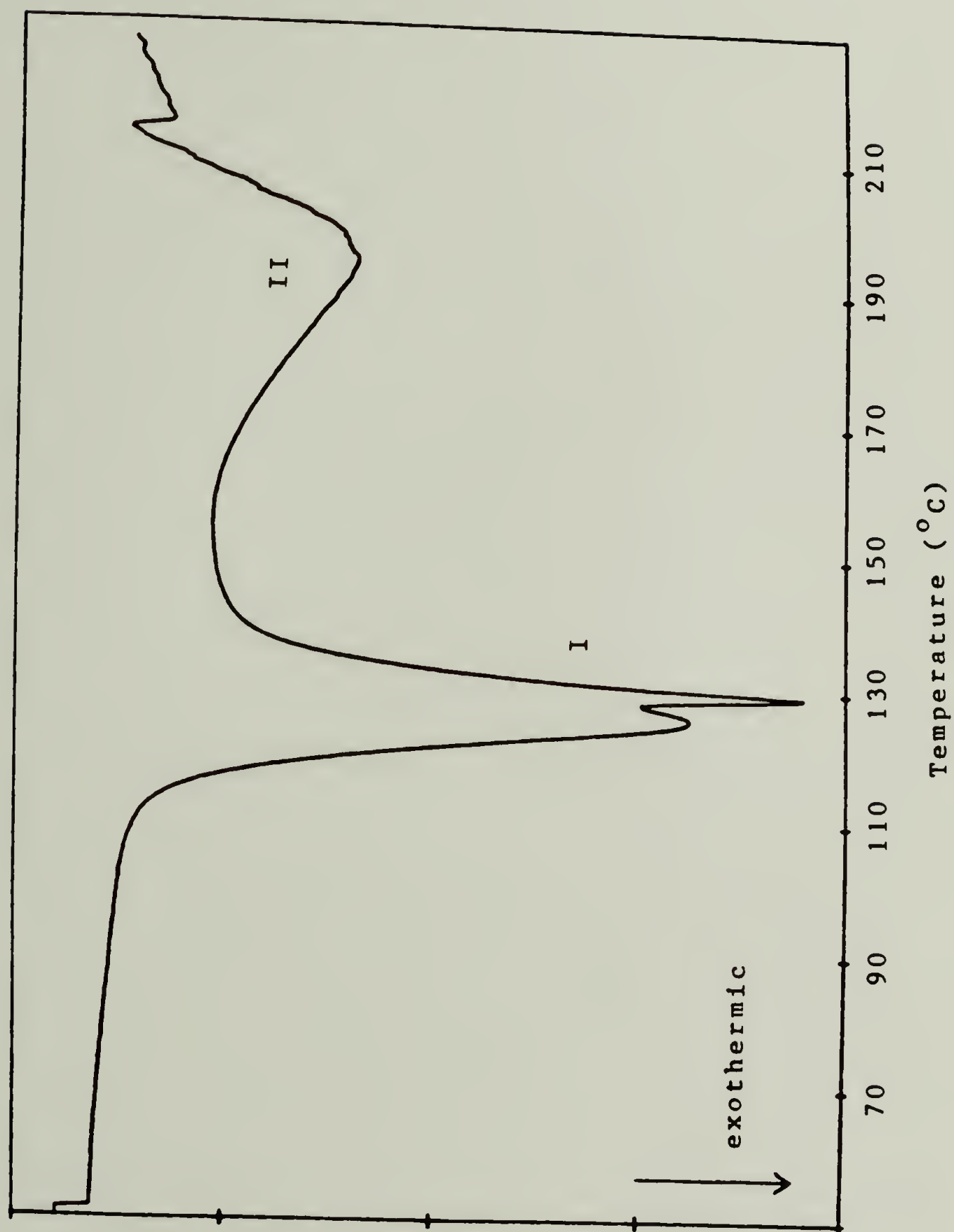


Figure 3-3: DSC temperature scan of 2:3 cyanamide/MGEBA at 5°C/min.



temperature of 130°C. This crystallization exotherm is similar to that seen in the DSC temperature scan of neat cyanamide, shown in Figure 2-7, indicating that a substantial amount of cyanamide dimerization had occurred when scanning through the initial exothermic region of this reaction. In order to determine the extent to which dimerization occurs in this system, cyanamide/MGEBA samples were scanned to 160°C, quenched, and analyzed by HPLC. The resulting chromatograms revealed the conversion of more than 50% of the cyanamide to dicy during these partial scans along with the consumption of a small amount of epoxide. Attempts were then made to limit cyanamide dimerization by isothermally reacting a range of cyanamide/MGEBA compositions at several temperatures for various lengths of time. In all cases over half of the available cyanamide was observed to dimerize to dicy.

Mixtures of cyanamide and MGEBA appear to be partially immiscible, even at the high temperatures required for reaction. Therefore, the high extent of cyanamide dimerization observed for this system is not surprising. HPLC analyses of isothermally reacted cyanamide/MGEBA mixtures, appear to indicate a rapid reaction between the cyanamide and MGEBA, generating several products which, along with the generated dicy, appeared to further react with MGEBA at a much slower rate. Due to the partial immiscibility of the reactants and the low concentration of initially formed products, this system could not be used to establish kinetic relationships for any of the various component reactions and, therefore, was not studied further. However, HPLC chromatograms of the initially formed cyanamide/MGEBA products were used to

tentatively identify components in chromatograms of the dicy/MGEBA reaction mixtures. In the study presented in chapter 4, use was made of the simplified cyanamide/MGEBA product mixtures to isolate purified products common to both the cyanamide/MGEBA and dicy/MGEBA reactions. Based on these identifications, the mechanism of the uncatalyzed cyanamide/MGEBA reaction, discussed in chapter 4, was postulated.

#### Thermal Analysis of the Dicy/MGEBA Reaction

While several dicy/MGEBA compositions were of interest to this study, mixtures with dicy/MGEBA compositions of 1:4 and 1:6 were primarily used for kinetic measurements. It was believed that the relatively high dicy loadings used in these mixtures would maximize the concentration of the initially formed intermediate products in the early stages of reaction, while minimizing the extent of etherification of longer reaction times. Compositions containing excess MGEBA were used to a lesser extent in order to identify products formed by etherification, as well as any other changes which might be attributable to low dicy concentration. Based on the results of the DSC temperature scans, isothermal reactions were conducted at temperatures of 167°, 172°, 187°, and 197°C. This temperature range was relatively narrow due to the high overall activation energy of the uncatalyzed reaction, and was similar to that used in the study of the uncatalyzed dicy/DGEBA cure.

The uncatalyzed 1:4 and 1:6 dicy/MGEBA compositions were isothermally reacted in the DSC in order to measure total heat of reaction for these compositions. Reactions were run at each of the isothermal

temperatures used in the HPLC kinetic study, so that a correlation could be made between product formation and generated heat. Identical values of 120 kJ/mole eq. epoxide were measured for each of these compositions at each of the four isothermal temperatures. Since vitrification does not occur and diffusion continues unabated throughout the course of this reaction, complete conversion was expected. However, while the measured heat of reaction is greater than the 108 kJ/mole eq. epoxide reported in the literature [23,27] for simple amine addition to epoxide, it is much less than the 155 kJ/mole eq. epoxide previously measured for the uncatalyzed dicy/DGEBA cure. Adjusting the DSC to maximum sensitivity, it was possible to discern a very small rate of reaction over long periods of time. A total heat of 160 kJ/mole was measured when including this long-term reaction. Correlations with the HPLC study discussed below indicated that this long term reaction occurred subsequent to complete epoxide consumption.

The extent of conversion at maximum rate of reaction, in the uncatalyzed model systems provided some insight into the physical nature of the uncatalyzed dicy/DGEBA cure. In the previous chapter, it was postulated that the conversion at maximum rate as measured by the partial heat of reaction is indicative of the average effective local concentration of dicy in the curing systems. While an unmilled 1:4 dicy/DGEBA mixture was found to have a maximum rate partial heat of 35 kJoules/mole eq. epoxide, a value of 60 kJoules/mole. eq. epoxide was measured for the milled sample. This latter value is identical to that measured for the uncatalyzed dicy/MGEBA mixtures of



similar composition. One of the questions was whether the lower average local dicy concentration in the unmilled sample was due to the larger size of the unmilled dicy particles or to diffusion control in the inhomogeneous system. Since unmilled dicy particles were used for the monoepoxide reactions, it appears that dissolution is not the controlling factor, thus supporting the build-up of regions of varying composition, postulated in the previous chapter for the cure of the unmilled dicy/DGEBA systems.

As in the case of the uncatalyzed dicy/DGEBA cure, the maximum rate extent of conversion for the uncatalyzed dicy/MGEBA reaction is invariant with respect to cure temperature. Thus, the time to maximum rate can be used to determine an overall energy of activation for the system. On this basis, a value of 150 kJ/mole was calculated, which is identical to that calculated by a similar means for the uncatalyzed dicy/DGEBA cure. Thus it appears that the rate controlling step for both the cure and model reaction are the same.

An attempt was made to assess the effect of catalyzation by BDMA on the overall activation energy of the dicy/MGEBA reactions. Isothermal DSC reactions were run in a range of 107° to 147°C. Again extent of conversion at maximum rate, determined by partial heat of reaction, was invariant with respect to cure temperature. Based on times to maximum rate, an energy of activation of 75 kJ/mole was calculated for the catalyzed dicy/MGEBA reactions. This value is identical to those reported in the literature for catalyzed dicy cured epoxies [39,42].



### HPLC Analysis of the Dicy/MGEBA Reaction

A single batch of MGEBA was used in formulating the mixtures used in the HPLC kinetic study of the uncatalyzed dicy/MGEBA reaction. This was done in order to prevent changes in reactivity which might occur due to variations in the amounts of trace contaminants. Because of the insolubility of dicy in the monoepoxide, there was some difficulty in obtaining uniform mixtures. Therefore, several unreactive samples were removed from each batch and analyzed for composition by HPLC, which indicated average variations in dicy concentration of less than 10%, while variations in MGEBA concentration were less than 1%. Samples were isothermally reacted in the DSC for specific lengths of time, quenched to room temperature and weighed. Samples experiencing weight losses greater than 0.5% were discarded. Solutions were made by dissolving mixtures in a solution of 5% H<sub>2</sub>O in THF. No attempt was made to refrigerate these solutions and some long term ageing was observed. The nature and extent of this ageing is discussed below.

A variety of separatory conditions, solvents, and columns were employed in the HPLC analysis of the dicy/MGEBA product mixtures. The goal was to separate as many of the individual components as possible into single chromatographic peaks which could then be identified and quantified. A typical chromatogram is shown in Figure 3-4 for an uncatalyzed 1:6 dicy/MGEBA composition, reacted at 197°C for 30 minutes. A THF/H<sub>2</sub>O mobile phase run at a 50 to 65%, 20 minute linear gradient, was used in this separation. The resultant chromatogram is deceptively simple in appearance. Aside from peak B, assigned to MGEBA, seven major product peaks are evident in this trace. However,

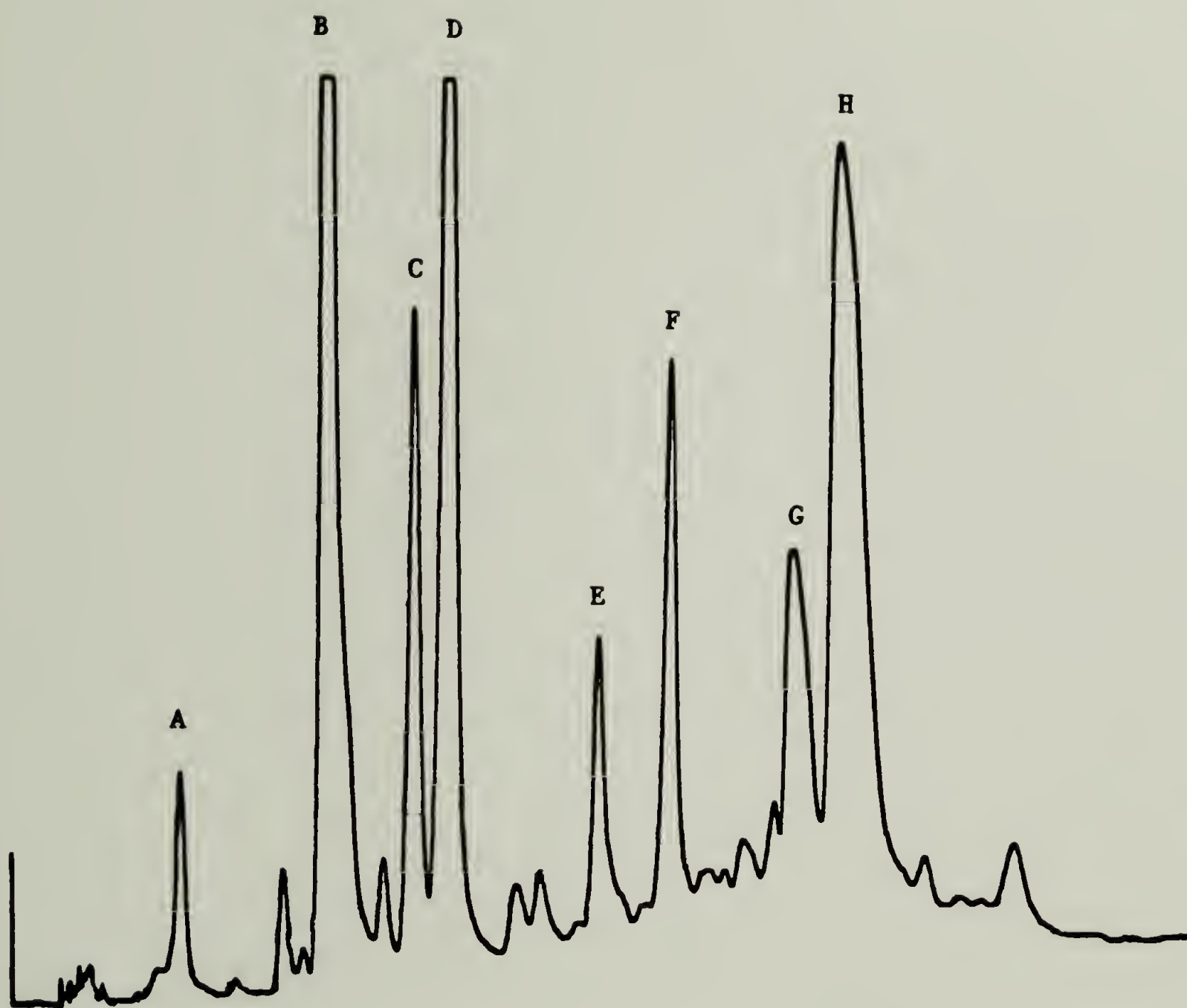


Figure 3-4: HPLC chromatogram of 1:6 dicy/MGEBA reacted at 197°C for 30 min; THF/H<sub>2</sub>O = 50-90%, over 40 min, at grad 6, analyzed at 280nm.

when examined under several different sets of conditions, it appeared that many of these product peaks contained multiple components. Although these different conditions might result in the appearance of several product peaks of different composition, the resolution of individual species could not be improved.

Difficulties were encountered in improving product resolution, due to the unknown number and identity of components contained in the mixtures. Depending on the relative rates of the various reactions and in the absence of etherification, thirteen potential products were anticipated from the dicy/MGEBA reaction in accordance with the mechanism proposed by Zahir. In addition, stereoisomers of these products, separable by reverse-phase HPLC, were expected to be formed by the incorporation of chiral epoxide units into multiply substituted adducts [69]. The presence of these stereoisomers in the dicy/MGEBA product mixtures was expected to further increase the number of components observed in these chromatograms especially for the most highly substituted species. However, due to the widely different rates of the several components reactions, it was found that the lifetimes of certain products were too short to allow the accumulation of detectable quantities.

#### Chromatographic Peak Identification

As discussed in the introduction of this chapter, longer elution times were generally expected for the dicy/MGEBA products with successively higher degrees of substitution. On this basis, peak A was thought to contain one or more monosubstituted adducts, while peaks C



and D were tentatively assigned to disubstituted species. Peaks F, G, and H were expected to contain the more highly substituted products of the dicy/MGEBA reaction. Peak E was known to contain a contaminant of the MGEBA resin, formed by the addition of two monomethyl bisphenol A molecules to epichlorohydrin. However, this peak also contained one or more products of the dicy/MGEBA reaction. A great multiplicity of components appeared to elute in the region of peaks F, G, and H. Subtle changes in the conditions used for separation resulted in large differences in the number, shape, and relative sizes of the peaks found in this region. Since the products eluting in this region had a higher degree of epoxide substitution, a large number of HPLC resolvable stereoisomers were expected for these products, thereby increasing the complexity of the chromatogram at longer elution times. Further complications in this region were also expected, due to the elution of products formed by the small amount of etherification which was believed to occur in the uncatalyzed system. Although difficulties were encountered in resolving the higher molecular products of the dicy/MGEBA reaction, the relatively polar, lower molecular weight fraction of the product mixture was found to consist of a simple combination of species, readily separable using a range of separatory conditions.

An attempt was made to identify the product peaks of the dicy/MGEBA chromatograms by comparison with the chromatograms of the products formed in the early stages of the uncatalyzed cyanamide/MGEBA reaction. An example of the latter, shown in Figure 4-5 of the following chapter, reveals the presence of cyanamide/MGEBA reaction



products coeluting with peaks A, C, and D, and to a lesser extent, peaks G and H in the dicy/MGEBA chromatogram. The cyanamide/MGEBA product, which coelutes with peak A of the dicy/DGEBA chromatogram is the initially formed product of the cyanamide/MGEBA reaction and was believed to be the 1:1 adduct. The products coeluting with peaks C and D of the dicy/MGEBA reaction mixture appeared to be disubstituted adducts of the cyanamide/MGEBA reaction. Since, as discussed in chapter 2, the cyclization of disubstituted 2-hydroxy cyanamides was expected to proceed rapidly at room temperature [70], it was believed that these peaks could be assigned to the cyclical products described by Zahir. Observations of these two peaks over the course of both the cyanamide/MGEBA and dicy/MGEBA reactions appeared to indicate the slow transformation of peak C into peak D when heated for prolonged periods of time. This observation was consistent with the designation of peak C as the disubstituted 2-imino oxazolidine and peak D as the disubstituted cyclical urea formed by the rearrangement of the 2-imino oxazolidine.

The products from peaks C and D of the dicy/MGEBA reaction mixtures were found to be coelutable with their cyanamide/MGEBA counterparts over a wide range of separatory conditions. Therefore, it appeared that identical products were formed by the two reactions, supporting the Zahir mechanism for the uncatalyzed dicy/epoxide reaction. According to the Zahir mechanism, these products are formed by the cyclization and dissociation of substituted dicy adducts. The measurement of the rate of formation of these products, relative to MGEBA consumption, was expected to provide an evaluation of the rela-

tive rate of amine/epoxide addition and cyclization/dissociation reactions for this system. However, some difficulties were anticipated. While the disubstituted 2-imino oxazolidine and cyclic urea appeared to be the predominant components of peaks C and D, respectively, in the dicy/MGEBA reaction mixtures, it was unknown whether other minor components might also be present in these peaks. In particular, no disubstituted dicy adducts were identified in these chromatograms. Although these products may have been too reactive to accumulate to detectable quantities in the reaction mixture, it was also possible that they coeluted as minor components of either peak C or D of the HPLC chromatograms. In order to determine the relative rate of formation of cyclical products, it was necessary to quantify the species formed by the further reactions of products C and D with MGEBA. Due to the complexity of the less polar, high molecular weight regions of the dicy/MGEBA product mixture chromatograms, it was difficult to assign specific peaks to these products. However, by following the course of the reaction it was assumed these additional assignments could be made.

#### Detector Wavelength and Product Quantification

In the chromatogram shown in Figure 3-4, eluting components were detected by the absorbance of ultraviolet light from a 280nm source. The areas of the chromatographic peaks, generated by the detector signal were directly proportional to the concentration of eluting components multiplied by the extinction coefficient of the individual species. Different extinction coefficients were expected for various reactants and products. Further, the specific extinction coefficients

were expected to be dependent on mobile phase composition and elutant concentration, resulting in a non-linear relationship between peak areas and component concentrations. However, when analyzed at 280nm, a linear relationship between component concentration and peak area was observed for MGEBA, BPA, and the several isolated products from the dicy/MGEBA reaction, as discussed in the following chapter. It was also found that at 280nm the molar absorbance of light for these compounds was directly proportional to the weight fraction of bisphenol A moieties contained in each of the eluting peaks. Thus, at this wavelength, the concentration of individual products could be directly ascertained from the chromatogram peak areas.

Since dicy does not absorb at 280nm, it was necessary to conduct analyses at 229nm, which is the wavelength of maximum ultraviolet light absorbance by dicy [3], in order to determine the rate of consumption of dicy. A typical chromatogram is shown in Figure 3-5 for a mixture analyzed using a 229nm detector. The product mixture and conditions of separation were identical to that used in the chromatogram of Figure 3-4. Aside from the peak assigned to dicy, eluting at the void volume [71], the chromatograms appear to be identical. However, the ratio of the areas of the product peaks relative to that of the MGEBA peak are different for the two chromatograms. It is believed that this difference is attributable to the higher relative molar absorbances of linearly substituted dicy adducts at 229nm compared with 280nm. It was felt that by examining the relative peak area ratios for mixtures analyzed at these two wavelengths, the identities and purities of the several major product



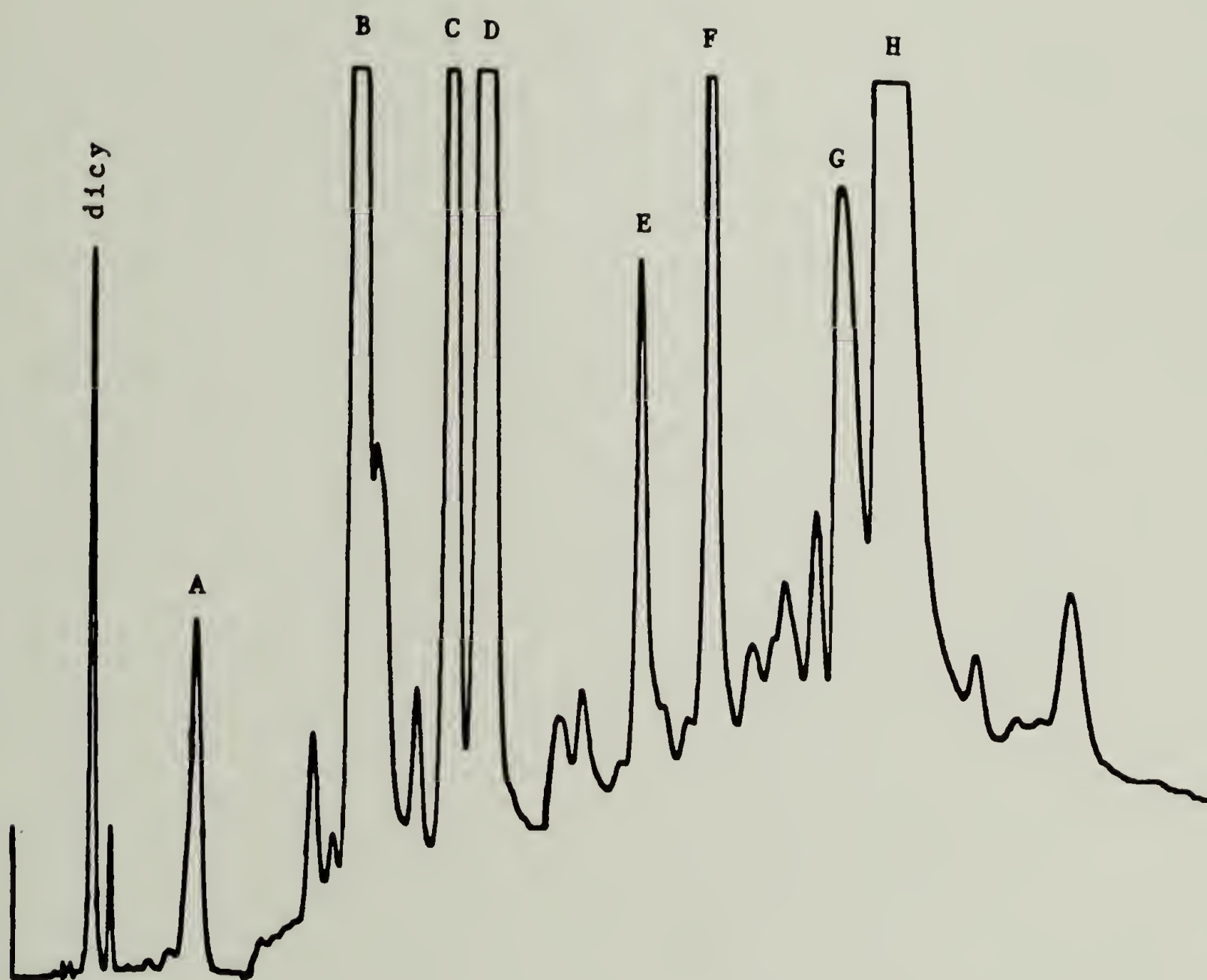


Figure 3-5: HPLC chromatogram of 1:6 dicy/MGEBA reacted at 197°C for 30 min; THF/H<sub>2</sub>O = 50-90%, over 40 min, at grad 6, analyzed at 229nm.



peaks could be qualitatively probed. However, it was found that only the areas of peaks A and C were increased relative to the area of the MGEBA peak when examined at 229nm as compared to 280nm. All other peak areas remained unchanged relative to MGEBA. Despite difficulties with baseline determination due to THF absorbance at 229nm, similar results were observed for a number of product mixtures. Based on these comparisons, it appears that no significant amounts of linear dicy adducts can be identified in the higher molecular weight region of the chromatogram.

#### Effect of Solvent

HPLC chromatograms of the uncatalyzed dicy/MGEBA reaction mixtures were also obtained using a mobile phase of acetonitrile and water. This is similar to the system used by Galy et al. [44] to separate the products of the catalyzed dicy/PGE reaction mixtures. A typical chromatogram using a Resolve C-18 column with the acetonitrile/H<sub>2</sub>O mobile phase is shown in Figure 3-6. Several of the peaks are alphabetically labelled to indicate their corresponding elution in the chromatogram of Figure 3-4. As can be seen, products assigned to peaks C and D are poorly resolved. In fact, when using the micron Bondapak column with this mobile phase, C and D were found to elute as a single peak. However, it was found that better resolution of the several minor components of importance to this study could be obtained using these conditions. For purposes of comparison, a chromatogram of the initial products of the uncatalyzed cyanamide/MGEBA reaction mixture, analyzed using identical separatory conditions is shown in Figure 3-7. Again, peaks C and D appear similar for the two mixtures.

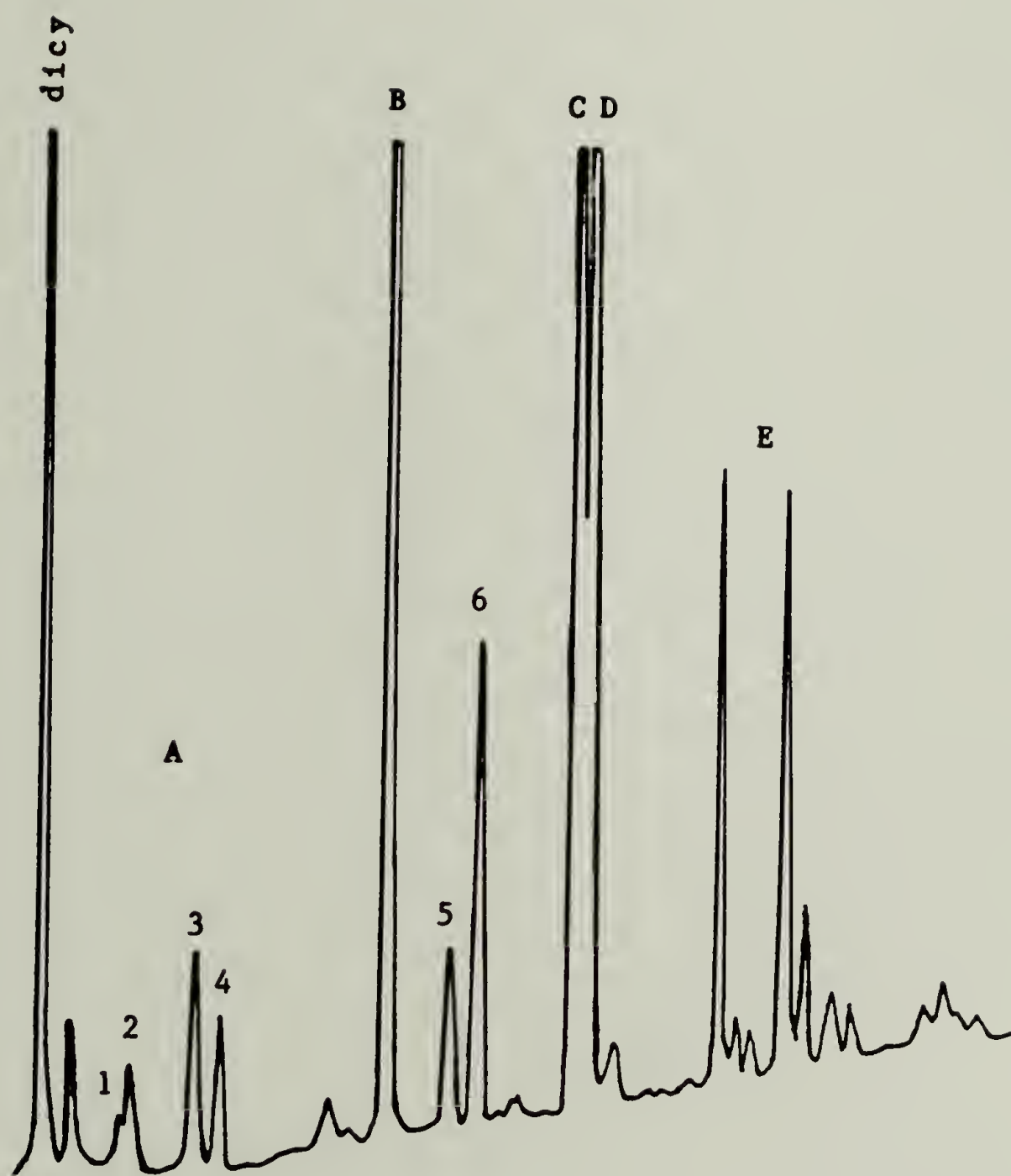


Figure 3-6: HPLC chromatogram of 1:4 dicy/MGEBA reacted at 197°C for 30 min, Acetonitrile/H<sub>2</sub>O = 50-100%, 10 min, grad 6, analyzed at 214nm.

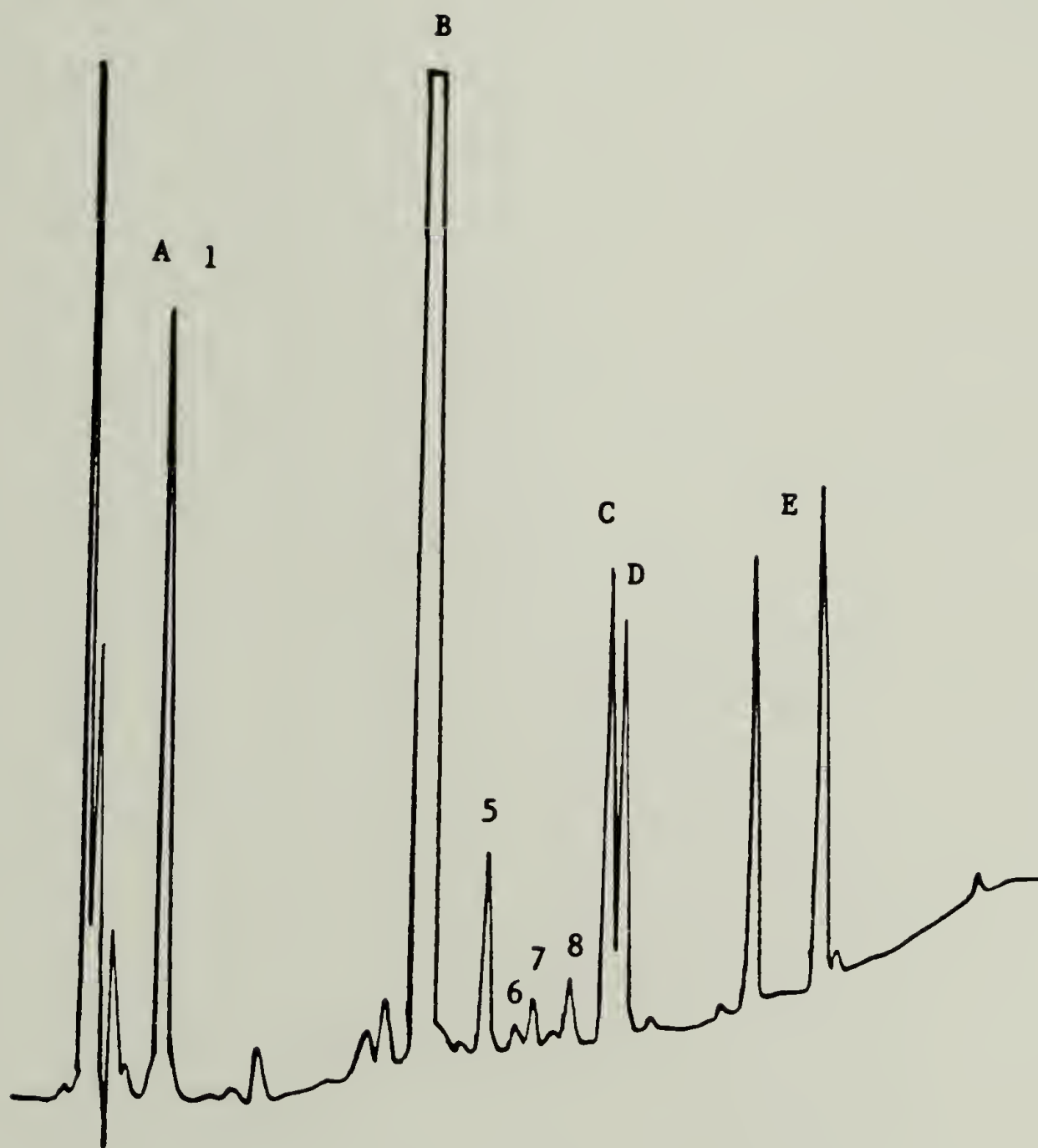


Figure 3-7: HPLC chromatogram of 1:2 cyanamide/MGEBA reacted at 127°C for 60 min, Acetonitrile/H<sub>2</sub>O = 50-100%, 10 min, grad 6, analyzed at 214nm.

However, differences were found in the resolution of peak A. For the dicy/MGEBA system this peak was found to contain four separate components, labelled 1 to 4. Peak A of the cyanamide/MGEBA system, on the other hand, appears to be composed of a single product, 1, which was, at best, only a very minor component of the dicy/MGEBA reaction mixture. Other differences exist in the region containing peaks 5,6,7 and 8. These peaks represent minor components in the reaction mixture, the significance of which is discussed in Chapter 4. Unseen in these chromatograms are any of the less polar, higher molecular weight species assigned to peaks F, G, and H of the chromatogram shown in Figure 3-4. These products were too non-polar to be eluted from either of the C-18 columns when using acetonitrile as the mobile phase. While PGE products are expected to be more polar than their MGEBA counterparts, the possible existence of uneluted material may significantly alter the interpretation of Galy's results.

#### Rates of Reactant Consumption and Product Formation

Plots of reactant and product concentrations versus time were constructed in order to elucidate the course of the uncatalyzed dicy/MGEBA reaction. The concentrations of MGEBA and the various products were determined by chromatographic peak areas obtained at 280nm, while dicy concentrations were based on analyses made at 214nm. Due to changes brought about by the room temperature aging of product solutions all measurements used in these plots were obtained within two weeks of product formation. In order to simplify the resulting plots, the concentrations of the disubstituted cyclical products C and D were combined. It was difficult to identify the products of the



further reactions of peaks C and D in the product chromatograms. However, peaks G and H appeared to exhibit a steady growth throughout the course of the reaction, and initially appeared to be assignable to the more highly substituted cyclical products. Therefore, the concentrations of these species were also combined and plotted. In order to determine changes in the rate of heat generation relative to epoxide consumption, the extent of reaction as determined by DSC was also plotted versus time.

Plots are shown in Figures 3-8 to 3-15, for the reactions of the 1:4 and 1:6 uncatalyzed dicy/MGEBA compositions at temperatures of 167° to 197°C. No major mechanistic changes are evident over the range of temperatures encompassed by these plots. Further, a comparison of these plots reveals a great similarity between the relative rates of reactant consumption, heat generation, and product formation for the two compositions over the temperature range. The isothermal DSC traces discussed in the thermal analysis section of this chapter appear to directly follow the course of epoxide consumption. Thus, the overall energies of activation determined from the times required to attain maximum rate of heat generation appear to be directly applicable to the dicy/MGEBA reaction.

Also, the extent of MGEBA consumption appears to increase linearly with the extent of dicy consumption over the initial 70 to 80% of the reaction. This is graphically illustrated in Figure 3-16. It is evident from this plot, that the rate controlling step for this system is the initial dicy/epoxide reaction. Based on the molar ratio of

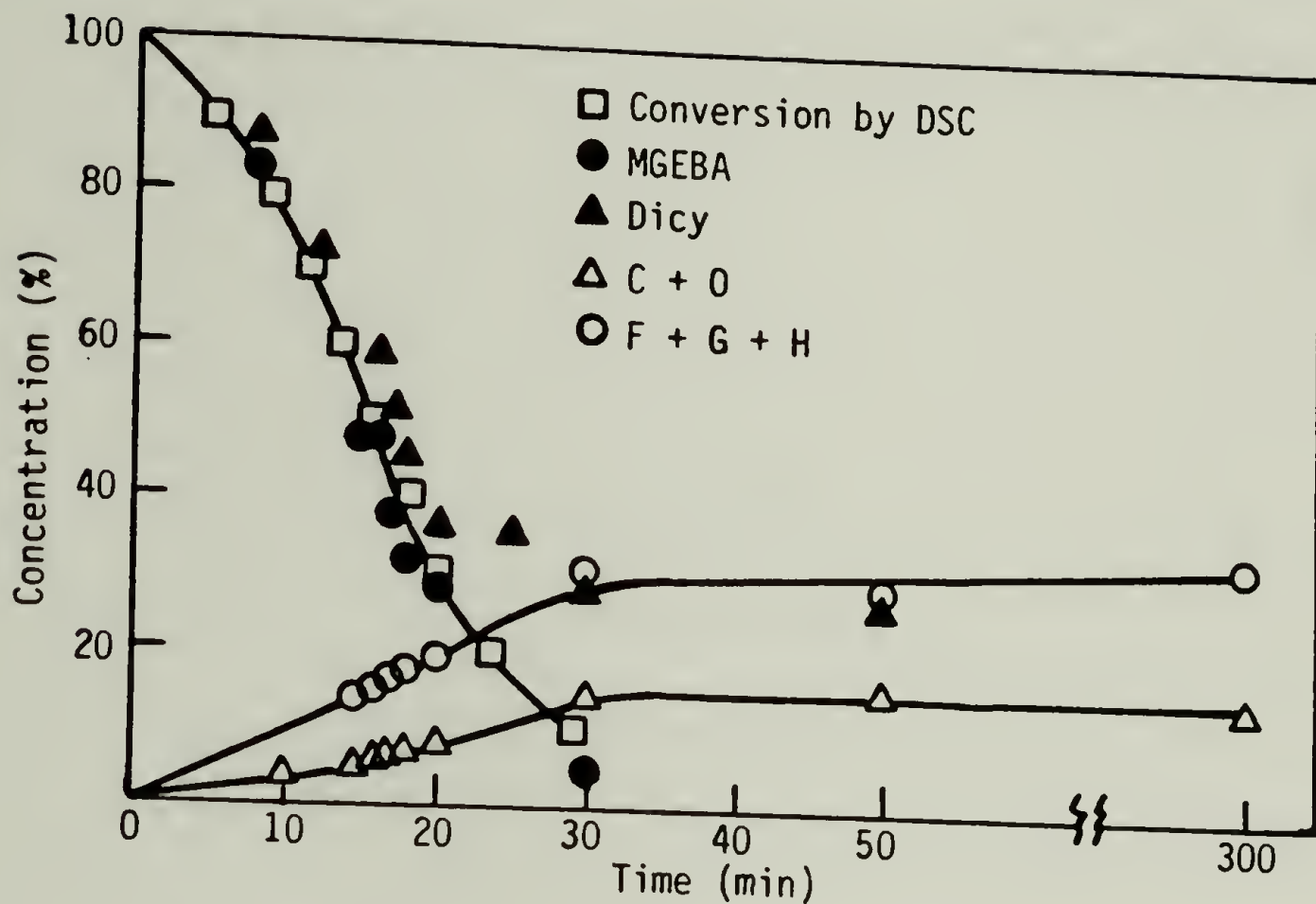


Figure 3-8: Products and reactants vs time for 1:4 dicy/MGEBA reacted at 197°C.

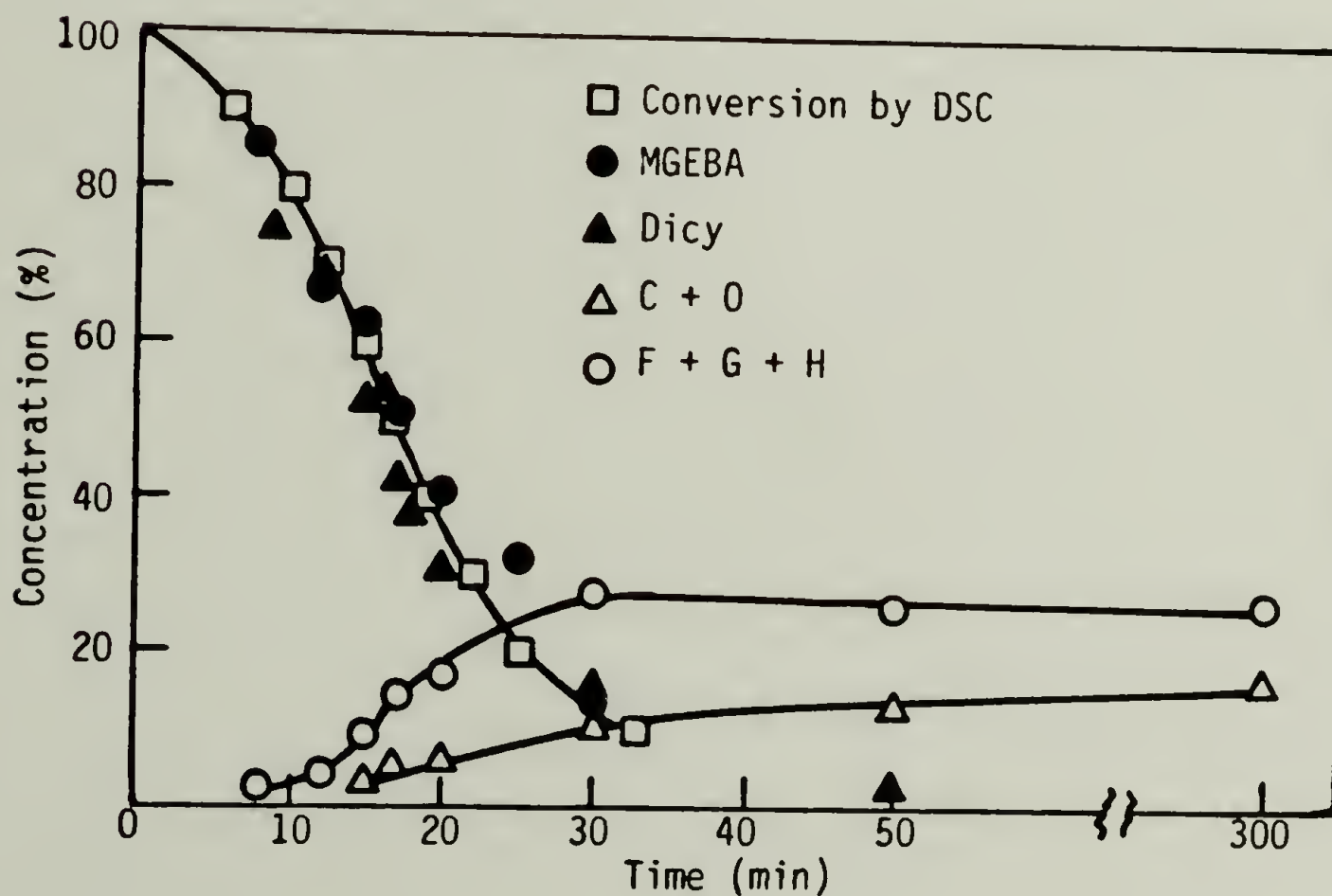


Figure 3-9: Products and reactants vs time for 1:6 dicy/MGEBA reacted at 197°C.

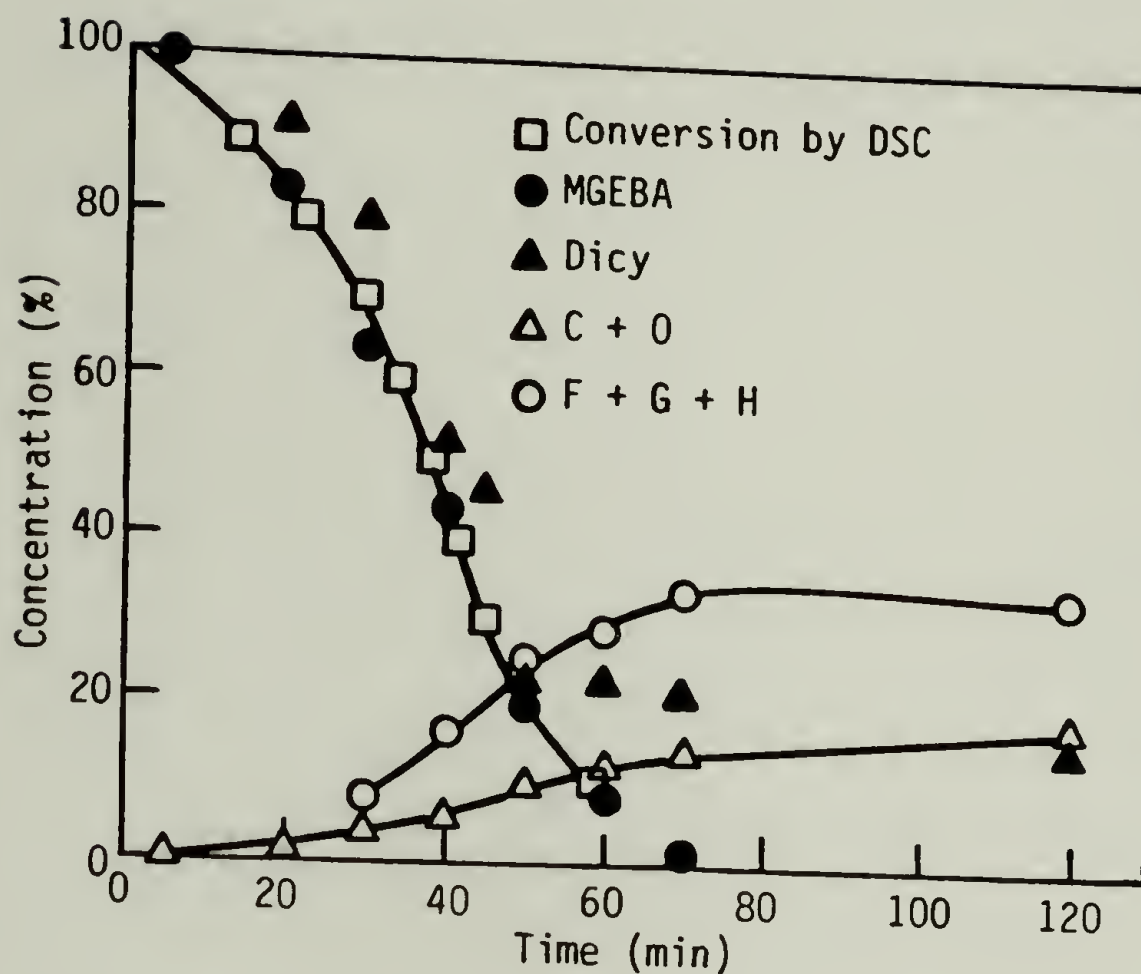


Figure 3-10: Products and reactants vs time for 1:4 dicy/MGEBA reacted at 187°C.

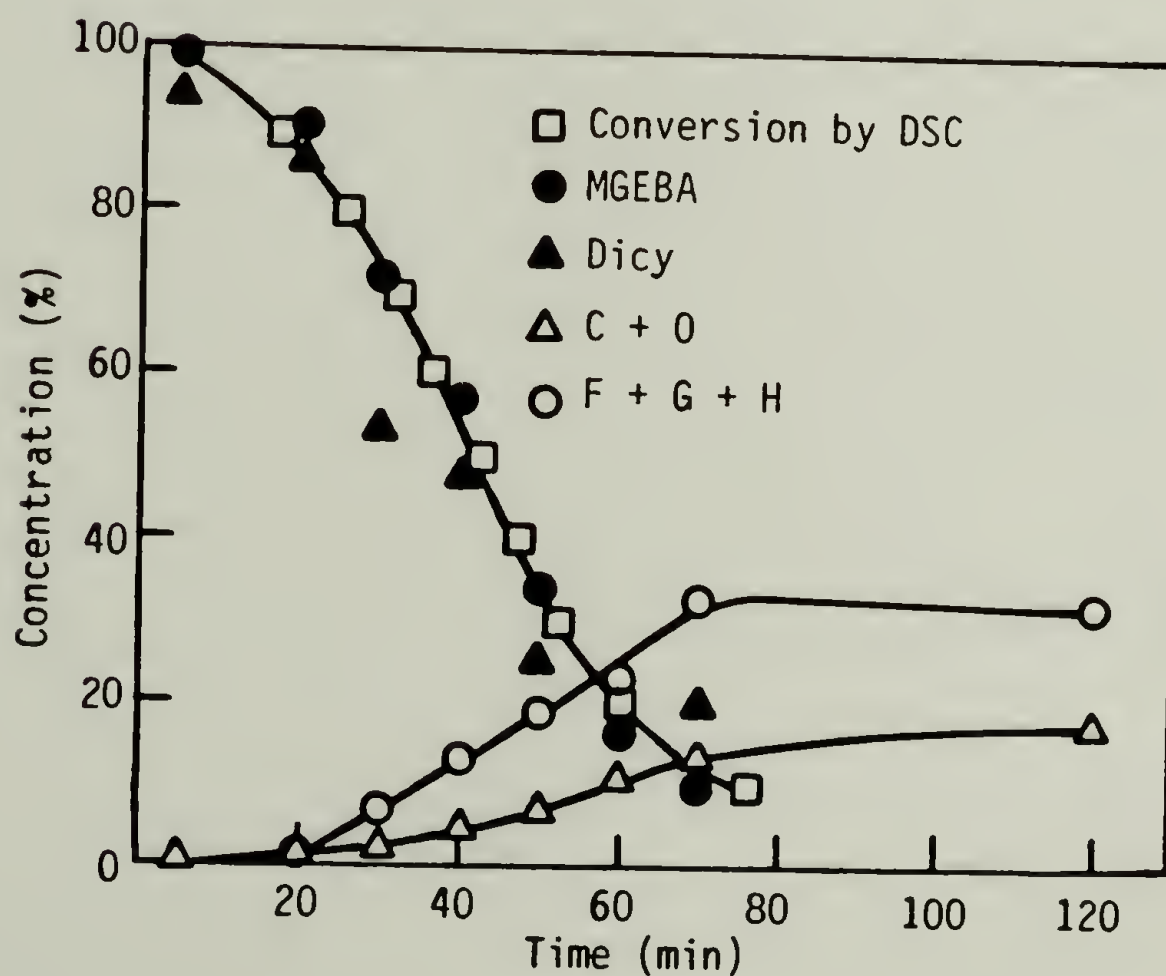


Figure 3-11: Products and reactants vs time for 1:6 dicy/MGEBA reacted at 187°C.

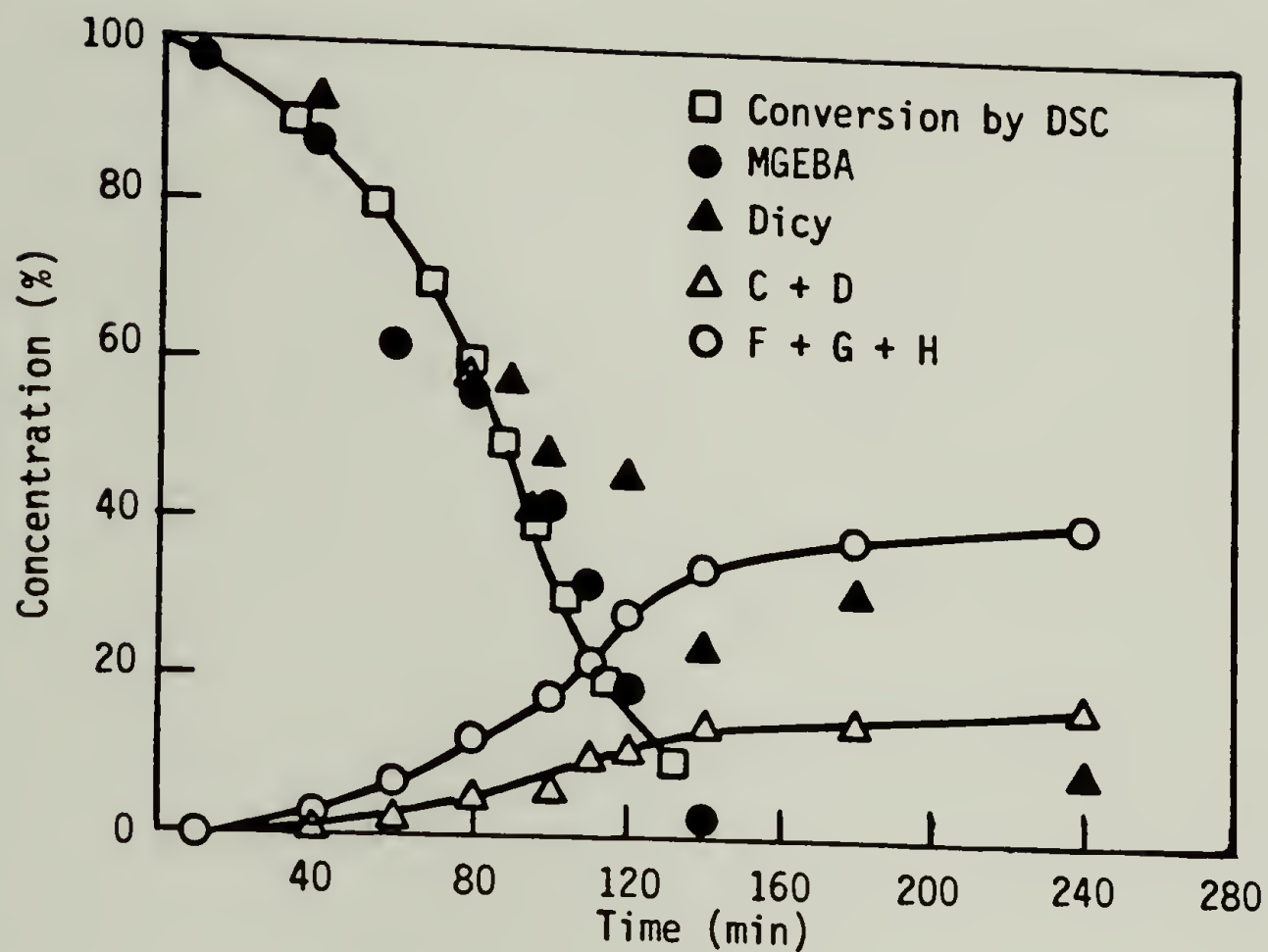


Figure 3-12: Products and reactants vs time for 1:4 dicy/MGEBA reacted at 177°C.

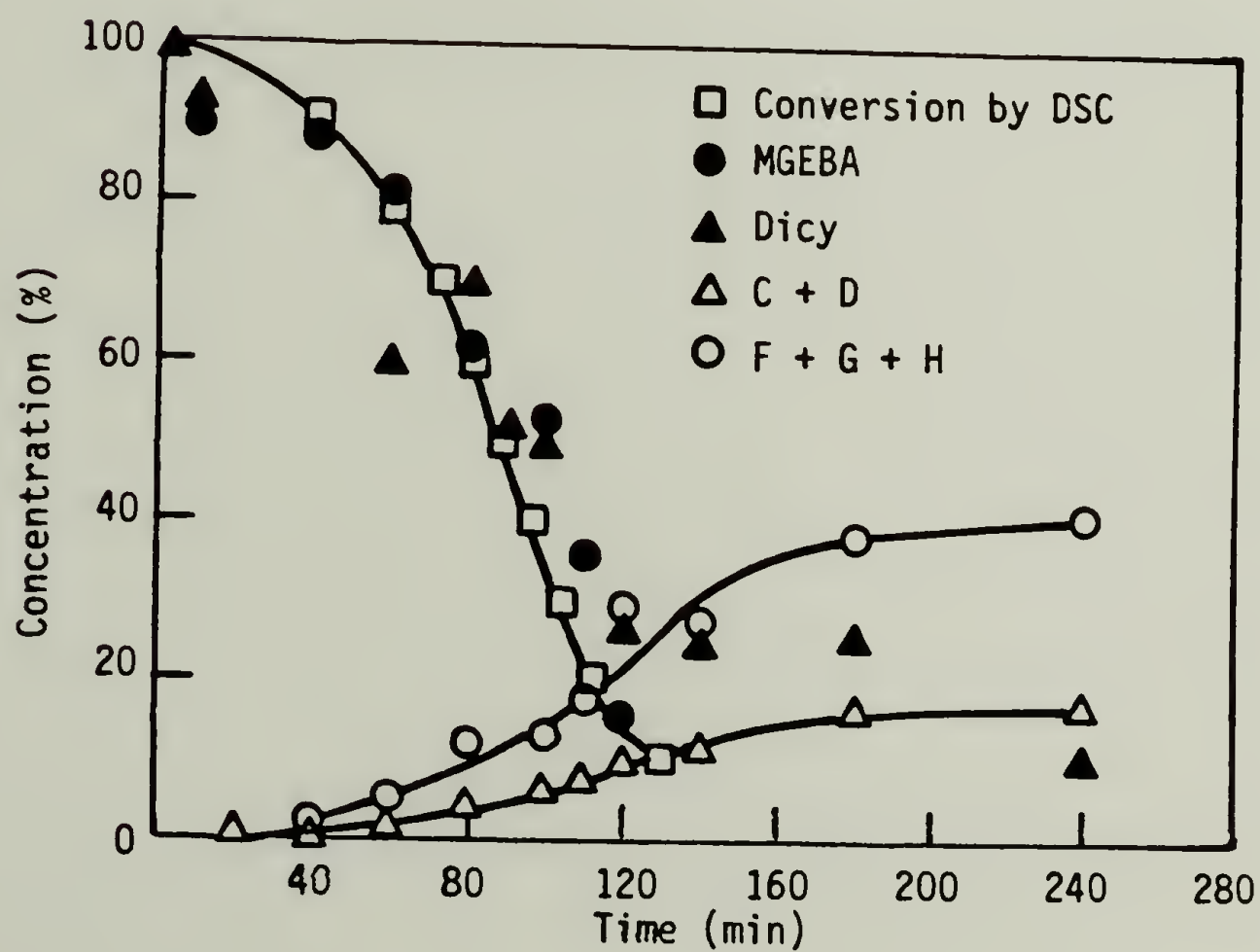


Figure 3-13: Products and reactants vs time for 1:6 dicy/MGEBA reacted at 177°C.



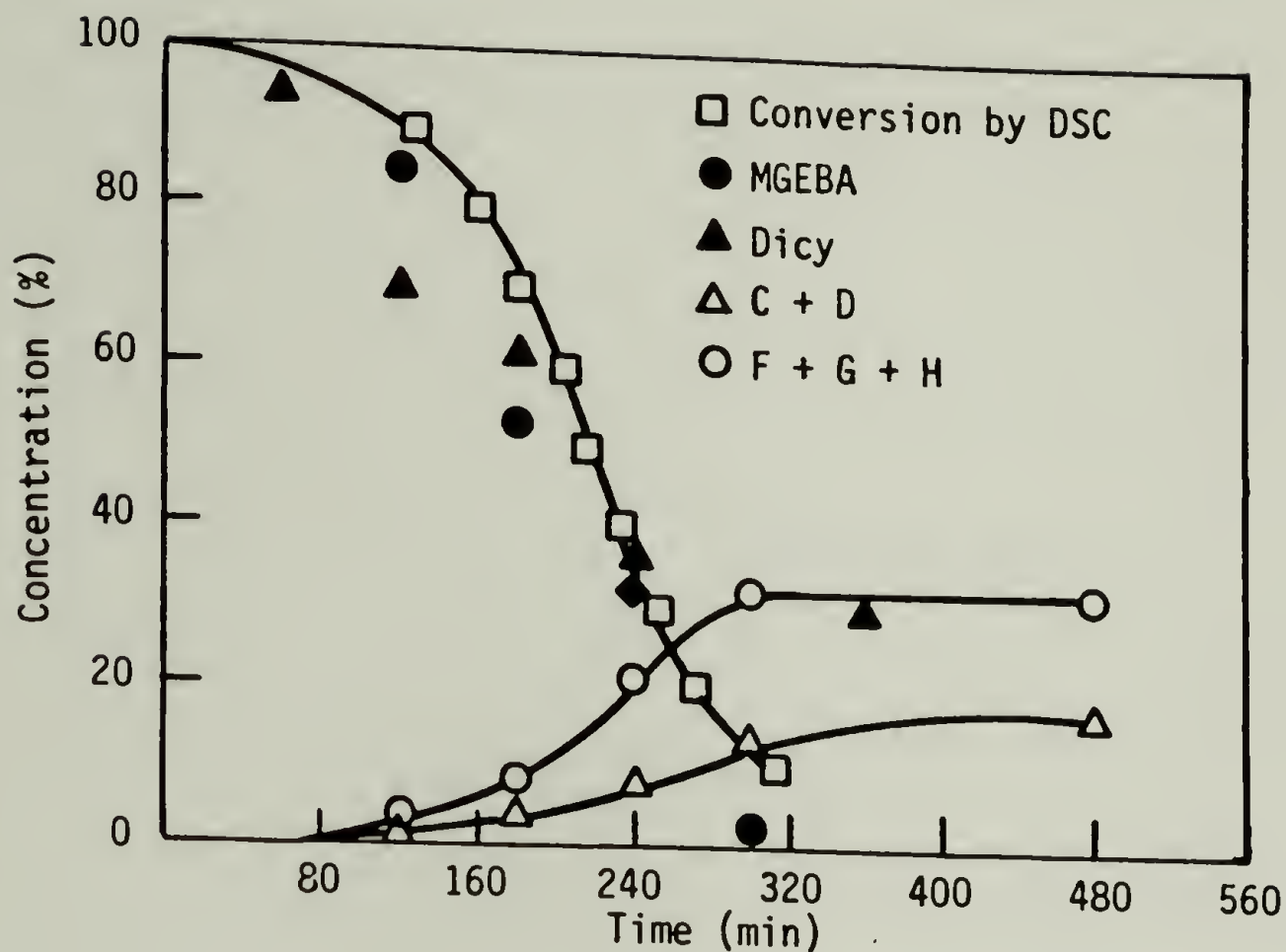


Figure 3-14: Products and reactants vs time for 1:4 dicy/MGEBA reacted at 167°C.

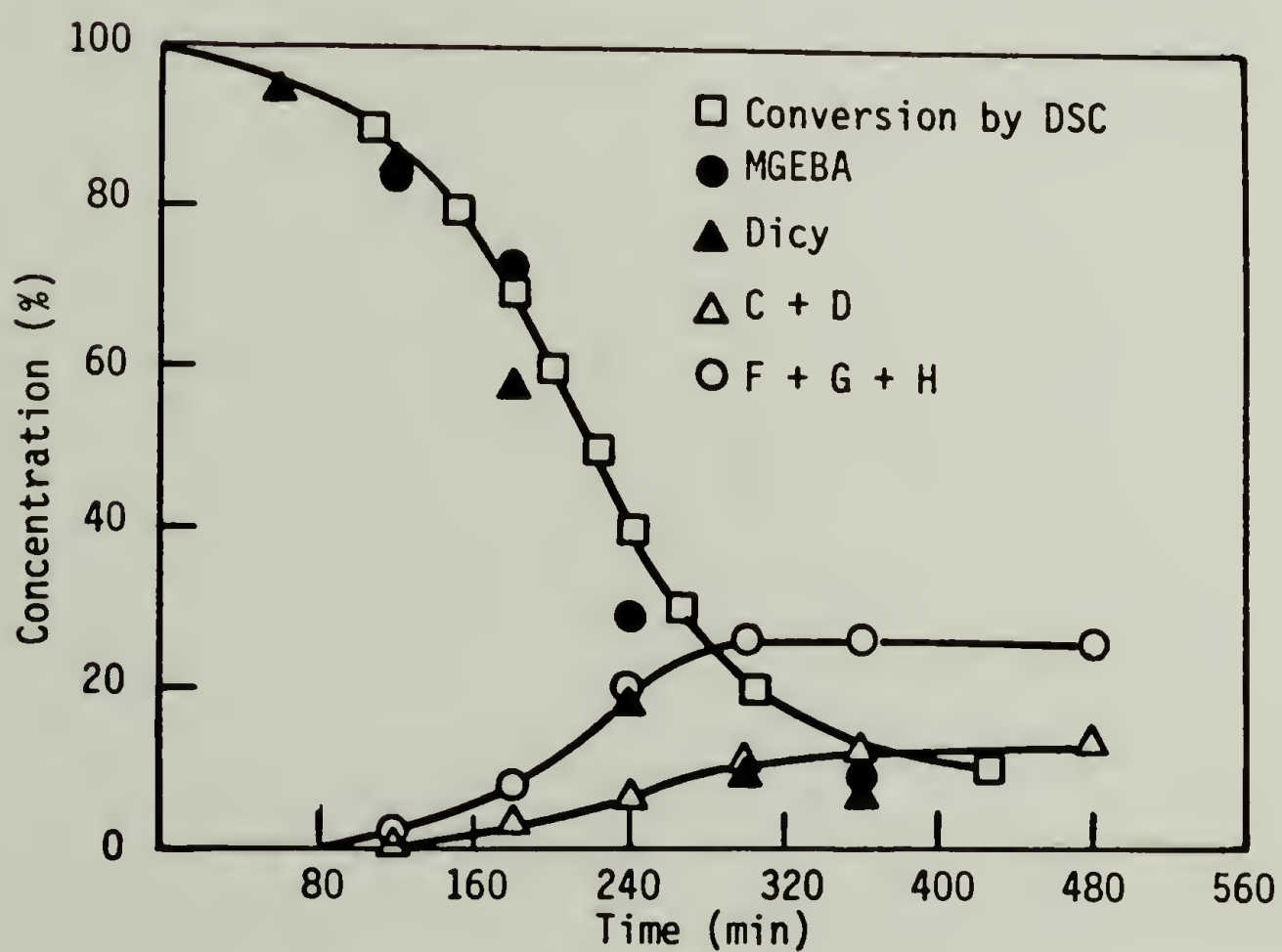


Figure 3-15: Products and reactants vs time for 1:6 dicy/MGEBA reacted at 167°C.

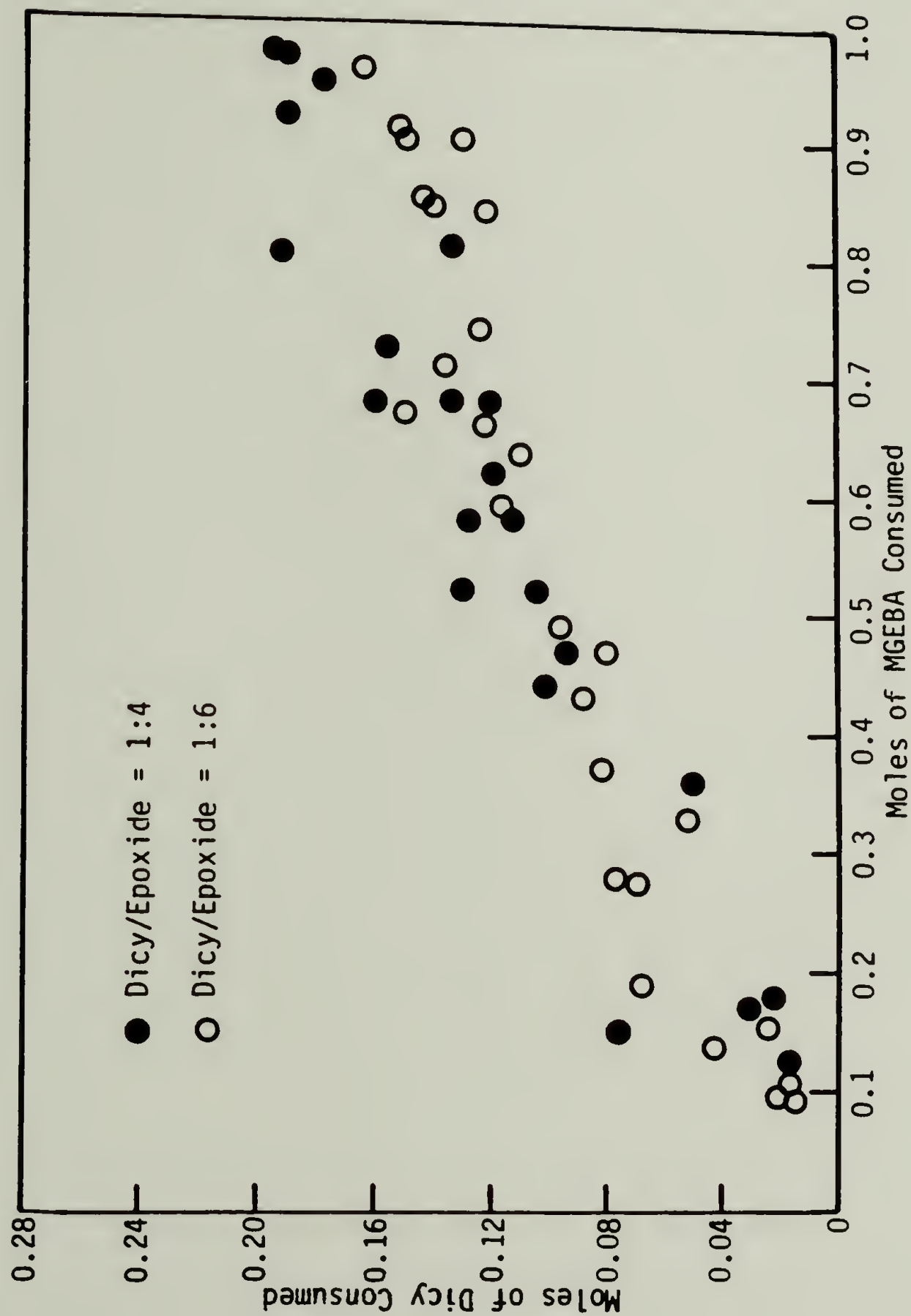


Figure 3-16: Dicy consumption vs MGEBA consumption 167°-197°C.

epoxide consumed relative to dicy consumption, it appears that the further reactions of the initially formed dicy/MGEBA adducts must then occur rapidly. The formation of cyclical products C and D, on the other hand, appears to be relatively slow during the initial 70 to 80 % of the epoxide consumption, advancing more rapidly only in the later stages of the reaction. Thus it appeared that amine/epoxide addition occurs at a much faster rate in this system than does the cyclization and dissociation reactions. Consequently, it was suspected that a substantial portion of the reaction mixture consisted of tetrasubstituted dicy molecules in the early stages of the dicy/MGEBA reaction. However, no evidence supporting this conclusion could be found in the HPLC chromatograms of the dicy/MGEBA reaction mixtures.

In the above plots, the consumption of dicy appears to have ceased in the last 20 to 30% of the reaction. Therefore, it was believed that the remaining epoxide was preferentially consumed by other means in the later stage of the reaction, presumably via reaction with dissociation products contained in peaks C and D. These products are observed to steadily increase in concentration throughout the course of the reaction and continue to be formed at a greatly reduced rate following the complete consumption of epoxide. Products contained in peaks G and H also appeared to have steadily increased as the reaction progressed. Following the completion of epoxide consumption, the total combined areas of peaks G and H did not vary with further heating, again supporting the initial assignment of these peaks to the more highly substituted analogs of cyclical products C and D.

### Extended Reaction Times

As previously discussed, a very small exotherm was detected for the product mixtures of the uncatalyzed dicy/MGEBA reaction, when held at the temperature of reaction for extended periods of time. In order to determine the origin of this excess heat, an attempt was made to assess the effects of long term heating on the dicy/MGEBA product mixtures. An uncatalyzed sample was heated to 197°C for 50 minutes resulting in complete consumption of the epoxide. The chromatogram of this product mixture was then compared to that of an identical sample which had been reacted at 197°C for 300 minutes. It was found that this extended heating had resulted in an increase in the concentration of peak D, from a value of 9% of the reaction mixture up to a value of 14%, while causing only a minimal decrease in the concentration of peak C. It was concluded that the excess heat, measured over the extended reaction times, was attributable to the formation disubstituted cyclical urea via the dissociation of higher molecular weight compounds. It was also observed that the concentration of peak D in the sample solutions gradually increased when held at room temperature over a period of a month or more. However, no decrease in peak C or change in the relative areas of any of the other major chromatographic peaks was observed for these solutions over the same period of time. The greatest increases in peak D were found in samples in which a moderate extent of reaction had occurred. Therefore, it was believed that these increases were due to the continued decomposition of substituted dicy adducts over long periods of time at room temperature.



### Excess Epoxide

The assignment of peaks C and D to disubstituted cyclical 2-imino oxazolidine and its cyclical urea rearrangement product, respectively, appeared to be well supported by the extensive observations presented in this chapter. However, some difficulty was encountered in identifying the components of peaks F, G and H, and in the determining the relationship between these components and those of peaks C and D. One of the problems was in locating the peaks assignable to the multiply substituted linear dicy/MGEBA adducts. As previously discussed, the HPLC kinetic study appeared to indicate the rapid accumulation of these species in the early stages of reaction. At longer times, these species were expected to decompose to form peaks C and D, which would then further react with any remaining epoxide to form higher molecular weight cyclical analogs. It was suspected that peaks F, G and H contained both the linear dicy adducts and the higher molecular weight cyclical analogs. In order to make specific peak identifications, it was necessary to eliminate one or the other of these two groups of products. Because of the slow rate of dicy dissolution and diffusion, it was not possible to overload the system with dicy in order to eliminate the high molecular weight cyclical analogs. Therefore, attempts were made to drive all of the reactions to completion by using an excess amount of MGEBA. Mixtures containing ratios of 1:8 and 1:16 dicy molecules per epoxide were reacted for periods of 12 hours at a temperature of 177°C. However, HPLC analyses revealed that the numbers of peaks contained in the non-polar region of the chromatograms of these mixtures were identical to those found in the case of the 1:4 and 1:6 dicy/MGEBA reaction mixtures. No peaks were elimin-

ated. In addition, substantial concentrations of C and D were observed in the 1:8 and 1:16 reaction mixtures, indicating that the further reaction of these disubstituted cyclical adducts with epoxide had not gone to completion. All attempts to complete the reaction of these species at higher temperatures and longer reaction times failed.

#### Base Catalyzed Reaction of Dicy with MGEBA

An attempt was made to assess the effects of base catalization on the mechanism of the dicy/epoxide reaction. BDMA samples of various compositions were reacted at temperatures of 127° and 147°C, and were analyzed with HPLC, using the conditions developed for the uncatalyzed reaction mixtures. A typical chromatogram is shown in Figure 3-17 for a catalyzed 1:8 dicy/MGEBA reaction mixture, heated to 147°C for 24 minutes. Evident in this chromatogram are many of the major components found in the chromatogram of the uncatalyzed dicy/MGEBA product mixture, shown in Figure 3-6. Thus, it appears that the addition of base does not alter the mechanism of the dicy/epoxide reaction. Several differences were also noted, which are believed to be attributable to increased rates of etherification in this system. One major difference between this chromatogram and that of the uncatalyzed system is seen in the region labelled A. In the catalyzed system, this region appears to contain only one component, peak 1. This peak was found to have the same elution time as peak 1 seen in the chromatogram of the cyanamide/MGEBA reaction mixture, shown in Figure 3-7. These peaks are each believed to contain the same compound, which is identified as product I in the following chapter. The significance of this will be discussed in the results section of that chapter.

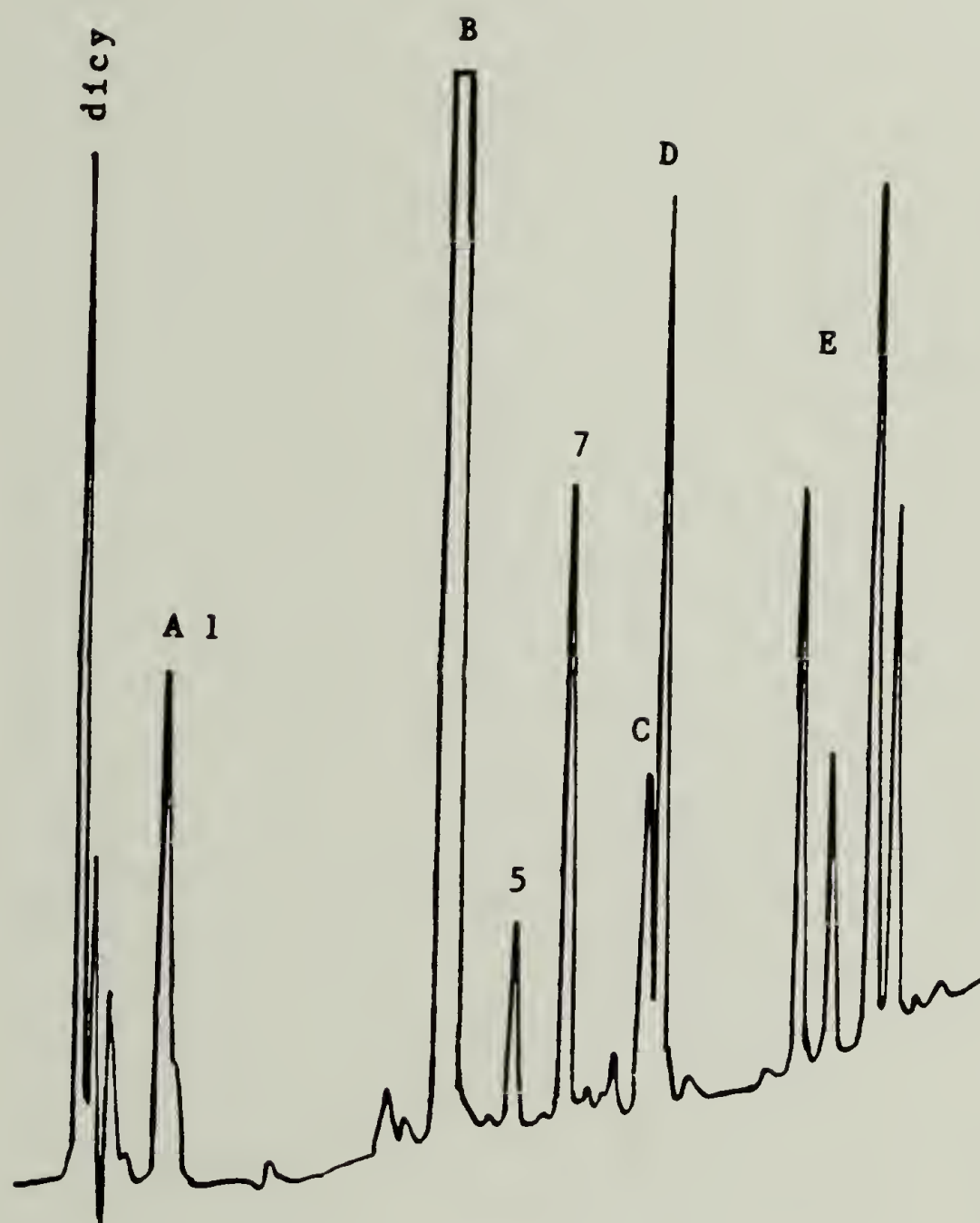


Figure 3-17: HPLC chromatogram BDMA catalyzed 1:8 dicy/MGEBA reacted at 147°C for 24 min; Acetonitrile/H<sub>2</sub>O = 50-100%, 10 min, grad 6, analyzed at 214nm.

### Summary

Initial dicy/MGEBA addition appears to be the rate controlling step in the reaction of the uncatalyzed model system. Following this reaction, further amine/epoxide addition appears to be rapid relative to the cyclization and dissociation reactions proposed by Zahir [40]. While it appeared that these later reactions produced the disubstituted 2-imino oxazolidine and cyclic urea compounds described by Zahir, it was difficult to discern the relationship of these cyclic compounds to the higher molecular weight species in the reaction mixture. Further, it appeared that the rate of the further addition of MGEBA to these compounds was slow, relative to the other reactions in this system. Based on these considerations, it appeared that tetrasubstituted dicy molecules constitute a large percentage of the reaction mixture throughout much of the reaction. However, no clear evidence for the presence of these compounds could be discerned in the HPLC chromatograms of the reaction mixtures. Further, following completion of epoxide consumption, no evidence was found for a large scale decomposition of the less polar peaks, via the formation of disubstituted cyclical products, as would have been expected if a large reservoir of tetrasubstituted dicy was present. Thus, the results of this study appeared to offer contradictory evidence in the determination of the relative rates of the reactions comprising the Zahir reaction mechanism.



## CHAPTER 4

### THE MECHANISM OF THE DICY/MGEBA REACTION

#### Introduction

The HPLC chromatograms in the previous chapter were initially interpreted in terms of the Zahir mechanism. Chromatographic peaks were tentatively assigned to Zahir structures based on the assumption of higher polarity for low molecular weight species, apparent order of formation, and the observed similarities between the product peaks of the dicy/MGEBA and cyanamide/MGEBA reaction mixtures. In order to verify these peak assignments, an attempt was made to isolate products from the dicy/MGEBA reaction mixture using preparative liquid chromatography (PLC), so that a definitive analysis of these products might be performed. It was believed that the use of PLC to isolate these products would provide a distinct advantage over the preparatory SEC used in the study by Zahir. With PLC, it was possible to obtain relatively pure compounds, instead of product mixtures of similar molecular size, greatly facilitating analysis and allowing an unambiguous characterization of the product structures.

The PLC column used in this experiment contained a reverse-phase packing material similar to that used by the HPLC in the study presented in chapter 3. The same general principals were expected to govern both separation techniques, so the HPLC results of the previous chapter were used to guide the isolation of products by PLC. As seen by HPLC, the dicy/MGEBA reaction mixture contains a large number of species with

similar elution times and often overlapping elution bands. Because it was not possible to isolate all of these products in pure form, the main effort was concentrated on isolating the high polarity chromatographic peaks, labelled A, C, and D in the HPLC chromatograms of the previous chapter. These peaks, which appeared to be relatively pure, were thought to contain the low molecular weight, initial products of the dicy/MGEBA reaction. As such, it was believed that, if these products were isolated in pure form, then they would have additional value as intermediates in the formation of higher molecular weight species. By reacting these compounds with MGEBA in the DSC and following the progress of the reaction with HPLC, a study could be conducted, similar to that of chapter 3, in which specific aspects of the dicy/MGEBA reaction could be isolated and examined. In this way, kinetic parameters could be measured free from the interfering effects of dicy dissolution and diffusion. Further, by comparing these HPLC chromatographs with those of the previous chapter, the structural identity of some of the less polar, higher molecular weight peaks might be ascertained.

Of primary interest to this study was the isolation of peak C. In the previous chapter this peak was tentatively assigned to the structure of bis-alkyl 2-imino oxazolidine. According to the Zahir mechanism, this compound is capable of undergoing several key reactions, including rearrangement to form a cyclic urea (peak D), and further reaction with epoxide via the imino functionality. Knowledge of the relative rate of this second reaction was thought to be extremely important. The results of chapter 2 had suggested that this reaction occurs at a much slower rate than cyanamide amine addition to epoxide, resulting in the forma-

tion of linear polymer at low cure temperatures. By isolating peak C and reacting it with MGEBA, the kinetics of this crosslinking reaction could be determined. In addition, the transformation of this 2-imino oxazolidine into a cyclic urea could be verified. Further, according to Zahir, the 2-imino oxazolidine acts as a strong base, catalyzing the cure and promoting etherification. Therefore, the study of this reaction using the isolated material was also thought to be of value in determining the kinetic parameters controlling the structure of a dicy cured epoxy.

The concentration of the desired compounds in the dicy/MGEBA reaction mixtures was low. In a typical amine/epoxide reaction, the concentration of those initial products can be enhanced by increasing the amine to epoxide ratio. However, due to the limited solubility of dicy in MGEBA, this could not be done. According to the results of the previous chapter, the maximum attainable concentration of these low molecular weight products appeared to be about 20% of the total by weight. Product yields were expected to be further reduced because of the low efficiency of the PLC and the requirements for high product purity. Thus, in order to obtain the bis-alkylated 2-imino oxazolidine in amounts sufficient for the above analysis, an attempt was made to synthesize this compound via the von Braun cleavage of MGEBA substituted tertiary amines with cyanogen bromide. It was believed that this material could not only be obtained in greater abundance with this synthesis, but could also be more easily purified. The details of this synthesis are given in the appendix.



## Experimental

### Materials

A general description of the structure and properties of MGEBA is provided in chapter 3, and the details of the synthesis and purification of this compound can be found in sections 1 and 2 of the appendix. Dicyandiamide and cyanamide, 97% and 99+% pure, respectively, were purchased from Aldrich and were used without further purification. Mixtures of these materials were reacted in a preheated oven, and no attempt was made to exclude air from the reacting mixtures. Solutions for PLC separation were made by dissolving the product mixtures in 100% THF, a solvent in which the excess dicy was nearly insoluble. These solvents were filtered to remove the excess dicy, and then distilled water was added in order to adjust the polarity of the solvent to that of the PLC mobile phase.

### Preparatory Liquid Chromatography

The PLC consisted of a 50 cm x 1.5 cm ID glass column, hand-packed with Waters Preparative C-18 bonded phase, silica gel packing material, with particle size ranging from 55 to 105 microns in diameter. The mobile phase consisted of THF, acetonitrile, or methanol adjusted to the desired polarity by the addition of distilled water. HPLC uv-grade solvents were used for this purpose. The mobile phase compositions are designated in the text by the volume percentage of organic solvent contained in the mixture. A single low pressure Waters solvent pump was used and solvent flow rates ranged between 3 and 15 ml/min. Mobile phases were, by necessity, isochratic, and the products were detected by



a Waters model 500 refractive index (RI) detector, equipped with a strip chart recorder. Fractions were collected by following the RI trace and were subsequently analyzed by HPLC, using the conditions developed in chapter 3. Following HPLC analysis, solvents were removed using a rotary evaporator. The isolated products were then dried overnight in a room temperature vacuum oven prior to further analysis.

### Product Analyses

Analyses of the products by Size Exclusion Chromatography (SEC) were performed using 3 IBM, 2A and 1C, low molecular weight, 5 micron columns in series. A Waters model 840 system controller, equipped with a Waters model 401 RI detector and an M 6000A solvent pump, was used for solvent programming and data acquisition. The mobile phase was 100% THF at a flow rate of 1 ml/min., and the column temperature was 40°C.

FTIR spectra were obtained using a Perkin Elmer 1550 FTIR spectrometer, equipped with a 7500 series data station. Sixty-four scans at a resolution of 4 cm<sup>-1</sup> were made of films cast on NaCl plates from methylene chloride solutions of the isolated products. Proton and carbon-13 NMR spectra were obtained using a Bruker MSL-200 FTNMR spectrometer at 200.13 and 50 MHz, respectively. Approximately 1% solutions of the products in CDCl<sub>3</sub> were used with TMS as an internal standard. Samples in 5 mm OD tubes were scanned 20 times for proton NMR spectra and samples in 10 mm OD tubes were scanned 200 times for carbon-13 NMR spectra. Fast atom bombardment mass spectra were obtained using a VG70-250SE mass spectrometer, and analyses were run on samples in a nitobenzyl alcohol matrix.

Mixtures of the isolated products with MGEBA were prepared for DSC analysis by combining the isolated products with MGEBA directly in DSC aluminum sample pans. Compositions were determined by weighing the sample pans on a microbalance before and after the addition of each of the reactants. A description of the DSC and DSC sample encapsulation process can be found in the experimental section of chapter 2. Mixtures were reacted in the DSC both isothermally and by temperature scans and the product mixtures formed by these reactions were analyzed by DSC in a manner identical to that previously described in chapter 3 for the dicy/MGEBA mixtures.

## Results and Discussion

### Dicy/MGEBA

Product mixtures were prepared by reacting a 1:4 molar ratio of dicy and MGEBA at 190°C for approximately one hour and the course of the reaction was monitored by HPLC. In order to avoid an uncontrollable exotherm, sample size was limited to 500mg and the mixtures were periodically stirred during the reaction to maximize dicy solubility. Attempts to use higher dicy loadings did not measurably increase the yield of the desired high polarity products. Figure 4-1 shows an HPLC chromatogram of a typical mixture from which products were isolated. In this case, peak C constituted about 10% of the product mixture.

### Product Isolation

A two-stage process was used to isolate peaks C and D from the above product mixture. First, it was necessary to partition the combined

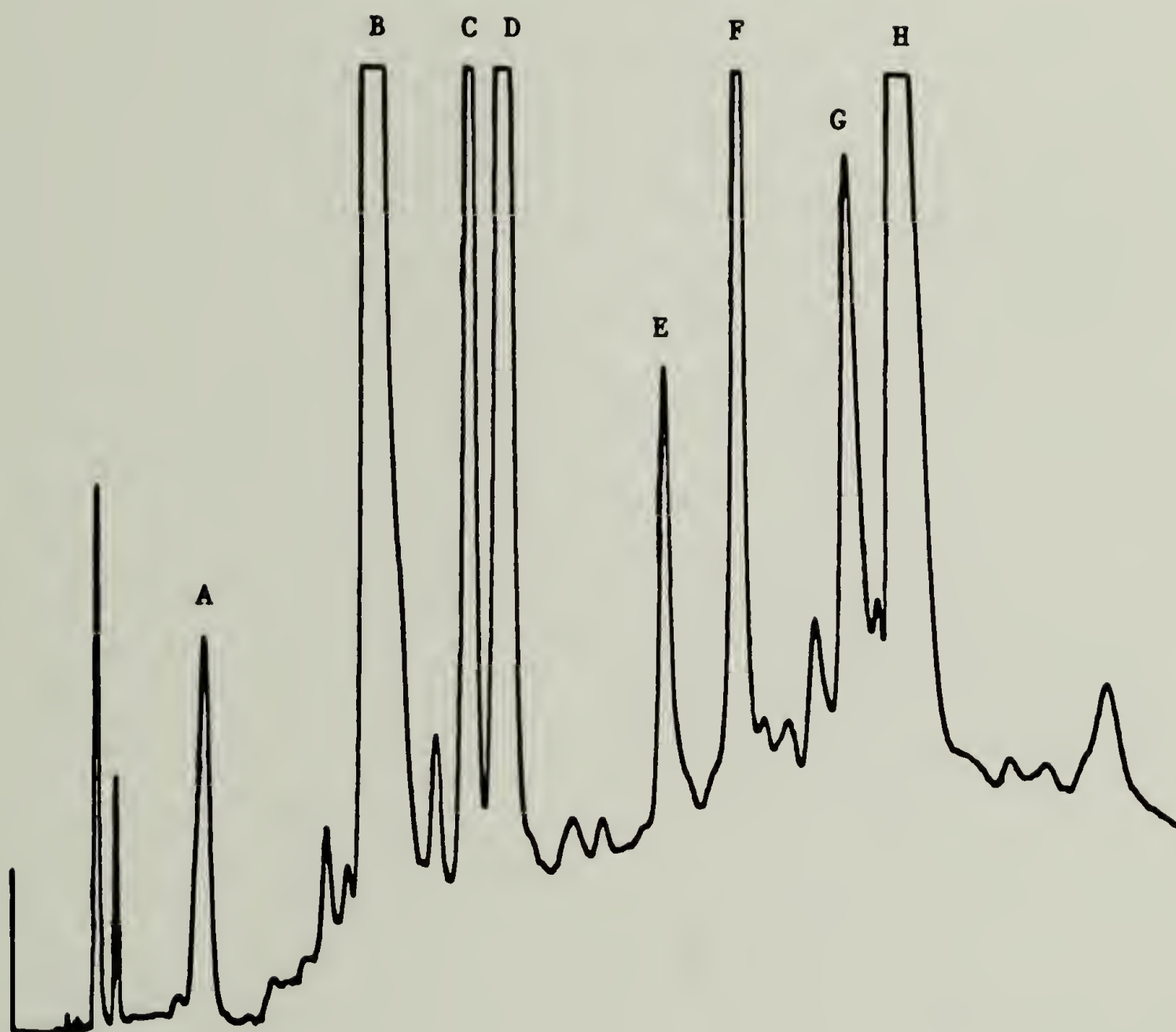


Figure 4-1: HPLC chromatogram of dicy/MGEBA reacted at 187°C for 60 min; THF/H<sub>2</sub>O = 50-90%, over 40 min, at grad 6, analyzed at 229nm.



peaks from the less polar species using the PLC with a low polarity mobile phase such as 90% methanol or 100% acetonitrile. The peaks were then separated from one another using a more polar solvent mixture. A variety of solvent combinations were tried, and the best separation was achieved using 55% THF as the mobile phase. However, the PLC was much less efficient than the HPLC, due to the large particle size of the packing material and the irregularities introduced by hand packing the column. Under optimum conditions, only a partial resolution of these peaks was possible during each product separation. Thus, in order to isolate the individual peaks it was necessary to combine fractions of similar composition, as determined by HPLC analysis, and to perform repeated separations. In this way it was possible to obtain samples progressively enriched in peak C or D. One of the main fears was that with repeated separations, the rigorous conditions required for solvent removal might have resulted in degradation or structural changes in the desired product. However, HPLC analyses of the product fractions before and after solvent removal revealed that no apparent change had occurred.

#### FTIR Analysis

After several separations, enough of each peak was isolated in sufficient purities for FTIR analysis. The spectra of peaks C and D are shown in Figures 4-2 and 4-3, respectively. Evident in each of these spectra are minor features indicative of small amounts of cross-contamination. However, several of the major absorbance bands appear to be unique to each of the isolated materials. The tentative designation of peak C as a 2-imino oxazolidine was supported by the appearance of a strong absorbance at  $1650\text{ cm}^{-1}$ . Bands at this frequency have been



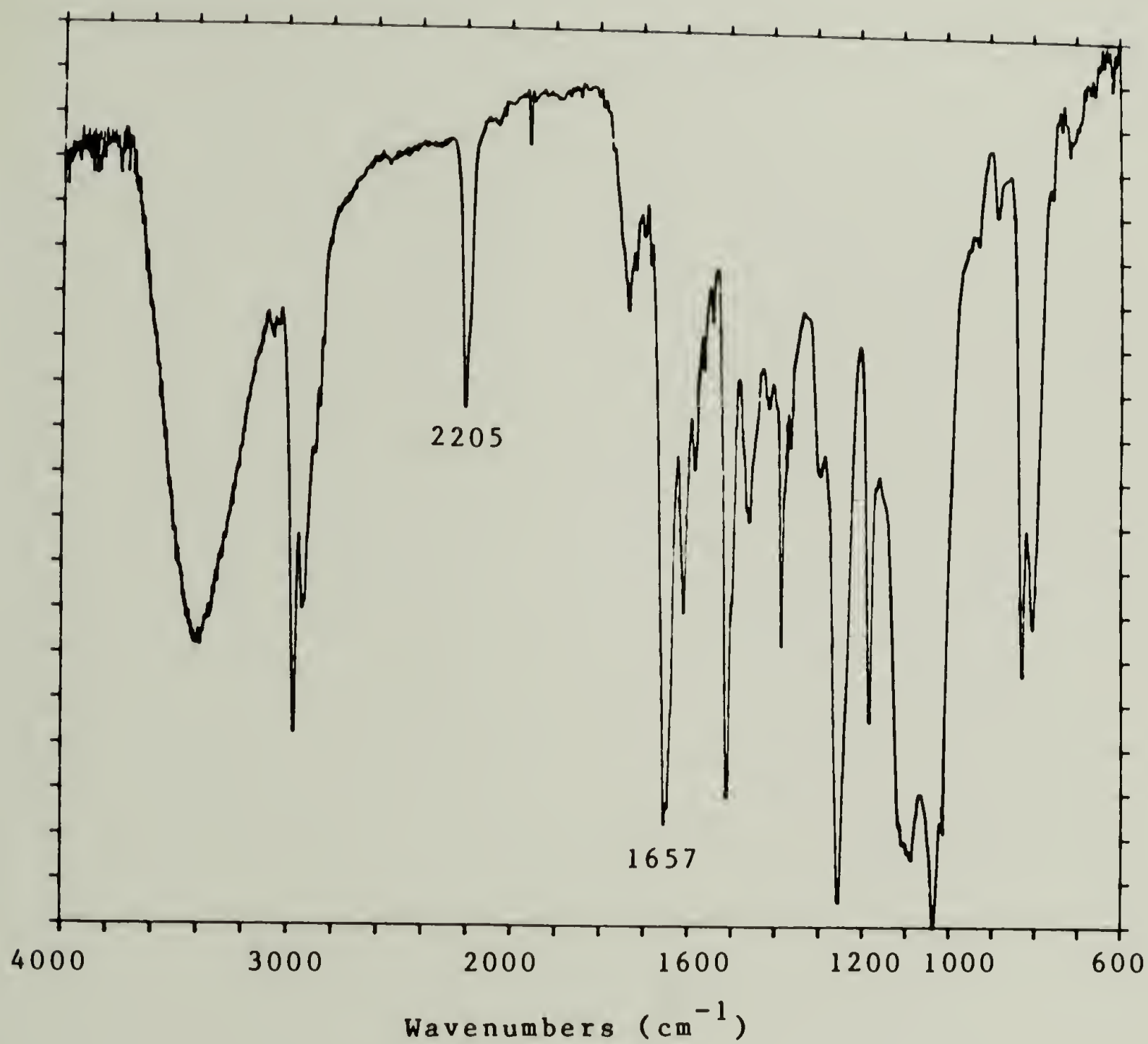


Figure 4-2: FTIR spectrum of isolated peak C.

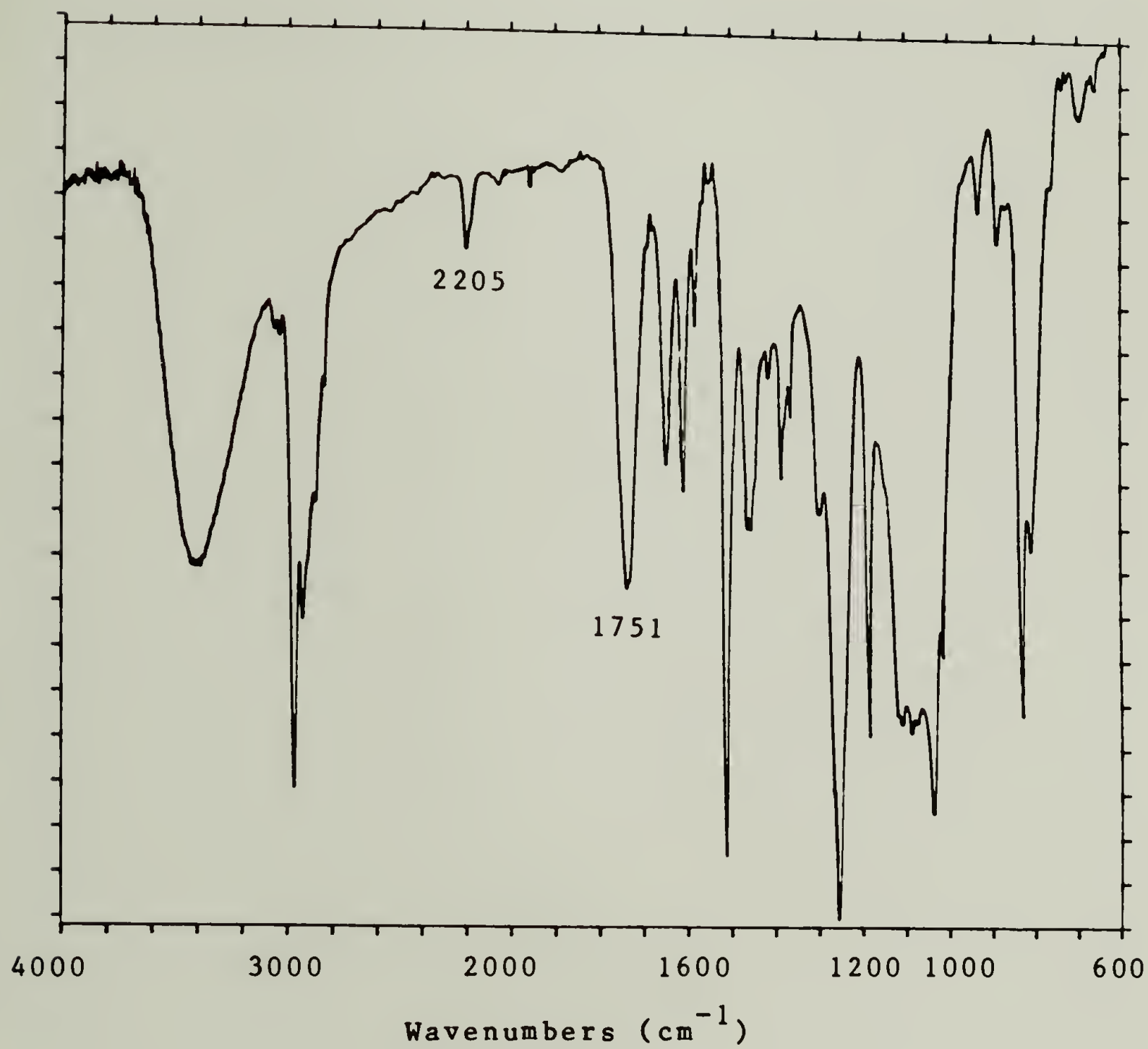


Figure 4-3: FTIR spectrum of isolated peak D.

previously observed in spectra of dicy cured epoxies [34,41,42] and were assigned by Zahir [40] to the imine stretch of the 2-imino oxazolidine. However, the spectrum of peak C also reveals a cyano absorbance band at  $2205\text{ cm}^{-1}$ , which contradicts this designation. While the appearance of both absorbance bands appeared to indicate the presence of a substituted dicy, it was also possible that peak C was composed of two separate compounds of similar polarities, which were indistinguishable by HPLC. Since the purity of this material was unknown, a definite structural determination could not be inferred from the FTIR spectrum. The spectrum of peak D, on the other hand, reveals only a single structurally significant absorbance band, which appears at  $1720\text{ cm}^{-1}$  in the carbonyl region. Similar bands were also reported in previous IR studies of the dicy/epoxy cure [4,34,41,42] and were assigned by Zahir [40] to cyclic urea products formed by the rearrangement of 2-imino oxazolidines shown in equation (14). The results of chapter 3 appeared to indicate that peak C was converted to peak D in the later stages of the dicy/MGEBA reaction. Because peak D contains a carbonyl, presumably generated by the rearrangement reactions proposed by both Saunders et al. [35] and Zahir [40], the results of chapter 3 appear to imply that peak C must contain the imino ester required for this transformation, apparently supporting the designation of this material as a 2-imino oxazolidine.

Peak A was also isolated from the dicy/MGEBA reaction mixture. Although this peak comprised only a few percent of the reaction mixture, as shown in Figure 4-1, it could be readily isolated from all other products by a single PLC separation using 60% acetonitrile as the mobile phase. An FTIR spectrum of this material is shown in Figure 4-4. This

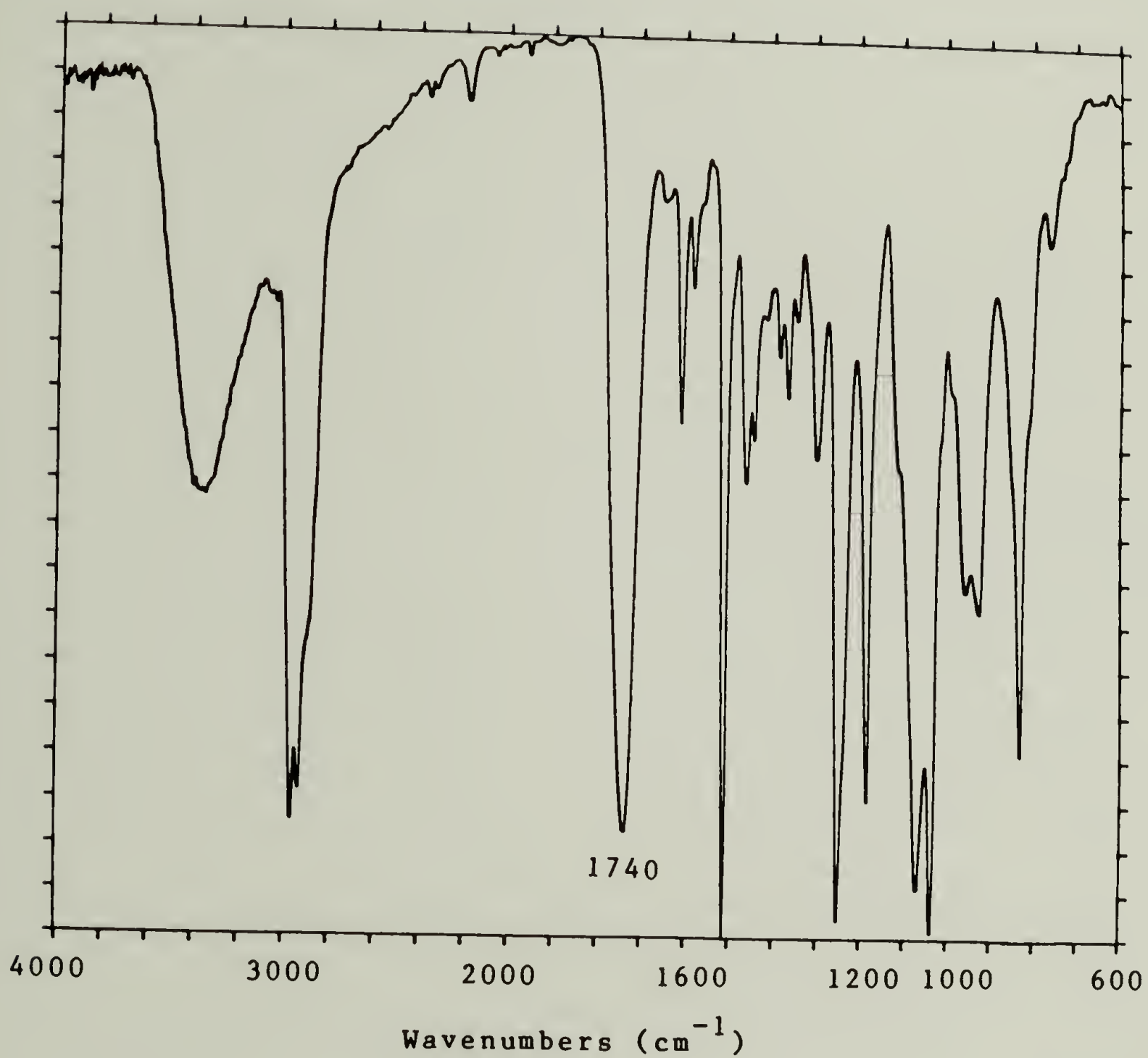


Figure 4-4: FTIR spectrum of isolated peak A.



material had been tentatively identified as a monoalkyl cyanamide or dicy, based on chromatographic comparisons with the cyanamide/MGEBA reaction mixture. However, the FTIR spectrum of this material revealed no evidence for the presence of either a cyano or imide group. Instead, a prominent carbonyl absorbance band was observed, and the spectrum was in general similar to that of isolated peak D. Thus, it appeared that this material was the monoalkyl cyclic urea.

The lack of cyano or imide groups in the spectrum of peak A was surprising considering that this material was isolated from a partially reacted mixture. Further, if product A contained monoalkyl cyclic urea, it was not understandable why the mono alkyl analogs of peak C were not also detectable. Based on these observations, the polar products of the partially reacted dicy/MGEBA mixture appeared to be heavily weighted with later-stage carbonyl containing species. While these appeared to be cyclic ureas as described by Zahir, other possibilities existed. Carbonyl bands in this region have been observed in the spectra of degradation products formed during relatively low temperature cures of epoxy resins with amines [72-75]. The results of chapter 3 revealed a late stage increase in the areas of chromatographic peaks A and D occurring after completion of epoxy composition, which indicated contamination of these peaks by degradation products.

In an attempt to clarify the structural identities of the isolated materials, an effort was made to determine their molecular weight by GC-MS. However, attempts to volatilize the material in the GC resulted in product degradation. Thus, neither a parent ion mass, nor other

structurally significant information could be obtained from the resulting spectrographs. The use of solid probe analysis resulted in a similar degradation of the materials by the electron beam, without the generation of any detectable parent ions for MS analysis.

#### Cyanamide/MGEBA

In order to obtain larger quantities of peaks C and D in greater purities, an attempt was made to isolate these products from the cyanamide/MGEBA reaction mixture. Advantage was taken of the increased solubility of cyanamide over dicy and high reactivity at low temperatures, in an attempt to form mixtures enriched in low molecular weight initial products. It was felt that the lower reaction temperatures would also decrease the possibility of potential degradation reactions, thus simplifying product purification.

The results in chapter 3 indicated that the rate of cyanamide dimerization to form dicy is competitive with that of cyanamide reaction with MGEBA. In several reaction studies, it was found that fully half of the cyanamide was converted to dicy, which was unreactive at the low temperatures used. Attempts to use a larger excess of cyanamide in these reactions resulted in an explosive exothermic reaction, accompanied by degradation and charring of the resin, even when small reaction masses were used. However, it was possible to form initial reaction products in large concentrations by the continuous addition of fresh cyanamide to the reaction mixture at set intervals. In this way a high effective concentration of cyanamide was maintained while avoiding an explosively

exothermic reaction. Reactions were run in a 100°C oven and sample size was again limited. The reaction was monitored by HPLC, and care was taken to insure that the concentration of cyanamide was not allowed to reach too high a level. An HPLC chromatogram of the product mixture thus formed, is shown in Figure 4-5. While the chromatographic peak placement is identical to that of the dicy/MGEBA mixture, the apparent concentrations of the high polarity products are higher. Especially evident is the high concentration of peak A, here believed to be the 1:1 adduct formed by the initial cyanamide/ MGEBA reaction.

#### Product Isolation

Product isolation proceeded in a manner similar to that used for the dicy/MGEBA reaction mixture. In this case peaks A and C were again found to contain one component each. However, variations in mobile phase composition revealed that peak D contained two components. The four components were designated by Roman Numerals to indicate their apparent order of formation, and the peaks in Figure 4-5 are thus labelled. Again repetitive separations were required to isolate the products of peaks C and D. However, two different mobile phase combinations were needed. Product II was first isolated from products III and IV using 70% acetonitrile, then III and IV were separated from one another using 55% THF. With repeated separations, it was possible to isolate products II-IV to purities of 90% as determined by HPLC. Product I from peak A, on the other hand, could be isolated to an apparent HPLC purity of 100%, using a single PLC separation with 60% acetonitrile.

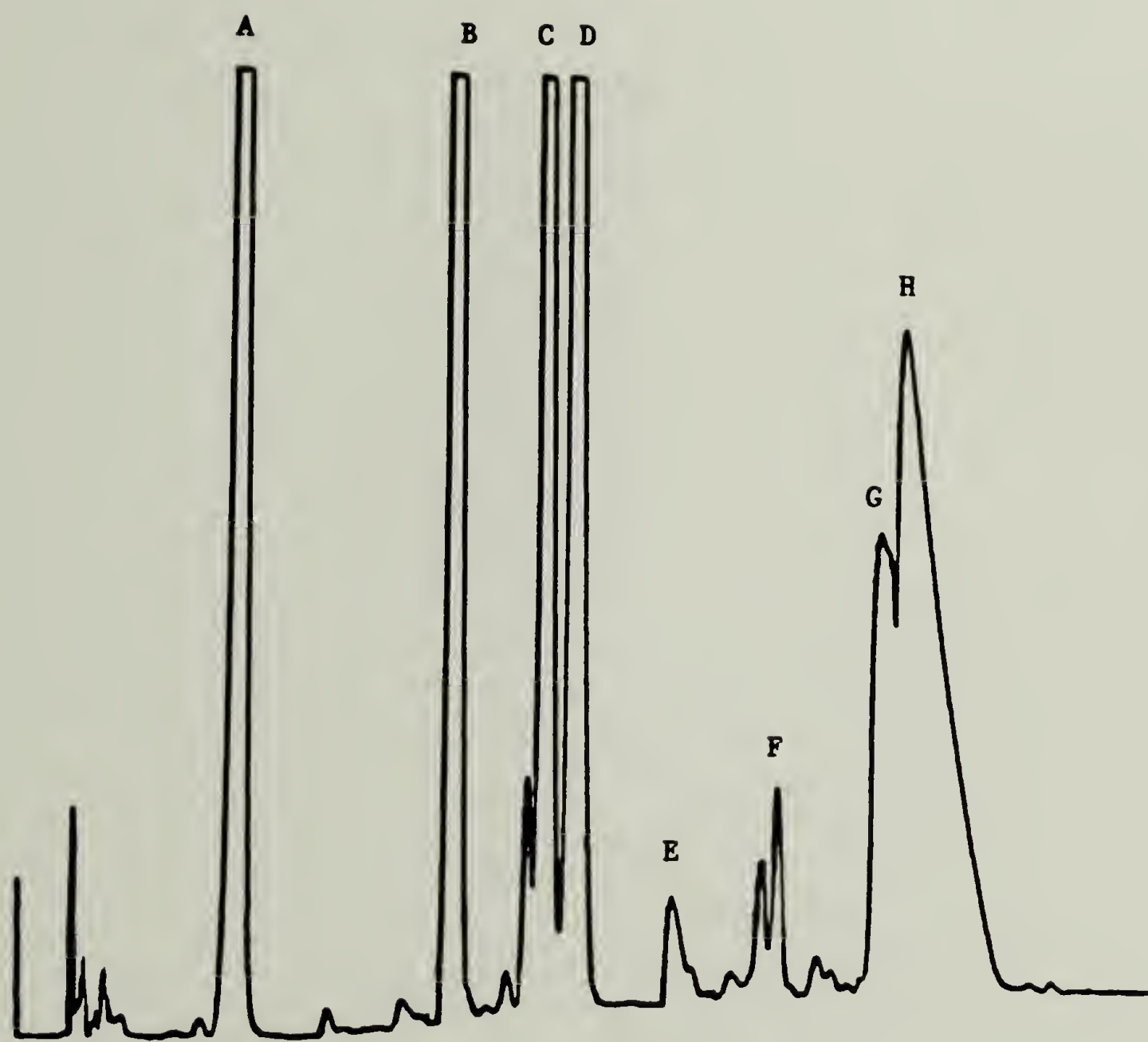


Figure 4-5: HPLC chromatogram of cyan/MGEBA product mixture;  
THF/H<sub>2</sub>O = 50-90%, over 40 min, at grad 6, analyzed at  
280nm.



### FTIR Analysis

The isolated products were analyzed by FTIR, and the spectrum of product I is shown in Figure 4-6. The strong cyano absorbance band at  $2174\text{ cm}^{-1}$  supported the tentative designation of this compound as the 1:1 adduct of MGEBA and cyanamide. An attempt to determine the molecular weight of this species using GC-MS, was only partially successful. While a small portion of the material was volatilized and eluted by the GC, the bulk of the material appeared to undergo a reaction, producing a higher molecular weight material, which could not be volatilized without degradation. A parent ion molecular weight of 342 AMU was determined for the eluted material, apparently confirming its identification as the monoalkyl cyanamide.

The spectrum of product II, shown in Figure 4-7, reveals a cyano absorbance band at  $2178\text{ cm}^{-1}$  and is similar in appearance to that of product I. However, the ratio of the height of this band to the height of the phenyl stretch at  $1511\text{ cm}^{-1}$  is about half of that found in the spectrum of product I. Product II, thus appeared to be the 2:1 adduct of MGEBA and cyanamide. The spectra of products III and IV are shown in Figures 4-8 and 4-9, respectively. These spectra are identical to those of peaks C and D isolated from the dicy/MGEBA reaction mixture, supporting the contention that both reactions yield the same products. Again the spectrum of product III reveals an imine absorbance at  $1651\text{ cm}^{-1}$  and a cyano absorbance band at  $2205\text{ cm}^{-1}$ . The appearance of both of these bands in identical proportions to those seen in Figure 4-2, supported the contention that either product III was a pure material or that it consisted of two materials in equilibrium. The spectrum of product IV

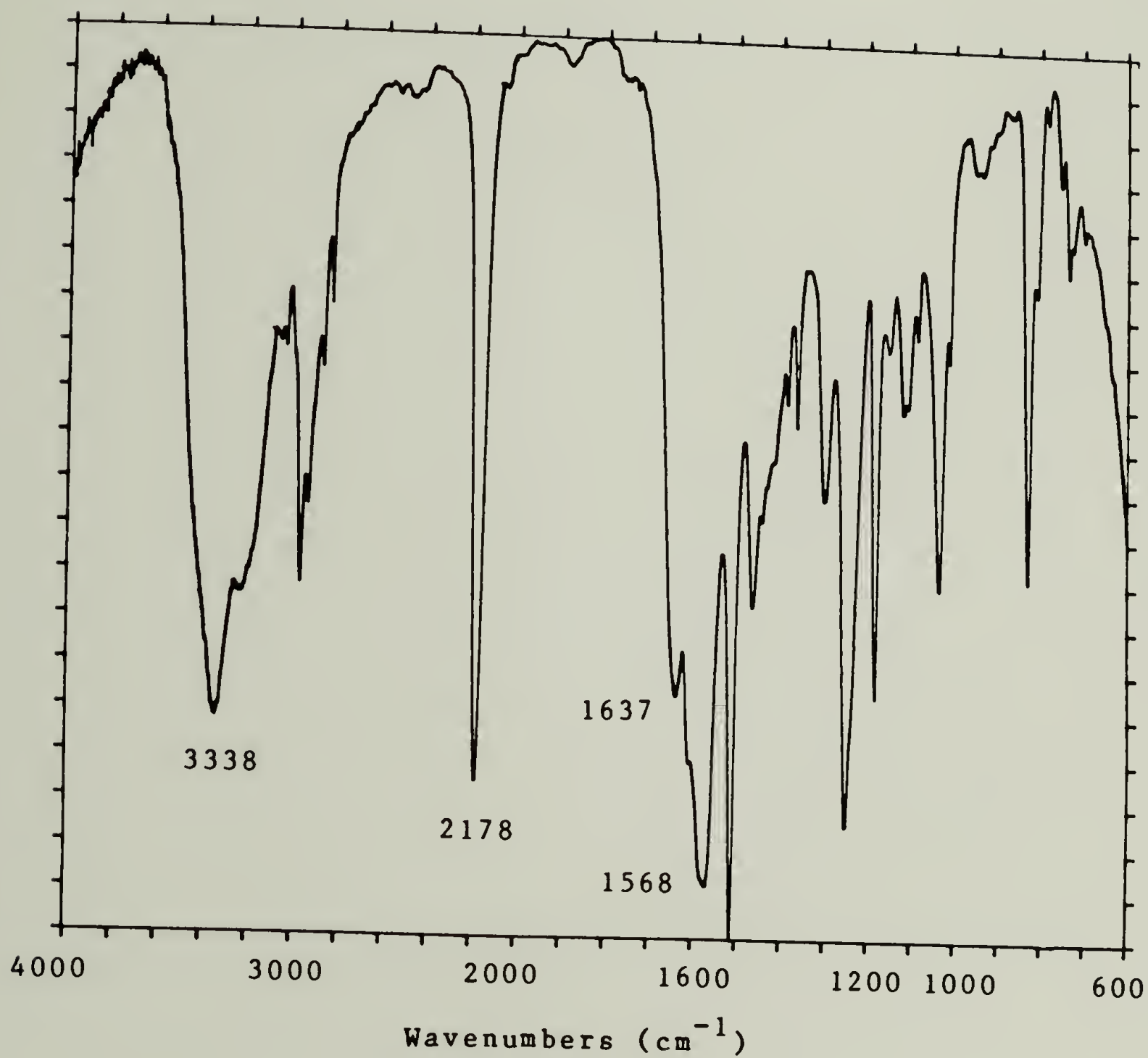


Figure 4-6: FTIR spectrum of product I.

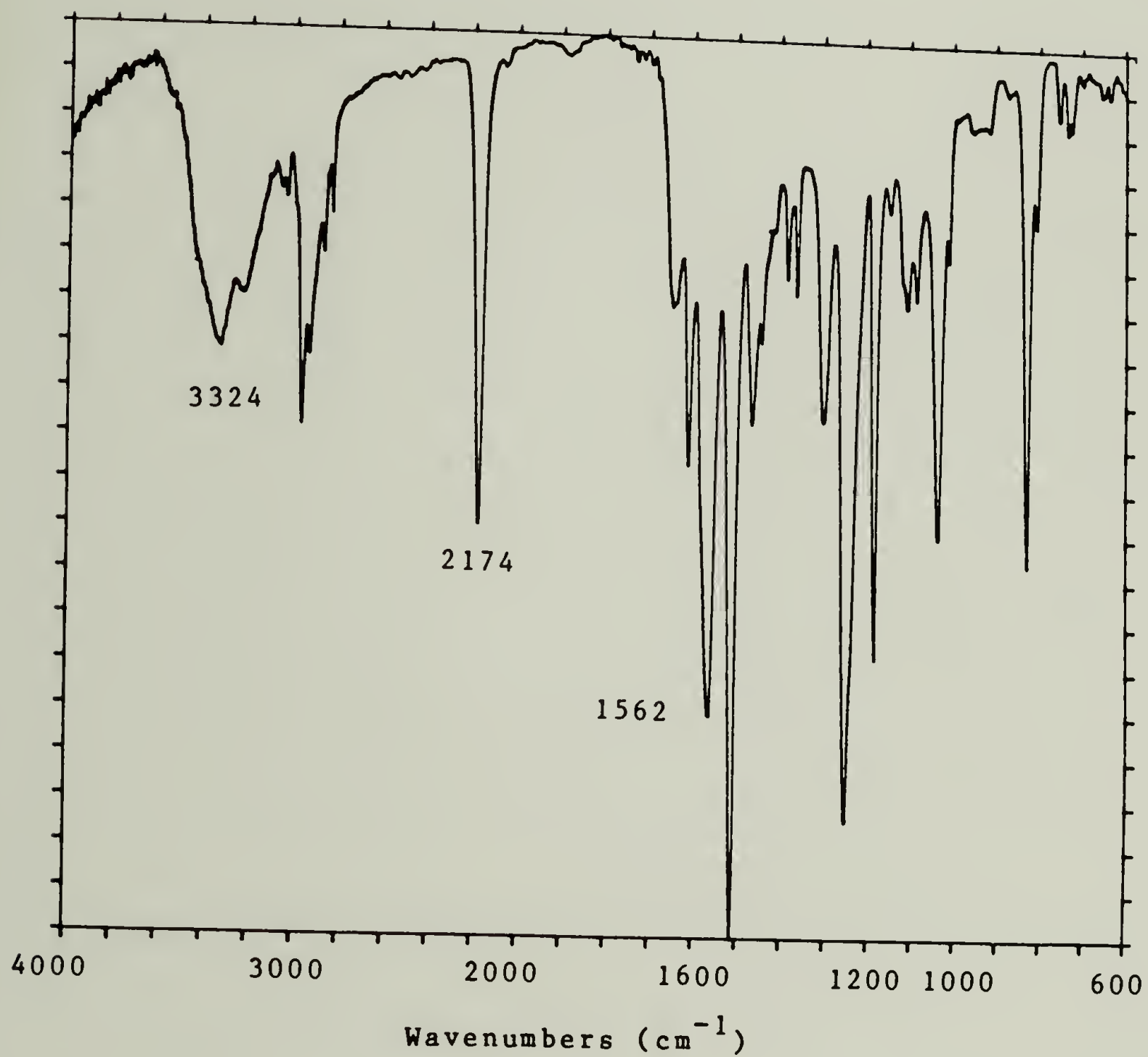


Figure 4-7: FTIR spectrum of product II.

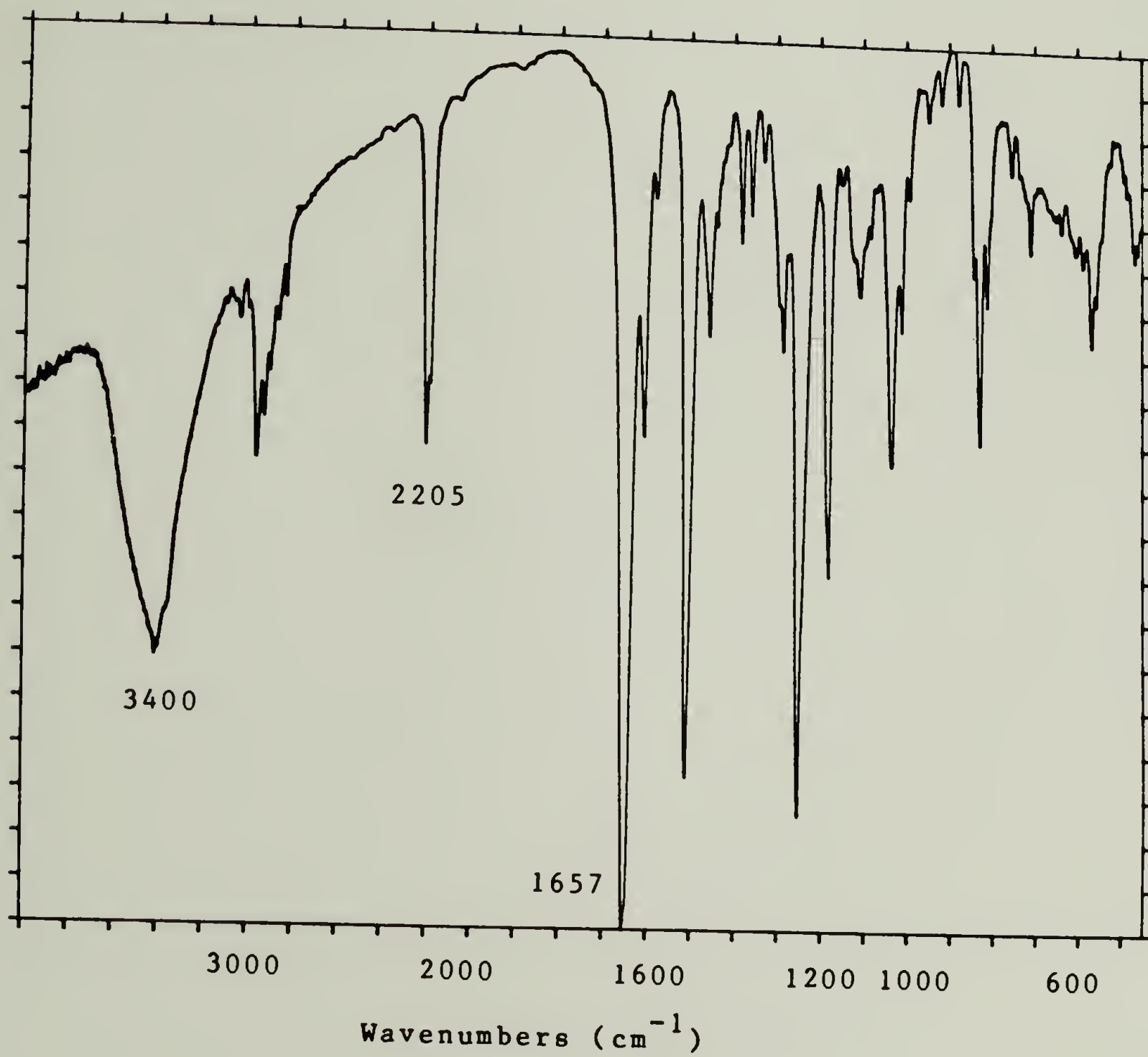


Figure 4-8: FTIR spectrum of product III.



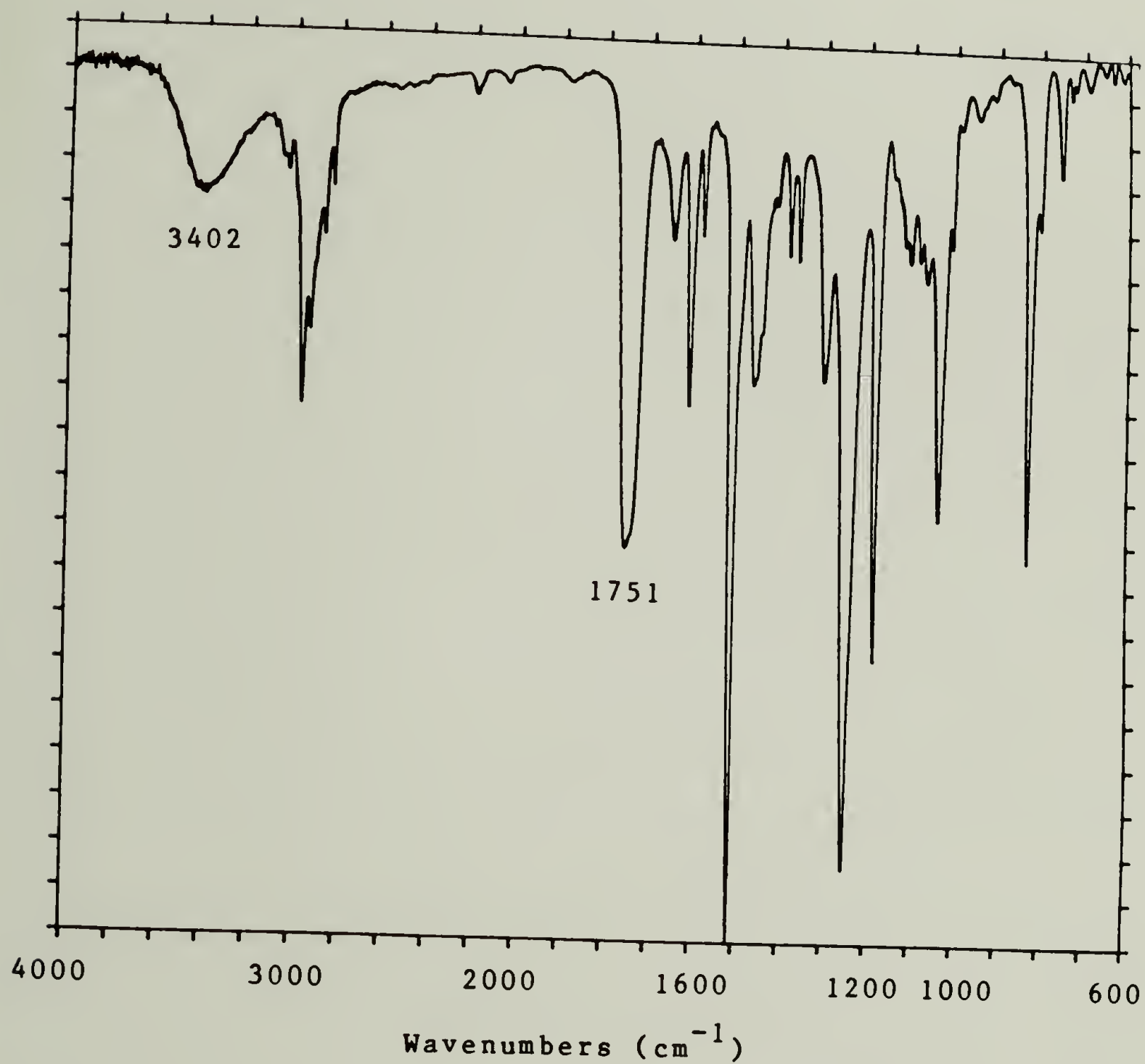


Figure 4-9: FTIR spectrum of product IV.

again shows a strong carbonyl centered at  $1750\text{ cm}^{-1}$ . The shift in this band to a higher frequency as compared with the spectrum of peak D in Figure 4-3, came about as a result of the increased purity and lower moisture content of this material when analyzed.

### SEC Analysis

Attempts to analyze products II, III, and IV by MS were unsuccessful, again due to the difficulties in volatilization and ionization of these materials. Therefore, these materials were analyzed by SEC in order to gain some insight into their relative molecular sizes. Products I-IV were analyzed along with MGEBA, and the resulting chromatograms are shown in Figure 4-10. Products II-IV appear to be of comparable size, with II slightly larger than III, and III slightly larger than IV. Product I, on the other hand, is intermediate in size between these compounds and MGEBA. This supported the assumption that product I was a monoalkylated species, while II-IV were bis-alkylated. It was also observed by HPLC that product II was converted into products III and IV by heating. Since the SEC results indicated that product III was of virtually the same molecular size as product II, it was felt that the thermal transformation of product II into product III was the result of an intramolecular reaction, presumably hydroxyl addition as described by Zahir.

### Further Reactions of Isolated Products

In order to obtain structural information on the higher molecular weight products, the isolated low molecular weight products were further reacted with MGEBA. The reactions were run in the DSC and the product

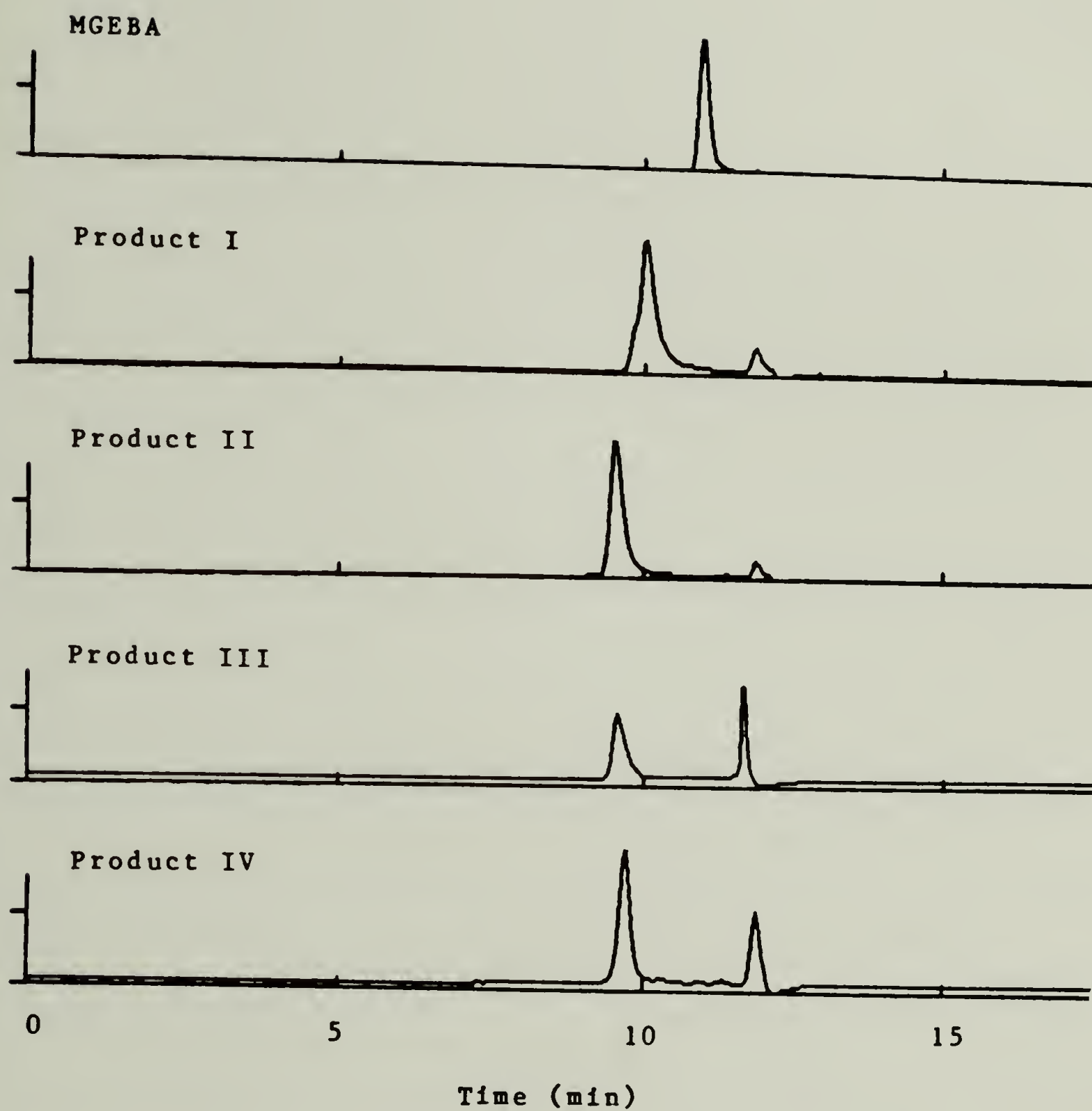


Figure 4-10: Comparison of SEC chromatograms of MGEBA and products I, II, III and IV.

mixtures were then analyzed by HPLC. A chromatogram of the mixture obtained from the reaction of product I with MGEBA is shown in Figure 4-11. In this example a 1:4 mixture of product I and MGEBA was isothermally reacted at 167°C for 15 minutes. The resulting chromatogram is identical in appearance to those obtained from the both dicy/ MGEBA and cyanamide/MGEBA reaction mixtures. Thus, product I appears to be the initial product from which all other products can be formed. The reaction of product II with MGEBA produced a similar product mixture, containing all other products except product I. A chromatogram of this mixture is shown in Figure 4-12, for a 1:8 II/MGEBA composition, isothermally cured at 167°C for two hours. This further supported the hypotheses that II was the 2:1 analog of product I. The results of additional reactions of this kind between product I and MGEBA can be found in Chapter 5.

Attempts were made to react products III and IV with MGEBA using similar conditions. However HPLC analyses of the product mixtures revealed that no reaction of III or IV had occurred. While some of the MGEBA was consumed by these reactions, and product III was observed to slowly transform into product IV, the sum total of III and IV in the reaction mixtures did not change. Further, no products identifiable as peaks F, G, or H appeared in the chromatograms. Attempts to promote the reaction by catalyzing with BDMA or product I failed, as did the use of extended reaction times or temperature scanning to 220°C. Peaks C and D, isolated from the dicy/MGEBA product mixture were found to be similarly unreactive toward further epoxide addition.



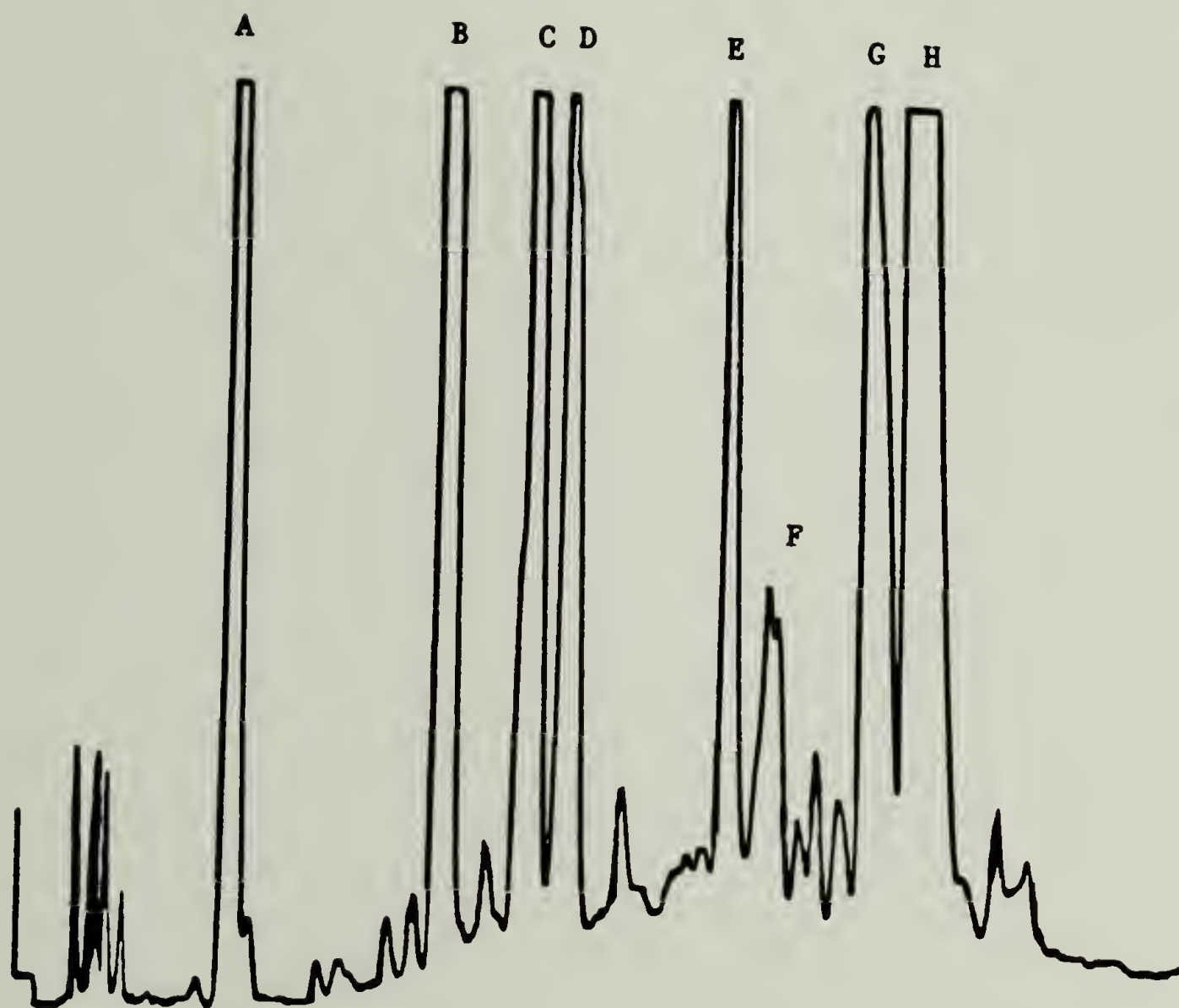


Figure 4-11: HPLC chromatogram of (1:4.5) I/MGEBA reacted at 167°C for 15 min; THF/H<sub>2</sub>O = 50-90%, over 40 min, at grad 6, analyzed at 229nm.

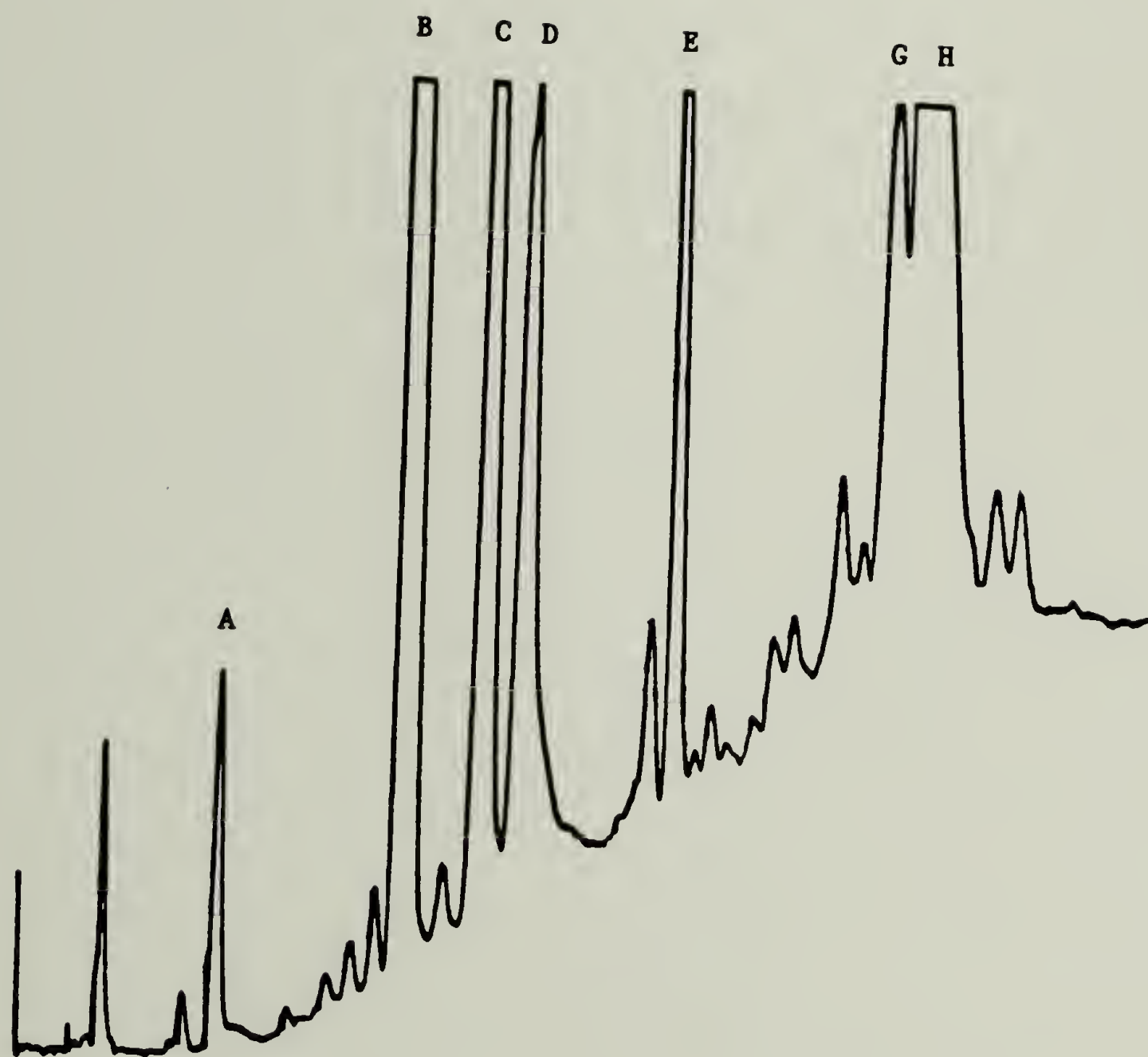


Figure 4-12: HPLC chromatogram of (1:9) product II/MGEBA reacted at 167°C for 120 min; THF/H<sub>2</sub>O = 50-90%, over 40 min, at grad 6, analyzed at 229nm.

A possibility existed that exposure to the rigors of solvent evaporation had structurally changed these compounds, making them inactive to further epoxide addition. In order to test this possibility, product II was transformed into product III by heating a neat sample in the DSC. Attempts to further react this converted product II with MGEBA also failed. Thus, the thermal transformation of product II rendered it inactive to further epoxide addition.

The non-reactive nature of products III and IV was surprising. According to the Zahir mechanism, as disubstituted cyclic products, these compounds should have been reactive either via imine or amide addition to the epoxide. Further, it was difficult to understand the relationship between product II and the less polar, higher molecular weight products. While the further reaction of this compound with MGEBA might have occurred via hydroxyl addition, it was unknown why hydroxyl groups present on III and IV would not react under similar conditions. An attempt was thus made to isolate higher molecular weight products in order to establish the nature of this relationship.

#### Less Polar Products

The less polar species of the dicy/MGEBA reaction mixture were not easily isolated. A variety of low polarity solvent combinations were used for the mobile phase, and these attempts revealed the complexity of the product mixture in this region. Chromatographic peaks G and H were found to contain several major components and a host of minor ones. Although peaks G and H could be separated from each other, they could not be separated from the components of peak F. Further, when exposed

to the conditions necessary for solvent removal, distinct changes were noted in the compositions of the isolated fractions, as determined by HPLC. Thus, it was difficult to obtain any of the products in pure form. FTIR was used to examine several of isolated fractions containing mixed components. While some of these spectra revealed the presence of several minor carbonyl absorbance bands, the bulk of the isolated material appeared to contain no cyano, carbonyl, or imide functionalities, thus no apparent kinship could be discerned between these materials and the previously isolated compounds. Further, although it was suspected that these products might be oligomers formed via etherification reactions, SEC analysis revealed a molecular size for these compounds which was only slightly larger than that of the bis alkylated species. Thus, neither the structure nor the mechanism of formation these species was readily evident.

#### Model 2-Imino Oxazolidines

Several model compounds were synthesized in an effort to clarify the spectroscopic results of the product characterization and to aide in understanding the structure and non-reactive nature of product III. The first of these was 2-imino-3-phenyl oxazolidine. This compound, was previously used in chapter 2 to model the imine reaction with DGEBA and the details of its synthesis are presented in section 4 of the appendix. An FTIR spectrum of the freshly prepared compound is shown in Figure 4-13. The imino stretch was readily apparent by an absorbance band at  $1670\text{ cm}^{-1}$ , which is comparable to that seen in spectrum of product III shown in Figure 4-8. However, the spectrum of the 2-imino-3-phenyl oxazolidine does not show any indications of a cyano absorbance band as



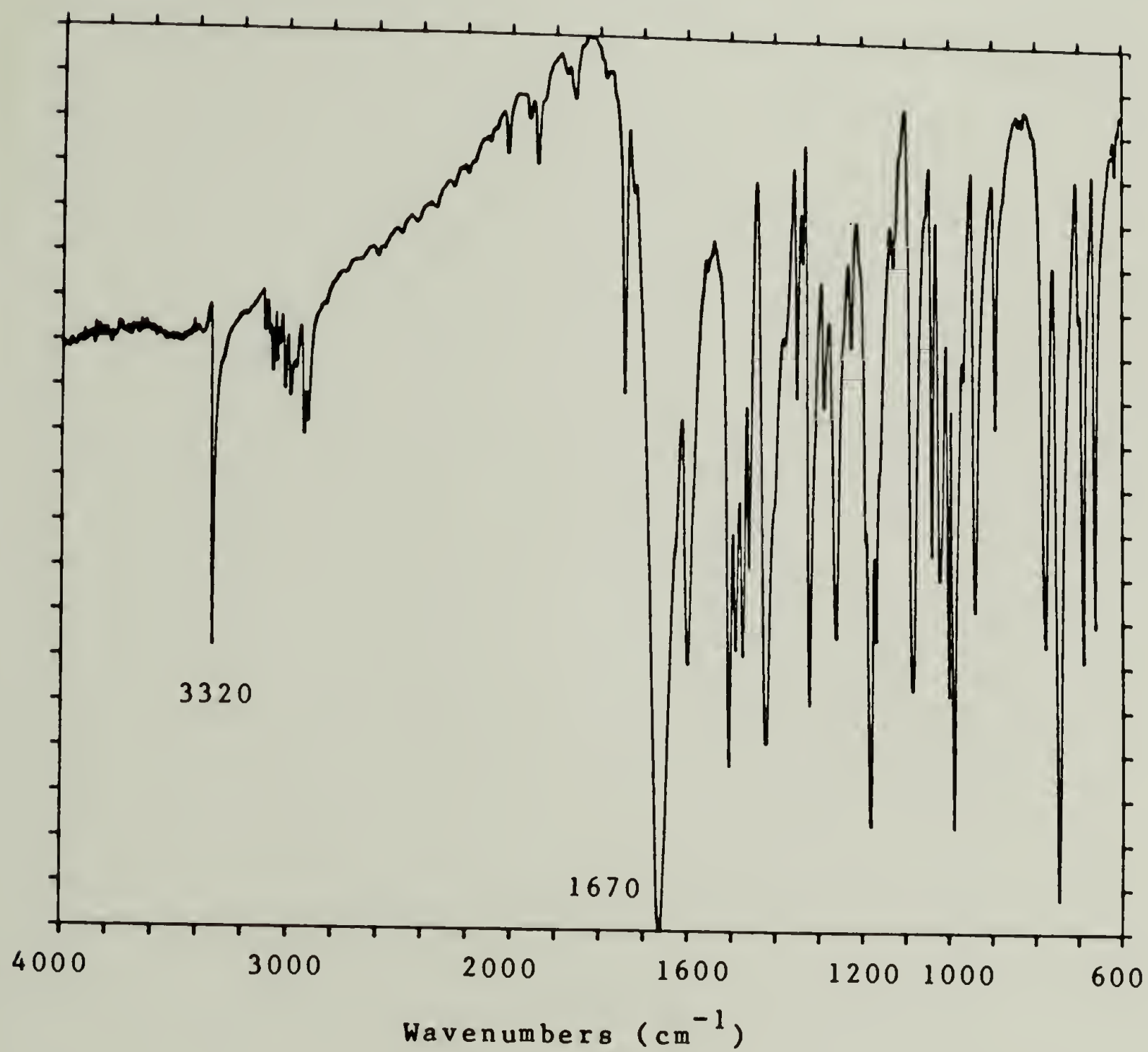


Figure 4-13: FTIR spectrum of 2-imino-3-phenyl oxazolidine.

might be expected if ring formation was an equilibrium reaction. Further, mixtures of the 2-imino-3-phenyl oxazolidine with MGEBA were found to be quite reactive, both when isothermally reacted at 167°C for two hours and when temperature scanned in the DSC to 220°C. An HPLC chromatogram of the product mixture from the isothermal reaction, shown in Figure 4-14, reveals a single major product believed to be the 1:1 adduct.

The 2-imino-3-phenyl oxazolidine was characterized by proton FT-NMR. The spectrum, shown in Figure 4-15, reveals a peak at 5.48 ppm which is assigned to the imine proton. This proton can be exchanged with deuterium from added D<sub>2</sub>O, resulting in complete elimination of the NMR peak. For purposes of comparison, an attempt was made to characterize isolated products I, II, and III by <sup>1</sup>H FT-NMR. Due to the large number of protons contained in the structurally invariant bisphenol A portion of the MGEBA substituents, the small quantities available for analysis, and the remaining impurities in these isolated compounds, there was some difficulty in assigning structures to the minor peaks. However, the spectrum of product III, shown in Figure 4-16, reveals a small peak at 5.10 ppm, which was not found in the spectra of products I and II. Although this peak was observed to have a chemical shift similar to the imine group of the model compound, all attempts to exchange this proton with D<sub>2</sub>O failed. Although product I was found to contain two exchangeable peaks at 6.3 and 6.6 ppm and product II showed one exchangeable peak at 6.2 ppm, the spectrum of product III revealed no peaks in this region. Due to the unpredictable chemical shifts and integrated values

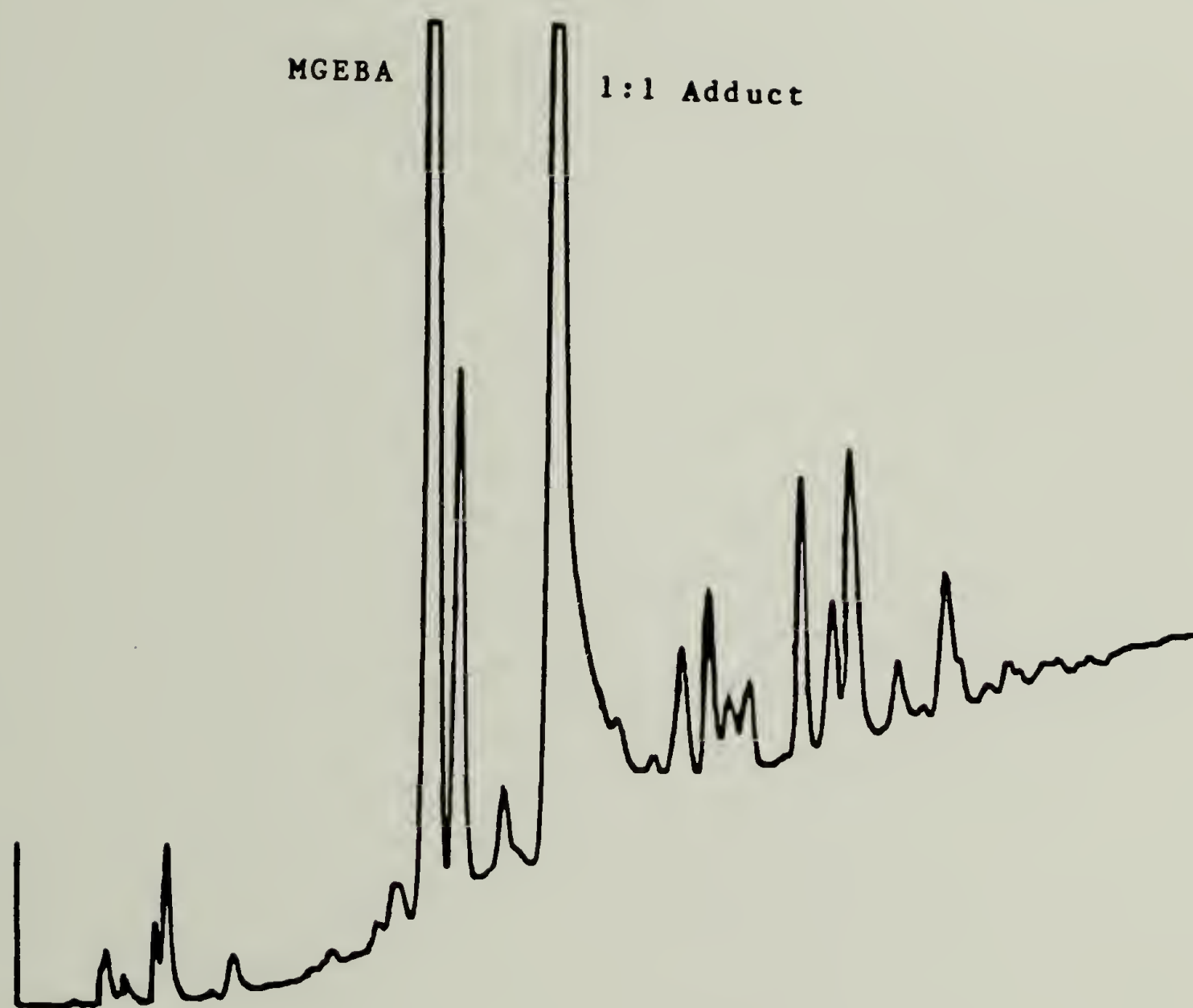


Figure 4-14: HPLC chromatogram of 1:2 2-imino-3-phenyl oxazolidine/DGEBA reacted at 167°C for 120 min; THF/H<sub>2</sub>O = 50-90%, over 40 min, at grad 6, analyzed at 229nm.

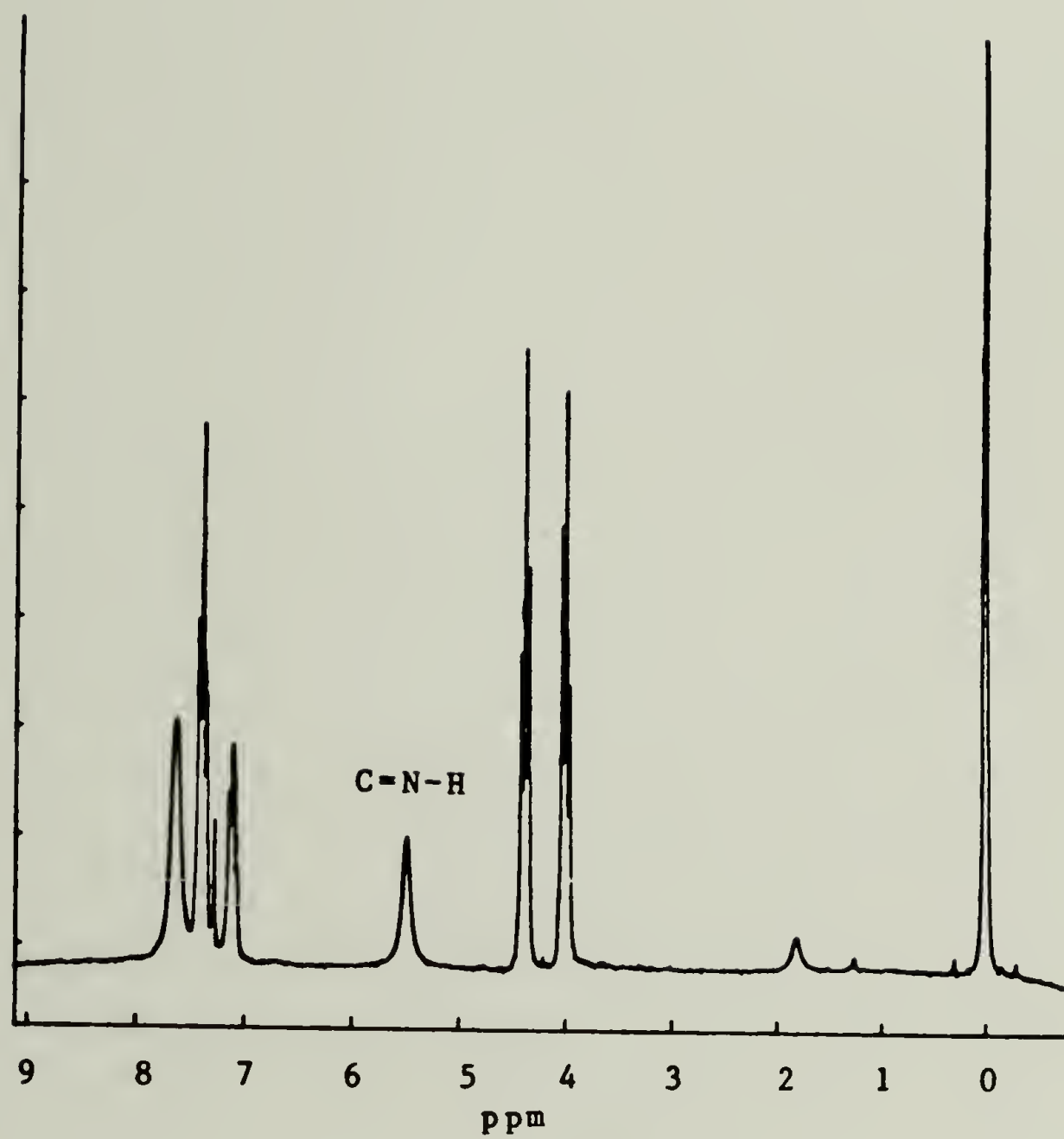


Figure 4-15:  $^1\text{H}$  NMR spectrum of 2-imino-3-phenyl oxazolidine.



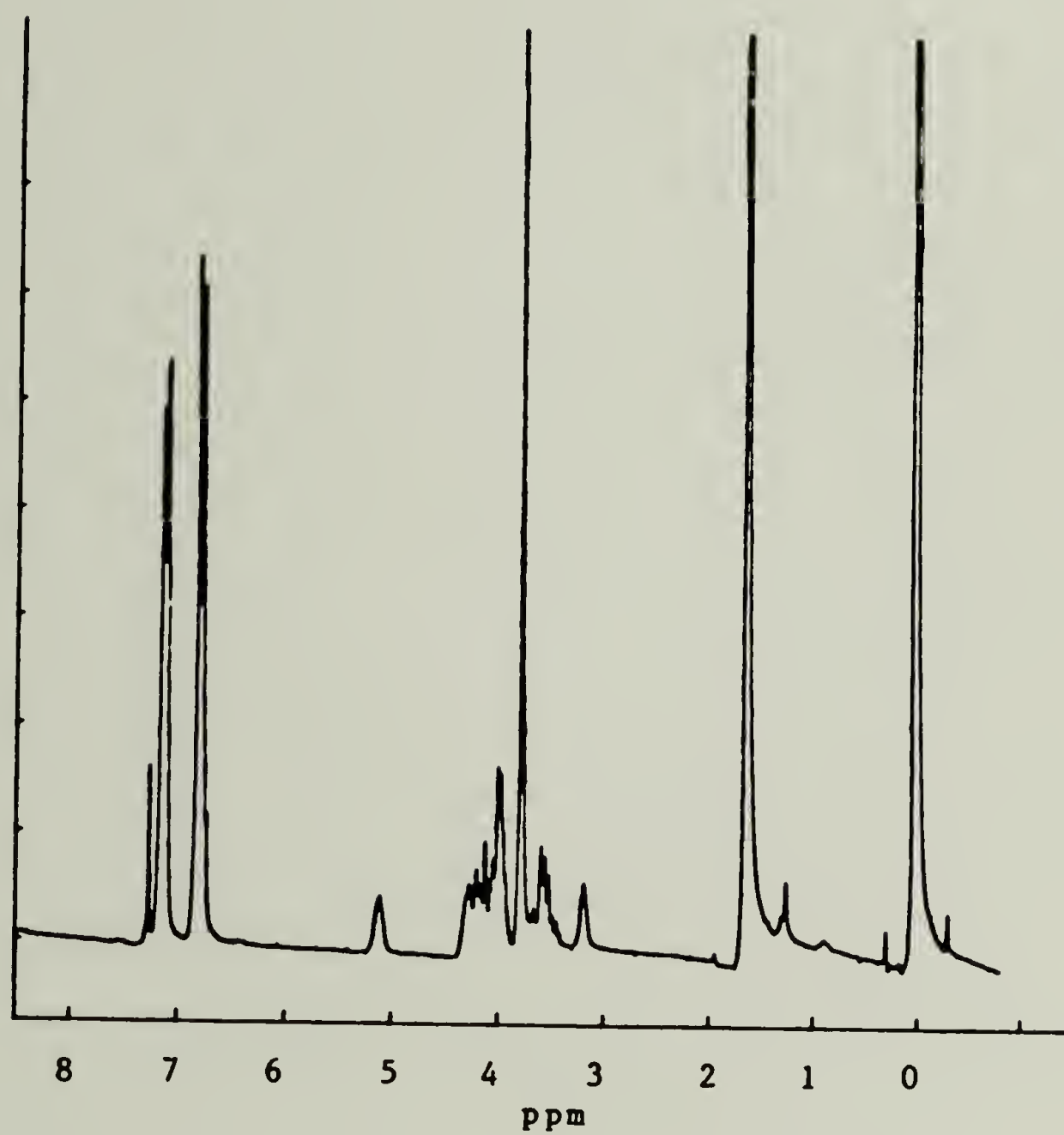


Figure 4-16:  $^1\text{H}$  NMR spectrum of product III.

of these heteroatom substituted protons, the accurate determination of these peak assignments required further structural verification.

As was discussed in the introduction of this chapter, an attempt was made to synthesize a disubstituted 2-imino oxazolidine from the reaction of MGEBA substituted tertiary amines with cyanogen bromide. The reaction was performed using 3:1 adduct of MGEBA and ammonia. However, this amine was found to be unreactive toward cleavage by cyanogen bromide. A second attempt using the 2:1 adduct of MGEBA and ammonia was more successful. An HPLC of the reaction mixture revealed several products as expected, one of which appeared to have the same elution time as product III. This material was isolated by PLC and analyzed by FTIR and  $^1\text{H}$  NMR spectroscopy. The FTIR spectrum of this synthesized compound, shown in Figure 4-17, appears to be identical to that of product III. The  $^1\text{H}$  NMR spectrum, shown in Figure 4-18, is also identical to that of product III, showing a peak at 5.10 ppm. This peak was similarly non-exchangeable with  $\text{D}_2\text{O}$ . The synthesized material was also unreactive toward further epoxide addition.

Since the synthesized product III was prepared in a manner similar to the 2-imino-3-phenyl oxazolidine by a known synthetic route, it appeared to confirm the tentative structure of product III. However, the spectral characterization and properties of this compound were again at odds with the assignment of this structure to a 2-imino oxazolidine. The details of the synthesis of this compound are presented in sections 3 and 4 of the appendix.

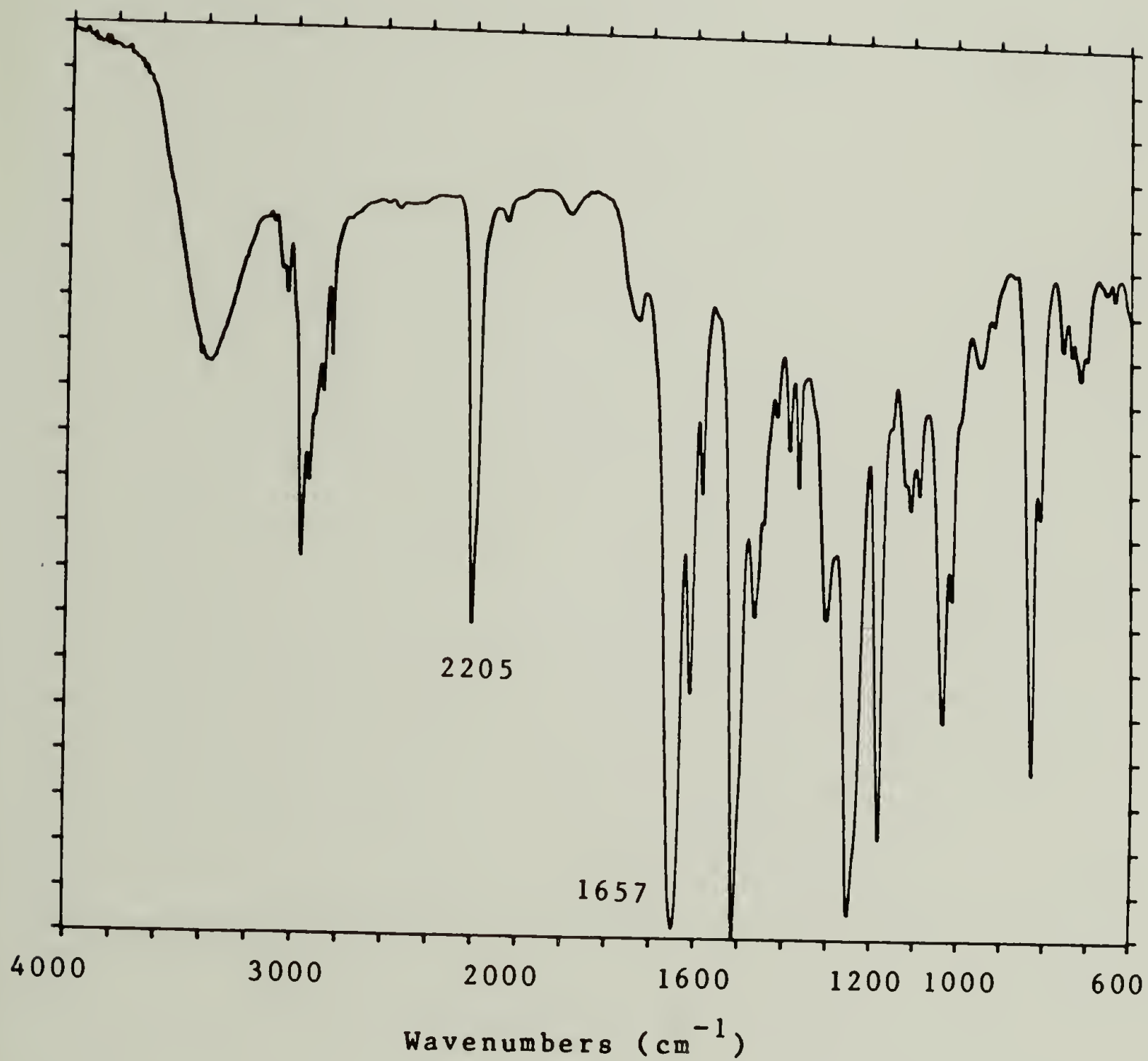


Figure 4-17: FTIR spectrum of synthesized product III.

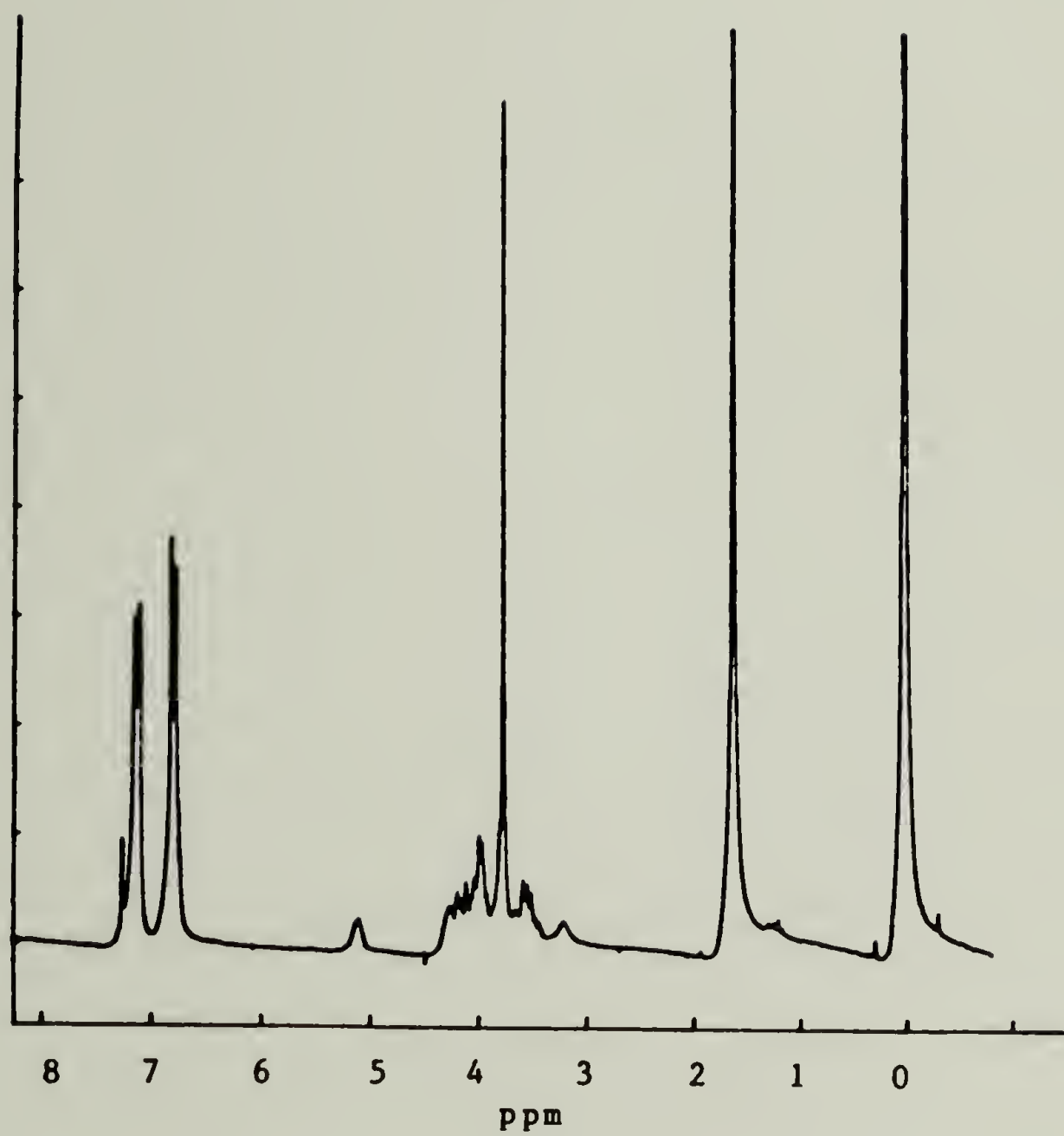


Figure 4-18:  $^1\text{H}$  NMR spectrum of synthesized product III.



### Purification and Identification of Isolated Products

In order to characterize products I, II, and III by  $^{13}\text{C}$  FT-NMR, it was necessary to further purify the materials in much larger quantities. This was done by repetitive isolations with the PLC, and in the case of products I and III, by recrystallization. It was found that products I and III could be crystallized by repeatedly dissolving them in methylene chloride and removing the solvent by vacuum evaporation at elevated temperatures. It is assumed that this process aided in removing the last traces of tenaciously held solvents, such as THF, from the materials. Following initial crystallization, product III could be purified by recrystallization from 100% methanol. Product I, on the other hand, was recrystallized from a methanol solution to which about 2% water was slowly added with mixing. Melting points of  $106^{\circ}$  and  $140^{\circ}\text{C}$  were measured for products I and III, respectively. Eventually, enough material was purified by this procedure so that  $^{13}\text{C}$  FT-NMR characterization could be performed. Further, the ultrapure nature of these materials made it possible to perform elemental analysis and most importantly, mass spectrometry on these compounds.

### Mass Spectrometry

Initial attempts to determine molecular weights by the techniques of GC and solid probe MS had failed due to the reaction or degradation of the isolated materials either at the temperatures required for volatilization or in the electron beam. However, a third attempt using fast atom bombardment mass spectroscopy (FABMS) proved to be successful. In this technique, materials were imbedded in an innocuous matrix of nitrobenzyl alcohol, and were ionized by the relatively soft technique of

Argon atom bombardment. Proton capture by individual molecules produced relatively stable parent ions which could then be analyzed by MS.

The FABMS spectra obtained for products I-III are shown in Figure 4-19 and the mass of the protonated parent ion are labelled. The molecular weights determined by this technique are listed in Table V, along with the results of elemental analysis. Products I and II were found to have molecular weights of 382 and 680 AMU, respectively. This indicated that products I and II were in fact the 1:1 and 2:1 adducts of MGEBA and dicy, respectively, and not alkyl cyanamides as originally believed. These designations were confirmed by elemental analysis, as shown in Table V. Product III was found to have a molecular weight of 663 which indicated a weight loss of 17 AMU in the transformation of product II into product III. Elemental analysis confirmed that this weight loss was due to the elimination of ammonia.

Based on these findings the mechanism and structures shown in Figure 4-20 were proposed. According to this mechanism, cyclization does not occur by the intramolecular addition of hydroxyl to cyano as proposed by Zahir. Instead, reaction occurs via the intramolecular nucleophilic substitution of hydroxyl at the imide carbon, resulting in the elimination of a molecule of ammonia. The proposed mechanism indicates that the cyano substituted imide group is not only quite stable, but that by acting concertedly, this group behaves very much like a carbonyl group in this reaction. The generation of ammonia by the dicy cure of epoxies had been previously reported by Saunders [35] and Fountain [11], both during the cure and in subsequent heatings of the cured material.

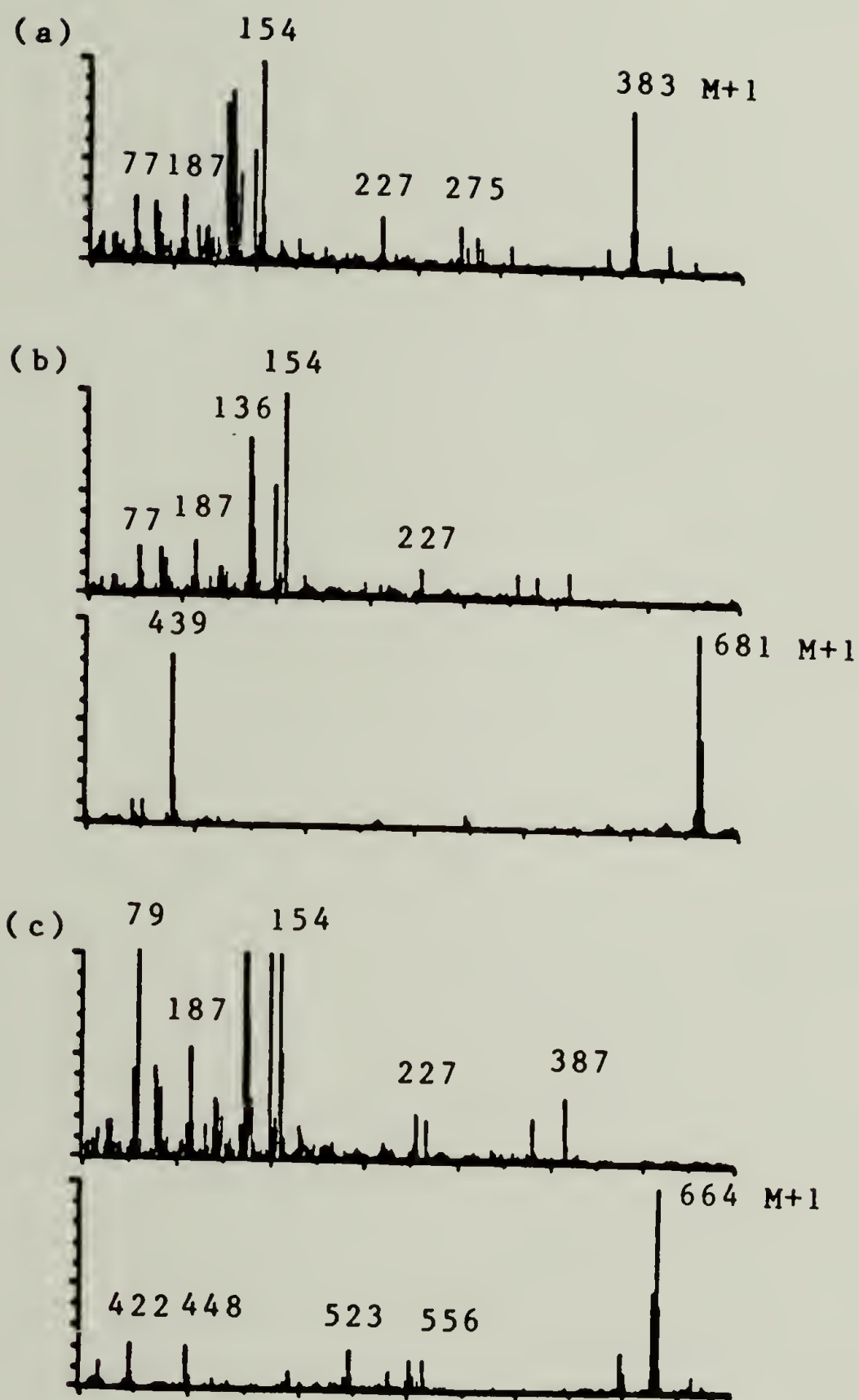


Figure 4-19: FABMS spectra of products I, II and III.

Table V  
MS and Elemental Analysis of Isolated Products

Product		Mass (AMU)	C	H	N
I	exp	382	64.14%	6.41%	14.22%
	theor		65.97%	6.81%	14.66%
II	exp	680	69.77%	7.25%	8.20%
	theor		70.59%	7.06%	8.24%
III	exp	663	71.99%	6.52%	6.24%
	theor		72.40%	6.79%	6.33%



## FORMATION OF PRODUCT III

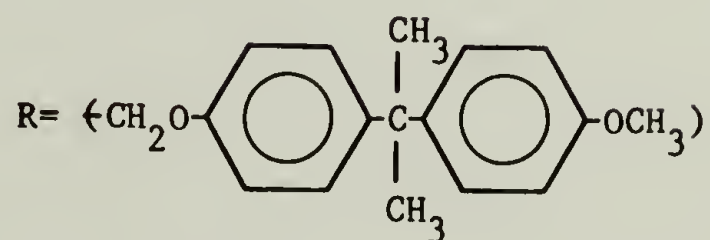
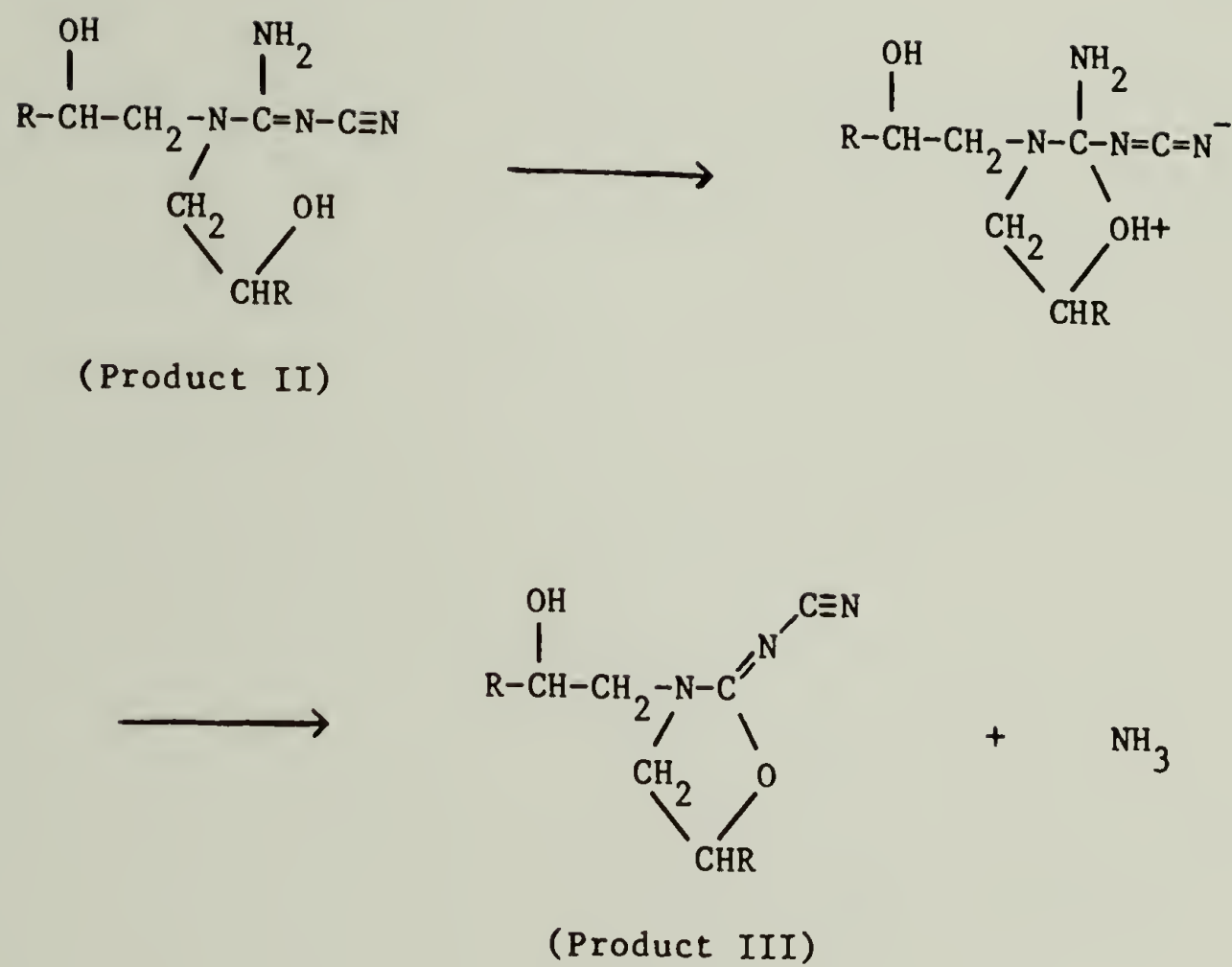


Figure 4-20: Mechanism of product III formation.

However, the ammonia was thought to be a minor by-product of dicy decomposition. The further implications of ammonia generation on the structure of the crosslinked resin will be addressed later in this chapter.

### Carbon-13 NMR Analysis

In order to confirm these structures, the purified products were characterized by  $^{13}\text{C}$  FT-NMR. For purposes of reference, a  $^{13}\text{C}$  NMR spectrum was also obtained for MGEBA and is shown in Figure 4-21. The various peaks in this spectrum are labelled to designate their assignments in the accompanying structure. Assignments were made, based on those previously reported for commercial epoxy resins [76]. As was the case for the  $^1\text{H}$  NMR spectra, most of the peaks are assigned to carbons in the bisphenol A portion of the molecule. Since the reaction of the oxirane functionality had little effect on the chemical shift of these peaks, no useful structural information could be obtained from their analysis in the spectra of the isolated products. However, the carbons contained in the oxirane functionality of the MGEBA were greatly affected by amine reaction and changes in their chemical shifts provided important structural information about these products. For purposes of clarity, the carbons, here assigned to peaks C and D at 46.1 and 51.5 ppm, respectively, will be referred to as carbon 1 (C1) and carbon 2 (C2).

In the  $^{13}\text{C}$  NMR spectrum of product I, shown in Figure 4-22, C1 and C2 have been assigned to peaks at 46.3 ppm and 71.1 ppm, respectively. This is indicative of the chemical change of C1 and C2 from oxirane

MGEBA

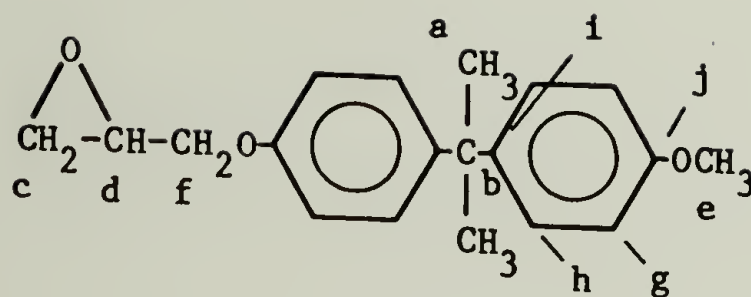
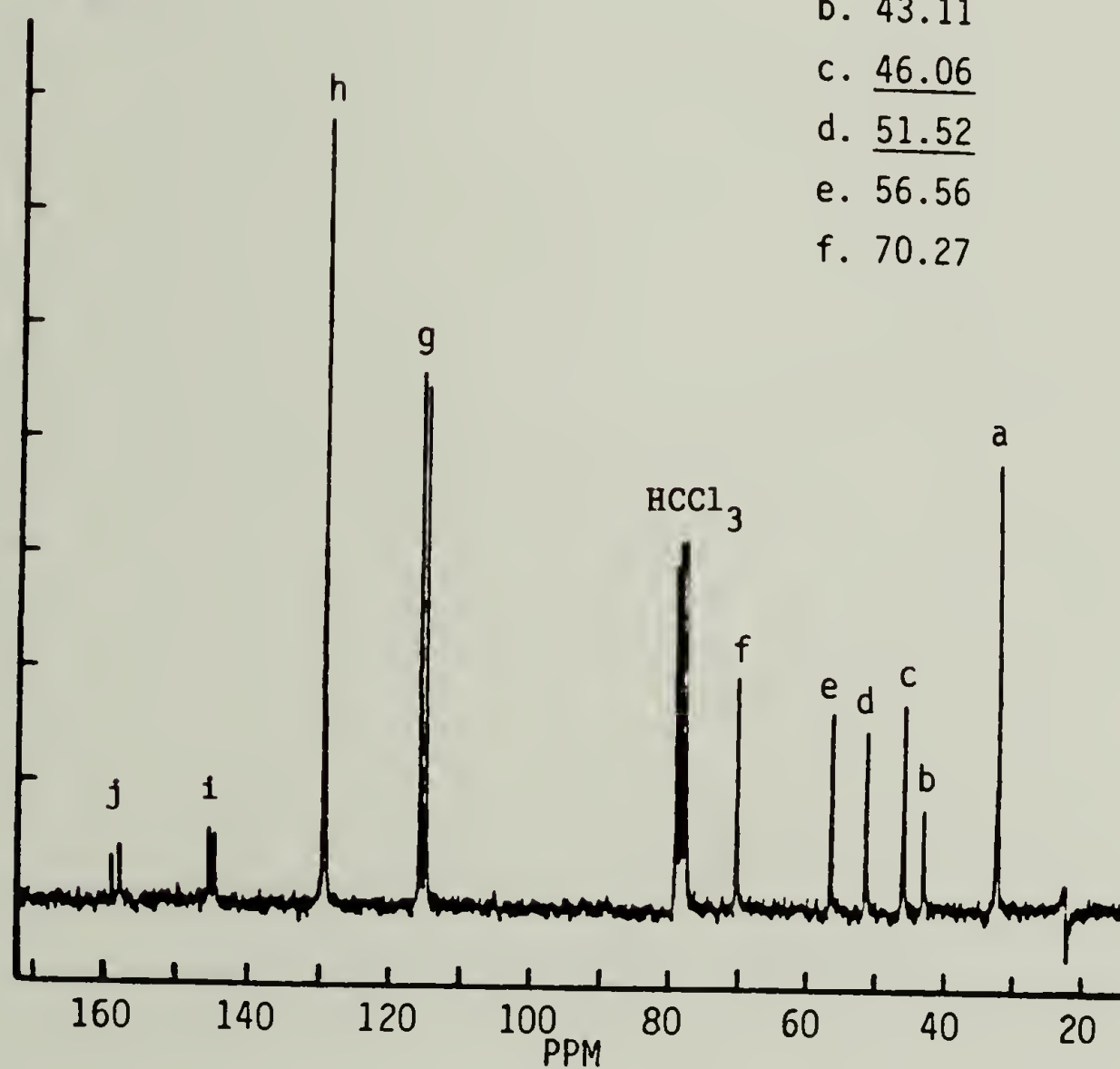
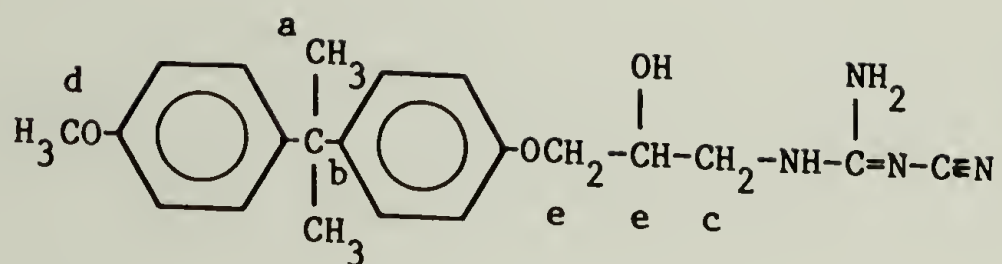
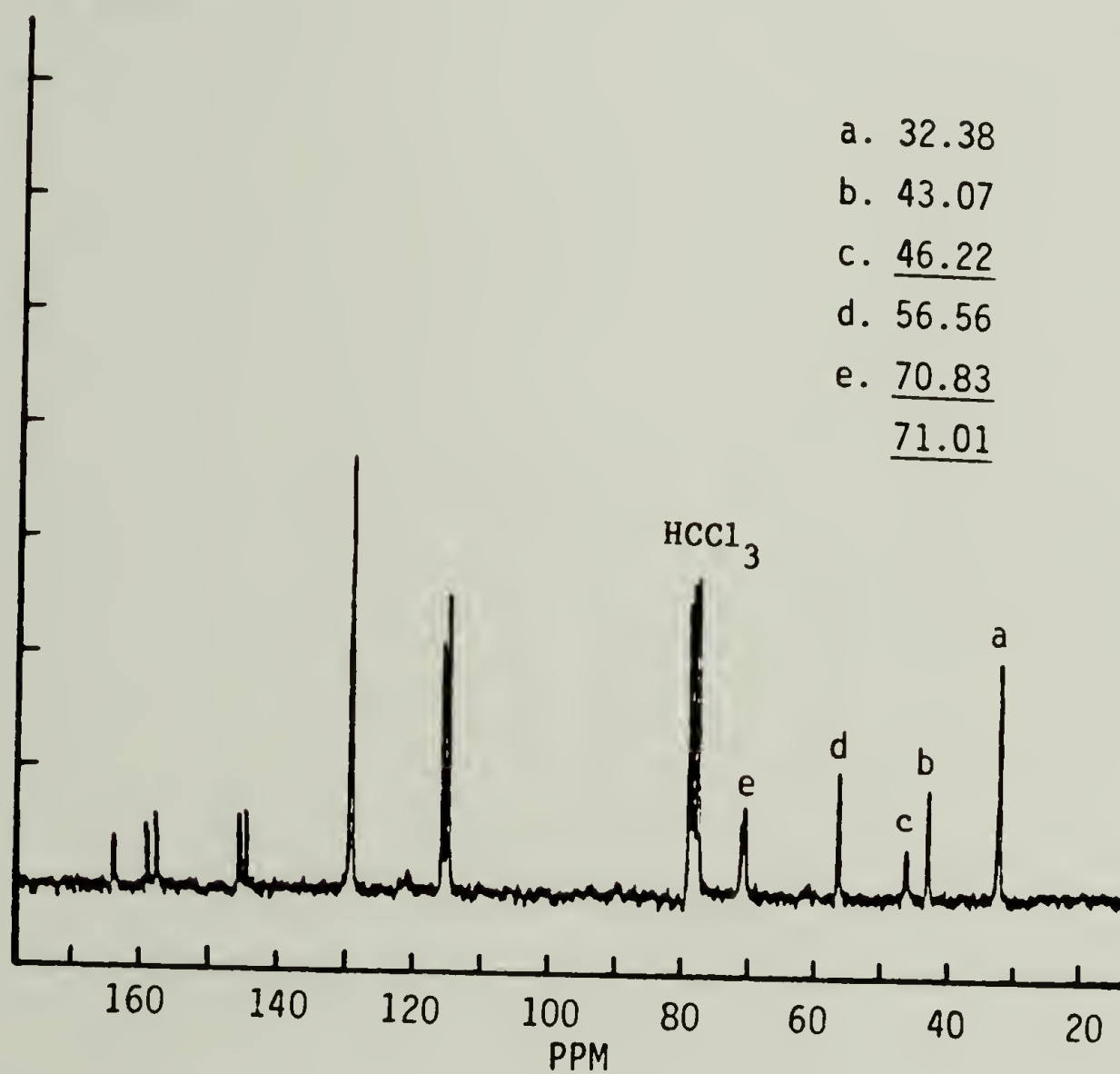
 $^{13}\text{C}$  NMR

Figure 4-21:  $^{13}\text{C}$  NMR spectrum of MGEBA.

## Product I

<sup>13</sup>C NMRFigure 4-22: <sup>13</sup>C NMR spectrum of product I.



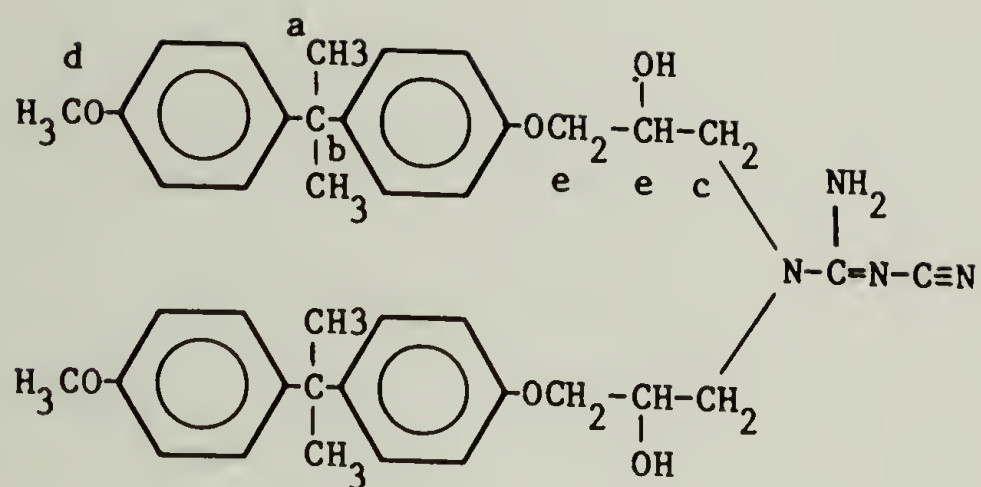
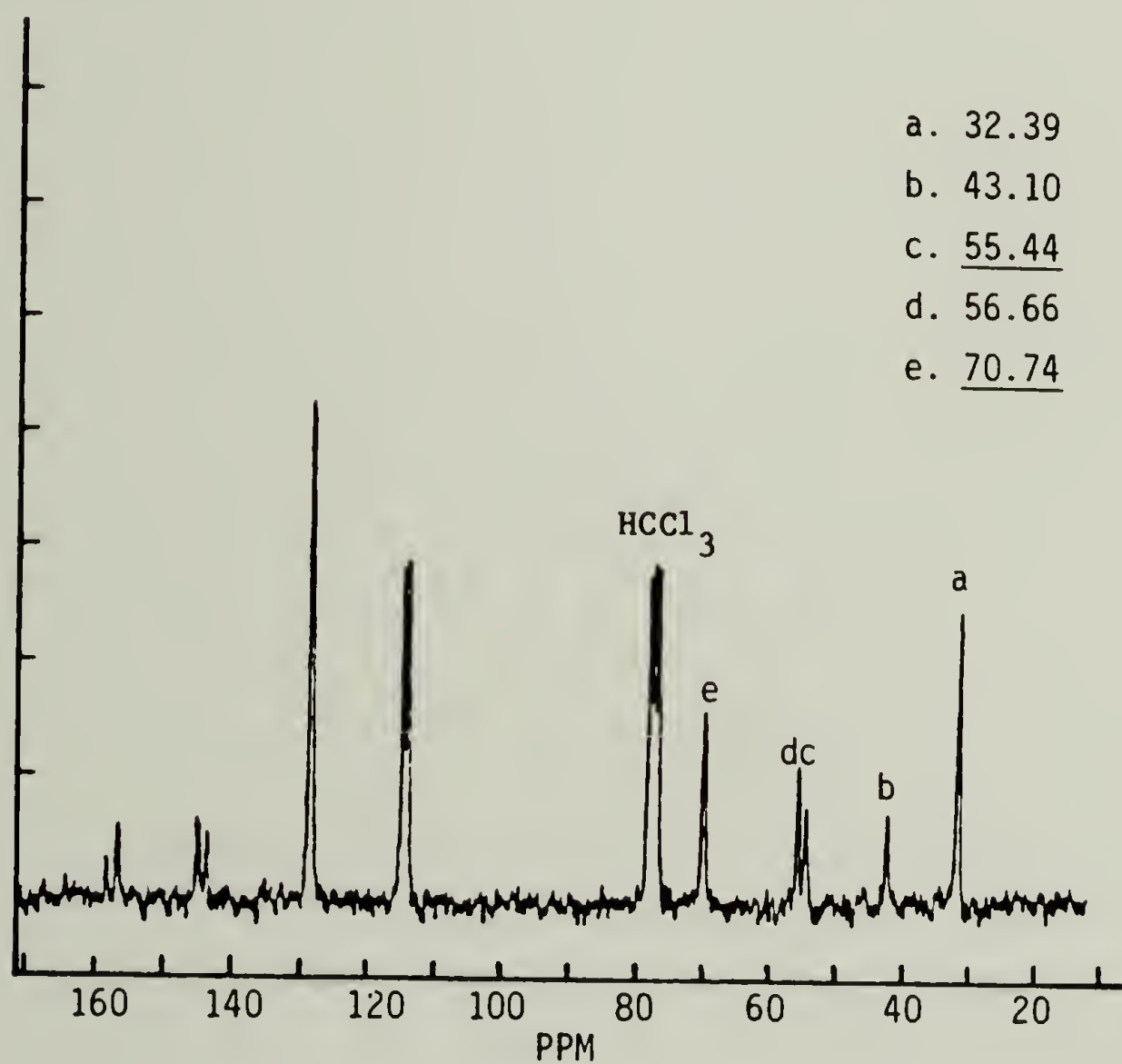
carbons to a secondary amine substituted carbon and a hydroxyl substituted carbon, respectively. Also evident in this spectra is a peak at 163.7 ppm, which is assigned to the imine carbon of the dicy structure, while a peak at 120.7 ppm, assigned to the cyano carbon, is barely perceptible.

In the case of the disubstituted product II, there are two C1 and two C2 carbons. However, the spectrum of product II, shown in Figure 4-23, reveals only one peak assigned to each of these types of carbons indicating the symmetric nature of the substitution. Further, the peak assigned to C1 is shifted downfield by 8.2 ppm in going from product I to product II. This downfield shift is indicative of the change in environment of C1 from that of a secondary amine substituted carbon to that of a tertiary amine substituted carbon.

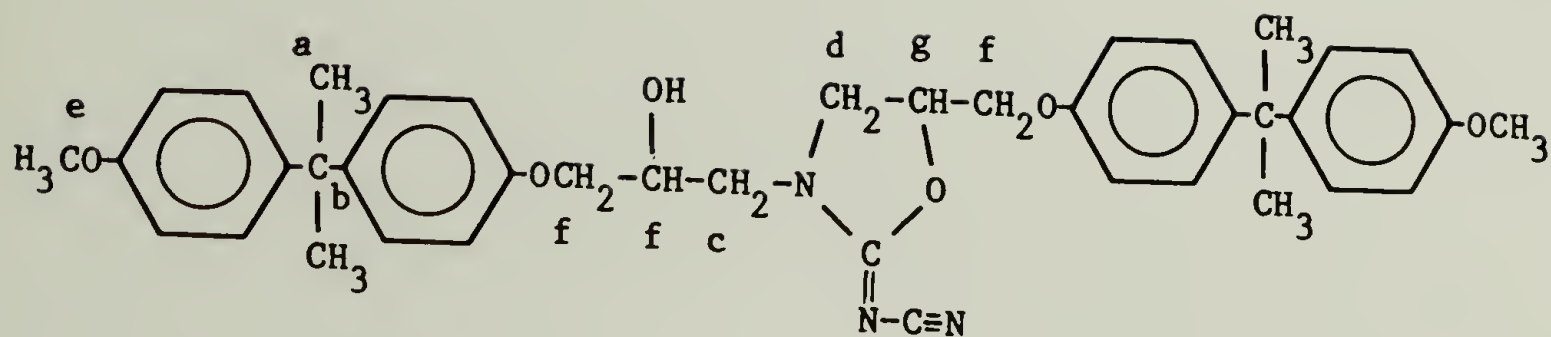
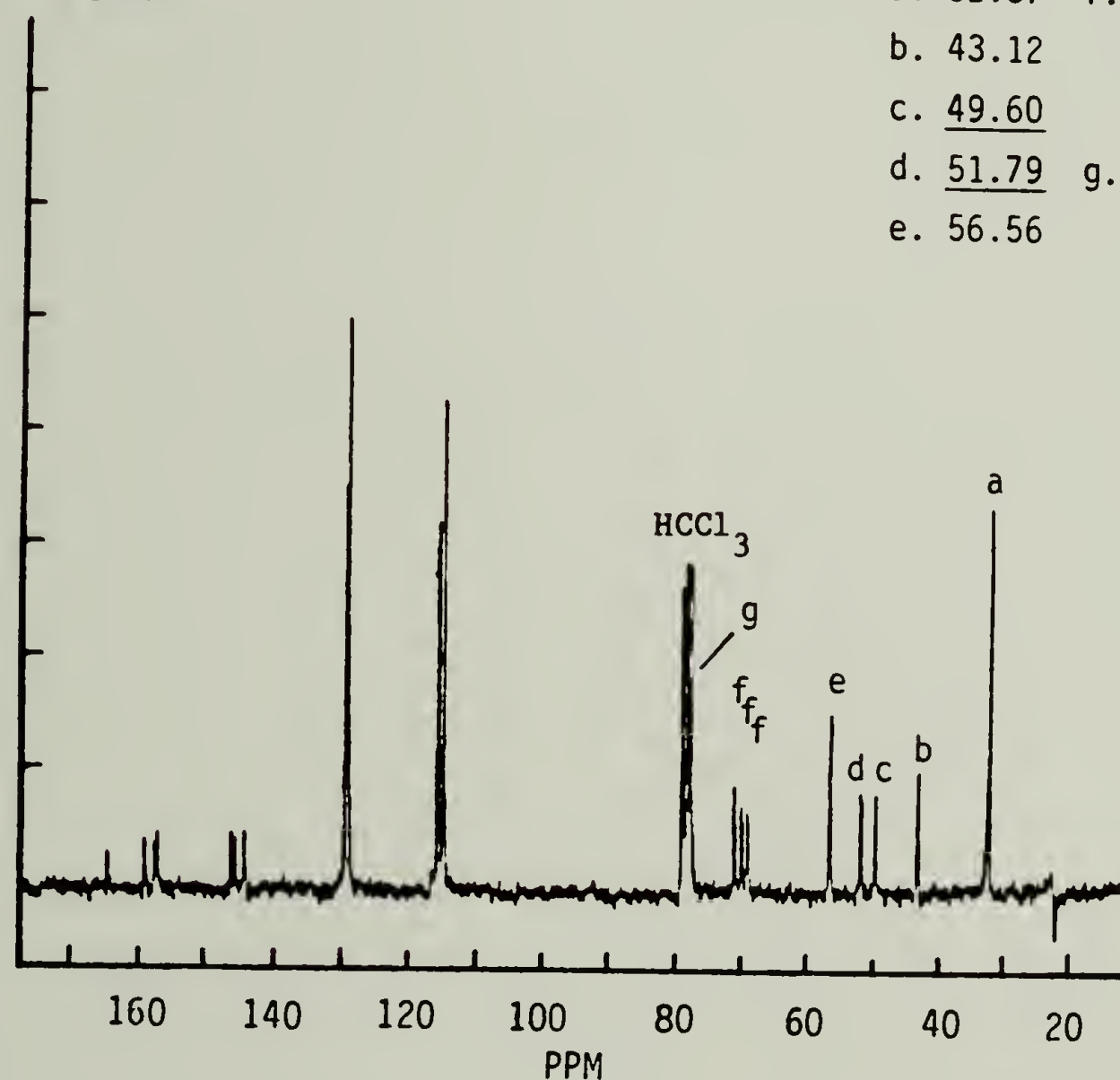
The spectrum of product III, shown in Figure 4-24, reveals two peaks assigned to C1, one at 49.7 ppm and the other at 51.8 ppm which are indicative of the now different environments of these amine substituted carbons. Further, only one of the two C2 carbons retains the chemical shift of a hydroxyl substituted carbon. The other has been shifted downfield to 78.2 ppm and is visible partially occluded by the chloroform triplet. The shift was due to the change in environment of this C2 carbon which occurred as a result of the intramolecular reaction of its attached hydroxyl functionality.

The  $^1\text{H}$  FT-NMR spectra of products I through III were reinterpreted in terms of the proposed structures and the key peaks from these spectra

## Product II

<sup>13</sup>C NMRFigure 4-23: <sup>13</sup>C NMR spectrum of product II.

## Product III

 $^{13}\text{C}$  NMRFigure 4-24:  $^{13}\text{C}$  NMR spectrum of product III.

are shown in Figure 4-25 along with the assigned structures. From this data, it can be seen that the proton attached to the C2 carbon also undergoes a downfield shift upon reaction of the hydroxyl group alpha to this carbon. While products I and II reveal one and two protons, respectively at 4.3 ppm assigned to the structure  $\text{=CH-OH}$ , product III shows only one proton at 4.3 ppm. The other has been shifted to 5.1 ppm. Previously, this shifted peak had been erroneously assigned to the imine group, which added to the difficulties in identifying this compound. The  $^1\text{H}$  FT-NMR peaks at 6.5 and 6.2 ppm are assigned to secondary and primary amine protons, respectively. Integration of these yielded two primary amine and one secondary amine proton for product I, while the spectrum of product II was found to contain only the two primary amine peaks, supporting the proposed structure of product II.

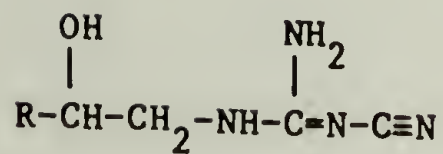
#### Carbonyl Formation in the Dicy/MGEBA Reaction

Product III is a relatively stable compound. In pure form it can be heated for several hours at  $167^\circ\text{C}$  without weight loss or structural change as determined by HPLC. However, when heated with MGEBA or when formed from II, product III is slowly transformed into product IV. As shown by SEC analysis in Figure 4-6, the molecular size of product IV appear to be only slightly smaller than product III. However the FTIR spectra, shown in Figure 4-8 and 4-9, reveals that this transformation results in the disappearance of both imide and cyano groups and the appearance of a broad carbonyl at  $1750\text{ cm}^{-1}$ . Thus, a simple rearrangement reaction as proposed by Zahir, was not a likely route for the formation of this compound. In order to determine the reaction responsible for this transformation, attempts were made to react product III both



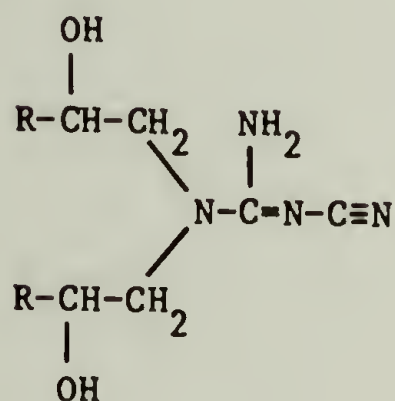
# PROTON NMR OF ISOLATED PRODUCTS

I



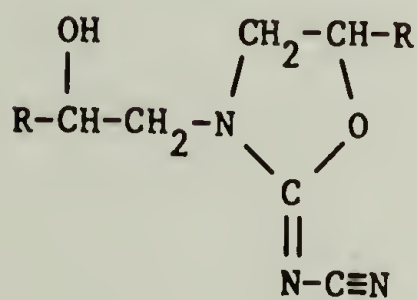
2 Protons at 6.2 ppm  $-\text{NH}_2$   
 1 Proton at 6.5 ppm  $-\text{NH}$   
 1 Proton at 4.3 ppm  $=\text{CH}-\text{OH}$

II



2 Protons at 6.2 ppm  $-\text{NH}_2$   
 2 Protons at 4.3 ppm  $=\text{CH}-\text{OH}$

III



No Amine Protons  
 1 Proton at 4.3 ppm  $=\text{CH}-\text{OH}$   
 1 Proton at 5.1 ppm  $=\text{CH}-\text{O}-\text{R}'$

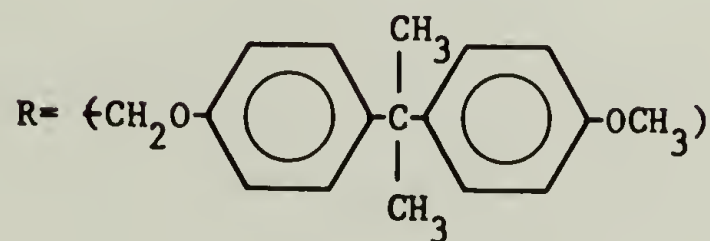


Figure 4-25:  $^1\text{H}$  NMR spectra and structures of products I, II and III.

with BDMA and with water. While the BDMA had only a slight effect, the added water drove the transformation almost to completion when reacted for two hours at 167°C. A hydrolysis reaction was proposed for this transformation yielding a dialkyl 2-oxazolidone. The proposed structure and mechanism of formation of product IV are shown in Figure 4-26. Confirmation of the proposed structure was obtained by FABMS analysis of the isolated material, which revealed the anticipated molecular weight of 639 AMU.

The proposed reaction scheme for the formation of the 2-oxazolidone, shown in Figure 4-26, indicated that cyanamide was generated by this reaction. The further hydrolysis of this generated cyanamide would yield urea. In addition, should the cyano group of product III be hydrolyzed first, a substituted urea would be generated. Each of these reactions would increase the concentration of amide protons available for epoxide addition. However, no compounds of this type were detected by the HPLC analysis of the above mixtures, or by the further reaction of hydrolyzed product III with MGEBA. These potential hydrolysis reactions will be addressed in a later section of this chapter.

#### Identification of the Less Polar Products

The formation of product III by intramolecular substitution, as shown in the proposed reaction scheme in Figure 4-20, results in the liberation of ammonia. Although it was initially believed that most of this ammonia would leave the system, it was thought that the reaction of some of the ammonia with MGEBA would form highly reactive primary amines. These in turn would then rapidly react to form tertiary amines.



In a recent study by Renner et al. [77] a cyanacetic acid ester, used as an epoxy curing agent, was found to liberate ammonia during the later stages of the cure. This liberated ammonia did not escape the system. Instead, it was found to act as a "satellite" curing agent, reacting immediately with the epoxide upon generation.

In order to confirm the ammonia/epoxide reaction in this system, an attempt was made to find these tertiary amine products in the dicy/MGEBA reaction mixture. Since these products were thought to be relatively nonpolar, the search began with chromatographic peaks G and H of the dicy/MGEBA reaction mixture, shown in Figure 4-1. As was previously discussed, the bulk of the materials eluting in this region appeared to contain no carbonyl, cyano, or imine peaks and were considered to be good candidates for the ammonia/MGEBA reaction products. With repeated isolations, it was possible to obtain peak H in relatively pure form. The material was then analyzed with FABMS and a parent ion with a molecular weight of 911 was detected, confirming the identification of this compound as the 3:1 adduct of MGEBA and ammonia. The pure compound was designated as product V and its FTIR spectrum is shown in Figure 4-27. A comparison of this spectrum with that of MGEBA, shown in Figure 3-1, reveals little in the way of distinguishable differences. It would thus have been difficult to detect the presence of this compound in a dicy/epoxide product mixture by means of spectral subtraction, as was used by Davidson [41]. Furthermore, by SEC analysis this material appeared to be insubstantially larger than products II, III, and IV, using THF as the mobile phase. Thus, these compounds would not have



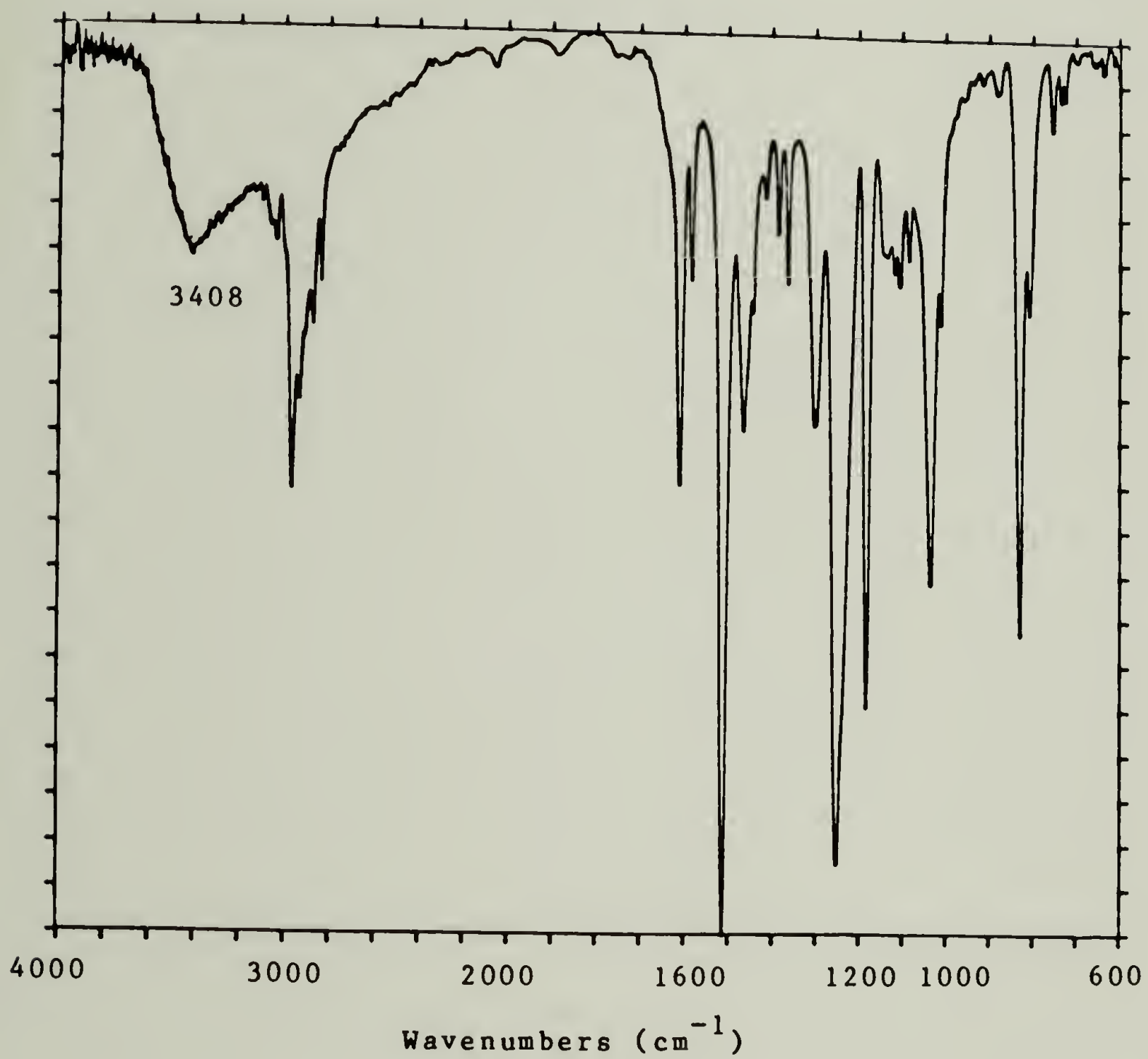


Figure 4-27: FTIR spectrum of product V.

been separated by the preparative SEC study performed by Zahir [40]. Only by PLC isolation, was it possible to identify this compound.

FTIR analyses indicated that the bulk of the materials isolated from peaks G and H are identical. It was therefore suspected that these peaks were composed of isomeric forms of product V [69]. As the 3:1 adduct of MGEBA and ammonia, product V has three chiral centers and thus eight stereoisomers. Due to molecular symmetry, these isomers were divided into two diastereomeric sets, one containing two isomers, and the other six, which are indistinguishable among themselves. Previous investigators have reported that each of the stereoisomers are formed in equivalent amounts in amine/epoxide reactions [64]. Thus the ratio of stereoisomers in the two diastereomeric sets should be reflected in the HPLC peak area ratios of product V. A review of the data in Chapter 3 indicated that indeed a ratio of approximately 1:3 is found for the areas of peaks G and H over a wide range of product compositions. Product IV was similarly found to be composed of a diastereomeric mixture, which could be separated into two equivalent peaks by the HPLC using an isochratic mobile phase of 50% THF. Attempts to resolve stereoisomers of products II and III, by a similar means, were unsuccessful.

Unlike peaks G and H, peak F could not be isolated without loss due to degradation. However, it was possible to isolate a mixture of peaks F and H without exposure to water or elevated temperatures by conducting a single separation with 100% methanol. An HPLC chromatogram of this isolated fraction, shown in Figure 4-28a, reveals that peak F constituted about 20% of the material while the balance was composed of product

V. In order to test the thermal stability of these compounds, the neat mixture was heated in the DSC at 167°C for fourteen hours and then analyzed by HPLC. The chromatogram, shown in Figure 4-28b, revealed that while product V remained unaffected by this heating schedule, peak F was degraded into several more polar peaks. Most notable of these were those which coeluted with peaks A and D of the dicy/MGEBA reaction mixture. An attempt was made to react the isolated mixture with MGEBA using an identical heating schedule. An HPLC chromatogram of the mixture resulting from this reaction, shown in Figure 4-28c, indicated that product V reacted with approximately its own weight in MGEBA, as determined by peak areas. The product from this reaction required a longer elution time than did product V, as would be expected for a higher molecular weight adduct. A comparison of the SEC chromatogram of this reaction mixture with that of the heated neat material is shown in Figure 4-29. The shorter elution time for the bulk of the material from the reaction mixture confirmed the larger molecular size of the reaction species. Thus product V, as a triethanol amine, appears to be capable of further reaction with MGEBA, presumably via amine catalyzed hydroxyl addition. Finally, the HPLC chromatogram shown in Figure 4-28c appears to indicate that a decomposition product of peak F, here labelled peak A, is capable of further reaction with MGEBA to yield peak D. Since this peak is probably identical to the peak D isolated from the dicy/MGEBA reaction mixture, it can be speculated that peak A from this mixture is composed of the monoalkyl 2-oxazolidone. This conclusion was further supported by the similarity of the FTIR spectra for isolated peaks A and D, shown in Figure 4-3 and 4-4. Although, the decomposition

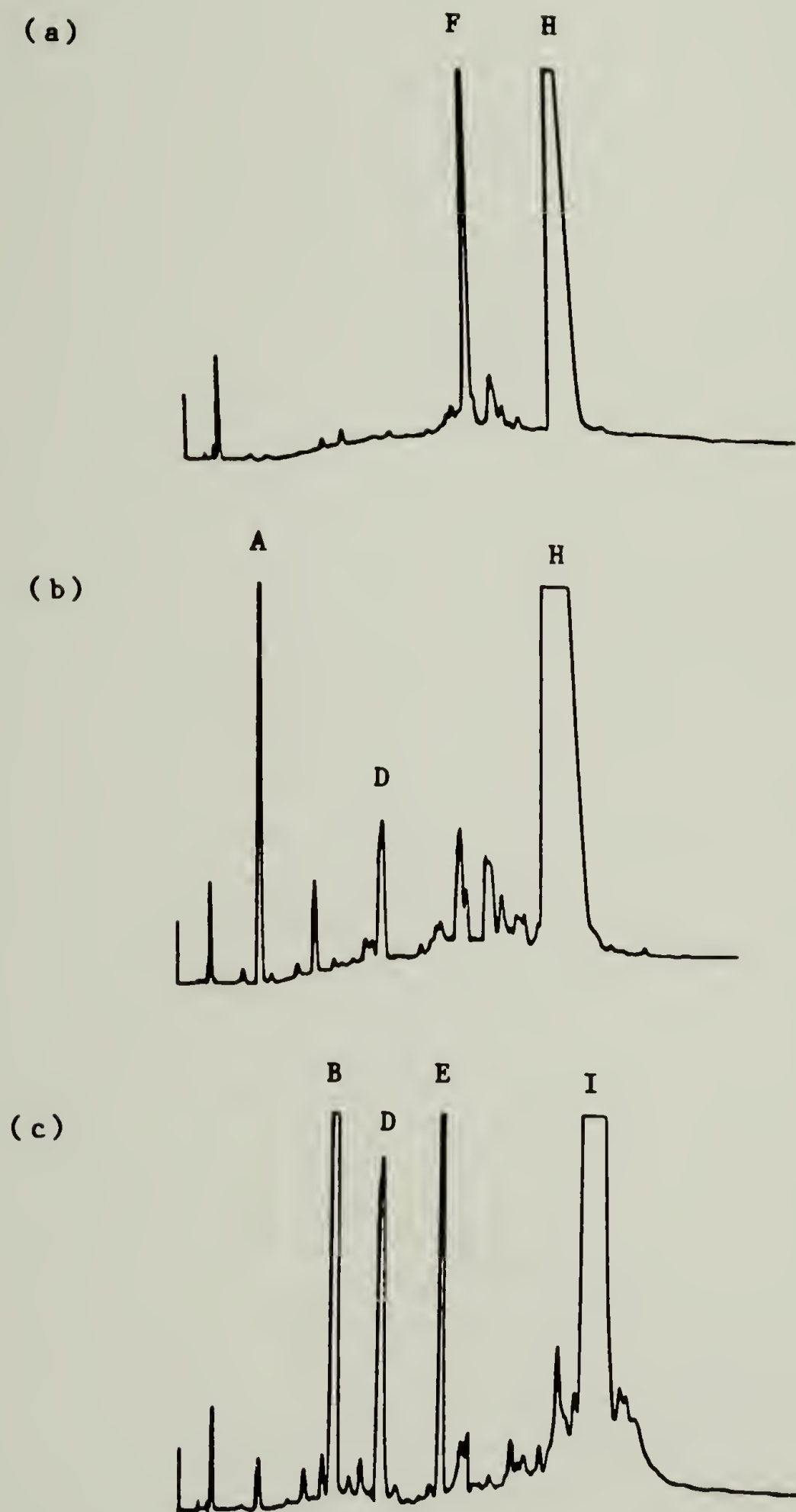


Figure 4-28: (a) HPLC chromatogram of isolated peaks F and H. (b) HPLC chromatogram of peaks F and H heated at 167°C for 120 min. (c) HPLC chromatogram of F+H/MGEBA reacted at 167°C for 120 min.



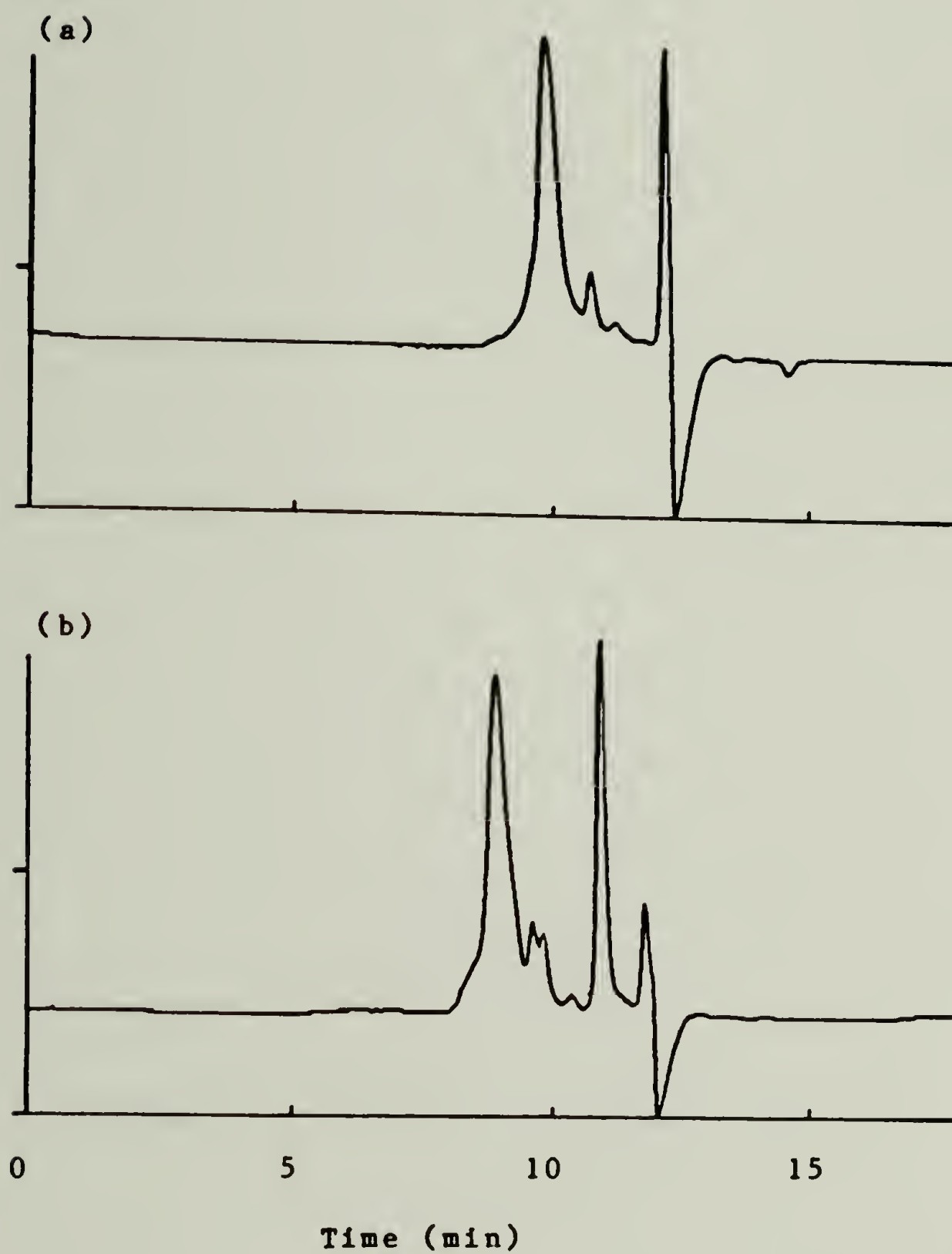


Figure 4-29: Comparison of SEC chromatograms of G+H heated neat and reacted with MGEBA.

of peak F may be an important contribution to the generation of 2-oxazolidones, further work is needed to confirm this hypothesis.

### Review of Previous Results

The combined evidence supports the proposed structures of the five isolated products and the proposed mechanism of their formation. Thus, alkylated dicy appears to form cyclical products via an intramolecular nucleophilic substitution reaction. This reaction liberates ammonia and/or amines which then react further with the epoxide. Carbonyl formation results, at least in part, from the hydrolysis of the dicy/epoxide products at the imide bond. Based on this proposed mechanism, the spectra of product II and III can now be reinterpreted. As shown in Figure 4-7, the spectrum of II contains an absorbance band at  $1570\text{ cm}^{-1}$ , which can be assigned to the conjugated imide bond. The transformation of product II into product III shifts this band to a higher frequency and greater intensity due to changes in the electronic and resonant structure of the imide bond. Thus, the appearance of a strong absorbance band at  $1650\text{ cm}^{-1}$  in the spectrum of product III was not due to the formation of an imine group, but rather to the changes in the environment of the imide bond as a result of cyclization.

Although products I and II were not isolated from the dicy/MGEBA reaction mixture, it is probable that product I was formed by the initial reaction of MGEBA with dicy. Further, the presence of products III, IV, and V in the reaction mixture confirms the applicability of the proposed mechanism to the dicy/MGEBA system. It was observed that the alkylated dicys were extremely reactive at the temperatures required by

the uncatalyzed reaction of dicy with MGEBA. Therefore once formed, the further reaction of these products would lead to the rapid formation of final products in the reaction mixture. Thus, the HPLC results of chapter 3 appear to be merely a documentation of the slow build-up of the virtual end-products in the dicy/MGEBA reaction mixture and the long term changes occurring therein. The rate controlling step appears to be the initial dicy/MGEBA reaction, which in turn is controlled by the dissolution and diffusion of dicy in the mixture.

A review of the HPLC chromatograms of the catalyzed dicy/MGEBA reaction mixtures, an example of which is shown in Figure 3-17, revealed the presence of significant amounts of products I and II. This is presumably due to the lower temperatures required for these reactions, thus lowering the relative rate of reaction of these products as compared to dicy dissolution. Also, the presence of products III and IV in these mixtures as determined by variations in HPLC conditions and detector wavelengths, confirmed the viability of the proposed mechanism for the base catalyzed system.

In the case of the cyanamide/MGEBA reaction mixture, it is probable that the isolated alkylated dicy products were formed by the subsequent addition of excess cyanamide to the initially formed mono and dialkylated cyanamides. This reaction sequence would explain the appearance of only the N,N-dialkyl isomer of product II in the reaction mixture, since this isomer could be easily formed by the addition of excess cyanamide to the dialkyl cyanamide formed in the initial reaction. The formation of the N,N'-dialkyl isomer on the other hand would have required the

further reaction of product I with MGEBA. The results presented in chapter 5 indicate that this reaction would have been relatively slow at the temperatures used.

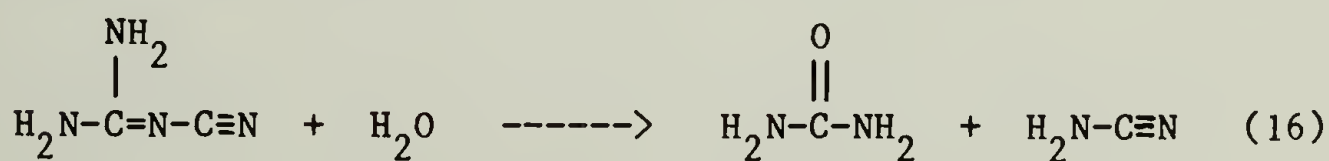
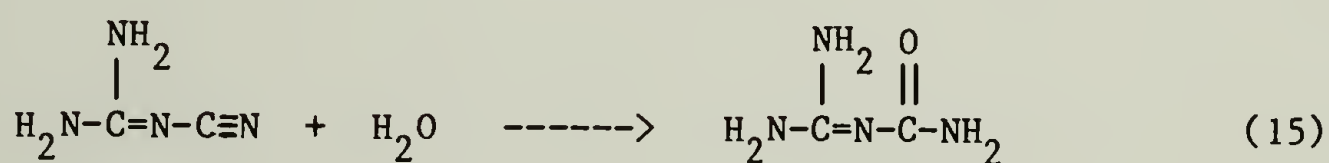
Some of the monoalkyl cyanamide produced in the cyanamide/MGEBA reaction mixture appears to have been a minor contaminant of the initially isolated product I. Thus, while product I reacted and degraded in the GC-MS analysis of the initially isolated material, the small amount of monoalkyl cyanamide present was volatilized, providing the erroneous assignment of 342 AMU as the molecular weight of product I in the that original attempt. Other minor products of the cyanamide/MGEBA reaction may also have been present as contaminants in the initially isolated products. Prior to purification by recrystallization, an attempt was made to analyze product III by FABMS. Although the material was 98% pure by HPLC, MS analysis revealed several prominent ion masses, most notably at 723 AMU, which made parent ion determination difficult. However, the several compounds isolated and purified in this study appear to represent the bulk of the material present in each of their respective peaks.

#### The Role of Water in the Dicy/Epoxide Reaction

According to the mechanism presented by the formation of product IV, water plays a significant role in determining the structure of the final crosslinked resin. Further, the hydrothermal stability of the resin would certainly be affected by the degree to which this reaction reached completion. A review of the literature revealed several studies in which the effect of water on the reaction and final properties of the

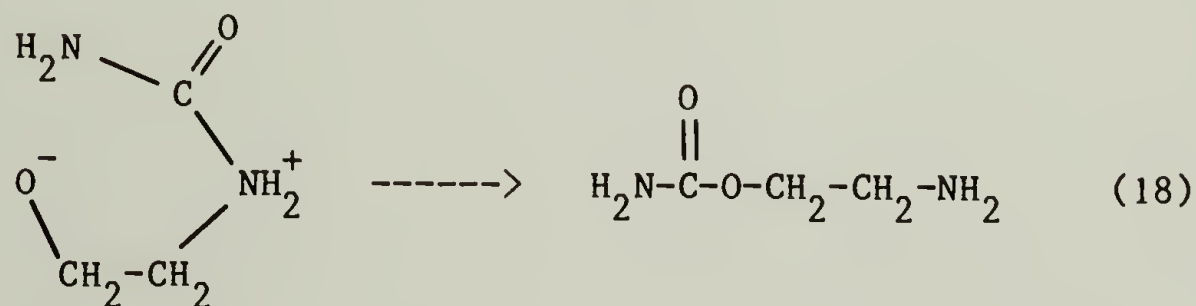
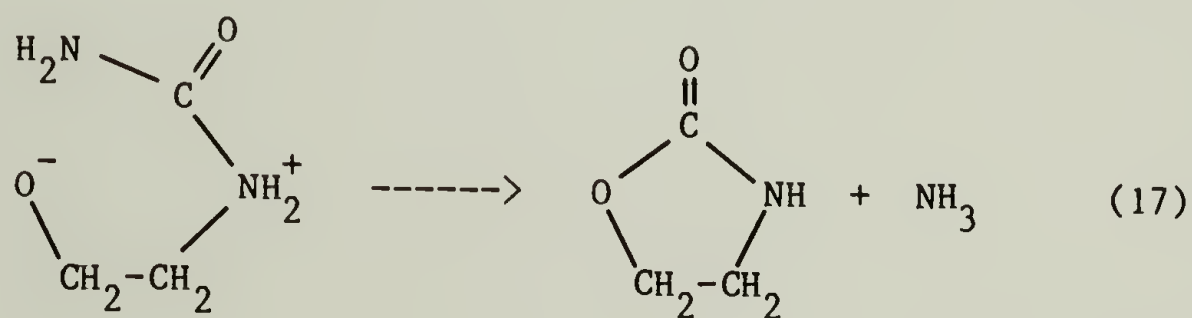


dicy cured resins was investigated. Brand [78] observed the plasticization of dicy cured laminated circuit boards by water, which resulted in swelling and circuit board failure. He reported that these effects were reversible. Illinger et al. [79], on the other hand, observed an irreversible sorption of water by a dicy cured TGMDA sample. The sample was allowed to absorb water until, without reaching equilibrium, it increased its weight by 10%. Upon desorption it was found that 1% of the sorbed water could not be removed. The slow initial sorption of the sample followed by rapid resorption in subsequent cycles led the authors to suspect that chain scission had occurred. Jones et al. [80] reported an irreversible reduction in modulus with hydrothermal ageing. Fountain et al. [11,80] reported that the lap shear strength of dicy cured adhesives was influenced by the amount of water in the curing system. These authors also reported that commercial dicy contains 7% by weight  $H_2O$  as measured by  $^1H$  NMR. Noll [81] studied the effects of moisture of B-staged dicy/epoxy composites using DSC to measure  $H$  and  $T_g$  and correlating these results with gel time and peel strength measurements. He found an optimum water concentration for maximum peel strength. Noll proposed that prior to reaction, dicy was hydrolyzed according to the reactions shown in equations (15) and (16). However, he offered no evidence supporting these reactions. While the reaction shown in equation



(15) has been reported to occur under acidic conditions (see chapter 1), there are no reports in the literature of the reaction depicted in equation (16).

Should carbonyl formation precede cyclization, then substituted ureas would be formed in the dicy/epoxide reaction mixture. If so, it was felt that those ureas, following reaction with epoxides, would form 2-oxazolidones via a mechanism analogous to that proposed for the conversion of product II into product III. A review of the literature revealed that this was so and thus provided further insights into the possible complications involved in this mechanism. Tousignant et al. [82] investigated the reaction of ethylene oxide with urea. Following the initial formation of  $\beta$ -hydroxyl ethyl urea, an intramolecular reaction occurred resulting in the formation of small amounts of 2-oxazolidone, equation (17), along with the main product  $\beta$ -amino ethyl carbonate, shown in equation (18). Iwakura et al. [83], on the other hand,



reported that only 2-oxazolidones were formed in the reaction of trisubstituted ureas with PGE. Further, the secondary amines generated by

this reaction were found to react with PGE at a much faster rate than the starting urea. This later result is similar to that found for the dicy/epoxide system, and indicated that cyclization was probably not affected by the size of the leaving group. Finally, the reaction of the accelerator Monuron with epoxide has been reported to yield an N-phenyl 2-oxazolidone and dimethyl amine [6]. The further reaction of the dimethyl amine with epoxide forms a tertiary amine, which acts as a catalyst for other epoxy reactions. The formation of  $\beta$ -amino ethyl carbonate, as reported by Tousignant and shown in equation (18), suggested the possibility that an analogous reaction might be responsible for some of the results discussed in the following section.

#### Uneluted Materials

In order to quantify the results of chapter 3, the five isolated products were analyzed by HPLC and an attempt was made to determine the relationship between product concentrations and peak areas. At 229nm, this relationship was found to be non-linear for all isolated products. However, at 280nm not only was a linear relationship found, it was also discovered that peak area was directly related to the concentration of phenyl rings in the injected sample, and this relationship was independent of the product injected. Thus the areas reported in chapter 3 for the peaks represented by these compounds were quantitative when analyzed at 280nm. Since these compounds represented the bulk of the material in these chromatograms, it was clear from a review of the data in chapter 3 that, as the extent of reaction increased, a progressively smaller amount of material was eluted by the column. It was therefore suspected that a compound or compounds were formed that were either so non-polar



that they were not eluted by 100% THF or so reactive that they bonded with the column packing material. Further evidence for this uneluted material was found in the SEC analysis of the product I/MGEBA product mixtures, shown in chapter 5, which revealed a product peak that could not be accounted for in the HPLC analysis of these mixtures. Based on these SEC chromatograms, the size of this material is somewhere between the size of product V and the etherification product of V, shown in Figure 4-29.

An attempt was made to isolate this material from the dicy/MGEBA reaction mixture using PLC. A freshly prepared mixture was injected into the PLC column using 100% methanol as the mobile phase. After elution of all of the known materials from the column, the column was back washed with 100% THF. Special effort was made to insure that only the THF was collected. Approximately three void volumes were passed through the column. The solvent was then evaporated from the collected sample, leaving behind a colorless, viscous material. Attempts to analyze this material by HPLC, using a variety of solvents, were futile because the material could not be eluted. Initial FTIR analysis revealed several carbonyl absorbance bands at 1774, 1758, and  $1722\text{ cm}^{-1}$ . However, further drying of this material revealed a single absorbance band at  $1699\text{ cm}^{-1}$ , as can be seen in an FTIR spectrum of this material which is shown in Figure 4-30.

Initially, it was suspected that this material might be a product of the partial hydrolysis of the alkylated dicy, akin to the guanyl urea structure proposed by Noll and shown in equation (15). The appearance



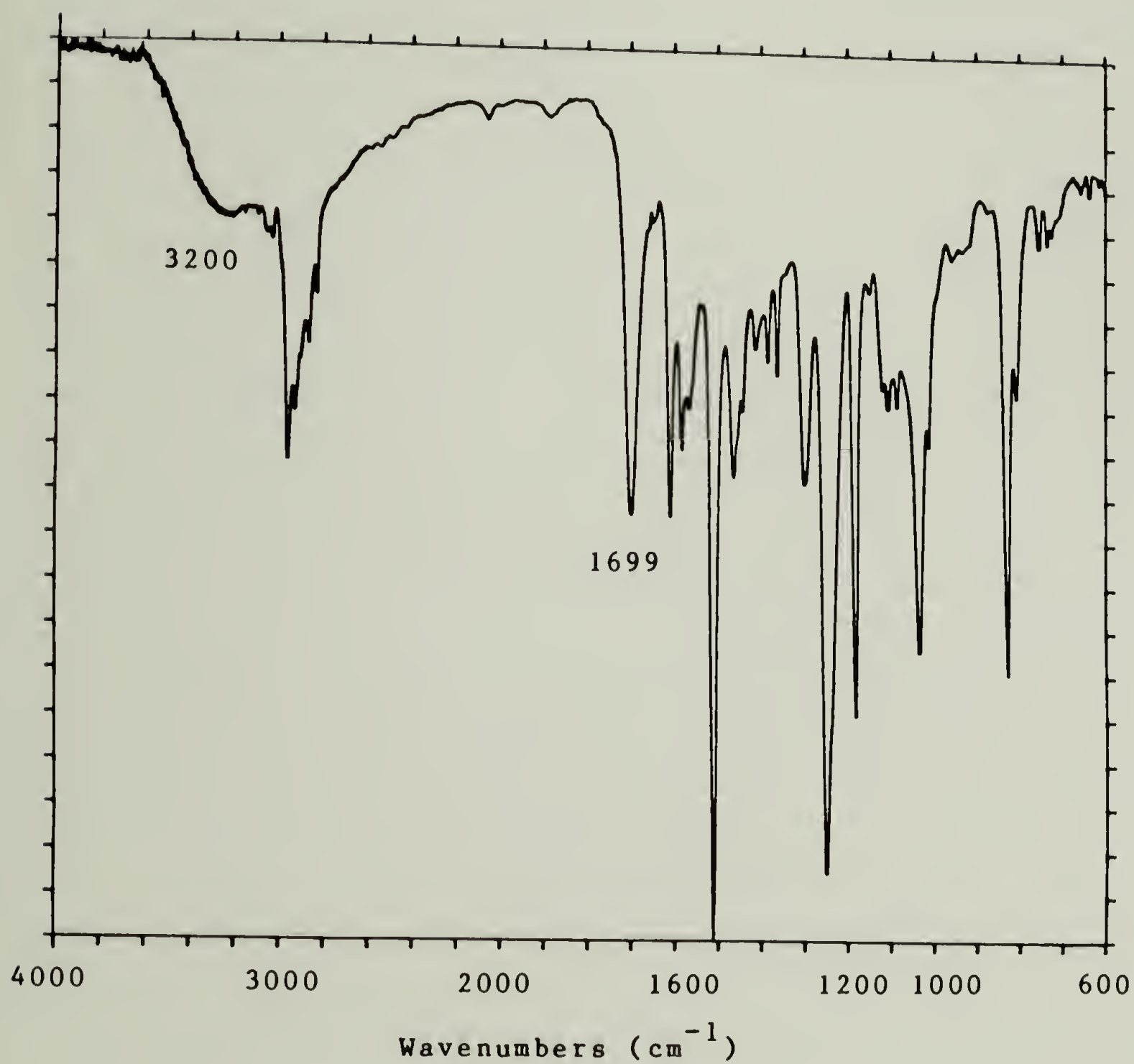


Figure 4-30: FTIR spectrum of uneluted material.

of a carbonyl absorbance band in the spectrum of this material would tend to corroborate this structure. However, it was also observed that when product II was thermally converted to product III and IV, the yield of these products accounted for only slightly more than half of the starting material. The remainder was converted into an unelutable material. The FTIR spectrum of thermally converted product II is shown in Figure 4-31. Aside from the peaks indicating a substantial portion of product III in this material, a number of unresolved bands are apparent in the region of 1670 to 1700  $\text{cm}^{-1}$ . It could be speculated that this material might have been formed by an intermolecular hydroxyl addition between two substituted dicy molecules. The hydroxyl group might have added to the imide carbon with elimination of ammonia in a reaction analogous to the intramolecular mechanism shown in Figure 4-20. On the other hand, the hydroxyl of one molecule might have added to the cyano group of another in a mechanism identical to that proposed by Saunders et al. [35], as shown in equation (10). Subsequent hydrolysis might then have generated carbonyl groups in the structures of the products of either of these reactions. However, no evidence favoring either of these reactions has been found and, therefore, no definite structures could be assigned. In order to establish the identity of this compound it would be necessary to isolate it using preparative SEC and then analyze it using FABMS.

While little was known about the structure of this material, the results of the following chapter indicate that it comprises approximately 40% by weight of the fully cured dicy/MGEBA product mixture. Products of this kind are expected to play an important role in the struc-

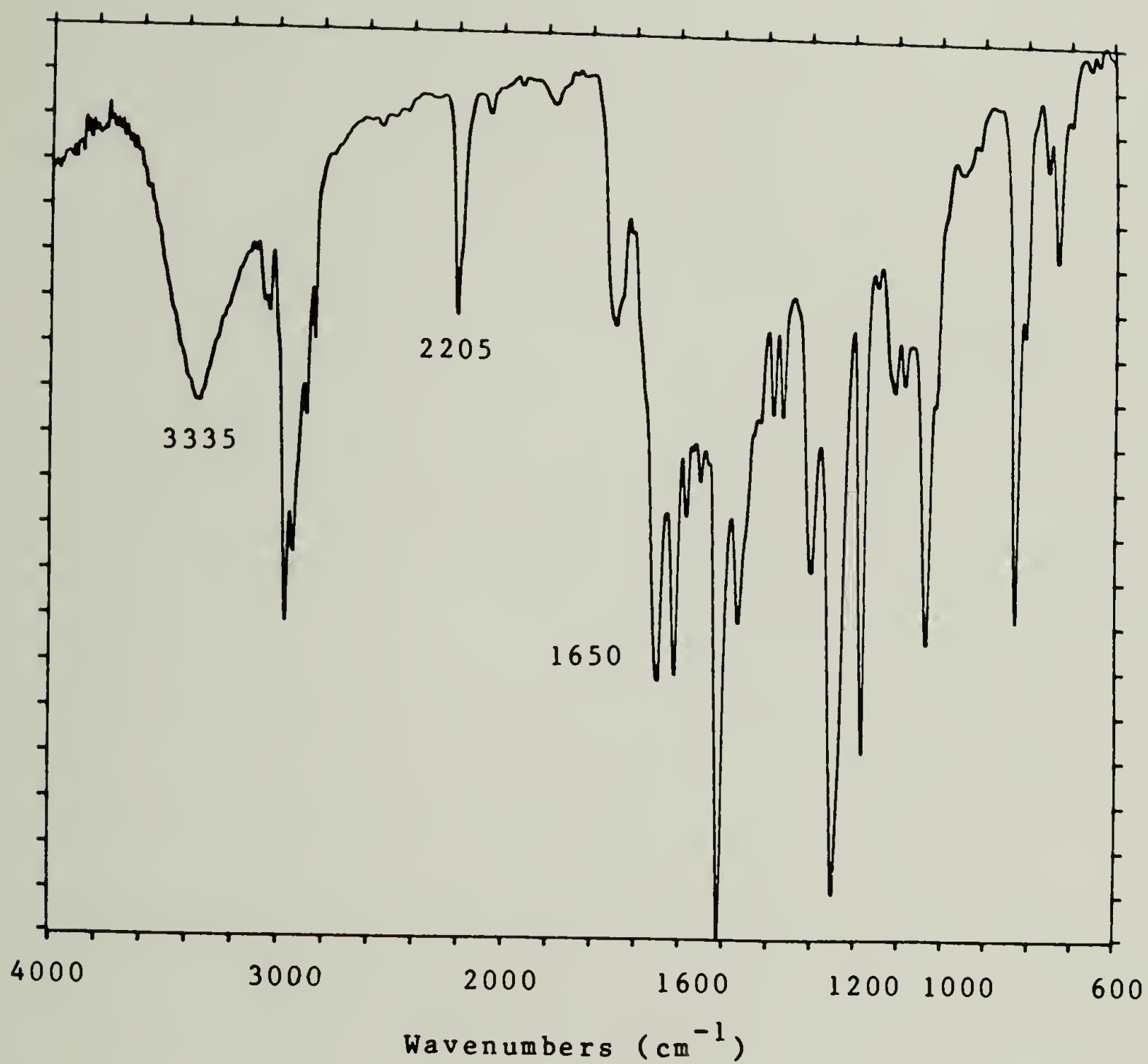


Figure 4-31: FTIR spectrum of product II heated to 167°C for 120 min.

ture of a fully cured dicy/epoxy system. These compounds represent the formation of more highly branched crosslink junctures in the cured material, relative to those obtained from structures analogous to products III, IV, and V. Thus, the relative rate of formation of this unknown material will affect both the onset of gelation and the crosslink density of the cured material.

#### FTIR Studies of the Dicy/Epoxide Reaction

In order to determine product differences in the catalyzed and uncatalyzed cures of MGEBA with dicy, an FTIR spectrum of the unresolved product mixtures from each of these reactions was obtained. Figure 4-32 shows the FTIR spectrum of an uncatalyzed 1:6 mixture of MGEBA and dicy, reacted for one hour at 187°C. Figure 4-33 shows the FTIR spectrum of a similar mixture catalyzed with BDMA and heated to 100°C for two hours. Several major differences are evident in these spectra. The most striking is the peak at 1686  $\text{cm}^{-1}$ , which is assigned to the carbonyl of the uneluted material. Although it is present in both spectra, it appears to constitute a higher proportion of the catalyzed reaction mixture. Also, the carbonyl peak at 1760  $\text{cm}^{-1}$ , assigned to the 2-oxazolidone (product IV), is much smaller in the catalyzed reaction mixture, indicating a lower concentration of this material in the catalyzed mixture, which was expected due to the lower temperature of this reaction. Finally, while both spectra show an absorbance band at 1651  $\text{cm}^{-1}$ , assigned to product III, differences are evident in the cyano region. In the spectrum of the catalyzed reaction mixture, the cyano absorbance band is centered at 2178  $\text{cm}^{-1}$ , supporting the identification of alkylated dicy adducts in the HPLC chromatograms of BDMA catalyzed reaction



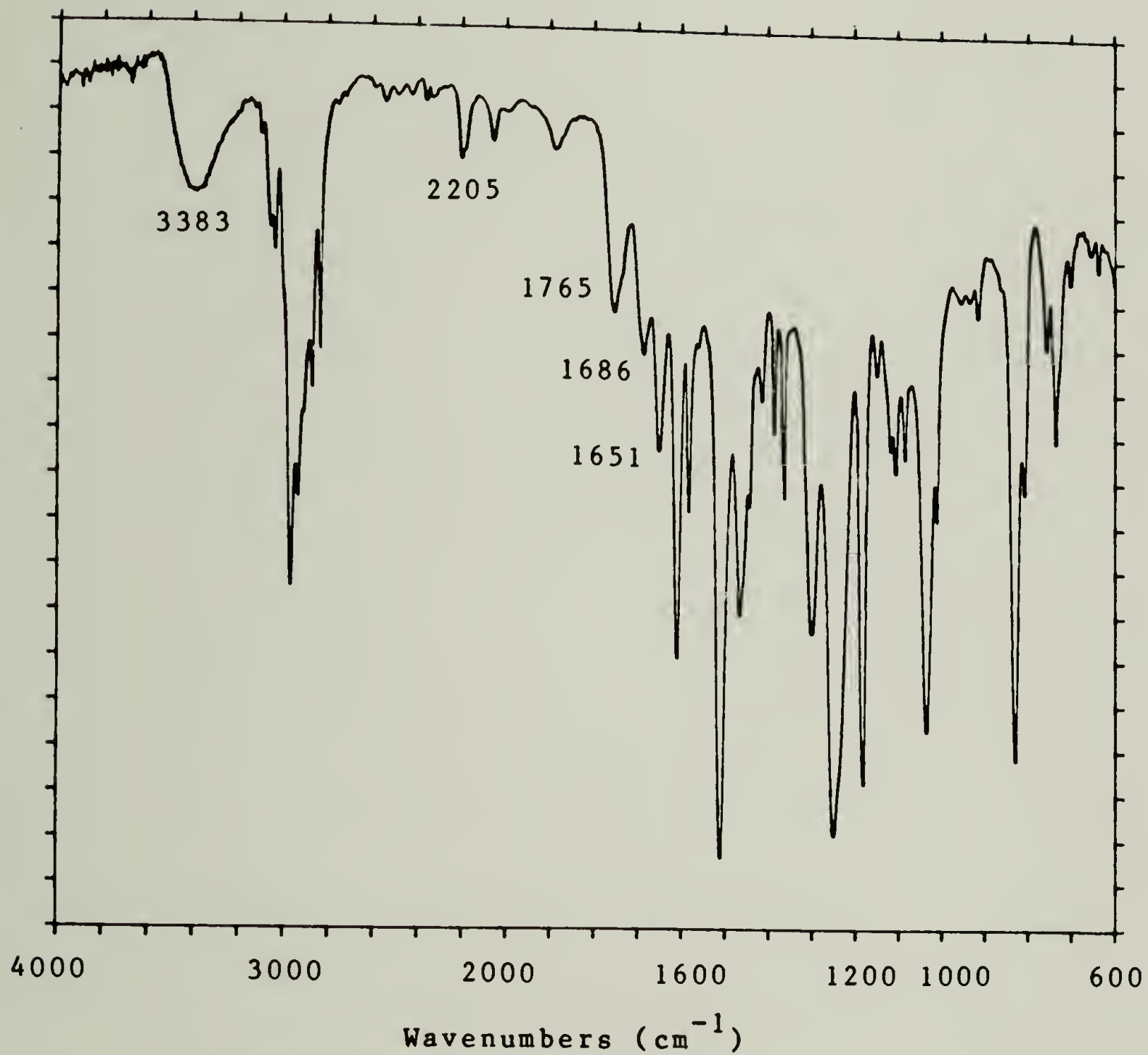


Figure 4-32: FTIR of unresolved product mixture formed by reacting 1:6 dicy/MGEBA at 190°C for 1 hour.

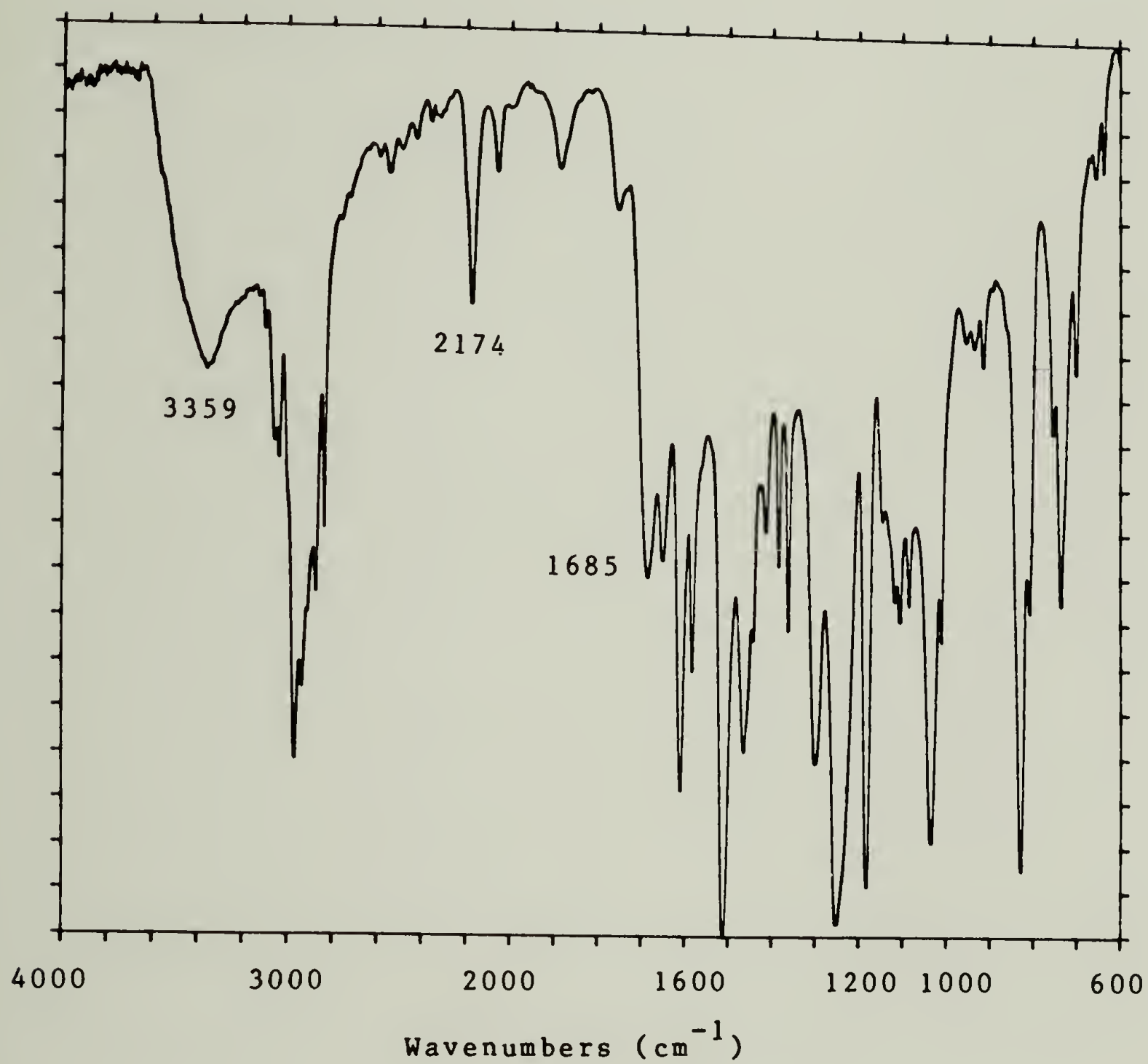


Figure 4-33: FTIR of unresolved product mixture formed by reacting BDMA catalyzed 1:6 dicy/MGEBA at 100°C for 1 hour.

mixtures. The cyano group in the uncatalyzed mixture was centered at  $2205\text{ cm}^{-1}$ , thus showing no indication of alkylated dicy, in agreement with the results of the HPLC study.

#### Correlation of Results with Previous IR Studies

An attempt was made to correlate the results of the present study with those of previous IR investigations of the dicy/ epoxy reaction. Using the FTIR spectra of the isolated products, it was possible to supply a structural interpretation to the IR observations of those studies. Further, by comparing the spectra with the observations made in those studies, the validity of the reaction mechanism proposed for the MGEBA model system could be extended to dicy curing systems reacted under a wide range of temperatures and compositions. In this way, the effects of these variations on the final crosslinked structure could also be assessed.

One of the most important studies was performed by Davidson [41], who used the spectral subtractive capabilities of FTIR to investigate the uncatalyzed dicy cure of DGEBA. In his study, Davidson reported the appearance of several absorbance bands which could be directly assigned to structures identified in the present work. The reacting mixture was observed to form a new band at  $2181\text{ cm}^{-1}$ , which could be assigned to alkylated dicy structures similar to products I and II. This assignment was verified by the reported appearance of an absorbance band at  $1570\text{ cm}^{-1}$ , which is assigned to a conjugated C=N functionality. An identical band can be seen in the spectrum of product II, shown in Figure 4-7. Davidson also reported the appearance of absorbance bands at 1760 and

1650  $\text{cm}^{-1}$ , which can be assigned to structures similar to products IV and III, respectively. The band at 1760  $\text{cm}^{-1}$  was observed to shift to 1748  $\text{cm}^{-1}$  as the reaction progressed. This shift may have been caused by hydrogen bonding. A similar shift was noted in the spectrum of product IV before purification. Finally, an absorbance band was reported at 1690  $\text{cm}^{-1}$ , indicating the presence of structures similar to that of the uneluted material described above.

The similarity of these observations to the results of the FTIR analyses of the isolated products helps establish a relationship between the reactions observed in the dicy/MGEBA model system, and the mechanism of the dicy/DGEBA cure. Thus, the mechanism proposed by the results of this study appeared to be applicable to the uncatalyzed dicy/DGEBA cure study presented in chapter 2. Further, Davidson cured his samples at 140°C. The observation of alkylated dicys in mixtures cured at this temperature, supports the view that the relative rate of reaction of these species compared to the rate of the initial dicy/epoxide reaction, is slower at this temperature.

The BDMA catalyzed dicy cure of DGEBA was followed by Lin et al. [42] over a range of temperatures using FTIR. At 100°C, the synchronous growth of absorbance bands at 2180  $\text{cm}^{-1}$  and 1650  $\text{cm}^{-1}$  was observed. At temperatures of 140°C and 160°C, the rate of growth of the 1650  $\text{cm}^{-1}$  band was faster than that of the 2180  $\text{cm}^{-1}$  band. This apparently indicates a higher activation energy for the intramolecular hydroxyl substitution reaction as compared to the initial dicy/epoxide reaction. Further, an absorbance band at 1740  $\text{cm}^{-1}$  was observed at long reaction



times in the high temperature cures. The appearance of this band, assigned to structures similar to product IV, reveals the presence of the hydrolysis reaction in the catalyzed cures and indicates a strong temperature dependence of this reaction.

Early workers such as Levine [34], Saunders et al.[35], and Eyerer [4] reported the appearance of many of these same absorbance peaks. Again the absorbance band at  $2180\text{ cm}^{-1}$  was observed in the early stages of the reaction, indicating the formation of alkyl dicy. At long reaction times or high temperatures, these authors reported the appearance of carbonyls at  $1740\text{ cm}^{-1}$ , which again can be assigned to structures similar to product IV. Also reported by Levine, was the appearance of the  $1690\text{ cm}^{-1}$  band, assigned to the uneluted material in the present study. Saunders et al. reported observing this band only in the model compound system. However, he used higher dicy loadings in the model system, probably enhancing the formation of this compound. A similar result was found in the product I/MGEBA reaction and is discussed in chapter 5.

Of great interest to the present study is the work of Zahir, who used FTIR to follow the reaction of cyanamide with PGE. It was reported in that study, that an absorbance band at  $2180\text{ cm}^{-1}$  appeared at the start of the reaction. This observation indicates that alkyl dicys were formed in this reaction, similar to those isolated in the present work. Also,  $^{13}\text{C}$  NMR analysis of the reaction mixture after removal of dicy, revealed peaks at 118 and 162 ppm, assigned to cyano and C=N groups, respectively. Similar peaks were seen in the spectra of product I,

shown in Figure 4-22. This further supports the contention that alkyl dicy structures are present in the cyanamide/PGE reaction mixture and are probably formed in all cyanamide/epoxide reactions, regardless of the initial concentration of cyanamide in the starting mixture.

In the Zahir study, the cyanamide/PGE reaction was carried out at the very low temperature of  $77^{\circ}\text{C}$ . At this temperature, the oxazolidone absorbance band at  $1740\text{ cm}^{-1}$  was not observed. However, a band at  $1700\text{ cm}^{-1}$  was found to form at a very slow rate. This band again is similar to that found in the spectrum of the uneluted material. After removal of dicy, the addition of HCL to the reaction mixture was found to result in an increase in the band at  $1700\text{ cm}^{-1}$ , as well as the formation of the  $1740\text{ cm}^{-1}$  band, similar to that observed in spectrum of product IV. This appears to support the contention that both carbonyl groups are formed by hydrolysis reactions. Exposure of the dicy-free product mixture to high temperatures was similarly reported to produce the carbonyl absorbance band at  $1740\text{ cm}^{-1}$ .

The reported observations of the previous spectral studies, indicate that the proposed dicy/epoxide reaction mechanism is applicable to the crosslinking dicy/epoxy system, cured over a broad temperature range with and without catalyst. Further, the observations of the present study, together with those of Zahir, have shown that dicy/epoxide adducts are the predominant products formed by the initial cyanamide/epoxide reaction. This finding has important implications in the interpretation of the results of chapter 2. In addition, the previous studies have revealed the effect of temperature on the relative rates of

formation of carbonyl bands at  $1690\text{ cm}^{-1}$  and  $1740\text{ cm}^{-1}$ . This later observation provides some insight into the reaction mechanism forming the unknown and extremely important structure assigned to the  $1690\text{ cm}^{-1}$  absorbance band. A further discussion of the possible structure of this species is presented in chapter 6.

## CHAPTER 5

### THE REACTION OF PRODUCT I WITH EPOXIES

#### Introduction

The analyses presented in chapter 4 revealed that the bulk of the HPLC elutable fraction of the dicy/MGEBA product mixture is composed of the species identified as products III, IV and V. When formed in a crosslinking system, in the absence of etherification, structures analogous to products III and IV are effectively difunctional chain extenders, while those analogous to product V are essentially trifunctional. Thus, based simply on the mechanism outlined in Figure 4-20, dicy should only be capable of providing crosslink junctures with an average functionality of 2.5, when used to cure epoxy resins. This low average functionality is in contradiction with the high modulus and  $T_g$ 's, characteristic of dicy cured epoxies [1], and indicative of a high crosslink density. It is apparent that a large concentration of other, more highly branched structures must be present in these systems. Further, it is believed that these structures are analogous to the non-HPLC elutable components of the dicy/MGEBA product mixture.

While little is known about the number, distribution and identities of these unelutable products, several possible structures have been postulated. These include tetrasubstituted dicy, the hydrolysis products of substituted dicy as discussed in chapter 1, and products formed by the oligomerization of substituted dicy via intermolecular hydroxyl additions, such as initially postulated by Saunders [35] and shown in equa-



tion (10). In an effort to differentiate between these structures, and to determine their respective concentrations, an attempt was made to quantify the rate and extent of formation of uneluted material in the dicy/MGEBA system. While this could not be done directly, due to the unelutable nature of these species, it was possible to estimate the weight fraction of these species in the reaction mixtures, by subtracting the amount of HPLC elutable species from the total amount of material contained in the starting mixtures. Thus, the extent of uneluted material formation could be followed throughout the course of the dicy/MGEBA reaction, using the HPLC data previously presented in chapter 3.

The intent of this study was not only to evaluate the relative rate and extent of formation of uneluted material in the model reaction, but also to establish the relationship between the eluting and uneluting species. One of the problems was to determine the extent to which the uneluted product fraction acts as a progenitor of the eluting species. As discussed in chapter 3, elutable species appear to be formed in the dicy/MGEBA reaction mixture, long after consumption of epoxide is complete, presumably via the decomposition of uneluted material. However, the extent to which this decomposition acts as a pathway for the formation of eluting species was unclear. By charting the formation of eluting and non-eluting products throughout the course of the reaction, it was believed that the order of formation of these product fractions would be evident, allowing some identification to be made.

As previously discussed, the rate of the initial dicy/MGEBA reaction is extremely slow relative to subsequent reaction steps. It appears

that the rate of reaction is controlled by the slow processes of dicy dissolution and diffusion. The net result is the gradual build up of virtual end-products in the reacting mixtures, while concentrations of intermediate species remain very small. Under these conditions, there was some difficulty in discerning the relationship between the identified products and the uneluted material. However, it was felt that these problems could be avoided by examining the further reactions of isolated product I with MGEBA. As was seen in chapter 4, this reaction is capable of forming a product mixture which is apparently identical to that formed by the dicy/MGEBA reaction. However, unlike dicy, product I is soluble in MGEBA and forms homogeneous mixtures. Using this reaction, it was thought that it would be possible to examine the chemical kinetics of the various dicy/epoxide reactions, free from the complicating effects dicy dissolution and diffusion. Further, it was believed that the homogeneity and relatively low temperatures required for reaction of these systems, would favor the accumulation of detectable and HPLC quantifiable amounts of the highly reactive intermediate species. In addition, since the composition of this homogeneous system could be controlled, it was felt that the effects of compositional variation could be readily ascertained.

A study was conducted which was similar to that performed in chapter 3. Mixtures of product I and MGEBA were reacted in the DSC at several temperatures for various lengths of time and the products were analyzed using the HPLC conditions developed in that chapter. In an attempt to determine the size and composition of the uneluted material, several samples were also analyzed using size exclusion chromatography (SEC).

In a further effort to examine the formation and decomposition of uneluted species, the cure of DGEBA with product I was studied using TBA. It was believed that, since the product I/DGEBA mixtures were homogeneous, changes in the developing network structure of this system could be directly assessed through changes in the mechanical properties. As a monosubstituted dicy, product I is essentially a trifunctional curing agent. However, upon undergoing intermolecular hydroxy addition and amine elimination, the average functionality of the resulting cyclic and amine products is reduced to a value of 2. Therefore, crosslinking in this system can only occur through the formation of either tetrasubstituted dicy structures or analogs to the other postulated structures comprising the uneluted material. Therefore, it was believed that, by studying this curing system, the functionality and long term stability of structures comparable to the uneluted material could be probed.

### Experimental

The isolation and purification of product I is described in chapter 4, the synthesis and purification of MGEBA is presented in the appendix, and the DGEBA was identical to that described in the experimental section of chapter 2.

Mixtures for the HPLC kinetic study were prepared by dissolving weighed amounts of product I in MGEBA on a hot plate at 50°C. Equipment and procedures for sample preparation, DSC reaction and HPLC analyses of the resulting mixtures have been previously described in the experimen-



tal section of chapter 3. For this study, micron Bondapak C-18 column was used with a mobile phase of THF/H<sub>2</sub>O = 50-90% over a 40 min linear gradient. The technique of SEC analysis is also discussed in chapter 3. The equipment and procedures utilized for the TBA study of the product I/DGEBA cures can be found in the experimental section of chapter 2. Composite specimens for this study were made by impregnating glass braids with 20% solutions of the I/DGEBA mixtures and air drying.

## Results and Discussion

### Thermal Analysis

A DSC temperature scan at 5°C/min is shown in Figure 5-1 for an uncatalyzed 1:2 I/MGEBA mixture. Evident in this trace is a broad exothermic region with an onset temperature of 120°C and two peak maxima at 155°C and 180°C. The area encompassed by this exotherm represents a total heat of reaction of 102 kJ/mole eq. epoxide, which is somewhat lower than the heats found by isothermal DSC, as discussed below. The second maxima in this DSC trace was thought to be due to hydroxyl addition reactions. To test that possibility, a neat sample of product I was scanned in the DSC at an identical rate. The resulting trace revealed an exotherm with an onset temperature of 170°C and a maximum rate at 205°C. Examination of the scanned sample by HPLC revealed the formation of a variety of products of lower polarity, and presumably higher molecular weight, than product I. Although further analysis has not been performed, it appears that the intermolecular addition of alkylated dicy molecules can occur.



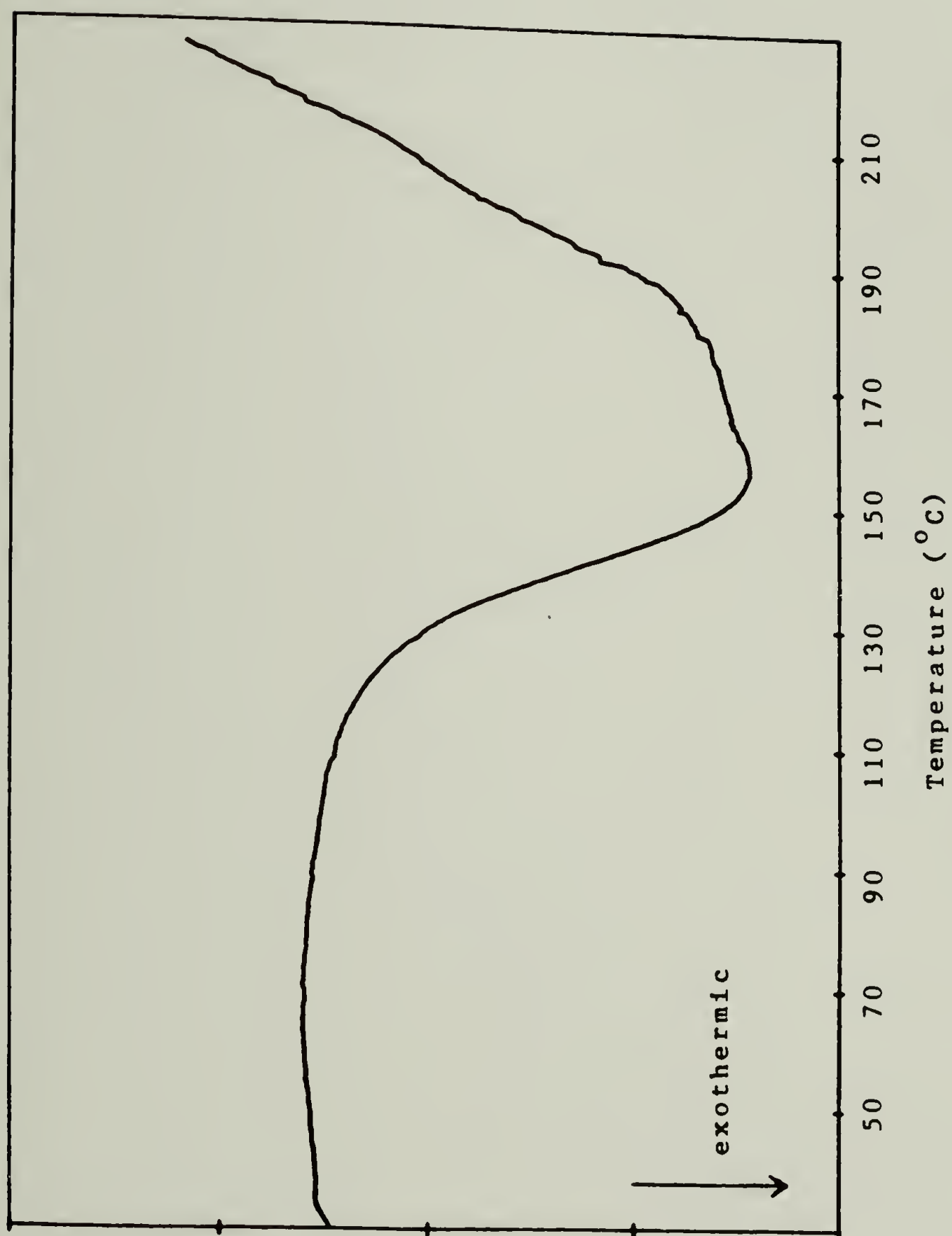


Figure 5-1: DSC temperature scan of 1:2 product I/MGEBA at 5°C/min.

Samples of the thermosetting product I/DGEBA system were also analyzed by temperature scanning in the DSC. The trace of a 1:4.5 product I/DGEBA mixture is shown in Figure 5-2. Again a single broad exothermic region is observed, with an onset temperature of  $110^{\circ}\text{C}$  and peak maximum at  $160^{\circ}\text{C}$ . A total heat of reaction of  $110\text{kJ/mole}$  was calculated for this exotherm. A rescan of the cured mixture, at  $5^{\circ}\text{C/min}$ , reveals a  $T_g$  midpoint of  $98^{\circ}\text{C}$ . This value is similar to those measured for the isothermally cured samples, discussed below.

Isothermal DSC measurements were made by reacting uncatalyzed product I/MGEBA mixtures at temperatures of  $107^{\circ}$  to  $167^{\circ}\text{C}$ . Values for heat of reaction are listed in Table VI. It was found that, as the temperature of reaction was increased, successively larger heat of reaction values were measured for the product I/MGEBA mixtures. It was believed that the excess heat of reaction at higher temperatures was representative of the relatively slow hydroxyl and  $\text{H}_2\text{O}$  addition reactions. Thus, it appeared that these reactions either did not occur at lower temperatures, or occurred at such a low rate as to be below the detectability limits of the DSC. A correlation between the heats of reaction and product mixture composition, presented in the following section of this chapter, supported this latter conclusion. Table VI lists the isothermal heats of reaction for the 1:4.5 product I/DGEBA cures at  $107^{\circ}$  and  $127^{\circ}\text{C}$ . Values for the curing system, measured over an identical temperature range, appear to be similar to those of the model system.

Due to variations in the total heat of reaction, overall energies of activation could not be readily assigned. correlations with HPLC pro-

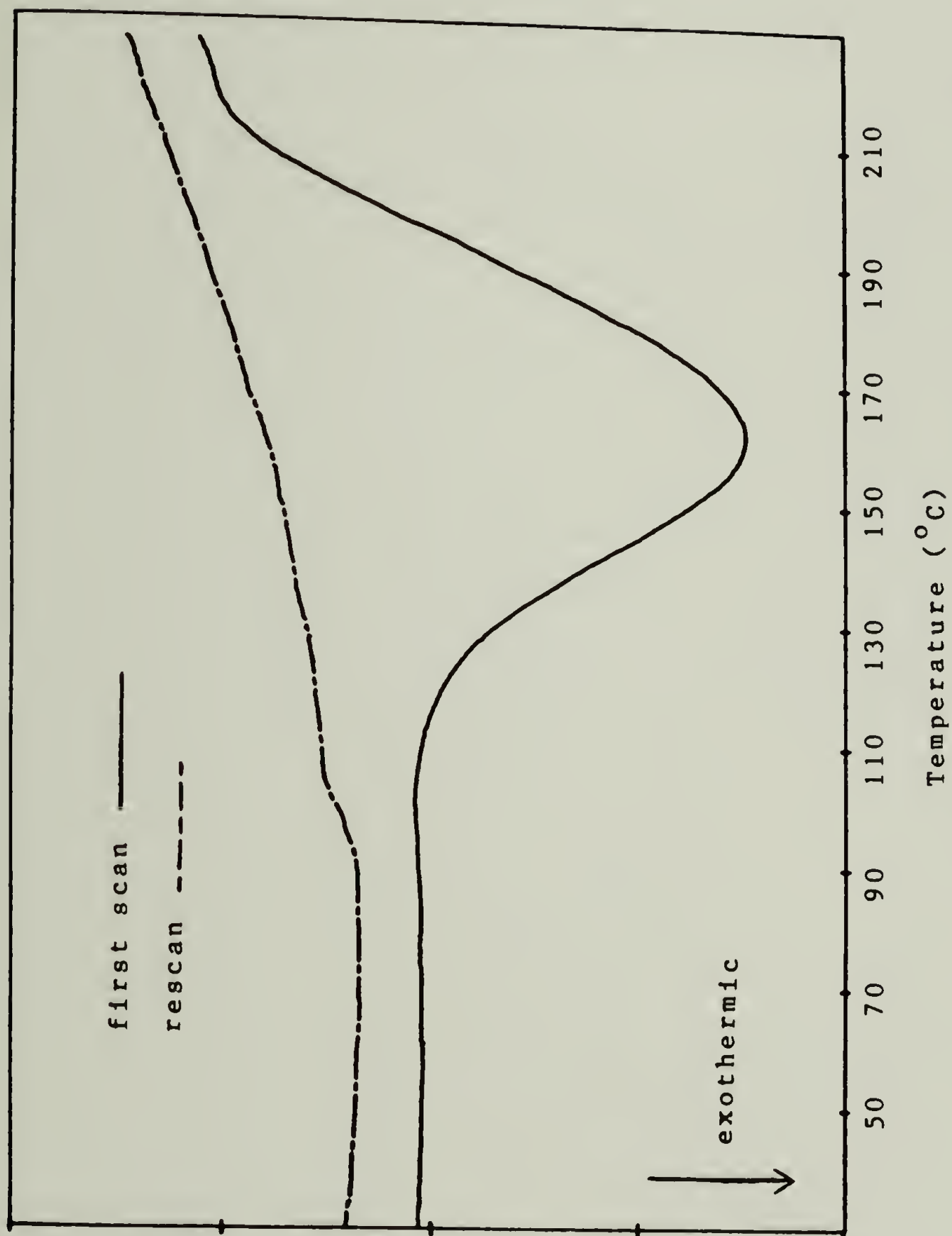


Figure 5-2: DSC temperature scan of 1:4.5 product I/DGEBA at 5°C/min.

TABLE VI  
Heats of Reaction of I/MGEBA and I/DGEBA

SAMPLE	TEMPERATURE	HEAT OF REACTION
	$^{\circ}\text{C}$	kJ/mole eq. epoxide
I/MGEBA	107	99
(1:4.5)	127	107
	147	136
	167	149
I/DGEBA	107	105
(1:4.)	127	114



duct analysis data revealed that the time to maximum rate for the product I/MGEBA system coincide with progressively higher extents of epoxide conversion for increasing temperatures of reaction. Therefore time to maximum rate cannot be used to determine reaction kinetics. However, it was possible to calculate an energy of activation of 85kJ/mole for the product I/MGEBA system, based on times to 50% epoxide conversion, as determined by HPLC. Using DSC conversions, a similar value was found for the I/DGEBA curing system. While, these values are much lower than those measured for the uncatalyzed dicy/MGEBA reaction in chapter 3, they are similar to those reported in the literature for the catalyzed dicy/DGEBA cure [4,39]. The low activation energy of the product I/MGEBA reaction is reflective of the chemical control. Activation energies for the dicy/MGEBA reaction (150 kJ/mole) appear to indicative of the dominating effects of dicy dissolution and diffusion in that system.

#### HPLC Kinetic Analysis

Samples for HPLC analyses were made by reacting uncatalyzed 1:4.5 product I/MGEBA mixtures in the DSC at temperatures of 127<sup>o</sup>, 147<sup>o</sup>, and 167<sup>o</sup>C for various lengths of time. Because this study was performed prior to the identification of product I, an inaccurate molecular weight was used in formulating these mixtures. This is reflected in the unusual molar ratios (1:4.5) used in these compositions. Although the rate of the product I/MGEBA reaction is extremely rapid at 167<sup>o</sup>C, an effort was made to follow the course of the reaction at this temperature in order to allow some overlap between the reaction conditions used in this study, and those previously used in the study of the the dicy/MGEBA reaction, presented in chapter 3. Due to the low availability of puri-

fied product I, only a limited number of reactions were run and no duplicate samples were made.

A typical HPLC chromatogram of a product mixture obtained reacting a 1:4.5 composition at 127°C for 2 hours is shown in Figure 5-3. Peaks A and B are assigned to the reactants I and MGEBA, respectively. Product peaks are assigned on the basis of species identification presented in chapter 4. Again, in this study, the peaks of primary interest are C and D assigned to disubstituted cyclical products III and IV, respectively, and G and H assigned to the trisubstituted isomers of product V. As discussed in chapter 4, products III, IV, and V are the unreactive end-products formed by the intramolecular hydroxyl addition/amine elimination reactions of substituted dicy molecules. Therefore, quantification of the areas of these peaks is expected to provide a measure of the extent to which intramolecular hydroxyl addition occurred in each of the analyzed samples. HPLC analyses were performed using a detector source of 280nm. Again, it was assumed that the product peak areas plotted in the above figures approximated the weight fractions of consumed MGEBA assignable to each of the product groups.

A plot of reactant consumption and product formation versus time is shown in Figure 5-4a for the uncatalyzed reaction of the 1:4.5 product I/MGEBA mixture at a temperature of 167°C. For purposes of simplicity, products were plotted as three distinct groups, the first assigned to the combined areas of peaks C and D, the second to the combined areas of peaks G and H, and the third to the uneluted material. In order to show more clearly the effects of long term heating, product concentrations

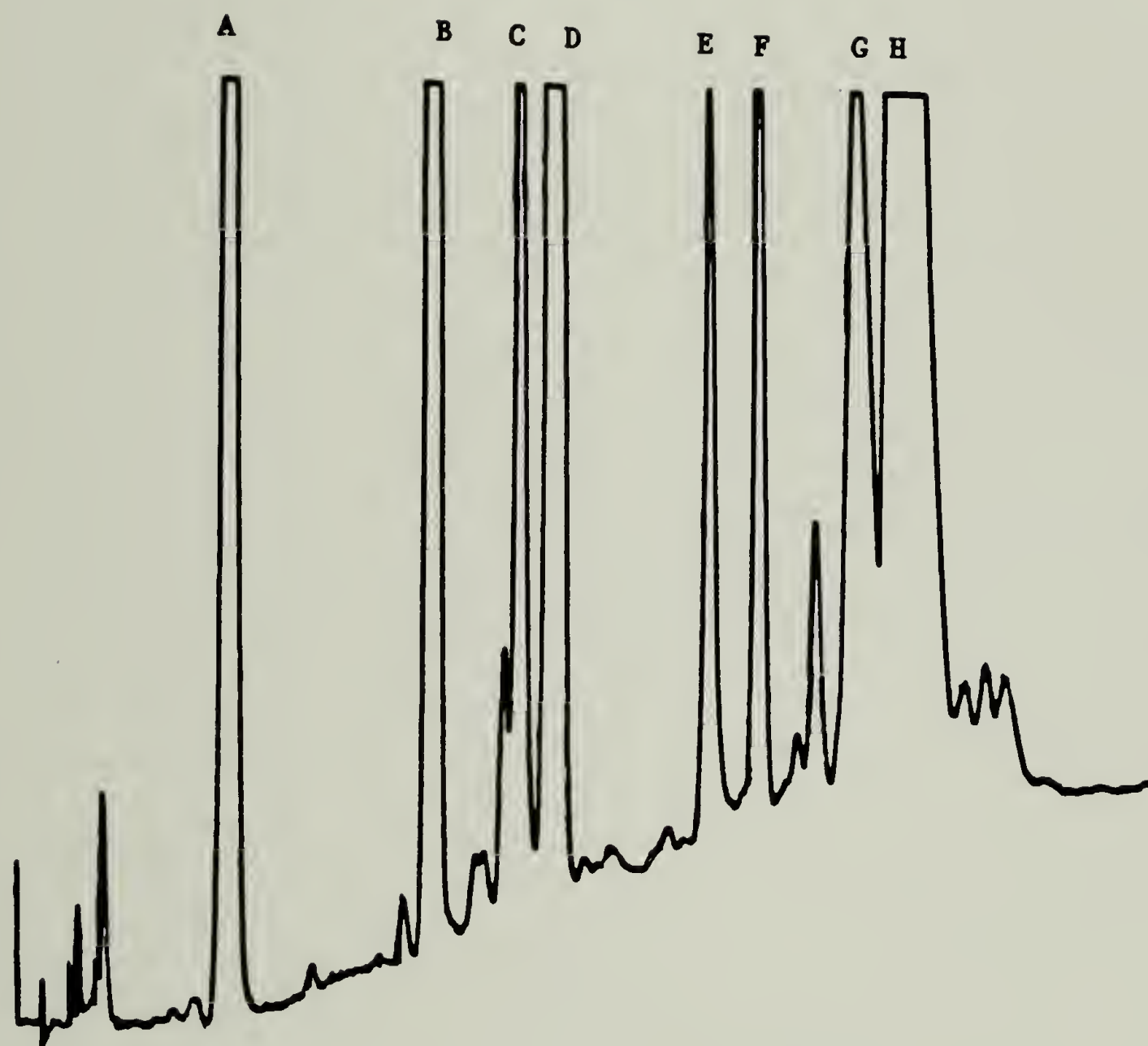


Figure 5-3: HPLC chromatogram of product 1:4.5 I/MGEBA reacted at 127°C for 121 min. THF/H<sub>2</sub>O = 50-90%, over 40 min, at grad 6, analyzed at 229nm.

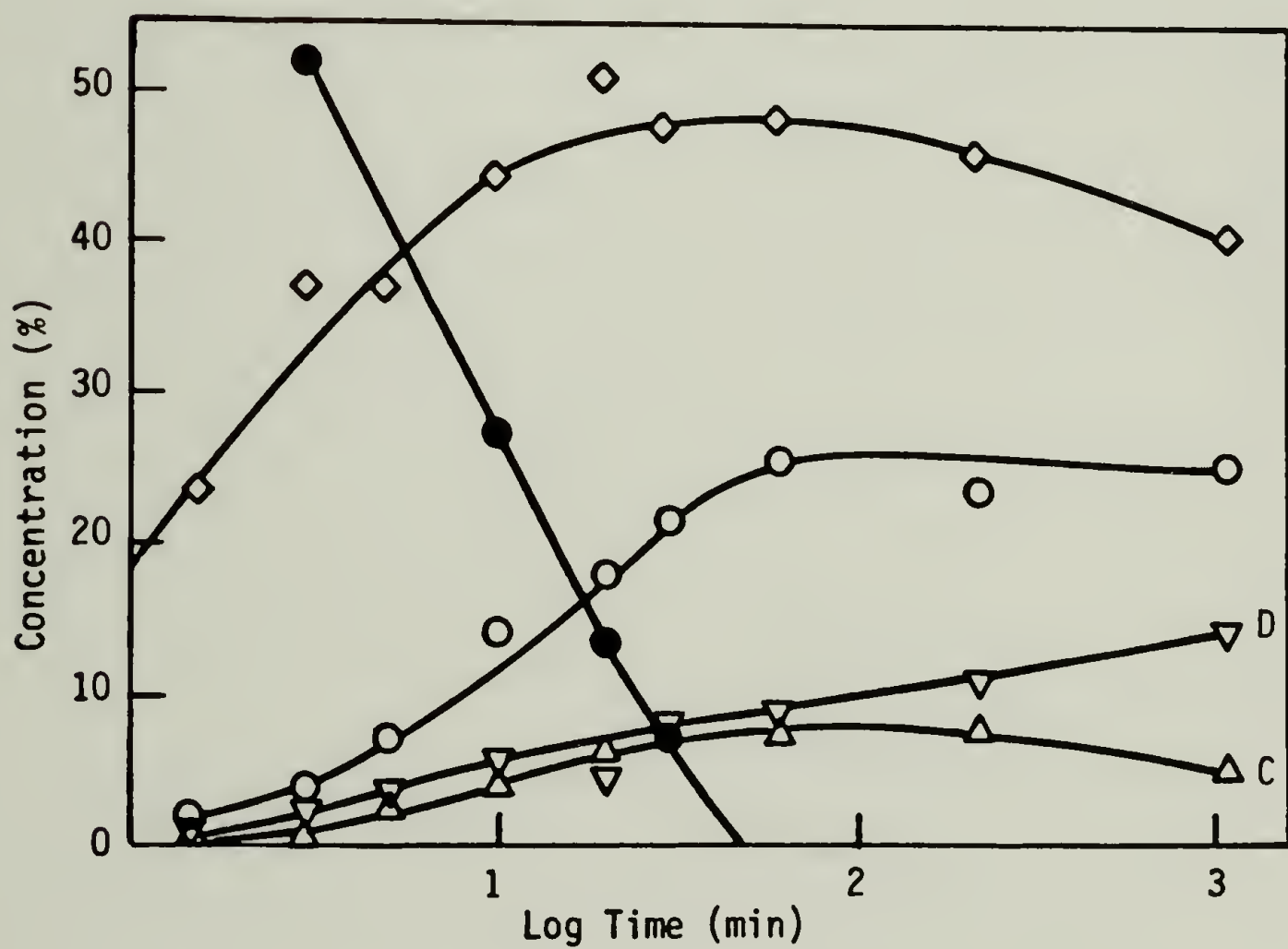
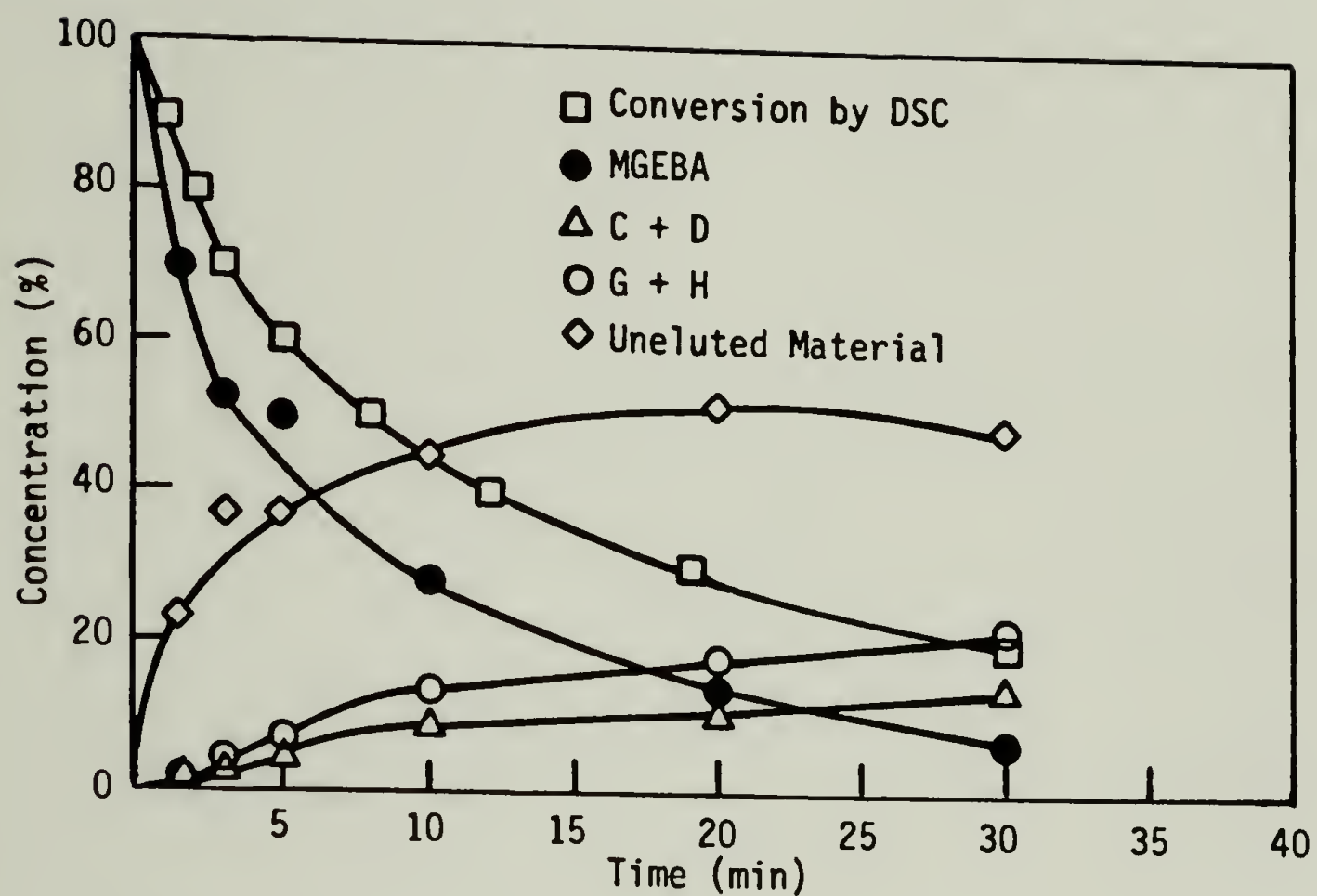


Figure 5-4: Products and Reactants vs time 1:4.5 product I/MGEBA reacted at 167°C.



were also plotted versus log time as shown in Figure 5-4b. Similar plots are shown in Figures 5-5 and 5-6 for the reactions of mixtures of identical composition at temperatures of 147° and 127°C, respectively.

Based on the mechanism presented in chapter 4, it was expected that the molar concentration of trisubstituted product V would be equal to the combined molar concentrations of disubstituted cyclic products III and IV. Consequently, the ratio of the combined areas of peaks G and H to that of combined peaks C and D was expected to equal a value of 3/2. This was generally found to be true for extents of reaction of 50-100% epoxide conversion, at each of the three reaction temperatures. However, prior to 50% epoxide conversion, G+H/C+D ratios were found to be much lower than 3/2. HPLC analysis of several of these low conversion samples at 229 nm revealed that the molar absorbance for the constituents of peak D, relative to MGEBA, is larger at 229 nm compared to that at 280 nm. As discussed in chapter 3, high 229/280 nm peak area ratios are indicative of the presence of molecules containing dicy moieties. Thus, it appears that disubstituted dicy molecules, such as product II, make a significant contribution to the area of peak D in the initial stages of the reaction. However, no evidence for the presence of disubstituted dicy was found at higher extents of epoxide conversion.

#### Concentrations of Eluting and Uneluting Species

According to the above plots, products eluting as peaks C,D,G and H appear to comprise only a tiny fraction of the product mixture in the early stages of the reaction. The predominant products formed during this early stage appear to be those contained in the uneluted material.

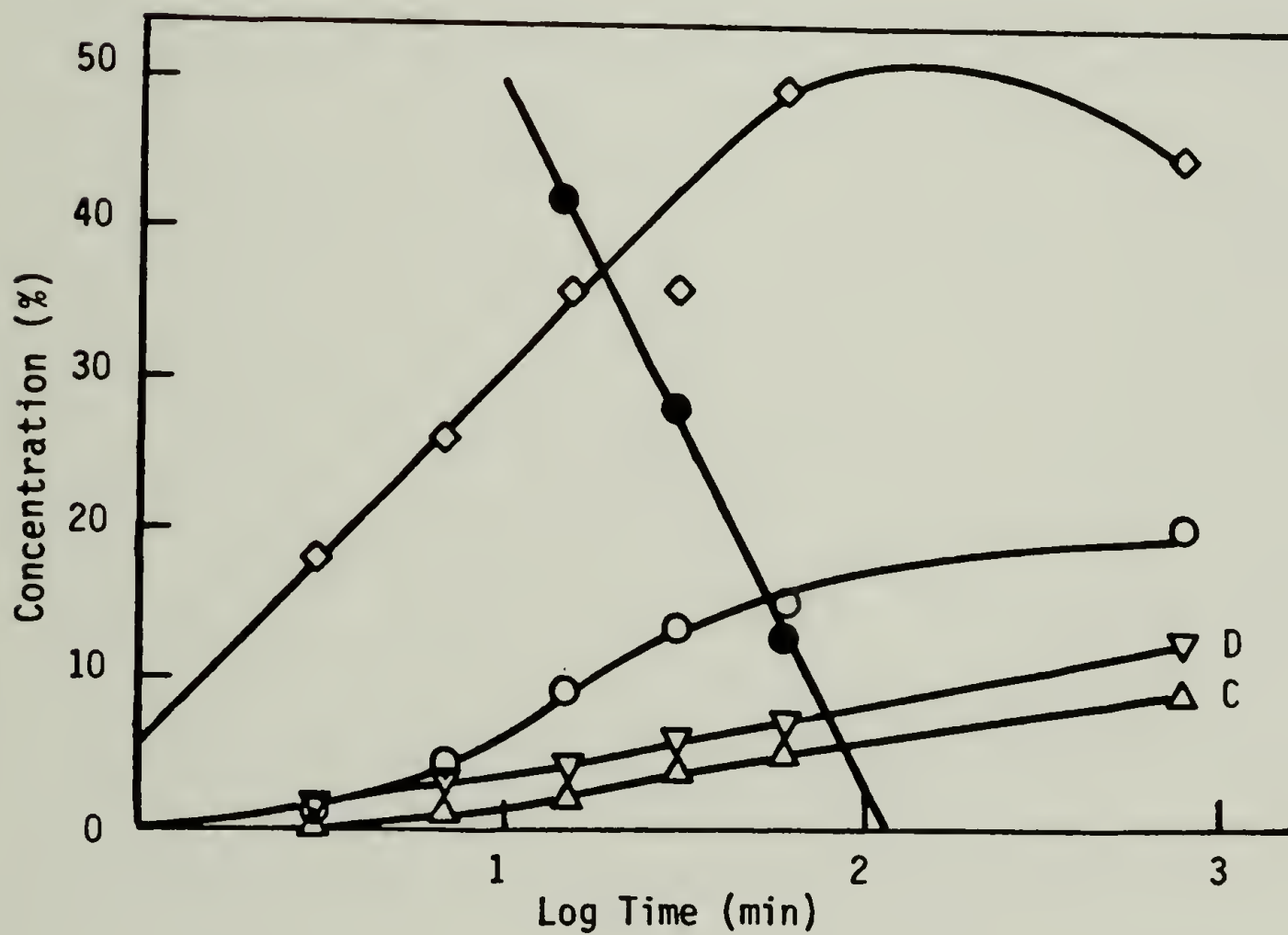
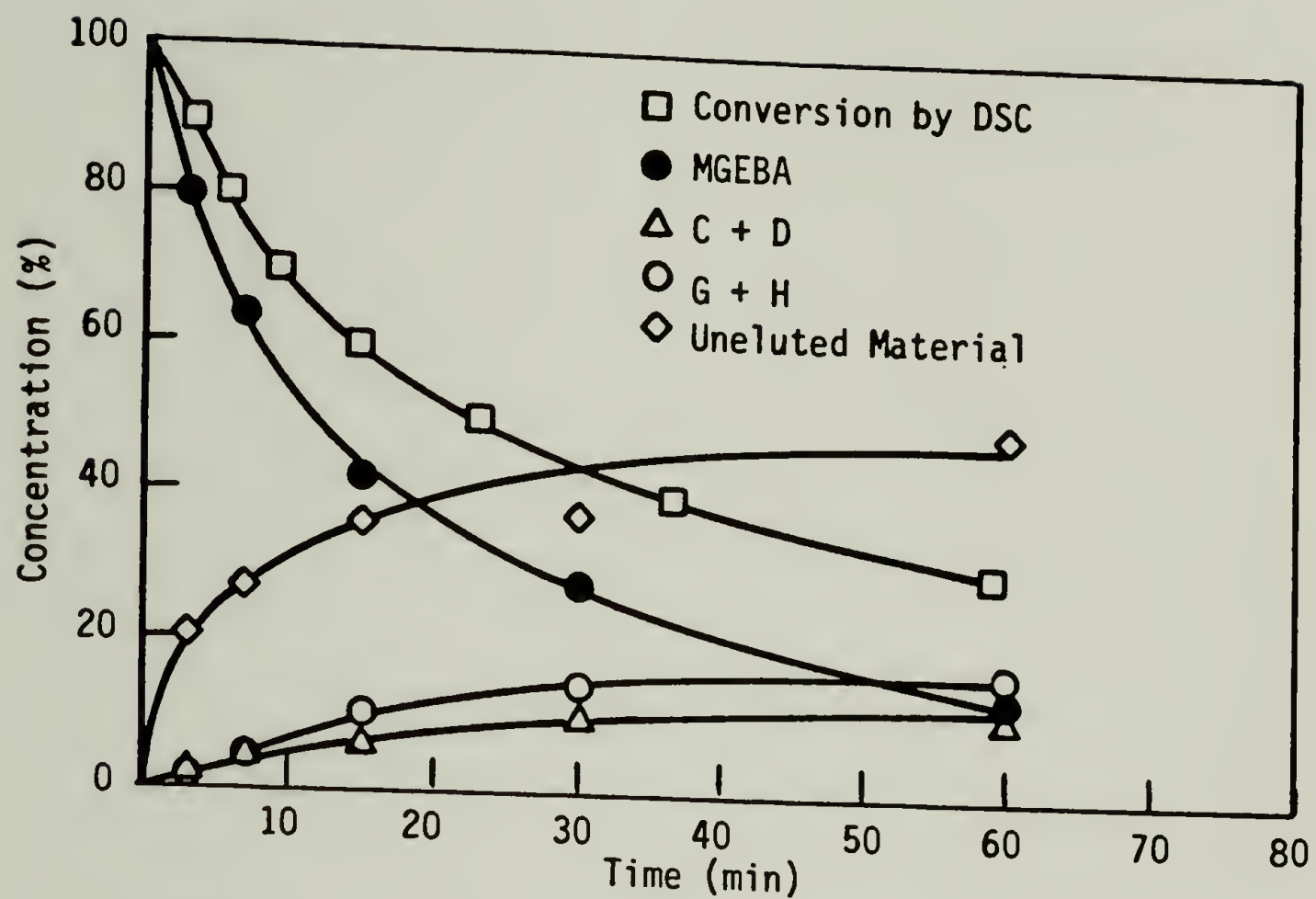


Figure 5-5: Products and Reactants vs time 1:4.5 product I/MGEBA reacted at 147°C.

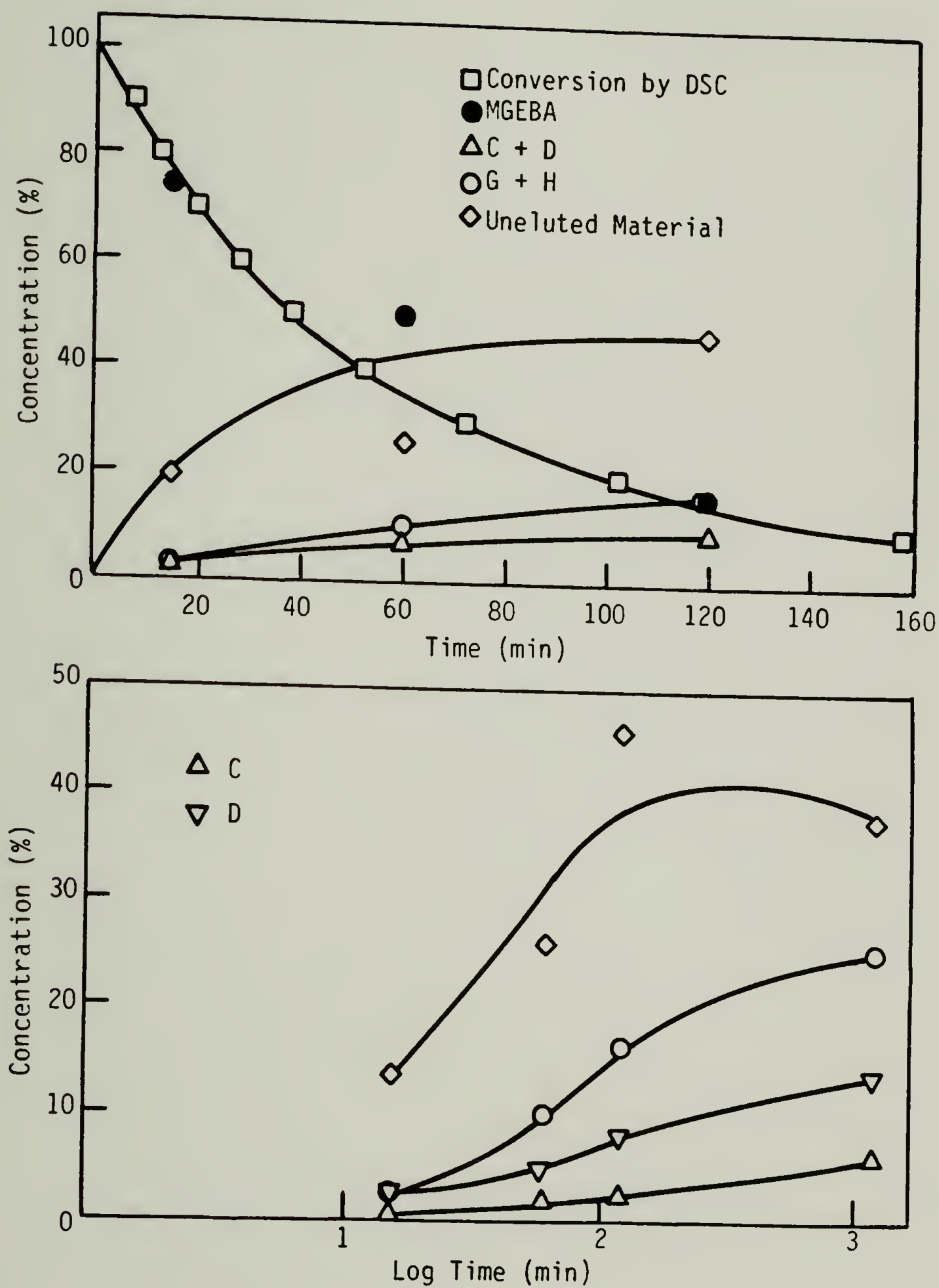


Figure 5-6: Products and Reactants vs time 1:4.5 product I/MGEBA reacted at 127°C.

It is only during the later stages of reaction that the formation of eluting species appears to be substantial. The question, therefore, arose as to the exact relationship between the eluting and uneluting products. It was unknown whether the eluting products were formed by a separate series of reactions or were instead formed by the decomposition of the uneluted material. As seen in Figure 5-4b, continued heating for very long times subsequent to complete epoxide consumption, results in a slow decrease in the weight fraction of uneluted material. In this case, the weight fraction of uneluted material appeared to decrease from 48 to 40% of the total product mixture, over a period of 18 hours. Simultaneously, the weight fraction of product IV appears to have increased, at the expense of both product III and the uneluted material. It was difficult to determine if primary or secondary alkyl amines were also generated by this reaction. As discussed in the previous chapter, these species are generated by the cyclization of both epoxide substituted dicy and urea molecules [84]. Thus, the generation of these species along with product IV would be indicative of substituted dicy or urea structures in the uneluted material. Due to the large number of species present and the potential for peak overlap, the assignment of chromatographic peaks to the generated primary or secondary amines was not readily obvious. These lower molecular weight amines would rapidly react in the presence of excess epoxide to form product V. However, no epoxide was present and virtually no change in the concentration of product V is evident over this period of time.

In an attempt to establish the relationship between the eluting and non-eluting products, the relative weight fractions of these materials



were plotted vs MGEBA consumption, as shown in Figure 5-7. The data plotted in this figure were taken from each of the three reaction temperatures. While some variation is noted, weight fractions measured at the three different reaction temperatures generally appear to fall along the same pair of curves. Evident during the first half of the reaction, is the apparent formation of eluted and uneluted materials at a constant molar ratio, with uneluted material comprising approximately 80% of the product mass. Beyond a point of about 50% epoxide conversion, the rate of formation of eluted species appears to increase relative to that of the uneluted material. If these two sets of products are formed by two competitive, unrelated series of reactions, then this behavior is indicative of an isoconversion change in the relative rates of the reactions comprising these two separate series. Otherwise, the increased rate of formation of eluting species in the later stages of reaction appears to support the contention that uneluted material is, in fact, the progenitor of the products III, IV, and V. Although no definite conclusions could be drawn, it was noted that the long-term decomposition of the uneluted material appeared to occur at a rate much slower than would be expected based on this latter scenario.

#### Relative Rates of MGEBA and Product I Consumption

In Figures 5-4 through 5-6, it is observed that the molar rate of consumption of MGEBA is much faster than that of product I. Since the mixtures were homogeneous, it appears that the initial addition of product I to epoxide is a relatively slow, rate controlling step. All subsequent steps in the amine/epoxide reaction appear to occur at a much greater rate. As in the case of the dicy/MGEBA reaction, the slow rate

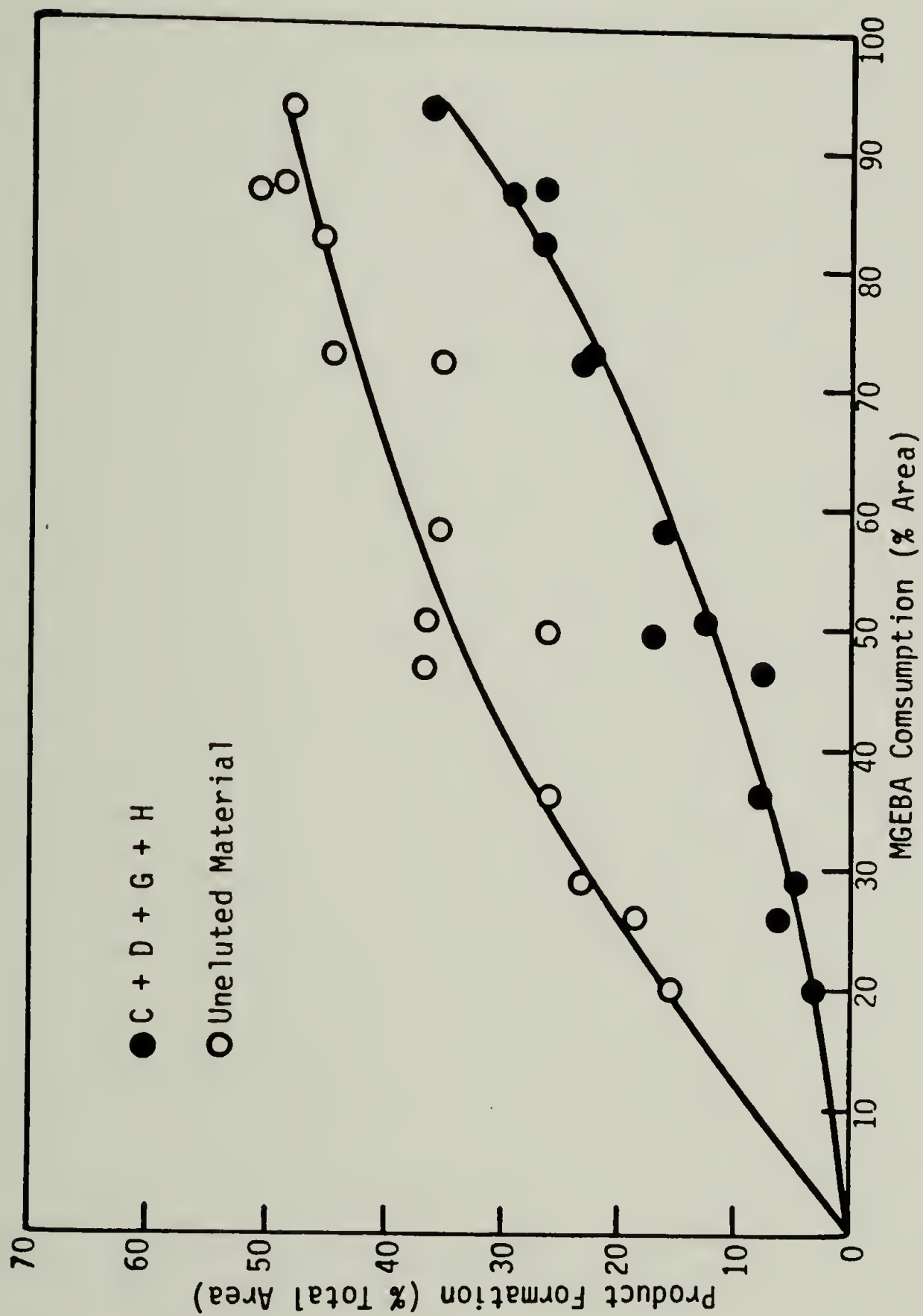


Figure 5-7: Formation of eluted and uneluted materials vs MGEBA consumption for (1:4.5) product I/MGEBA at 127<sup>o</sup>-167<sup>o</sup>C.

of the initial I/MGEBA reaction results in the steady formation of a low concentration of intermediate species, such as product II, in the reaction mixture, throughout the course of the reaction. Thus, if reaction conditions more favorable to cyclic and triamine product formation did arise in the later half of the reaction, then a substantial supply of reactive intermediate species was readily available. Figure 5-8 shows a plot of the molar consumption of product I vs that of MGEBA, for the 1-4.5 mixture reacted at 127°-167°C. Again, data from each of the three temperatures appears to fall along a single curve, confirming the initial reaction as the rate controlling step. At an epoxide conversion of 50%, a change in the slope of this curve is evident, apparently reflecting an increase in the amount of hydroxyl addition/amine elimination reactions. The rate of alkyl amine reaction is extremely rapid, relative to product I reaction, the diminished rate of product I consumption at this point in the reaction, appears to indicate an increase in the rate of alkyl amine generation. This, in turn implies that a reservoir of multiply substituted dicy species must be present from which alkyl amines can be generated. Otherwise, a change in mechanism would have had to have occurred. Thus, it appeared that the uneluted material was, to some extent, composed of multiply substituted dicy molecules. However, it can be seen that, prior to the change in slope of Figure 5-8, reactants appear to be consumed at a rate of 6 epoxide groups per product I molecule, which gives some indication of the high degree of substitution expected for the bulk of the uneluted material.

At longer reaction times, beyond completion of epoxide consumption, an increase in the area of peak A was observed. HPLC analyses at 229 nm

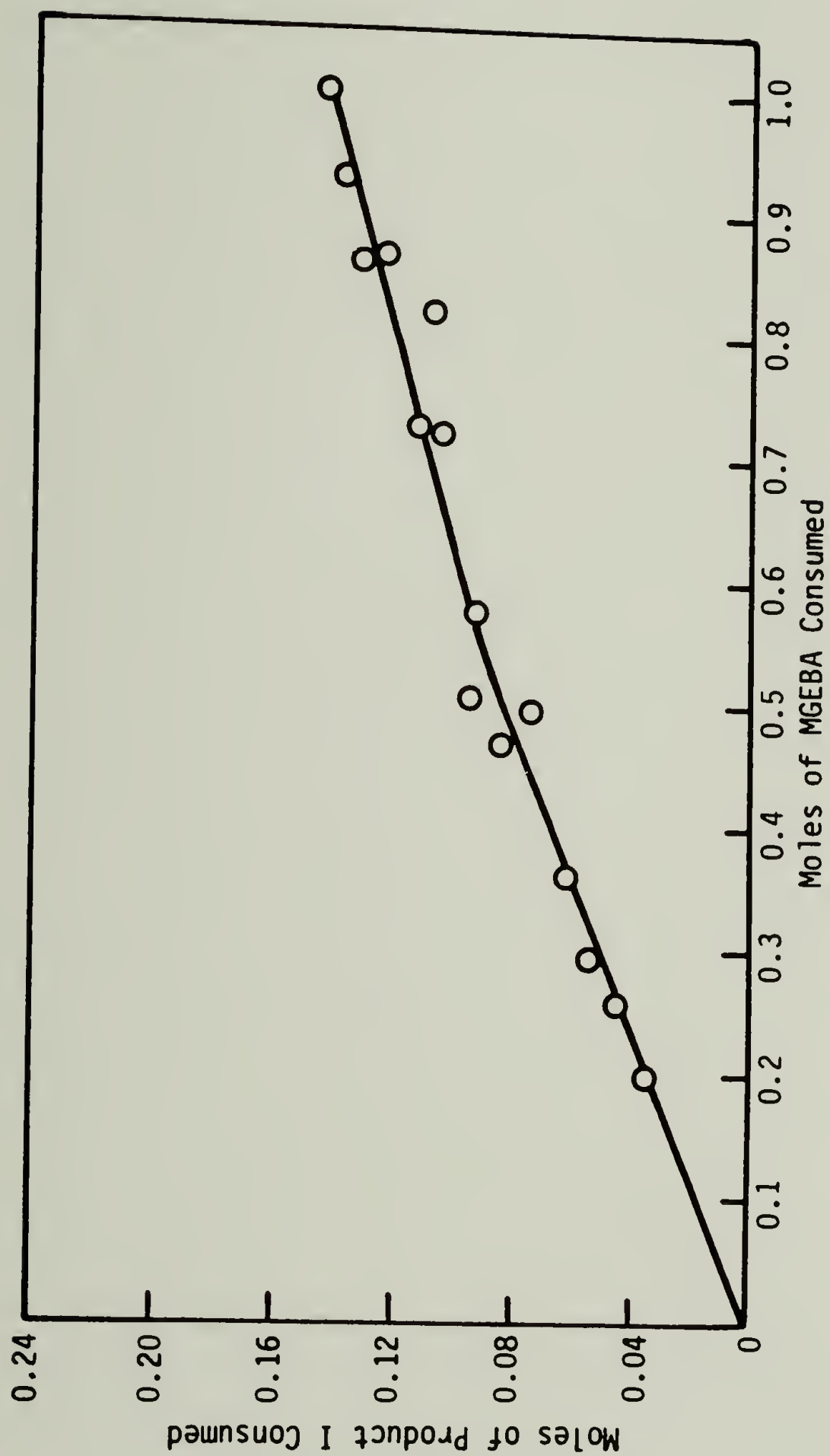


Figure 5-8: Consumption of product I vs consumption of MGEBA consumption for (1:4.5) product I/MGEBA at 127°-167°C.



indicated that this peak, at long reaction times, was composed entirely of a non-dicy based product, presumably identical to that isolated from peak A of the dicy/MGEBA reaction mixture and characterized by FTIR in chapter 4. Substantial amounts of this product appeared to be present only after epoxide consumption was complete. Thus, it is believed that this product represents a sizable portion of the material formed by the long term decomposition of the uneluted material. After 19 hours at 167°C, this compound was found to comprise 5% of the total mass of the consumed MGEBA.

#### Uneluted Material in the Dicy/MGEBA Reaction

In the case of the uncatalyzed dicy/MGEBA reaction, discussed in chapter 3, the extremely slow rate of the the initial dicy/epoxide addition and the high temperatures required for reaction results in the slow accumulation of non-reactive end-products in the reaction mixtures. A typical plot of reactant consumption and product formation for this reaction, shown in Figure 5-9, reveals the apparent linear growth of eluting and non-eluting species. Further the relative weight fraction ratios of the three groups of products plotted in this figure appear to remain constant over the course of the reaction. However, a plot of the weight fractions of eluting and non-eluting materials vs MGEBA consumption, shown in Figure 5-10, reveals an increase in the rate of formation of eluting species relative to that of non-eluting materials, at an epoxide conversion of 70%. This conversion is comparable to the the 50% conversion of the, effectively staged, product I/MGEBA reaction, supporting conversion, or in actuality the extent of hydroxyl formation, as a controlling factor in the observed ratio in the relative rates of

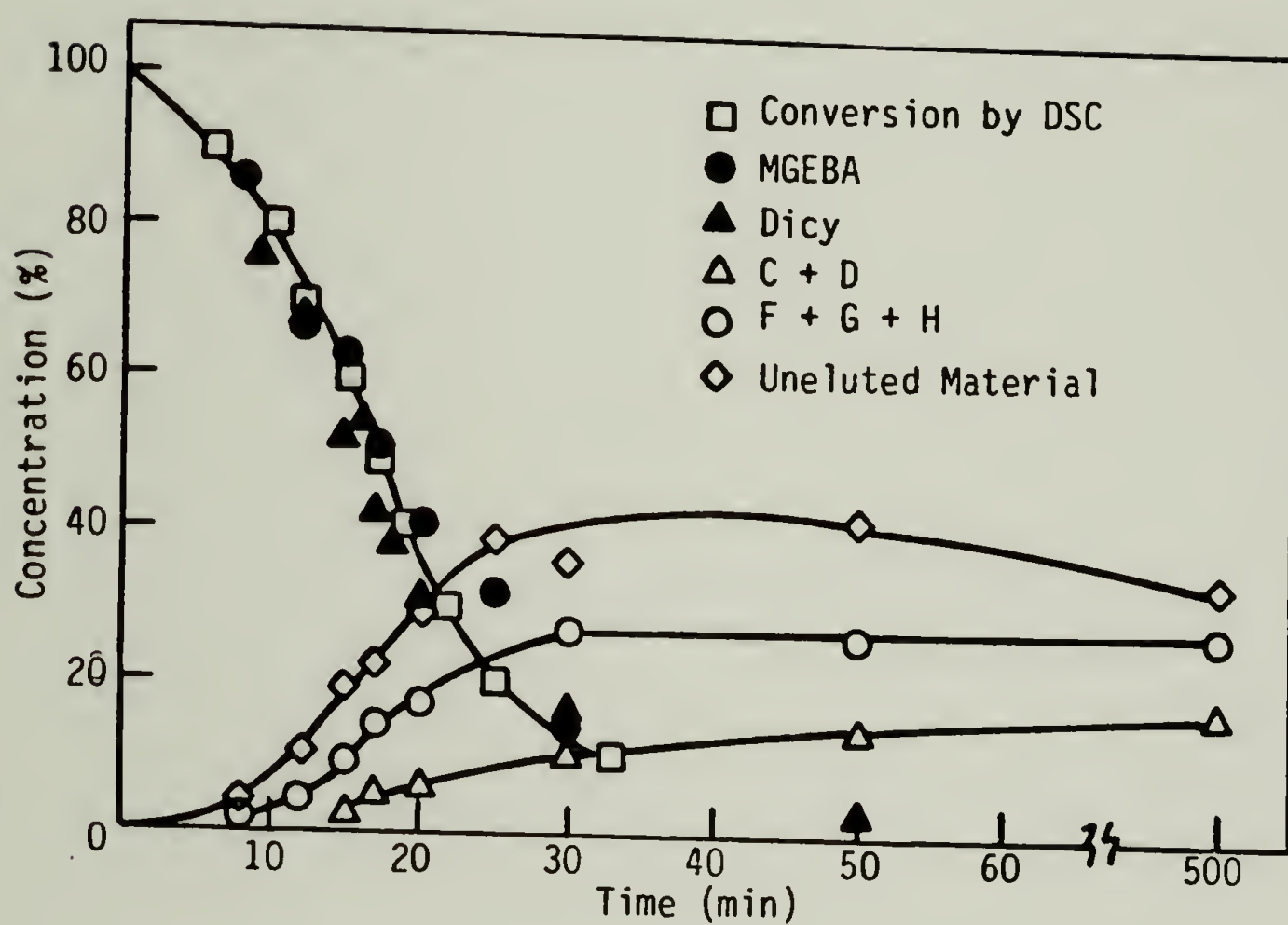


Figure 5-9: Product and reactant concentration vs time for 1:6 dicy/MGEBA reacted at 197°C.

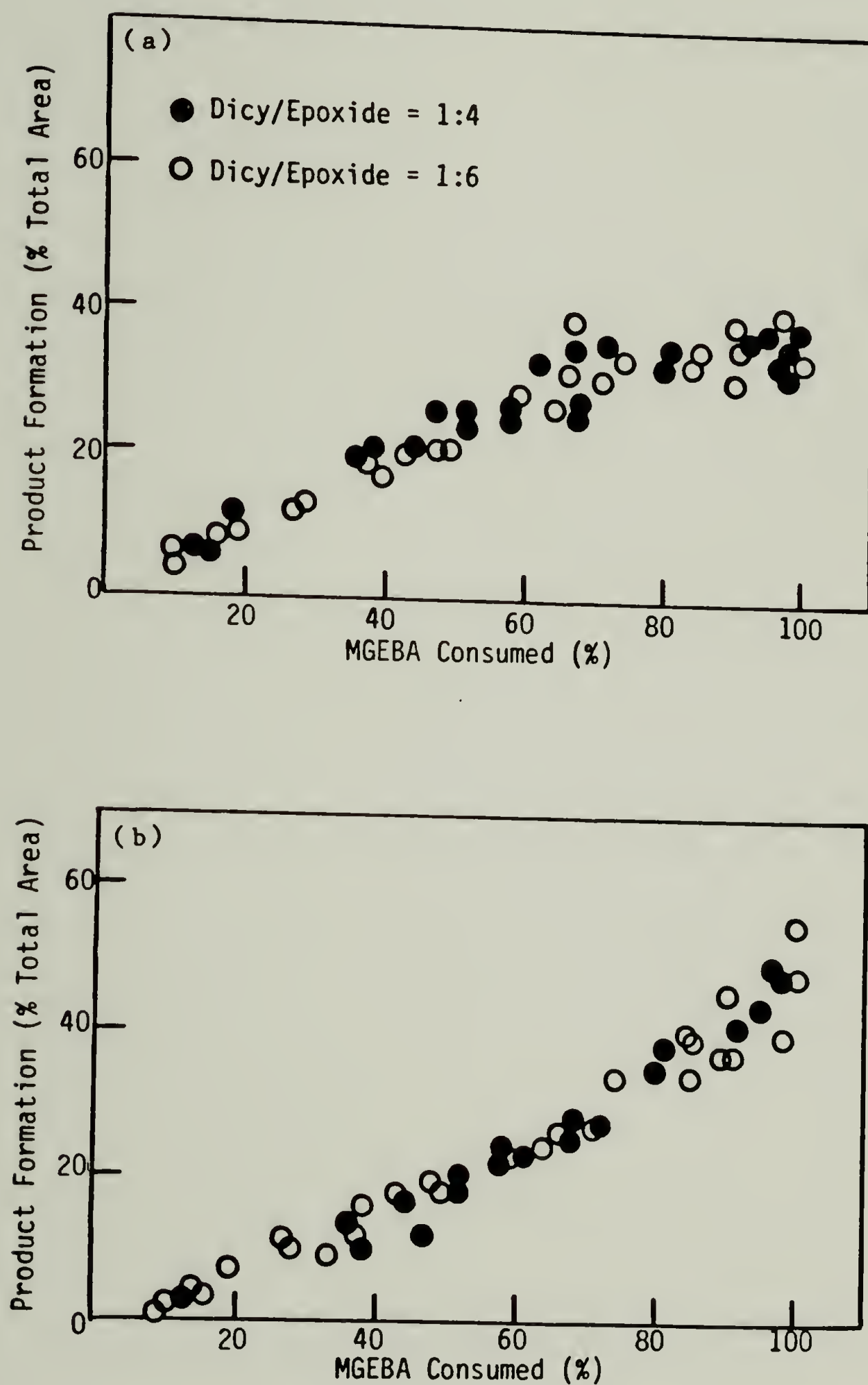


Figure 5-10: (a) Formation of uneluted materials vs MGEBA consumption for dicy/MGEBA. (b) Formation of eluted materials vs MGEBA consumption for dicy/MGEBA. Temp. = 167°-197°C.

formation of eluting and non-eluting products. Despite the differences in temperature and kinetic control, similar distributions of products were found for these two systems.

### Size Exclusion Chromatography

Based on mass balance calculations for the reaction mixtures used in the HPLC kinetic study, it appears that the uneluted material is formed by the addition of an average of 6 to 8 MGEBA molecules to each dicy molecule. Since a significant amount of etherification may have occurred during the course of this reaction, it is difficult to assign tentative structures to the uneluted material according to these ratios. In an attempt to further clarify the size and numbers of these products, several of the samples used in the HPLC kinetic study were analyzed by SEC. Figure 5-11 shows a series of SEC chromatograms for the product mixtures formed by the 1:4.5 composition, reacted at a temperature of 167°C for a period of 5-30 min. Four major peaks are evident in these chromatograms. Of these, peaks w and x are assigned to MGEBA and product I, respectively, while peaks y and z are assigned to the eluting and non-eluting materials. The relative sizes and rate of growth of these product peaks appear to support the results found in the HPLC kinetic study. As discussed in the previous chapter, based on these SEC chromatograms, the molecular size of the products composing the uneluted material appear to be somewhat smaller than that of the 6:1 etherification product of the V/MGEBA reaction. However, due to the differences in structures and solvent interactions, this finding is not conclusive. In the first example, shown in Figure 5-11a, the mixture has been reacted to an epoxide conversion of 50%. The uneluted material again appears



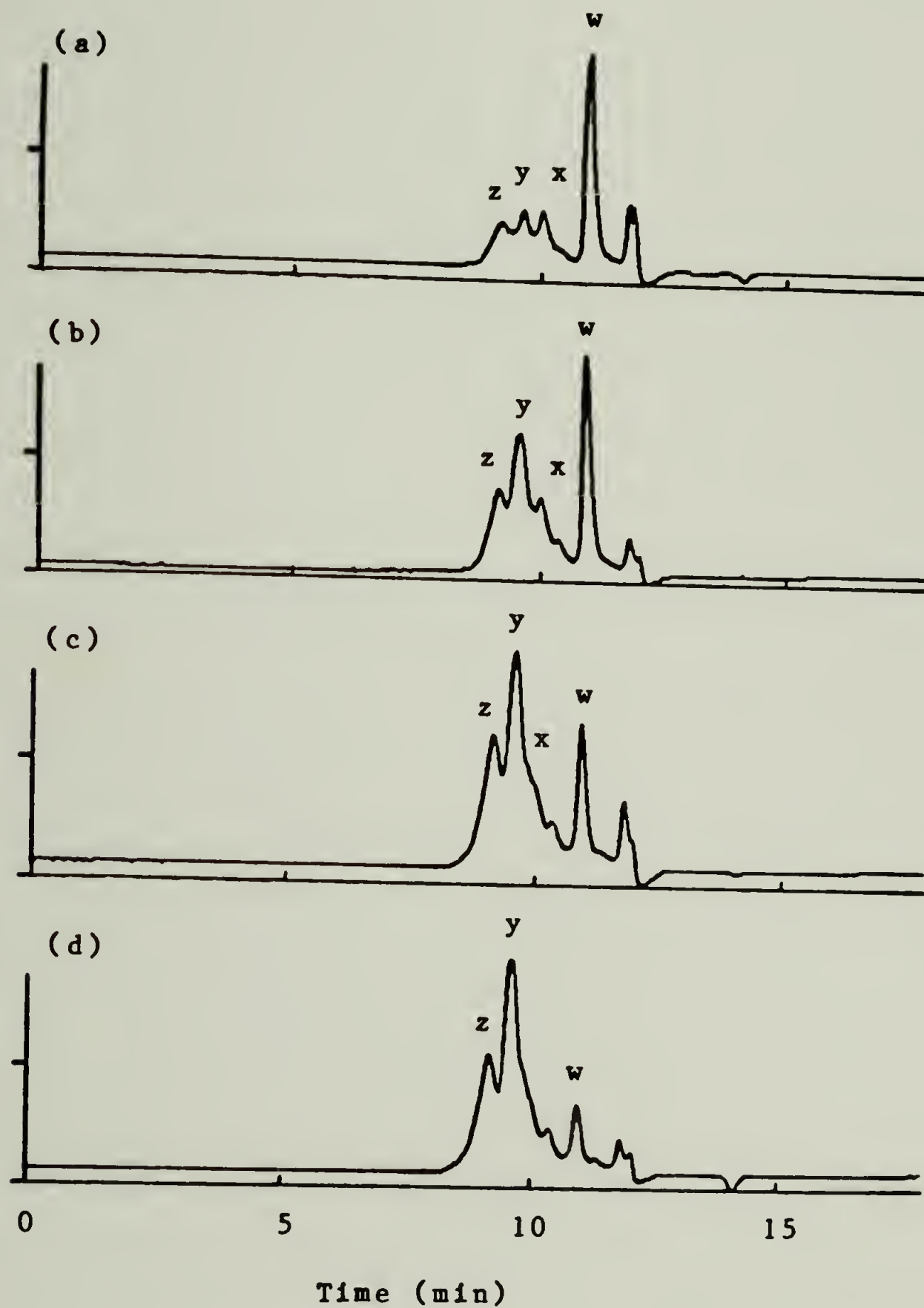


Figure 5-11: Comparison of SEC chromatograms of product I/MGEBA reacted at 167°C for (a) 5 min, (b) 10 min, (c) 20 min, (d) 30 min.

to be the predominant product, forming a broad peak z in this chromatogram, while the HPLC eluting products appear as a minor shoulder y. With increasing epoxide conversion, Figures 5-11b through 5-11d, peak y is observed to rapidly increase, accompanied by only a moderate increase in the size of peak z. It was unclear whether the higher molecular weight uneluted material formed by a reaction mechanism unrelated to, and competitive with, those reactions forming the eluting species, or was instead the source from which the eluting species were formed.

#### Compositional Variation

In a further attempt to answer this question, the combined techniques of SEC and HPLC were used in order to determine the effects of compositional variation on the distribution of products formed in the I/MGEBA reaction. An uncatalyzed 1:9 product I/MGEBA mixture was reacted at 167°C for 425 minutes resulting in complete epoxide consumption. HPLC analysis revealed only a slight reduction in the concentrations of cyclic compounds and uneluted materials for this mixture compared with that formed by reaction of the 1:4.5 mixture. However, a number of non-polar peaks were observed, which were apparently attributable to the products formed by etherification reactions. Again, an SEC chromatogram indicated that these products were larger in size than the products of the uneluted material. Despite the large amount of etherification, the distribution of eluting and uneluting species appeared to be similar to that found in the 1:4.5 product mixtures.

Using the product I/MGEBA system, it was possible to determine the effects of high dicy loading on the distribution of products. For pur-

poses of comparison, product mixtures were obtained by reacting 1:1 and 1:4.5 I/MGEBA compositions at a temperature of 167°C for one hour. HPLC analyses revealed nearly identical uneluted material weight fractions of 56% and 47% for the 1:1 and 1:4.5 product mixtures, respectively. However, while the the weight fractions of products III and IV in the 1:1 mixture were found to be somewhat reduced, the amount of product V in this mixture was almost nonexistent. SEC chromatograms for the two mixtures, shown in Figures 5-12a and 5-12b, reveal peaks assigned to the uneluted material, which were apparently identical in shape and elution time. Based on product distribution and the results of the HPLC kinetic study presented earlier, it appears that the uneluted material was rapidly formed in the initial stage of the reaction, resulting in the depletion of deficient MGEBA. Subsequent heating apparently resulted in the formation of cyclical products and amines through the apparent decomposition of higher molecular weight species. In the absence of epoxide, the further reaction of these products could not occur, resulting in the low concentrations of products III, IV and V in this system. Mass balance considerations indicate that a large concentration of the less substituted analogs of these products should be present in this mixture, and these apparently elute in the HPLC at positions designated as peaks A and E in Figure 3. Thus, in the case of high product I loadings, the formation of substantial amounts of both high molecular weight uneluted material, and low molecular weight species was observed.

#### Variation of Reaction Temperature

As discussed above, temperature dependent differences in the product mixtures obtained by reacting the 1:4.5 I/MGEBA mixtures in the range of

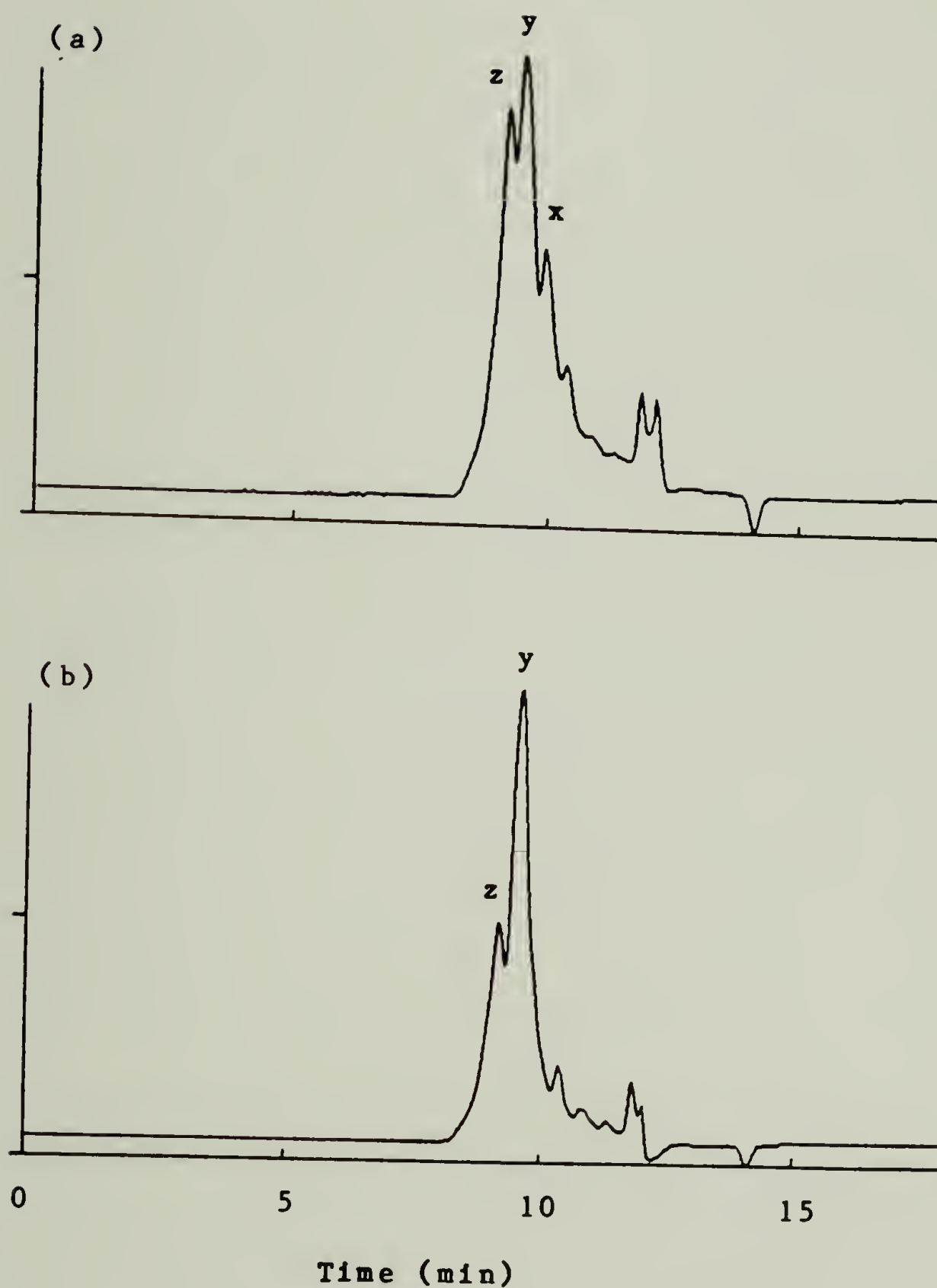


Figure 5-12: (a) SEC chromatogram of 1:1 product I/MGEBA reacted at 167°C for 60 min. (b) SEC chromatogram of 1:4.5 product I/MGEBA reacted at 167°C for 60min.



127 to 167°C were minimal. However, the reaction of this composition at a temperature of 107°C resulted in the formation of a product mixture containing a disproportionately high concentration of uneluted material. The weight fraction of this material was 64% of the product mixture, as determined by HPLC analysis, while the combined weight fraction of products III, IV, and V was found to be only 22%. Thus, it appears that the relative rate of decomposition of the uneluted material is to some degree temperature dependent. The SEC chromatogram of this mixture revealed no changes in the shape or positioning of the uneluted product peak.

#### Analysis of the Product I/DGEBA Cure by TBA

TBA was used to follow the cures of a range of product I/DGEBA compositions at temperatures of 107°C to 167°C. A typical trace of a 1:5 product I/DGEBA mixture cured at 107°C is shown in Figure 5-13a. Two maxima are evident in the damping curve of this trace. As discussed in chapter 2, the first of these, at 175 min, is associated with gelation, while the second, at 625 min, is assigned to vitrification. For reasons presented in the introduction of this chapter, the structures analogous to products III, IV and V were not expected to be effective crosslink junctures when formed in the I/DGEBA system. Therefore, network formation in this system is entirely dependent on the functionality and extent of formation of structures analogous to the uneluted material. Figure 5-13b shows a temperature scan of the cured 1:5 sample at a scan rate of 1.5°C/min. In the first scan, a  $T_g$  midpoint of 128°C is observed. However, after scanning to 200°C, a rescan of the sample reveals a reduction in the  $T_g$  midpoint to a temperature of 112°C. All

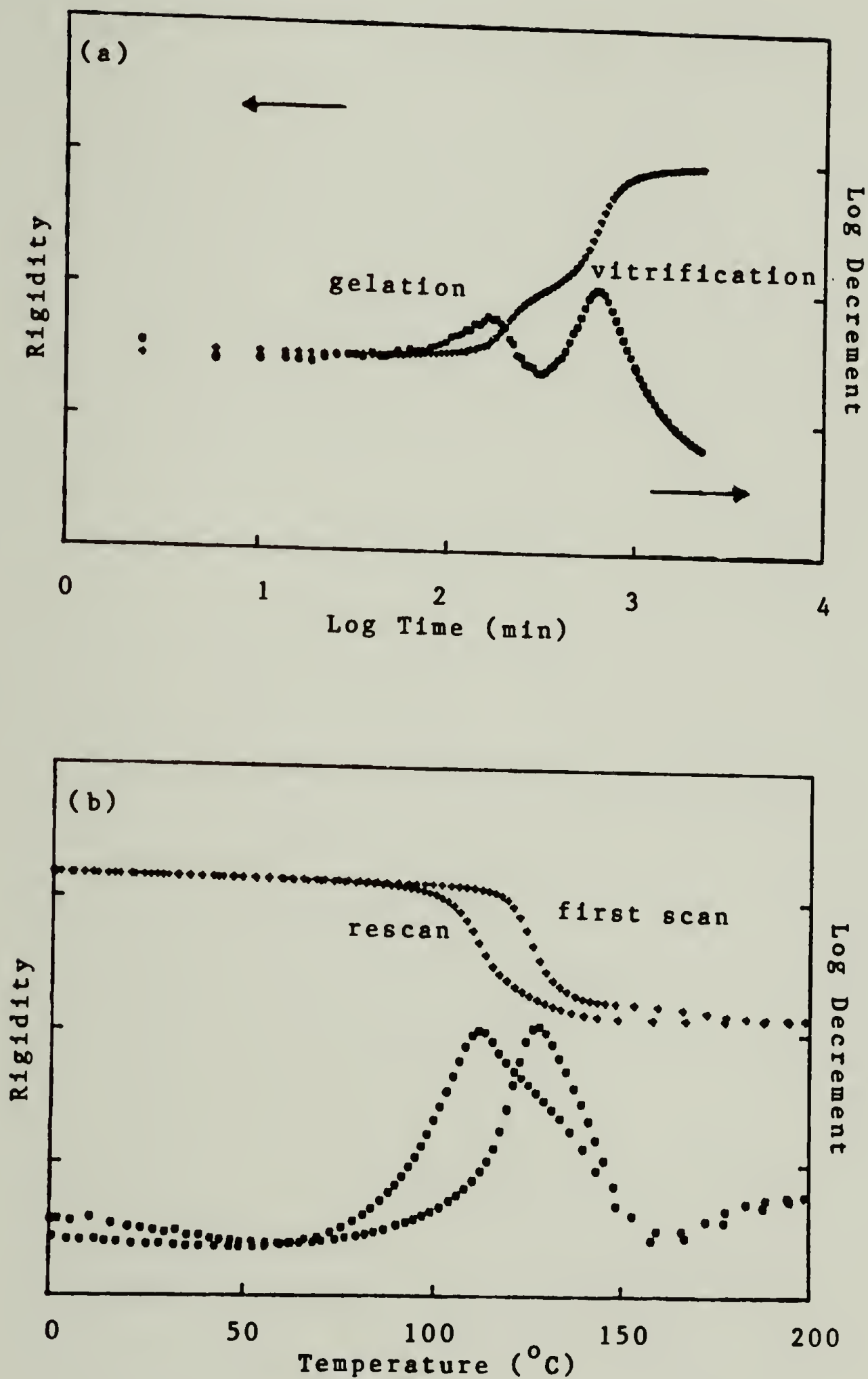


Figure 5-13: (a) TBA trace of 1:5 product I/DGEBA cured at 127 $^{\circ}\text{C}$ .  
 (b) TBA temperature scan at 1.5 $^{\circ}\text{C}/\text{min}$ .

ing scans revealed only a slight increase in the  $T_g$  midpoint, apparently due to high temperature crosslinking. Several similar, although smaller, reductions in  $T_g$  have been reported for other amine/epoxy cures. In these cases,  $T_g$  reduction was attributed to supercooling [31,84]. However, attempts to increase post scan  $T_g$  in the present system by cure temperature annealing for a period of several days failed to produce any significant changes. Thus, it is believed that  $T_g$  reduction can be attributed to degradation, presumably of the structures analogous to the uneluted material.

Under certain conditions, it is possible to observe  $T_g$  reduction in the TBA trace of an isothermal product I/DGEBA cure. An example of this is shown in Figure 5-14 for the cure of a 1:7 product I/DGEBA mixture at  $147^{\circ}\text{C}$ . Although this temperature is  $20^{\circ}\text{C}$  above the ultimate  $T_g$  midpoint of the cured sample, it is possible to discern the slight rise in modulus indicative of the onset of vitrification. At long times, this modulus reaches a maximum value and then decreases, again apparently due to the degradation of the network structure via the decomposition of structures analogous to the uneluted material. In chapter 2, identical behavior was observed in the TBA traces of the isothermal cures of the uncatalyzed dicy/DGEBA system. Since, based on the MGEBA reaction studies, the mechanism of the dicy/ epoxy reaction appears to be identical to that of the product I/epoxy reaction, it appears that the mechanisms governing long term degradation in these systems are identical.

An attempt was made to determine the effects of compositional variation on network formation and the development of physical properties in

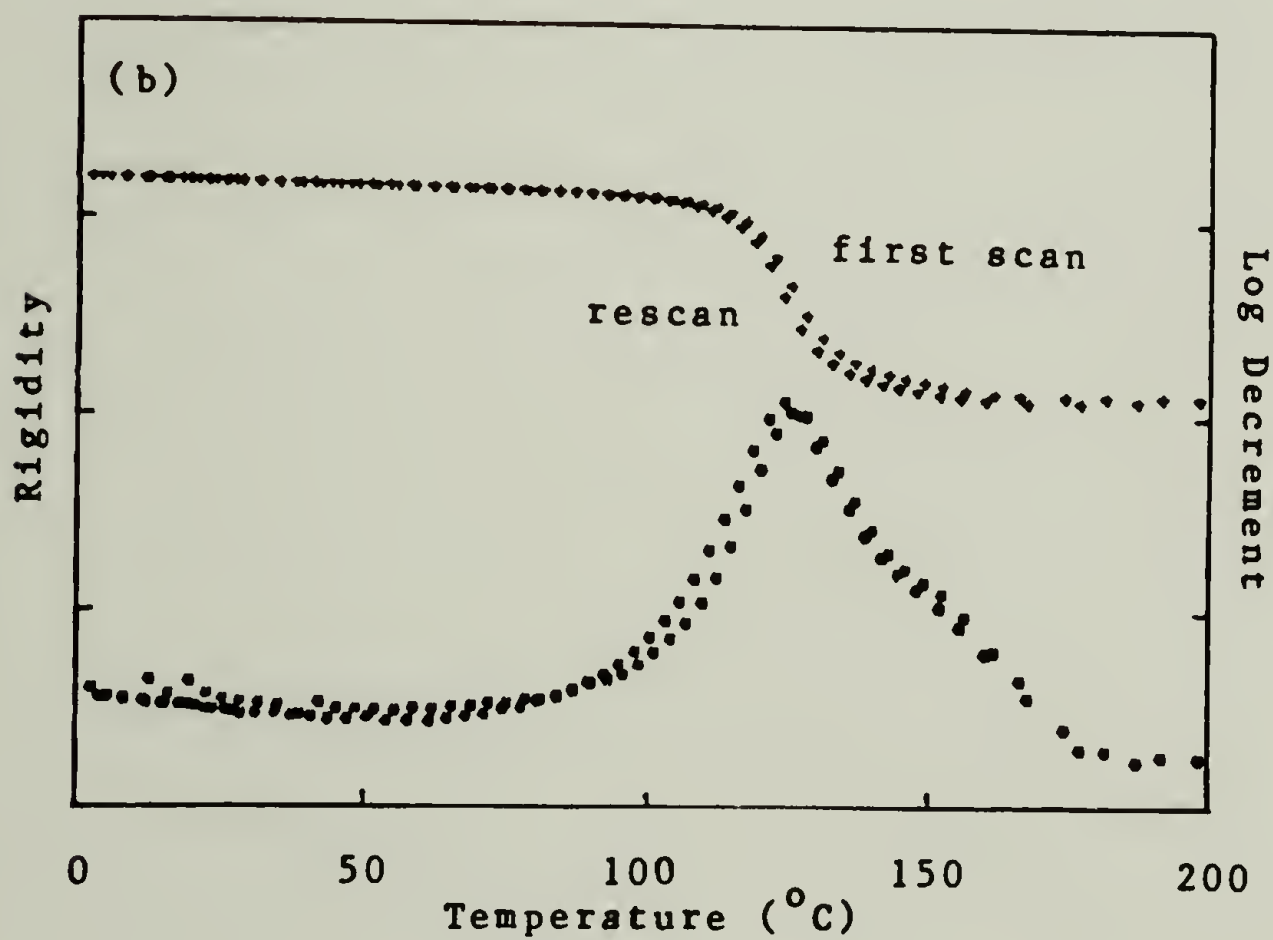
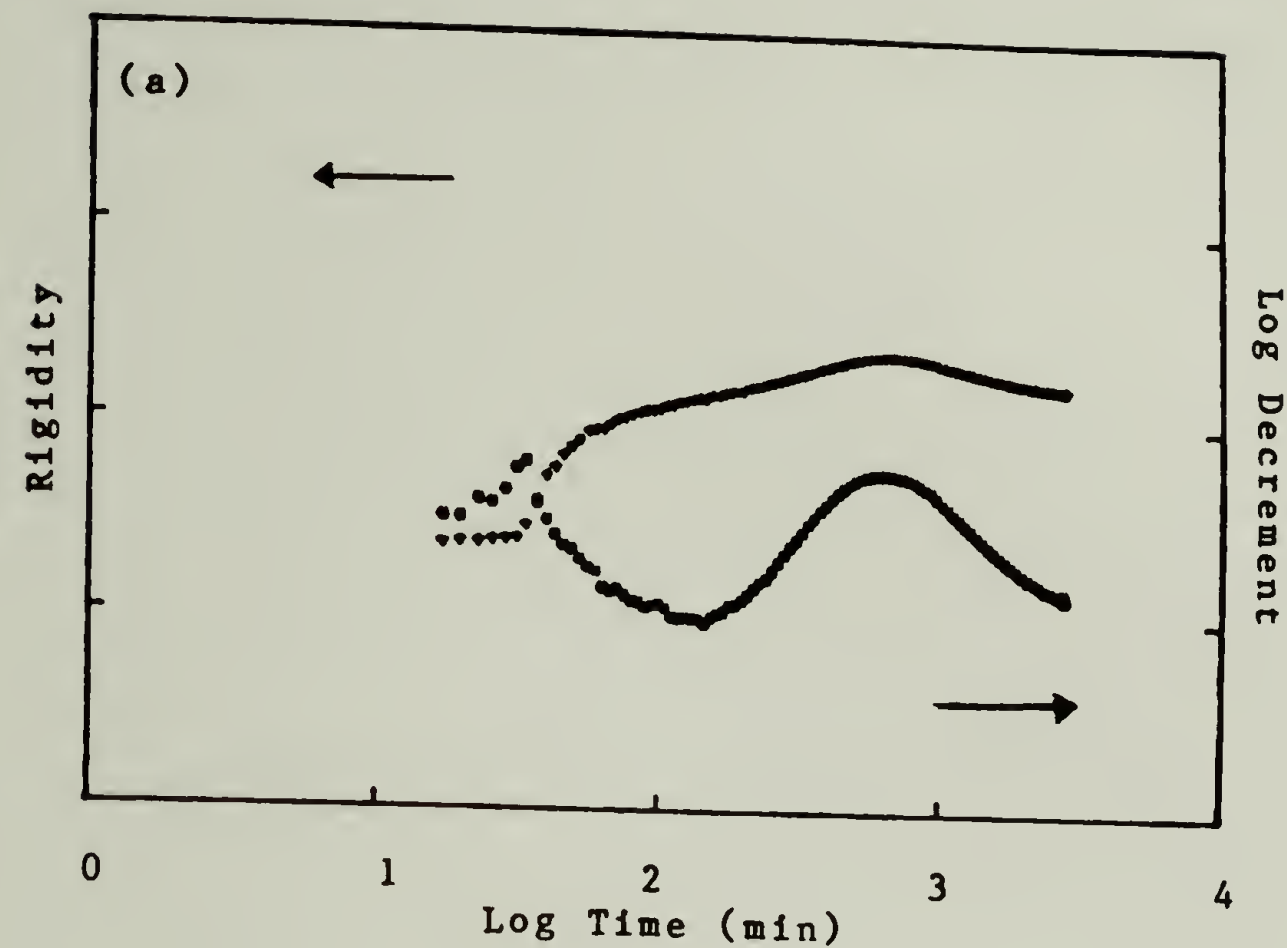


Figure 5-14: (a) TBA trace of 1:7 productI/DGEBA cured at 147°C.  
(b) TBA temperature scan at 1.5°C/min.



the product I/DGEBA cure. Table VII lists the  $T_g$  midpoint values, obtained both before and after scanning to  $200^{\circ}\text{C}$ , for a series of product I/DGEBA compositions cured at  $127^{\circ}\text{C}$ . Cures were run until a plateau value in maximum rigidity was obtained. Of interest were the post-scan  $T_g$ 's, and the extent of  $T_g$  reduction seen for the various compositions.  $T_g$  reduction appears to be greatest for the 1:5 and 1:7 compositions. The 1:3 composition did not appear to undergo decomposition at all. However, based on isothermal observations, it appears that the overall rate of  $T_g$  reduction is proportional to the concentrations of product I in each of the starting mixtures. Thus, at  $127^{\circ}\text{C}$ , the rate of the degradation reaction appears to be competitive with crosslinking in the 1:3 composition. The highest prescan  $T_g$  was observed for the 1:7 mixture, which is believed to be closest in composition to the stoichiometry required for uneluted material formation. Finally, only a slight  $T_g$  reduction is observed for the 1:9 composition. To some degree, this is expected, since a large extent of the crosslinking in this system can be attributed to etherification. However, it was also possible that some amount of stabilization is afforded this system due to the consumption of hydroxyl groups via these etherification reactions, as was suggested by Lin et al. [42]. It is noted that the final  $T_g$ 's of the several compositions were invariant toward further heating. Thus, it appears that the decomposition of structures, analogous to the products comprising the uneluted material of the dicy/MGEBA reaction mixtures, only occurs to a partial extent.

Gel times, as determined by TBA, are listed in Table VIII, for several product I/DGEBA compositions, cured over a range of temperatures.

TABLE VII

$T_g$  Midpoint vs Composition for the Product I/DGEBA Cure

Composition	$T_{g \text{ init.}}(^{\circ}\text{C})$	$T_{g \text{ final}}(^{\circ}\text{C})$
1:3	106	110
1:5	130	114
1:7	142	125
1:9	140	136

TABLE VIII

Times to TBA Gel Point for I/DGEBA Cure (min)

Composition	107°C	127°C	147°C	167°C
1:3	-----	33	-----	-----
1:5	176	57	18	9
1:7	305	100	34	16
1:9	-----	156	-----	-----

Based on the results of the product I/MGEBA reaction study, it was assumed that the initial product I/epoxide reaction would be the rate controlling step in the initial reaction, and that this reaction would result in a linear increase in the extent of uneluted product formation with epoxide conversion. Further, it was believed that the gel times, measured by TBA, represent the time to formation of a specific concentration of structures analogous to the uneluted material, independent of the starting composition of the mixture. Thus, for the range of compositions cured at  $127^{\circ}\text{C}$ , it was believed that these gel times would reveal the relative rate of uneluted product formation. Using these gel times,  $E_a$ 's of 70-75 kJ/mole were calculated for the 1:5 and 1:7 compositions, in the temperature range of  $107^{\circ}\text{C}$ - $147^{\circ}\text{C}$ . At  $167^{\circ}\text{C}$ , deviations from the Arrhenius value appeared to indicate an increase in the relative rate of the decomposition reaction for both of these mixtures.

### Summary

The results of the HPLC kinetic study of the product I/MGEBA reaction revealed the rapid formation of the, as yet unidentified, uneluted material in the early stages of reaction. At a later stage in the reaction, the rate of HPLC elutable species formation appears to increase at the expense of uneluted material formation. At long reaction times, following the completion of epoxide consumption, the uneluted material appears to decompose to form elutable species. These observations appeared to indicate that tetrasubstituted was the major component of the uneluted material, with decomposition occurring via the mechanism described in Figure 4-20. However, this conclusion is not supported by



the incomplete and slow rate of decomposition observed for the uneluted material, at long reaction times. Thus, it appears that other, as yet unidentified, products comprise the bulk of the uneluted material. Although the structures of these products are not known, the products appear to be of moderate mass, having been formed by the reaction of 5 to 8 epoxide molecules with each dicy molecule. The formation of these uneluted products appears to be competitive with the formation of eluting species via the intramolecular hydroxyl addition/amine elimination reactions, described in Figure 4-20. The reason for change in the relative rates of formation of eluting and uneluting species at a specific conversion will be discussed in chapter 6, and possible structures for the uneluted compounds will be described along with the mechanisms for their partial decomposition.

## CHAPTER 6

### CONCLUSIONS

#### The Dicy/Epoxide Reaction Mechanism

##### The Mechanism

A schematic representation of the mechanism of the dicy/epoxide reaction, in the absence of etherification, is shown in Figure 6-1. The initial phase of the reaction, depicted by equation (a), consists of simple amine/epoxide addition reactions, which result in the formation of a series of linearly substituted dicy/epoxide adducts, including those analogous to products I and II. Once formed, these adducts are capable of cyclizing via intramolecular hydroxyl addition at the imido carbon. As shown in equation (b), this reaction is accompanied by the elimination of ammonia or alkyl amine, leading to the formation of 2-cyanimido oxazolidines, analogous to product III. Thus, contrary to the mechanism proposed by Zahir and shown in equations (12) and (13), cyclization does not occur via hydroxyl addition to the cyano group, nor does dicy dissociate to form cyanamide and 2-imino oxazolidine.

The ammonia and/or alkyl amines, generated by cyclization reaction (b), undergo further addition of epoxide, ultimately yielding structures analogous to product V, as demonstrated in equation (c). Structures analogous to product III are thermally stable and are incapable of further reaction with epoxide. However, these structures are susceptible to hydrolysis at the imide bond, as shown in equation (d), forming 2-oxazolidone products, analogous to product IV. Hydrolysis appears to

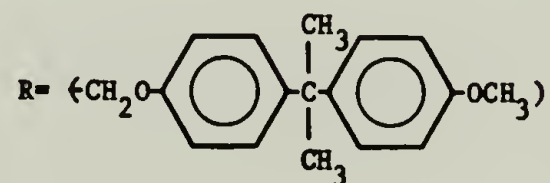
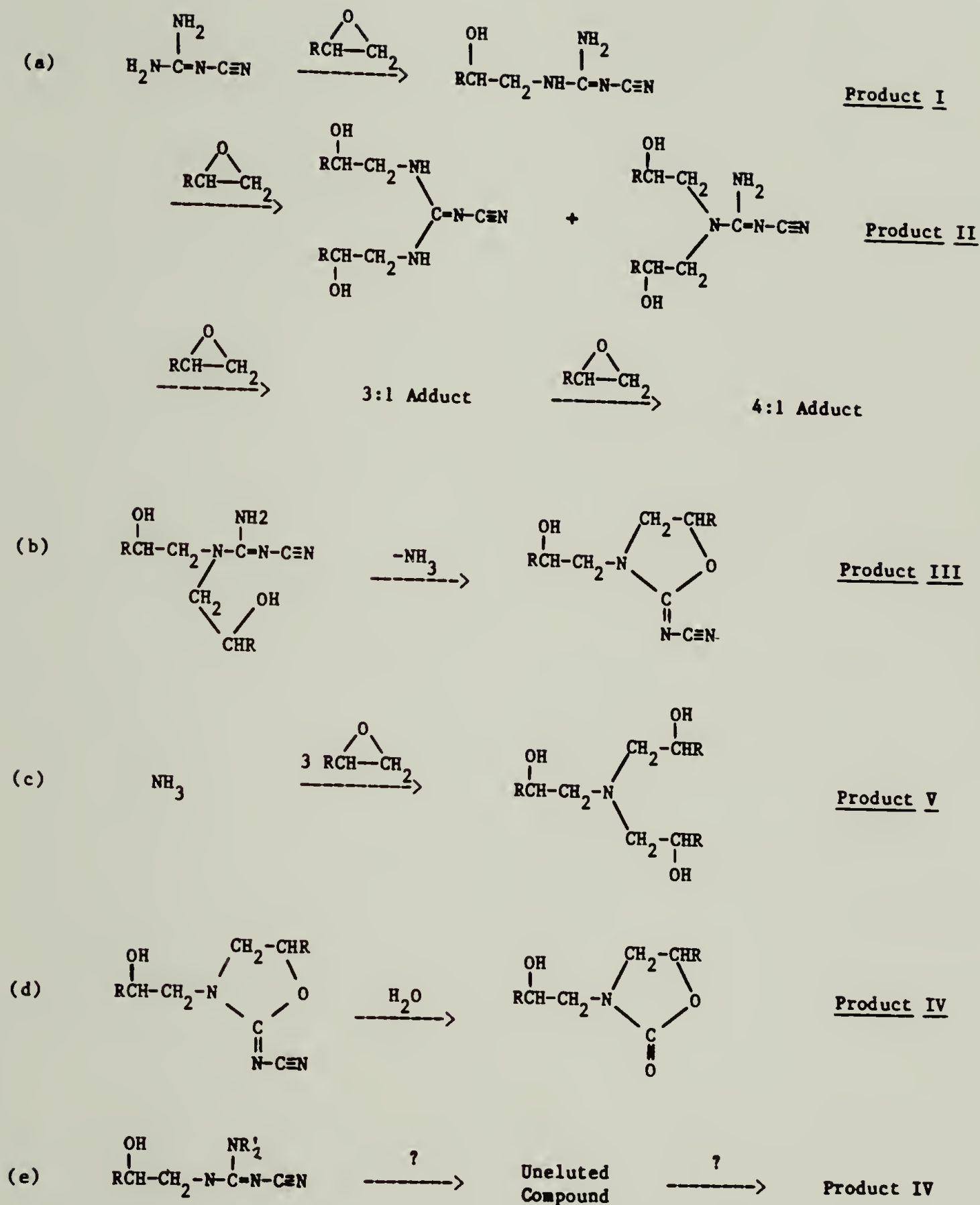


Figure 6-1: Dicy/MGEBA reaction scheme.

be the only mechanism of carbonyl generation. Structural rearrangements, as proposed by Saunders [35] and Zahir [40], and shown in equations (11) and (14), respectively, do not occur.

Finally, the linearly substituted dicy adducts formed in equation (a), appear to be capable of avoiding cyclization reaction (b) by undergoing an as yet unknown, competitive transformation into structures analogous to the non-HPLC elutable fraction of the dicy/MGEBA product mixture. As depicted in equation (e), this material also appears to be partially susceptible to a very slow decomposition reaction, leading to the formation of structures analogous to product IV.

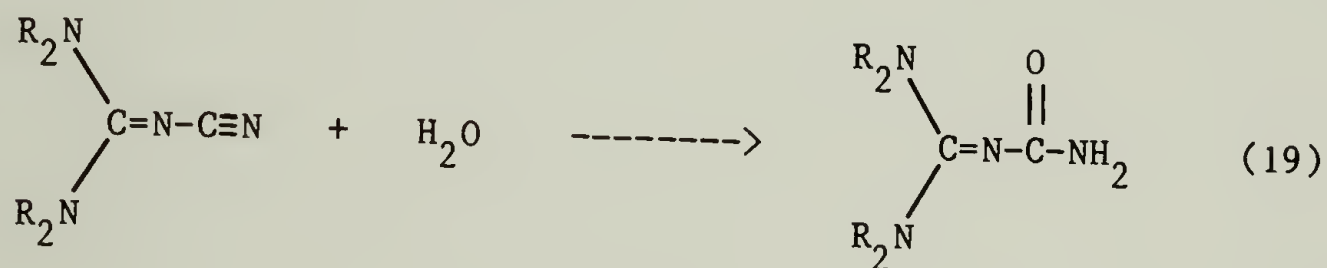
#### Postulated Identity of Uneluted Material

Although no definitive analyses have been made, much is known about the components comprising this non-HPLC elutable material. Based on SEC analyses, a molecular size of 4 to 6 MGEBA molecules has been estimated for these species, while mass balance calculations have indicated a consumption ratio of 6 to 8 moles of MGEBA per mole of dicy, in the formation of the uneluted products. These products do not increase in size when further reacted over a reasonable period of time, even in the presence of excess epoxide. Thus, based on these considerations, it is possible to rule out both oligomerization of substituted dicy molecules by intermolecular hydroxyl addition, and etherification reactions, as the mechanisms by which the uneluted products are formed.

FTIR analyses have revealed a predominant carbonyl absorbance band at  $1699\text{ cm}^{-1}$ , both in the spectra of the unresolved product mixtures,



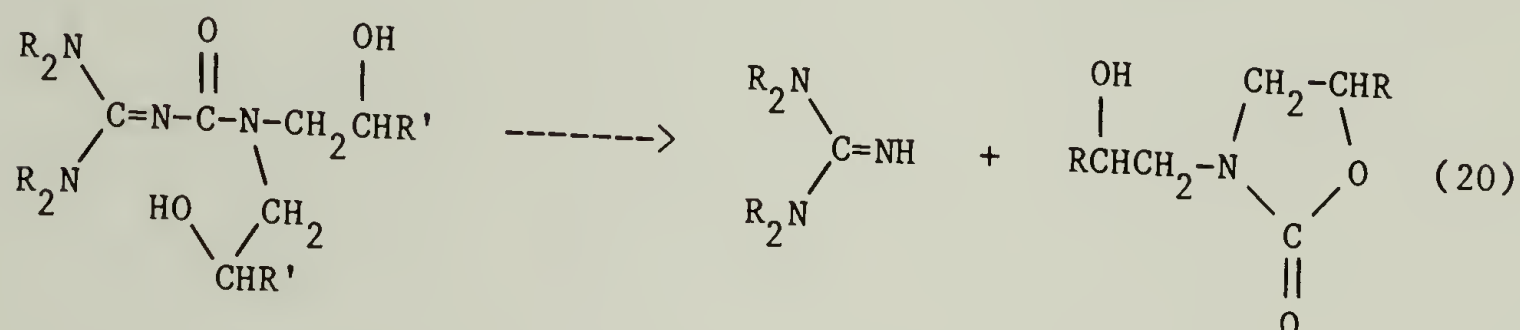
and in that of the isolated, non-HPLC elutable material. This band can be assigned to linear urethane or urea carbonyls. Previous studies have shown that the intensity of this band is increased by the acid catalyzed hydrolysis of the dicy/epoxide reaction product mixtures [40]. Thus, it is postulated that the formation of some fraction of the non-elutable material is attributable to the hydrolysis of linear dicy/epoxide adducts. As discussed in chapter 1, this reaction results in the formation of guanyl urea, cyanourea, guanidine and urea. Of these, guanyl urea appears to most suitably account for the observed properties of the non-elutable material. This product can be formed by the reaction depicted in equation (19), which is similar to that initially proposed



by Noll [82]. However, in the present case, reaction appears to occur via the hydrolysis of substituted dicy molecules.

Further reaction of the substituted guanyl ureas with epoxide would ultimately lead to the formation of the hexasubstituted adduct. In line with the work of Tousignant [83] and Iwakura [84], this compound can be expected to undergo a cyclization/elimination reaction similar to that depicted in equation (b) of Figure 6-1. In the case of the hexasubstituted adduct, hydroxyl addition would primarily occur at the urea carbonyl, as shown in equation (20), resulting in the elimination of guanidines and the formation of structures analogous to product IV. It is

probable that the rate of this decomposition reaction is slower than that observed for the cyclization of the substituted dicy molecule,



since the high basicity of the guanyl urea should render it less susceptible, than substituted dicy, to nucleophilic attack by hydroxyl groups.

In its further reactions with epoxide, guanidine is effectively pentafunctional. Thus, a single dicy molecule should be capable of reacting with as many as seven epoxide groups, via simple amine/epoxide addition reactions. Further, due to their high basicity, the several postulated hydrolysis and degradation products can be expected to act as catalysts for both amine/epoxide additions and etherification reactions, in the dicy/epoxide system. It should be noted that, as strong bases, both substituted guanidines and guanyl ureas will tenaciously bind to the silica gel packing material of the C-18 HPLC column, making them virtually unelutable. Therefore, it appears that the mechanism presented in equations (19) and (20) adequately explains the unelutable nature and slow partial decomposition observed for the components of the non-HPLC elutable fraction of the dicy/MGEBA product mixtures. Several other possible reactions, such as melamine formation, have not been included in the mechanism depicted in Figure 6-1. While these reactions may occur to some extent, no evidence has been found for the large scale participation of these reactions in the dicy/epoxy cure.

### Crosslinking and Long Term Stability

Depending on their initial composition and cure schedule, dicy cured epoxy resins can be expected to contain a specific quantity of each of the structures depicted in figure 6-1 and equations (19) and (20). In the crosslinked resin, the amount and distribution of these structures will determine not only the crosslink density,  $T_g$  and modulus, but also the thermal, hydrolytic and long term stability of the end use material. In the absence of etherification, structures analogous to products III and IV are difunctional chain extenders, while those analogous to product V are essentially trifunctional. As such, these products do not make a sizable contribution to the crosslink density of the curing system. However, each of these structures imparts a high degree of thermal stability to the cured material. In particular, structures analogous to product IV have been shown to act as chain stiffeners, increasing both the  $T_g$  and thermal stability of resins into which they have been incorporated [86]. A similar effect may be expected from the incorporation of structures analogous to product III. Further, products IV and V are both hydrolytically stable, and while product III is susceptible to hydrolysis as shown in equation (d), this reaction will not result in chain cleavage.

Structures analogous to products I, II and the more highly substituted dicy/epoxide adducts may also be present in a dicy cured epoxy resin. Fully substituted, these alkyl dicys will act as tetrafunctional crosslink junctions, imparting a relatively high degree of crosslink density to the cured resin. However, at high temperatures, these struc-

tures will undergo the cyclization/elimination reactions depicted in equation (b). Cyclization can also be expected to occur at lower temperatures, even in a vitrified resin, at a rate which is dependent on the activation energy of this reaction. In a cured resin, this reaction will result in network degradation, and consequently, a reduction in both the  $T_g$  and modulus of the material. It has been suggested that, in the case of a base catalyzed cure, these structures might be afforded some protection by the consumption of  $\beta$ -hydroxyl groups via etherification reactions [42]. However, these structures will remain susceptible to attack by any hydroxyl containing species, which may be present in the cured resin.

Structures analogous to the products comprising the unelutable material appear to provide a high degree of crosslink density, as well as a certain amount of thermal and hydrolytic stability to the cured resin. As guanyl urea and guanidine derivatives, the fully substituted structures will act as hexafunctional and pentafunctional crosslink junctures, respectively. Although the guanyl urea is susceptible to thermal degradation via the mechanism postulated in equation (20), the effect would not be as catastrophic as in the case of tetrasubstituted dicy, due to the higher effective functionality of the eliminated products. Since it is postulated that these uneluted products are formed by the hydrolysis of substituted dicy adducts, it appears that the amount of trace water contained in a dicy/epoxy system is a key factor in determining the structure, crosslink density and long term stability of the cured material.



Finally, it is noted that reactions which do not occur during the cure of dicy/epoxy system, can and will occur during the service life of the end-use product. While vitrification of the resin does result in the cessation of long range molecular motions, stopping the overall cure, the short range motions required for intramolecular reactions such as hydroxyl addition will be much less affected. In addition, the diffusion of water throughout the system can result in the continued hydrolysis of the system. These reactions will not only decrease the crosslink density of the cured resin, but will also change overall polarity and dielectric constant of the material. Further, hydrolysis reactions may lead to the formation of small polar molecules, which can plasticize the resin and which may be leached into the environment of the cured material.

#### Reaction Kinetics

According to the mechanism presented in Figure 6-1, a stoichiometric dicy/epoxy mixture, cured for a sufficient length of time, should yield only those structures analogous to the products formed by reactions (c), (d) and (e). However, substantial quantities of alkylated dicy structures can accumulate during the cure. Truncation of the cure, prior to the completion of reactions (b) and (e), will result in the incorporation of these adducts in the network structure. In accordance with the above discussion, the  $T_g$ , modulus and long-term stability of the end-use material will depend upon the degree of this incorporation. Therefore, these properties are directly dependent on the relative rates of reactions (a), (b) and (e).

Due to the indeterminant role of water and the remaining unknowns in the dicy/epoxide reaction mechanism, There is some difficulty in assessing the effects of composition and temperature on the relative rates of these reactions. However, some generalizations can be made. In the model product I/MGEBA system, reaction (e) appeared to occur at a much faster rate than reaction (b), in the early stages of reaction, while reaction (b) appeared to predominate in the later stages. It is believed that this apparent change in mechanism is due to the depletion of water in the reacting mixtures, resulting in a reduction in the rate of postulated reaction (19). However, the concentration of water in these reaction mixtures was unknown, and it is possible that other factors may be involved. Intuitively, and by observation of isolated products I and II, it is expected that the rate of reaction (b) will increase with the degree of substitution of a specific dicy molecule, while the rate of reaction (e) should be unaffected by the degree of substitution. Based on mass balance equations, it appears that the unresolved uneluted material may contain substantial amounts of tetrasubstituted dicy during the early stages of the reaction. Thus, the increase in the rate of reaction (b), relative to that of (e) in the later stages of reaction, may be to some extent, a reflection of the accumulation of tetrasubstituted dicy in the reaction mixture.

Although kinetic parameters have not been assigned, cyclization reaction (b) appears to have a higher energy of activation than do the amine/epoxide addition reactions depicted in equation (a). Thus, the accumulation of substituted dicy adducts is favored by low temperature curing. Exposure of these kinetically favored, but thermally unstable

structures to higher temperatures, or continued curing for long periods of time at low temperatures will result in their decomposition via reaction (b). These decomposition reactions are responsible, in part, for the decreases in  $T_g$  observed in the TBA traces of both the dicy and product I cures of DGEBA. Other contributions to this  $T_g$  reduction may have come from the postulated degradation reaction of guanyl urea, shown in equation (20).

The products eliminated by the above decomposition reactions, ammonia, alkyl amines and perhaps guanidine, will react at a much faster rate than dicy with any epoxide remaining in a curing system. However, in the case of excess dicy, the depletion of epoxide in the early stages of cure, by the reactions depicted in equation (a), can prevent the incorporation of eliminated products in the crosslink network from occurring. This is apparently what happened in the case of the (1:2) cyanamide/DGEBA cure discussed in chapter 2. There, a sample was precured at 100°C for 19 hours, resulting in the reaction of most of the epoxide, and then post cured at 177°C, along with an unprecured sample of identical composition. A much lower ultimate  $T_g$  was observed for the precured mixture, apparently due to the inability of the eliminated alkyl amines to participate in the cure.

### The Inhomogeneous Cure

The overall rate of cure of the inherently inhomogeneous dicy/epoxy mixture, is dominated by the processes of dicy dissolution and diffusion. Compositional gradients formed early in the cure result in the



formation of regions of varying composition throughout the curing system. In the vicinity of the dicy particles, rapid reaction results in the depletion of epoxide and the build up of structures analogous to the uneluted material and the less substituted products of decomposition reaction (b). These domains are separated from those deficient in dicy by regions of stoichiometric composition and high crosslink density. Vitrification in these regions can prevent the diffusion of reactants into the areas in which they are deficient, leading to a diminished overall rate of cure. At long cure times, decomposition of network structure occurs via the reactions depicted in equations (b) and (20), leading to continued diffusion and cure. Under these conditions, the overall homogeneity of the curing system is dependent on the relative rates of dicy dissolution and diffusion vs that of dicy/epoxide reaction.

#### Future Work

The most important remaining unknowns are the identities of the non-elutable products and the role of  $H_2O$  in the dicy/epoxide mechanism. Using preparative size exclusion chromatography, it should be possible to isolate the non-HPLC elutable products to a degree of purity sufficient to allow useful analyses by FABMS to be conducted. A direct assessment of the role of water in the mechanism can be made by adding small amounts to an assiduously dried product I/MGEBA reaction mixture and analyzing the products by HPLC and SEC.

The ease of formation and purification of product I provides a convenient means of studying dicy cure mechanism over a wide range of



temperatures and compositions, free from the effects of dicy insolubility. Further studies should be conducted using this compound in order to explore the full effects of low temperature reactions on the relative rates of product formation and product stability. In addition, it may be possible to make analogs of this compound using DGEBA. These analogs could then be used as curing agents, allowing the full potential of the dicy/DGEBA cure to be assessed.

Finally, the mechanism of the dicy/epoxide reaction suggests potential modifications which could be performed on the dicy molecule. Nucleophilic substitutions could be attempted at the imido carbon using a variety of hydroxyl and amine containing compounds. These modifications could result in lower use temperatures and increased homogeneity, while maintaining the room temperature latency and relative inexpense of this hardener.

## APPENDIX

### Section 1. Synthesis of Monomethyl Bisphenol A (mMBPA) [87]

#### Materials:

Bisphenol A (BPA), gold label, 99+% pure was obtained from Aldrich and used with out further purification; dimethyl sulfate, reagent grade, was obtained from Kodak.

BPA	22.8grms	(0.1 moles)
DMS	10-12mls	(0.105-0.126 moles)
NaOH	8grms	(0.2 moles)
MeOH	app. 300mls	

#### Procedure:

1. Place BPA in 3-necked round bottom flask, equipped with a stirring bar, magnetic stirrer, reflux condensor, thermometer, and pressure equalizing dropping funnel. Add 150mls of MeOH to the BPA under nitrogen with stirring. Dissolve NaOH in 10gms H<sub>2</sub>O and add to 100mls of MeOH. Slowly add NaOH/MeOH solution to round bottom flask with stirring.

2. Carefully pour dimethyl sulfate into pressure equalizing dropping funnel. (Beakers with ammonia/methanol solutions should be placed in hood near reaction. All glasswear should be washed with these solutions after use. In case of dimethyl sulfate spill, flood contaminated area with these solutions.) Purge system with nitrogen,

heat water bath to methanol reflux. Add dimethyl sulfate over a period of one half hour. Continue heating for one half to one hour.

3. Cool reaction mixture to room temperature and remove all methanol with a rotary evaporator. Dissolve white precipitate in warm aqueous NaOH (3-4grms NaOH in 300mls H<sub>2</sub>O). Place solution in separatory funnel and wash with three 75ml portions of cyclohexane. Wash combined cyclohexane fractions with 50mls portions of aqueous NaOH solution twice. Cyclohexane fractions will contain the dimethyl bisphenol A.

4. Wash combined aqueous fractions with 100ml portions of either diethyl ether or methylene chloride. Repeat 5-6 times. Combine ether extracts and wash with 100mls 1M HCL. Remove ether by rotory evaporation. The free mMBPA is a clear viscous liquid at room temperature. Further purification can be obtained by recrystallizing mMBPA from cold aqueous NaOH solution.

## Section 2. Synthesis of MGEBA [88]

### Materials:

Epichlorohydrin, gold label, 99+% pure was obtained from Aldrich. Sodium hydride was obtained from Aldrich as a 60% dispersion in oil. The material was purified by washing pentane, followed by cyclohexane, followed by THF. Reagent grade THF was dried over sodium and purified by distillation prior to use. Free mMBPA was obtained via the above procedure.

mMBPA	7grms	$(2.89 \times 10^{-2} \text{ moles})$
Epichlorohydrin	50grms	$(0.54 \text{ moles})$
NaH	1.5grms	
THF	app. 500mls	

Procedure:

1. Place NaH in a 3-necked round bottom flask equipped with a reflux condensor, stirring bar, magnetic stirrer and pressure equalizing dropping funnel. Dissolve the mMBPA in 300mls of THF and place in dropping funnel. Add solution to NaH slowly, with stirring and cooling. After addition is complete, stirring is continued for one half hour to complete the reaction. The THF solution is then filtered to remove excess NaH.
2. Dissolve Epichlorohydrin in 200mls of THF in a 1-liter, 3-necked round bottom flask, equipped with a thermometer, reflux condensor, pressure equalizing dropped funnel, stirring bar, magnetic stirrer, nitrogen purge, and hot water bath. Place the mMBPA/THF solution in the pressure equalizing dropping funnel. Heat the bath to THF reflux, and add the mMBPA solution to the round bottom flask over a period of several hours. After addition is complete, continue the reaction at THF reflux for a period of twenty-four to thirty-six hours.
3. Remove THF and excess epichlorohydrin by distillation at reduced pressures. Dissolve MGEBA in diethyl ether and wash with 100mls of cold dilute aqueous NaOH and 100mls of H<sub>2</sub>O. Remove diethyl ether by rotory evaporation and dry product in a vacuum oven.



4. Further purification was obtained by solvent fractionation using acetonitrile and cyclohexane. The material purified in this way was used to conduct the HPLC cure studies in chapter 3 and 5. MGEBA was also purified by vacuum distillation at  $204^{\circ}\text{C}$  and 0.8mm.

### Section 3. Formation of Triamines

Several attempts were made to form triamines from MGEBA, which could then be cleaved by reacting with cyanogen bromide ( $\text{BrCN}$ ), as discussed in following section, in order to produce the disubstituted 2-imino oxazolidine, in accordance with a procedure described by Thursten [71]. In the first attempt, an effort was made to react MGEBA directly with ammonia using a procedure described by McManus [89]. Equimolar amounts of MGEBA and water were charged into a reaction bomb along with a 10:1 excess of liquid ammonia. The bomb was placed in a  $70^{\circ}\text{C}$  oven for 2 to 4 hours, then cooled, and the ammonia allowed to evaporate. The contents were then extracted with THF. HPLC analysis revealed that no reaction had occurred, apparently due to the immiscibility of the reactants. A variety of other conditions were attempted, including the use of a cosolvent, higher reaction temperatures and longer reaction times. These attempts were to no avail.

A simpler procedure was attempted using the chlorohydrin formed by the reaction of MGEBA with  $\text{HCl}$ , and reacting with ammonia. The chlorohydrin and equimolar amounts of water were again placed into a reaction bomb along with a 10:1 excess of liquid ammonia, and the reaction

was again run at 70<sup>0</sup>c for 2 hours. After cooling, and bleeding off the excess ammonia, the contents of the bomb were extracted with diethyl ether. The extract was washed three times with 10% NaHCO<sub>3</sub> to liberate the amines from their HCl salts. HPLC analysis of the liberated amines revealed the formation of a single product peak, believed to be the triamine (yield 90%).

The triamine formed by the above reaction proved to be unreactive toward cleavage by BrCN. This can be attributed to the low propensity of the bulky MGEBA substituents to act as a leaving group in this reaction. It was felt that the use of a disubstituted benzyl amine would offer a better chance for success, due to the high activity of the benzyl group toward cleavage by BrCN [90].

#### Procedure:

1. Dissolve MGEBA in diethyl ether, and place in a separatory funnel. Wash ether solution with 3 portions of 5% aqueous HCl at room temperature. Evaporate the diethyl ether.
2. Place the MGEBA chlorohydrin (7.5 grms) in a reaction vial, along with benzyl amine (3.85grms). Seal the reaction vial and place in a 120<sup>0</sup>C oven for 1 hour.
3. Extract the products from vial with diethyl ether. Wash ether extract with 2 portions of 10% aqueous NaHCO<sub>3</sub> and 1 portion water. Evaporate diethyl ether.
4. HPLC analysis revealed the presence of several impurities presumably including the secondary amine. The triamine was purified by preparatory liquid chromatography using a 65% THF solution. A

discription of this technique can be found in the experimental section of chapter 4.

#### Section 4. The von Braun Cleavage of Tertiary Amines [90]

##### Synthesis of 3-phenyl-2-imino oxazolidine [71]

##### Materials:

2-Anilinoethanol, 98% pure was obtained from Aldrich and was purified by vacuum distillation at 110°C and 1mm; cyanogen bromide (BrCN), 97% pure was obtained from Aldrich and used without further purification.

2-Aniloethanol	15.0 grms (0.109 moles)
BrCN	25.0 grms (0.236 moles)
Toluene	app. 100 mls

##### Procedure:

1. Place BrCN in a 3-necked round bottom flask, equipped with a stirring bar, reflux condensor, thermometer, and pressure equalizing dropping funnel. Add 50 mls of toluene under nitrogen with stirring. Cool to 10°C with an ice bath.

2. Dissolve 2-aniloethanol in 50 mls toluene and place in pressure equalizing dropping funnel. Slowly add to BrCN with stirring over a period of 30 min, taking care that temperature of the flask does not rise above 10°C. Reaction will form a yellowish precipitate. Con-

tinue stirring for another hour, then allow temperature to increase to ambient.

3. Remove condensor and allow flask to vent into hood for several hours in order to evaporate excess BrCN. Extract product by washing toluene with 2 100 ml portions of distilled water. Combine extracts and add 10% aqueous NaOH, in order to liberate the 3-phenyl 2-imino oxazolidine. The liberated product will form a white precipitate.

4. The filtered product was dried over night in a vacuum oven at room temperature, and was found to have a melting point of 97°C (yield 4.39 grms).

#### Synthesis of Product III Analog

##### Materials:

The synthesis and purification of di-MGEBA benzyl amine is described in section 3 of the Appendix. BrCN was identical to that described above.

di-MGEBA benzyl amine	1.0 gram	( $1.42 \times 10^{-3}$ moles)
BrCN	25.0 grms	(.236 moles)
Toluene	app. 50 mls	

##### Procedure:

1. This reaction was conducted using a procedure identical to that used above. The di-MGEBA benzyl amine, dissolved in 25 mls of toluene was slowly added to the BrCN, also dissolved in 25 mls of toluene.

2. HPLC analysis of the product mixture revealed a very low extent



of conversion. Therefore, the reaction temperature was elevated to 50°C and the reaction was allowed to continue for several hours. No precipitate was observed.

3. Following reaction, the toluene was removed by rotory evaporation, and the products, dissolved in THF were analyzed by HPLC, revealing a complex mixture, including what appeared to be product III.

4. The synthetic product III was isolated from the reaction mixture by preparatory liquid chromatography, using 70% acetonitrile.

5. Characterization of this product by FTIR and  $^1\text{H}$  NMR, discussed in chapter 4, reveals that it is indeed product III, the structure of which is shown in Figure 4-20, and not that of a 2-imino oxazolidine. It is believed that product III was preferentially formed in this synthesis, due to the huge excess of BrCN and rigorous conditions used. This reaction may be useful in the future preparation of these products.

## REFERENCES

1. J. Bolger in "Treatise on Adhesion and Adhesives, vol. 3," R. L. Patrick (ed.), New York: Marcel Dekker, Inc., 61-66 (1973).
2. F. A. Hudock and R. B. Grauer, "Applications for Aqueous Dispersions of Epoxy Resins," Org. Coat. Appl. Polym. Sci., Prepr., Proceedings, 46, 183<sup>rd</sup> Nat. Meeting, Las Vegas, 665-671, 3/25-4/2 (1982).
3. G. L. Hagnauer and D. A. Dunn, "Dicyandiamide Analysis and Solubility in Epoxy Resins," J. Appl. Polym. Sci., 20, 1837-1840 (1981).
4. P. Eyerer, "Reaktionsverlauf Wahrend der Hartung eines Epoxidharzes mit Dizyandiamid," J. Appl. Polym. Sci., 15, 3069-3088 (1971).
5. P. N. Son and C. D. Weber, "Some Aspects of Monuron-Accerlerated Dicyandiamide Cure of Epoxy Resins," J. Appl. Polym. Sci., 17, 1305-1313 (1973).
6. B. R. LaLiberte and J. Bornstein, "Mechanism of Monuron-Accelerated Dicyandiamide Cure of Epoxy Resins," AMMRC TR 81, 34.
7. L. Ritter, "Dicyandiamide," Ullman's Encyclopedia, Band 10, 145-149.
8. W. D. Kumler, "Acidic and Basic Dissociation Constants and Structure," J. Org.Chem., 20, 700 (1955).
9. R. F. Stockel, "Dicyandiamide (Cyanoquanidine)," Textbook Errors, 90, J. Chem. Ed., 46(6), 391-392 (1969).

10. A. Y. Kretov, "Dicyanodiamide and Its Reactions," *Usp. Khim.*, 23, 105-122 (1954).
11. R. Fountain, "Characterization and Control of a Structural Epoxy Adhesive," *Polym. Eng. Sci.*, 14(9), 597-603 (1974).
12. L. Shechter, J. Wynstra, and R. E. Kurkijy, *Ind. Eng. Chem.*, 48, 94 (1956).
13. J. P. Bell, "Structure of a Typical Amine-Cured Epoxy Resins," *J. Poly. Sci., Part A-2*, 6, 417-436 (1970).
14. S. Lunak and K. Dusek, "Curing of Epoxy Resins II. Curing of Bisphenol A Diglycidyl Ether with Diamines," *J. Polym. Sci., Symposium* 53, 45-55 (1975).
15. C. A. Byrne, G. L. Hagnauer, N. S. Schneider, and R. W. Lenz, "Model Compound Studies on the Amine Cure of Epoxy Resins," *Org. Coat. and Plast. Chem. Proc., Prepr.*, 41, 178<sup>th</sup> Nat. Meet., Wash. D. C., 293-298, 9/9-9/14 (1979).
16. I. T. Smith, "The Mechanism of the Crosslinking of Epoxide Resins by Amines," *Polym.*, 2, 95-108 (1961).
17. G. Odian, "Principles of Polymerization, 2<sup>nd</sup> Ed.," New York: John Wiley and Sons, 113-123 (1981).
18. N. S. Isaacs and R. E. Parker, "The Mechanism of Epoxide Reactions. Part II. The Reactions of 1,2-Epoxyethylbenzene, 1,2 Epoxy-3-Phenylpropane, and 1,2 Epoxy-3-Phenoxypropane with Benzylamine," *J. Chem. Soc.*, 3497 (1960).
19. J. H. Harrod, "Reactions of Primary Amines with Epoxies," *J. Appl. Polym. Sci.* 6(24), 363-364 (1962).

20. J. Charlesworth, "An Analysis of the Substitution Effects Involved in Diepoxide-Diamine Copolymerization Reactions," J. Polym. Sci., Polym. Chem. Ed., 18, 621-628 (1980).
21. P. Johncock, L. Porecha, and G.F. Tudgey, "The Relative Reactivity of Primary and Secondary Amine Hydrogen Atoms of Aromatic Amines with Epichlorohydrin and N- and O- Glycidyl Compounds," J. Polym. Sci., Polym. Chem. Ed., 23, 291-301 (1985).
22. S. Lunak, J. Vladyka, and K. Dusek, "Effect of Diffusion Control in the Glass Transition Region on Critical Conversion at the Gel Point During Curing of Epoxy Resins," Polym., 19, 931-933 (1978).
23. K. Horie, H. Hiura, M. Sawada, I. Mita, and H. Kambe, "Calorimetric Investigation of Polymerizations Reactions. III. Curing Reaction of Epoxides with amines," J. Polym. Sci., Part A-1, 8, 1357-1372 (1970).
24. T. Murayama, and J. P. Bell, "Relations Between the Network Structure and Dynamic Mechanical Properties of a Typical Amine-Cured Epoxy Polymer," J. Polym. Sci., 8(A-2), 437-445 (1970).
25. C. A. Byrne, G. L. Hagnauer, N. S. Schneider, and R.W. Lenz, "Model Compound Studies on the Amine Cure of Epoxy Resins," Polym. Composites, 1(2), 71-76 (1980).
26. M. A. Acitelli, R. B. Prime, and E. Sacher, "Kinetics of Epoxy Cure: (1) The System Bisphenol-A Diglycidyl Ether/M-Phenylene Diamine," Polymer, 12, 335-343 (1971).



27. S. Sourour and M. R. Kamal, "Differential Scanning Calorimetry of Epoxy Cure: Isothermal Cure Kinetics," *Thermochi. Acta*, 14, 41-59 (1976).
28. K. Dusek, J. Plestil, F. Lednický, and S. Lunak, "Are Cured Epoxy Resins Inhomogeneous?," *Polym.*, 19, 393-397 (1978).
29. U. T. Kreibich and R. Schmid, "Inhomogeneities in Epoxy Resin Networks," *J. Polym. Sci., Symposium*, 53, 177-185 (1975).
30. P. J. Aspbury and W. C. Wake, "The Super Molecular Structures Found in Cured Epoxy Resins," *Br. Polym. J.*, 11(1), 17-27 (1979).
31. J. Mijovic and J. A. Koutsky, "Correlation Between Nodular Morphology and Fracture of Cured Epoxy Resins," *Polym.* 20, 1095-1107 (1979).
32. E. Kontou, G. Spathis, and P.S. Theocaris, "The Heterogeneity of the Network Structure of Epoxy Polymers Studied by Dynamic and DSC Tests," *J. Polym. Sci., Polym. Chem. Ed.*, 23, 1493-1503 (1985).
33. J. P. Bell, "Epoxy Resins: Effect of Extent of Mixing on Properties," *Org. Coat. and Appl. Polym. Sci. Proc., Prepr.*, 46, 183<sup>rd</sup> Nat. Meeting, Las Vegas, 585-591, 3/25-4/2 (1982).
34. H. H. Levine, "Reaction of Dicyandiamide and Epoxy Resins: Preliminary Mechanism Study," *Amer. Chem. Soc.*, 148<sup>th</sup> Nat. Meet., Chicago, 17T 41, 8/-9/ (1964).
35. T. F. Saunders, M. F. Levy, and J. F. Serino, "Mechanism of the Tertiary Amine-Catalyzed Dicyandiamide Cure of Epoxy Resins," *J. Polym. Sci., A-1* 5, 1609-1617 (1967).

36. E. Sacher, "Kinetics of Epoxy Cure: 3. The System Bisphenol-A Epoxides/Dicy," *Polym.*, 14, 91-95 (1973).
37. Muroi, Souichi, H. Ishimura, and M. Otsuka, "Reactivity of Epoxy Resin in Dispersed Dicyandiamide of the Resulting Product," *J. Appl. Polym. Sci.*, 32, 5095-5104 (1986).
38. G. L. Hagnauer, B. R. LaLiberte, and D. A. Dunn, "Isothermal Cure Kinetics of an Epoxy Resin Prepreg," *ACS Symposium Series*, 221, Epoxy Resins Chem. II, R. S. Bauer, Editor.
39. N. S. Schneider, J. F. Sprouse, G. L. Hagnauer, and J. K. Gillham, "DSC and TBA Studies of the Curing Behavior of Two Dicy-Containing Epoxy Resins," *Polym. Eng. Sci.*, 19(4), 304-312 (1979).
40. S. A. Zahir, "The Mechanism of the Cure of Epoxide Resins by Cyanamide and Dicyandiamide," *Adv. Org. Coat. Sci. Technol. Ser.*, 4, 83-102 (1982).
41. R. G. Davidson, "Computer Assisted IR Spectroscopy of the Dicyandiamide-Epoxy Reaction," *Polym. Mech. Sci. Eng. ACS Polym. Prepr.*, 50, 194 (1984).
42. Y. G. Lin, H. Sautereau, and J. P. Pascault, "BDMA-Catalyzed DDA-Epoxy Resins System: Temperature and Composition Effects on Curing Mechanism," *J. Polym. Sci., Polym. Chem. Ed.*, 24, 2171-2184 (1986).
43. J. Galy, A. Sabra, and J. P. Pascault, "Characterization of Epoxy Thermosetting Systems by Differential Scanning Calorimetry," *Polym. Eng. Sci.*, 26(21) 1514 Dec. (1986).

44. J. Galy, D. Gulino, J. P. Pascault, and Quahg Tho Pham, "Study on the Mechanism of 1-Cyanoquanidine Cure of Epoxy Resins Using Model Compounds," *Die Makromole. Chem.*, 188, 7-19 (1987).
45. R. A. Fava, "Differential Scanning Calorimetry of Epoxy Resins," *Polym.*, 9, 137 (1968).
46. R. B. Prime, "Differential Scanning Calorimetry of the Epoxy Cure Reaction," *Polym. Eng. Sci.*, 13(5), 365-371 (1973).
47. J. M. Barton, "Monitoring the Curing Reaction of an Aromatic Amine/Epoxy Resins System by Differential Scanning Calorimetry (DSC): Determination and Significance of the Activation Energy," *D. Makromole. Chem.*, 171, 247-251 (1973).
48. M. E. Ryan and A. Dutta, "Kinetics of Epoxy Cure: A Rapid Technique for Kinetic Parameter Estimation," *Polym.* 20, 203-206 (1979).
49. R. B. Prime, "Thermosets: Thermal Characterization of Polymeric Materials," Edith Turi Ed., Chapter 5, 435-563 (1981).
50. O. R. Abolafia, "Application of Differential Scanning Calorimetry to Epoxy Curing Studies," *SPE Tech. Papers* 15, 610-616 (1969).
51. T. Olcese, O. Spelta, and S. W. Vargiu, "Curing Kinetics of Epoxy Resins," *J. Polym. Sci., Symposium* 53, 113-126 (1975).
52. R. L. Miller and M. A. Oebser, "Determination of Cure Times and Activation Energies of One-Container Epoxy Resins Systems by Isothermal DSC," *Thermochimica Acta*, 36, 121-131 (1980).

53. P. G. Babayevsky and J. K. Gillham, "Epoxy Thermosetting Systems: Dynamic Mechanical Analysis of the Reactions of Aromatic Diamines with the Diglycidyl Ether of Bisphenol A," *J. Appl. Polym. Sci.*, 17, 2067-2088 (1973).
54. J. K. Gillham, "A. Semimicro Thermomechanical Technique for Characterizing Polymeric Materials: Torsional Braid Analysis," *J. A. I. Chem. Eng.*, 20(6), 1066-1079 (1974).
55. J. B. Enns and J. K. Gillham, "Time-Temperature-Transformation (TTT) Cure Diagram: Modeling the Cure Behavior of Thermosets," *J. Appl. Polym. Sci.*, 28, 2567-2591 (1983).
56. N. S. Schneider and J. K. Gillham, "TBA Studies of Prepreg Curing Behavior," *Polym. Composites*, 1(2), 97-102 (1980).
57. W. X. Zukas, D. A. Dunn, and M. D. Gilbert, "Analysis of the Amine Cure of Epoxy Resins Using Model Compounds," *Polym. Mat. Sci. Eng., Prepr.*, 56, Denver, 346-350 (1987).
58. G. A. Senich, W. J. MacKnight, and N. S. Schneider, "A Dynamic Mechanical Study of the Curing Reaction of Two Epoxy Resins," *Polym. Eng. Sci.*, 19(4), 313-318 (1979).
59. C. Y. M. Tung and P. J. Dynes, "Relationship Between Viscoelastic Properties and Gelation in Thermosetting Systems," *J. Appl. Polym. Sci.*, 27, 569-574 (1982).
60. B. Wunderlich in "Thermal Characterization of Polymeric Materials," E. Turi (ed.), New York: Academic Press, 92-234 (1981).
61. E. H. Catsiff, H. B. Dee, J. F. D. Prima, and R. Seltzer "Cyanamides of Primary Aromatic Amines: New High-Performance Epoxy Curing Agents," *Polymer Preprints* 22, #2 (1981).



62. R. J. Morgan and E. T. Mones, "The Cure Reactions, Network Structures and Mechanical Response of Diaminodiphenyl Sulfone Cured Tetraglycidyl 4, 4'-Diaminodiphenyl Methane Epoxies," Polymer.
63. R. E. Smith, F. N. Larsen, and C. L. Long, "Epoxy Resin Cure II. FTIR Analysis," J. Appl. Polym. Sci., 29, 3713-3726 (1984).
64. H. H. Hoehold, J. Klee, H. Schutz, and R. Radeaglia, "Unvernetzte Epoxid-Amin-Additions-Polymere, 15,  $^{15}\text{N}$ -NMR-Spektroskopie von DGEBA-Anilin-Additions-Polymeren," Die Angewandte Makromole. Chem., 144, 109 (1986).
65. M. F. Grenier-Loustalot et P. Grenier, "Reaction Epoxy-Amine: Sui vi du Mechanisme Reactioniel et de la Cinetique par RMN  $^{13}\text{C}$ ,  $^{15}\text{N}$  et HPLC,"
66. K. Dusek, M. Bleha, and S. Lunak, "Curing of Epoxide Resins: Model Reactions of Curing with Amines," J. Polym. Sci., Polym. Chem. Ed., 15, 2393-2400 (1977).
67. C. A. Byrne, G. L. Hagnauer, and N. S. Schneider, "Effects of Variation in Composition and Temperature on the Amine Cure at an Epoxy Resin Model System," Polym. Composites, 4(4), 206-213 (1983).
68. S. A. Mestan and C. E. M. Morris, "Chromatography of Epoxy Resins," J. Macromol. Sci.- Rev. Macromol. Chem. Phys., C24(1) 117-172 (1984).
69. R. W. Yost, L. S. Ettre, and R. D. Conlon, "Practical Liquid Chromatography: An Introduction," Perkin-Elmer, (1980).

70. D. Doskocilova, L. Matejka, S. Pokorny, M. Brezina, J. Stokr, I. Dobas, and K. Dusek, "Epoxy Resins, Curing of Epoxy Resins: 'Configurational Structure and Reactivity of Stereoisomers in the Model Reaction of Diglycidylamine with N-Methylamine'," Polym. Bulletin, 14, 123-129 (1985).
71. J. T. Thursten, "Oxazolidines and a Method of Preparing the Same," Patent (U. S.), 2, 479,525.
72. G. L. Hagnauer and I. Setton, "Compositional Analysis of Epoxy Resin Formulations," J. Liq. Chromato., 1(1), 55-73 (1978).
73. J. C. Paterson-Jones, "The Mechanism of the Thermal Degradation of Aromatic Amine-Cured Glycidyl Ether-Type Epoxide Resins," J. Appl. Polym. Sci., 19, 1539-1547 (1975).
74. M. A. Grayson and C. J. Wolf, "Low-Temperature Thermal Decomposition of an Epoxy Resins," J. Polym. Sci., Polym. Chem. Ed., 22, 1897-1907 (1984).
75. V. Bellenger and L. Verdu, "Oxidative Skeleton Breaking in Epoxy-Amine Networks," J. Appl. Polym. Sci., 30, 363-374 (1985).
76. G. A. Luoma and R. D. Rauland, "Environmental Degradation of an Epoxy Resin Matrix," J. Appl. Polym. Sci., 32, 5770-5790 (1986).
77. C. F. Poranski jr., W. B. Moniz, D. L. Birkle, J. T. Kopfle, and S. A. Sojka, "Carbon-13 and Proton NMR Spectra for Characterizing Thermosetting Polymer Systems, I: Epoxy Resins and Curing Agents," NRL Report 8092 (1977).

78. A. Renner, R. Moser, M. Bellus, H. Fuhrer, and M. A. Spitzer, "Cure of Epoxy Resins with Esters of Cyanoacetic Acid," J. Polym. Sci., Polym. Chem. Ed., 23, 2341-2359 (1985).
79. J. Brand, Tech. Pap. IPC-TP Inst. Printed Circuits, IPC-TP-152 (1977).
80. J. L. Illinger and N. S. Schneider, "Water Vapor Transport in an Epoxy Resin Based on TGMDA and Dicy," Polym. Eng. Sci., 20(4), 310-314 (1980).
81. J. F. Jones, T. T. Bartels, and R. Fountain, "The Processing and Aging of Boron/Epoxy Composite Materials," Polym. Sci. Eng., 14(3), 240-245 (1974).
82. T. E. Noll, Tech. Pap. IPC-TP, Inst. Printed Circuits, IPC-TP-140 (1975).
83. W. F. Tousignant and A. W. Baker, "Reaction of Ethylene Oxide with Urea," J. Org. Chem., 22, 166 (1957).
84. Y. Iwakura and S. I. Izawa, "Glycidal Ether Reactions with Urethanes and Ureas. A New Synthetic Method for 2-Oxazolidones," J. Org. Chem., 29, 379-382 (1964).
85. W. Fisch, W. Hofmann, and R. Schmid, "Chemistry of Epoxide Resins. XVII. Influence of Structure and Curing Conditions on the Density, Degree of Cure, and Glass Transition Temperature During the Curing of Epoxide Resins," J. Appl. Polym. Sci., 13, 295-308 (1969).
86. P. Kordomenos, J. E. Kresta and K. C. Frisch, "Kinetics of the Initial Stage of Thermal Decomposition of Isocyanate Based Model Compounds and Polymers," Org. Coat. and Plast. Chem. Proc., 38, 175<sup>th</sup> Nat. Meet., Anaheim, 450-455 (1978).

87. G. S. Hiers and F. D. Hager, "Anisole," Organic Syntheses, Collective Volume I, N. Y.: J. Wiley and Sons, Inc., 1, 58 (1967).
88. N. S. Enikolopyan, M. A. Markevitch, L. S. Sakhonenko, S. Z. Rogovina, and V. G. Oshmyan, "Kinetics of Epoxide Resin Formation from Epichlorohydrin and Bisphenol-A," J. Polym. Sci., Polym. Chem. Ed., 20, 1231-1245 (1982).
89. S. P. McManus, C. A. Larson, and R. A. Hearn, "The Synthesis of Aminoalcohols from Epoxides and Ammonia," Synthetic Communications, 3(3), 177-180 (1973).
90. H. A. Hageman in "Organic Reactions, vol. VII," R Adams (ed.), New York: John Wiley and Sons, 198-262 (1953).



